THESE

Pour obtenir le grade de

DOCTEUR

de l'Université Louis Pasteur de Strasbourg

Spécialité: **CHIMIE**

Présentée par

Suyun JIE

Synthèse de nouveaux complexes des métaux de transition et application en catalyse d'oligomérisation et/ou de polymerization de l'éthylène

---

Soutenue le 11 Avril 2008 devant la commission d'examen:

Prof. P. BRAUNSTEIN	Directeur de recherche CNRS à l'Université Louis Pasteur, Srasbourg *Directeur de Thèse*
Prof. W.-H. SUN	Professeur à l'Institut de Chimie, Académie des Sciences de Chine, Pékin (Chine) *Directeur de Thèse*
Prof. K. MUNIZ	Professeur à l'Université Louis Pasteur, Strasbourg *Rapporteur Interne*
Prof. B. HAN	Professeur à l'Institut de Chimie, Académie des Sciences de Chine, Pékin (Chine) *Rapporteur Externe*
Prof. R. HUA	Professeur à l'Université Tsinghua, Pékin (Chine) *Rapporteur Externe*
Prof. D. WANG	Professeur à l'Institut de Chimie, Académie des Sciences de Chine, Pékin (Chine) *Examinateur*
Prof. X. WAN	Professeur à l'Université de Pékin (Chine) *Examinateur*
Prof. P. J. T. TAIT	Professeur à l'Université de Manchester (UK) *Examinateur*

Remerciements

Ce travail a été effectué au Laboratoire de Chimie de Coordination, UMR 7177 du CNRS, de l'Université Louis Pasteur de Strasbourg, et à l'Institut de Chimie, Académie des Sciences de Chine, Pékin.

Je tiens tout d'abord à remercier mes directeurs de thèse le Dr. Pierre Braunstein, Directeur de Recherche au CNRS et membre de l'Académie des Sciences en France, et Dr. Wen-Hua Sun, professeur à l'Institut de Chimie, Académie des Sciences de Chine à Pékin, pour m'avoir accueilli au sein de son laboratoire, pour avoir encadré ce travail, et l'ambassade de France en Chine pour sa confiance.

Je remercie les membres de mon jury, Messieurs K. Muniz, B. HAN, R. HUA, D. Wang, X. Wan, et P. J. T. Tait, qui ont accepté de juger mon travail.

Mes remerciements vont aussi à tous ceux qui ont contribué à ce travail: Dr. Tianzhu Zhang, Dr. Wen Zhang, Shu Zhang, Yingxia Song, et Dr. Anthony Kermagoret, Dr. Magno Agostinho.

Je tiens aussi à remercier André DeCian, Lydia Brelot et Richard Welter pour la détermination des structures, Anne Degrémont pour la synthèse des précurseurs métalliques et Marc Mermillon-Fournier pour son aide avec les problèmes techniques.

Un grand merci aux membres du Laboratoire de Chimie de Coordination: Jacky, Soumia, Marc, Catherine, Abdelatif, Adel, Roberto, Riccardo, Magno, Anthony, Günter, Sabrina, Farba, Matthieu, Lisa, Shuanming, Christophe. Merci aussi aux collogues à Pékin: Dr. Tianzhu Zhang, Dr. Wen Zhang, Dr. Xiubo Tang, Dr. Dongheng Zhang, Dr. Junxian Hou, Dr. Wenjuan Zhang, Fei Chang, Tielong Gao, Shu Zhang, Weiwei Zuo, Kefeng Wang, Peng Hao, Yanjun Chen, Rong Gao, Min Zhang, Miao Shen, Shaofeng Liu, et les autres.

Merci à mes amis, non chimistes, de Strasbourg et Pékin.

Enfin, j'adresse un merci à mes parents et ma soeur en Chine.

SOMMAIRE/CONTENTS

Composition du document et organisation de la bibliographie

Ce document se divise en 7 sections principales: une introduction générale, 5 chapitres et une conclusion générale.

L'introduction générale est rédigée en anglais.

Les chapitres I–V sont rédigés en anglais:

Le chapitre I a été publié dans le journal *J. Organomet. Chem.*, il dispose en sa fin de sa propre bibliographie;
Le chapitre II a été publié dans le journal *Organometallics*, il dispose en sa fin de sa propre bibliographie;
Le chapitre III a été publié dans le journal *C. R. Chim.*, il dispose en sa fin de sa propre bibliographie;
Le chapitre IV a été publié dans le journal *Eur. J. Inorg. Chem.*, il dispose en sa fin de sa propre bibliographie;
Le chapitre V a été publié dans le journal *Dalton Trans.*, il dispose en sa fin de sa propre bibliographie.

La Conclusion Générale est rédigée en anglais.

Introduction Générale

General Introduction

Polyolefins show a rapidly growing potential because they contain only carbon and hydrogen atoms, which are inert, stable to water, and can be easily recycled or used as a source of energy for incineration. Although it has been half a century since polyethylene's commercialization, polyolefins remain highly technology-driven, which are the fastest-growing segment of polymer industry. The three major classes of polyethylene are described by the acronyms HDPE, LDPE, and LLDPE.[1,2] High-density polyethylene (HDPE) is a linear, semicrystalline ethylene homopolymer ($T_m \approx 135$ °C) prepared by Ziegler-Natta and chromium-based coordination polymerization technology. Linear low-density polyethylene (LLDPE) is a random copolymer of ethylene and α-olefins (e.g., 1-butene, 1-hexene, or 1-octene) produced commercially using Ziegler-Natta, chromium, and metallocene catalysts. Low-density polyethylene (LDPE) is a branched ethylene homopolymer prepared in a high-temperature and high-pressure free-radical process.

Linear α-olefins are also major industrial reactants owing to their growing demand most notably as comonomers with ethylene (C_4–C_8 to yield branched linear low-density polyethylene (LLDPE) with impressive rheological and mechanical properties), for the synthesis of poly-α-olefins and synthetic lubricants (C_{10}), as additives for high-density polyethylene production and for the production of plasticizers (C_6–C_{10}) and surfactants (C_{12}–C_{20}).[3] Ethylene is a readily available feedstock, and its oligomerization represents the main source for α-olefins in industry.[4] And the products in ethylene oligomerization possess exclusively an even number of carbon atoms and represent commercially most valuable products.[2,5] The selective synthesis of C_4–C_{20} linear α-olefins has therefore become a topic of considerable interest in both academia and industry.

The lower oxophilicity and the greater functional group tolerance of late transition metals relative to early transition metals, such as Ti, Zr, and Hf, make them likely targets for the development of catalysts for the homo- and copolymerization of ethylene with polar comonomers under mild conditions. This endows their complexes with possibilities of synthesizing new polymers with special microstructures and polar monomers and value-added products, such as linear α-olefins, wax, and polyethylenes.

for references, see page 11

Nickel-based catalysts

Shell's very well-known Schell Higher Olefin Process (SHOP) for the production of linear α-olefins is an excellent example of the utility of Ni(II) complexes bearing monoanionic [P,O] ligands (**A**, Scheme 1) for ethylene oligomerization.[6] These catalysts are very selective for the insertion of ethylene versus α-olefins, and β-hydride elimination is competitive with olefin insertion, giving high-quality, linear α-olefins (C_6–C_{20}) from ethylene.

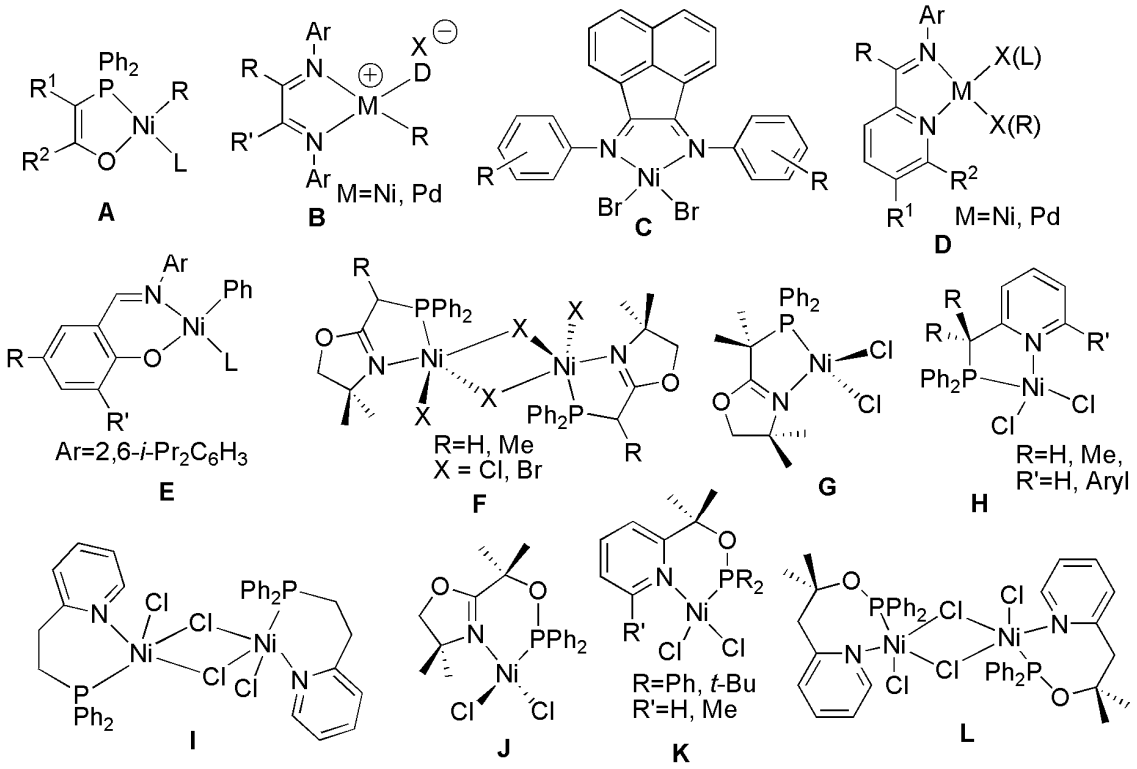

Scheme 1.
Nickel (palladium) complexes bearing various chelate bidentate ligands.

The area of ethylene polymerization with late transition metal catalysts was rejuvenated when Brookhart and his co-workers reported a family of new cationic Ni(II) and Pd(II) α-diimine catalysts (**B**, Scheme 1) for the polymerization of ethylene, α-olefins, and cyclic olefins and the copolymerization of nonpolar olefins with a variety of functionalized olefins in 1995.[7] The steric and electronic properties of the α-diimine ligands can be readily adjusted by modifying the imino carbon and nitrogen substituents, and hence a large number of structural variations have been reported in the academic literatures.[2,5b,8] The fact that these complexes produce high-molecular-weight polymer is a consequence of slow chain transfer relative to chain propagation. In these d^8 square planar systems, chain transfer is proposed to occur by associative olefin displacement and is hindered by the axial bulk provided by the *ortho*-substituents of the aryl rings.

for references, see page 11

For example, nickel(II) complexes containing para- and unsubstituted aryl α-diimine ligands (**C**, Scheme 1) in combination with MMAO are highly active and efficient catalysts for the oligomerization of ethylene to linear α-olefins in the C_4–C_{26} range with selectivities as high as 94% and Schulz-Flory product distributions.[9] Several groups have reported that neutral and cationic Ni and Pd complexes with unsymmetrical imino-pyridine ligands (**D**, Scheme 1), and generally greatly reduced ethylene polymerization activities and reduced molecular weights were obtained.[10] The related bridged bis-pyridylimino dinuclear nickel complexes and their catalytic behavior for ethylene oligomerization and polymerization will be described in Chapter I.

A series of neutral salicylaldiminato nickel complexes (**E**, Scheme 1), bearing bulky imino substituents, were reported by Grubbs and co-workers.[11] The bulky groups retard associative displacement reactions in much the same way as for cationic α-diimine nickel systems. A dependence of activity on R' was observed, and the catalyst activity, as well as molecular weight and linearity, increases in the order ^{t}Bu < Ph < 9-phenanthrenyl < 9-anthracenyl, after activation of **E** (L = PPh_3) by $Ni(COD)_2$. This family of neutral catalysts also exhibited good functional group tolerance and remains active in the presence of polar or protic solvents.[12] Ethylene oligomerization uing a number of neutral nickel complexes bearing anionic [N,O] and [O,O] chelating ligands has been investigated by Carlini and co-workers, and generally low to moderate activities were obtained at elevated pressure.[13]

Phosphinoimine ligands have only recently attracted attention for the late transition-metal-catalyzed oligomerization, polymerization, and copolymerization of ethylene.[2,8,14,15] Considering that the use of nonenolizable imine donors should be beneficial to catalyst thermal and chemical stability, we have examined the synthesis, structure, and catalytic properties of various mono- and dinuclear Ni(II) complexes with phosphino-oxazoline and phosphino-pyridine ligands (**F**–**I**, Scheme 1).[16] In all cases, one of our goals was to use as little cocatalyst as possible, not only for economical reasons but also for a better understanding of the ligand influence on the catalytic properties of the metal complexes.[17] Phosphinito-imines have rarely been used in the oligomerization of ethylene. The phosphinito-oxazoline and phosphinito-pyridine nickel complexes (**J**–**L**, Scheme 1) were prepared, but in the presence of MAO and $AlEt_3$, only decomposition of the complexes was observed.[17] The consequence of the replacement of a phosphine by a phosphinite donor, which also resulted in a increase of the chelate ring size from 5 to 6, was noted when comparing the TOF values observed in the presence of 6 equiv of $AlEtCl_2$.[16a,18] Within this large family of P,N ligands, variables

for references, see page 11

include the basicity of the N-donor moiety, from pyridines to less basic oxazolines, and the stereoelectronic properties of the phosphorus donor, from a phosphine, phosphinite, or phosphonite type. Relatively small variations in the ligand steric and/or electronic properties may favor mononuclear structures for their metal complexes, and a comparison between mono- and dinuclear catalyst precursors thus becomes available. We have always attempted to use as little cocatalyst as possible, and it was even possible to use only 1.3 equiv of $AlEtCl_2$ with complexes **K**.[18] In this thesis, some of phosphino-oxazoline and phosphinito-oxazoline ligands were chosen for their cobalt(II) complexes. Their catalytic behavior for ethylene oligomerization were investigated in the presence of MAO and $AlEtCl_2$, and also compared with the corresponding nickel complexes (see Chapter V).

Both ethylene oligomerization and polymerization reactions can be represented by a general mechanism that involves common organometallic elementary steps (Scheme 2).

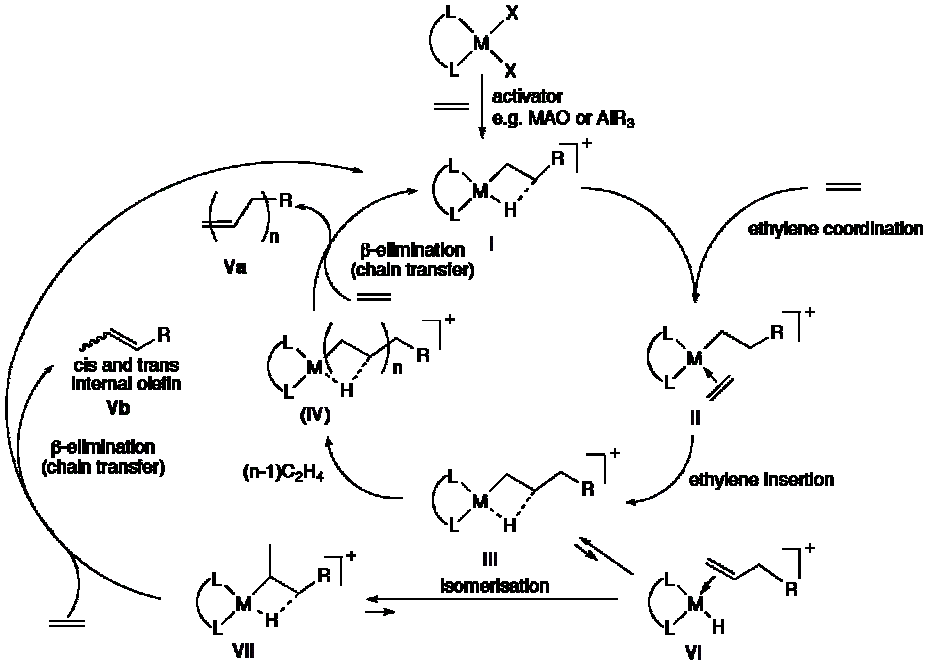

Scheme 2.
Catalytic mechanism for ethylene oligomerization and polymerization.

First, a coordinatively unsaturated species is generated, which is stabilized after ethylene insertion by a *β*-agostic interaction **I**.[19] The coordinated ethylene in complex **II** inserts into the M-alkyl bond to give **III**. Finally, after (*n*–1) further insertions leading to **IV**, the product molecule **Va** is eliminated. The exact mechanism that leads to the liberation of the olefin, chain transfer/*β*-H elimination, still deserves detailed studies.[20] For values of *n* ranging from 1 to 40, oligomers are formed, and for larger values of *n*, polymers are eliminated (Scheme 2). Isomerization leading to internal olefins **Vb** is accounted for by species **VI** and **VII**. The reaction sequence **II**–**IV** depends strongly on

for references, see page 11

the ethylene concentration (pressure) because the rate of chain transfer relative to chain isomerization increases with the ethylene concentration.[2,9a] Brookhart and coworkers have noted that an increase in ethylene pressure led to an increased selectivity for α-olefins and in the Schulz-Flory constant α. Therefore, any change in the ethylene concentration, e.g., pressure, reaction temperature, and ethylene solubility, will have a decisive influence on the branching ratio in polymerization or on the α-olefin content in oligomerization reactions.[2]

Recently, more attention has been also paid to pentacoordinate nickel complexes bearing various tridentate ligands, such as N^N^O (**A** and **B**, Scheme 3),[21] N^P^N (**C**, Scheme 3),[22] P^N^N (**D** and **E**, Scheme 3),[23] P^N^P (**F**, Scheme 3)[23a] and N^N^N (**G**–**L**, Scheme 3) ligands.[24,25] Our group in Beijing has reported a number of nickel complexes bearing tridentate-N_3 ligands, for example, 2-benzimidazolyl-6-iminopyridines (**H**, Scheme 3),[21b,25a] 2-quinoxalinyl-6-iminopyridines (**I**, Scheme 3),[25b] 2-imino-1,10-phenathrolines (**J**, Scheme 3),[25c] 2-benzimidazolyl-1,10-phenanthrolines (**K**, Scheme 3),[25d] *N*-((Pyridin-2-yl)methylene) quinolin-8-amine (**L**, Scheme 3),[25e] and all of them showed moderate to good catalytic activity for ethylene oligomerization and very high activity in the presence of PPh_3 as an auxiliary ligand. In this thesis, the related nickel complexes bearing 2-imino-9-phenyl-1,10-phenanthrolines will be discussed in Chapter IV.

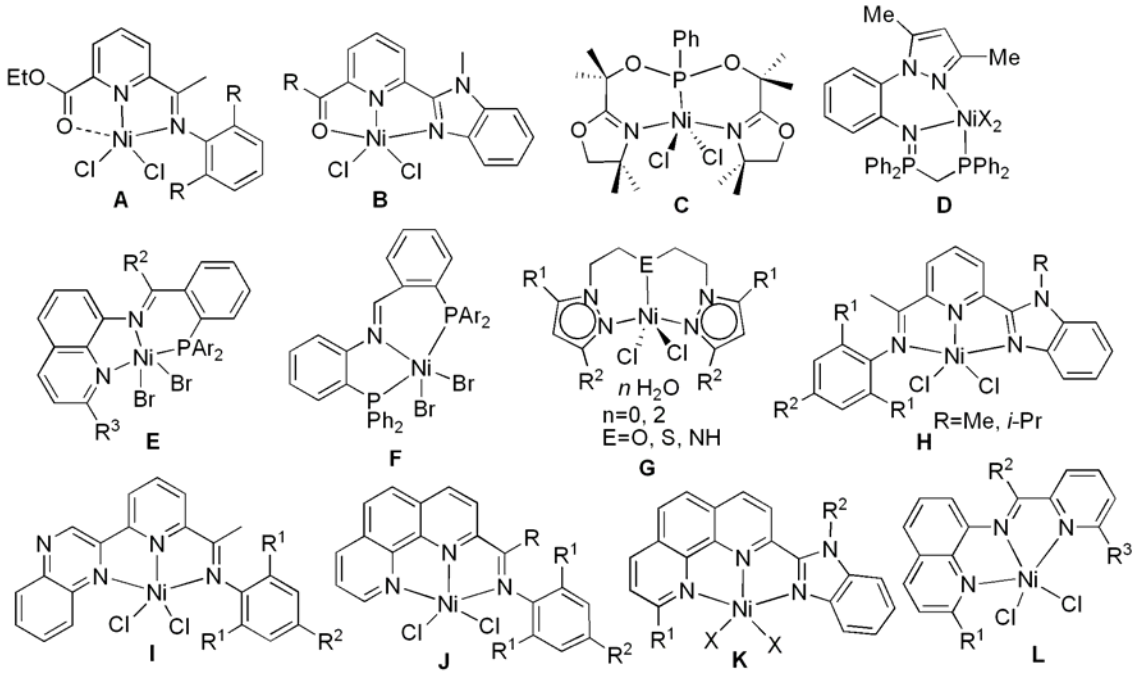

Scheme 3.
Nickel complexes bearing various neutral tridentate ligands.

for references, see page 11

Iron- and cobalt-based catalysts

In 1998, Brookhart[26] and Gibson[27] independently discovered that five-coordinate 2,6-bis(arylimino)pyridyl iron(II) and cobalt(II) dihalides (**A**, Scheme 4), activated by MAO, are very effective catalysts for the conversion of ethylene to high-density polyethylene or to α-olefins with Schluz-Flory distribution. Remarkably, the productivities were as high as those of most efficient metallocenes. The advantages of these Fe and Co catalysts over other types of single-site catalysts for ethylene homopolymerization (e.g., metallocenes, CGC) are manifold, spanning from the ease of prearation and handling to the use of low-cost metals with negligible environment impact. Another intriguing feature of these catalysts is provided by the facile tuning of their polymerization activity by simple modifications of the ligand architecture. It has been shown that the size, nature and regiochemistry of the substituents in the iminoaryl groups are of crucial importance in controlling the polymerization and oligomerization of ethylene.[28] Moreover, due to the good compatibility with various early and late metal copolymerization catalysts, bis(arylimino)pyridyl Fe(II) and Co(II) dihalides can be used as oligomerization catalysts in tandem catalytic systems for the production of branched PE as well as in reactor blending to give PE with controlled molecular weight distribution.[29]

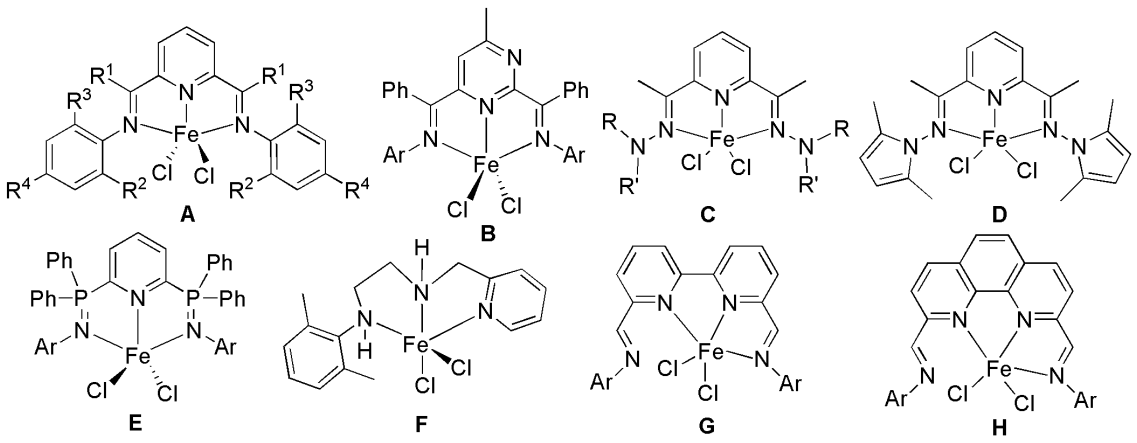

Scheme 4.
Some five-coordiante iron complexes bearing neutral ligands.

Extending the iron complexes containing alternative tridentate-N_3 ligands, however, commonly leads to lower catalytic activities for ethylene oligomerization and polymerization.[30,31] Restricting the discussion to five-coordiante complexes in meridional fashion, some examples of iron complexes are also shown in Scheme 4. The complexes **B**–**D** show only slight variations from the bis(imino)pyridyl species. In

for references, see page 11

complex **B**, the central pyridine ring has been replaced by a pyrimidine ring; the resultant catalysts were reported to be somewhat less active than **A**.[30a] Complexes of type **C**, in which dialkyl or diaryl hydrazines were used instead of anilines to generate the similar structure, exhibited substantially lower activity than **A**.[30b] Catalyst activity increased, though, when 1-amino-2,5-dimethylpyrrole was used to form the tridentate ligand (**D**, Scheme 4). The steric similarities of **D** to **A** are obvious; the lower molecular weight of the polymer made by **D** relative to the 2,6-dimethylsubstituted aryl-imine analogues was noted.[30b] On activation with MAO or Et_2AlCl, the sterically hindered iminophosphorane complexes of iron (**E**, Scheme 4) showed only low activity for ethylene polymerization.[30c] The iron complexes bearing flexible tridentate-N_3 ligands (**F**, Scheme 4) just acted as modest ethylene oligomerisation catalysts on activation with MAO, giving linear α-olefins with a Schulz–Flory distribution.[30d] The X-ray study reveals that only one imine arm is coordinated in iron complexes **G** and **H** bearing bis(imino)bipyridines and bis(imino)phenanthrolines, affording a severely distorted trigonal-bipyramidal iron center. Neither **G** nor **H** is catalytically active in the presence of MAO.[31]

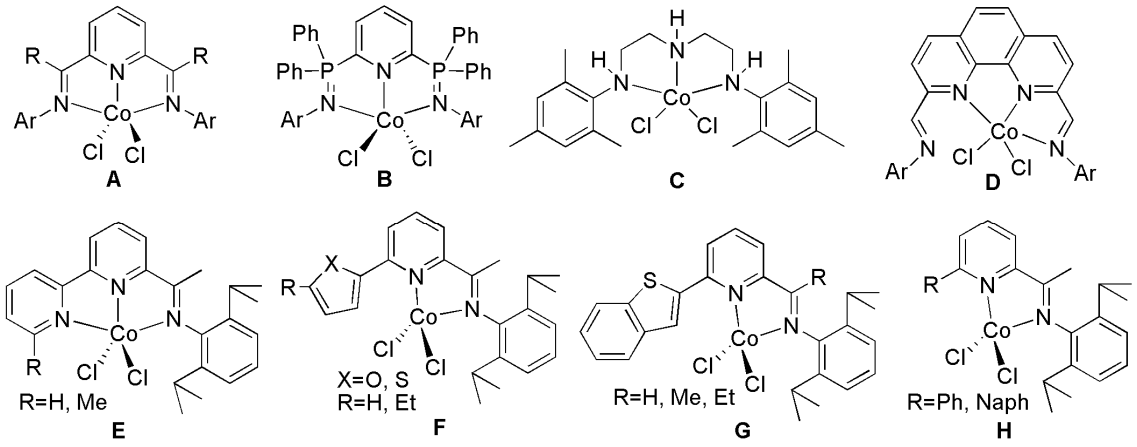

Scheme 5.
Some examples of cobalt complexes.

New advances in olefin polymerization catalysts using cobalt complexes have also been based mainly on the bis(imino)pyridine ligand framework (**A**, Scheme 5). Generally their activities are an order of magnitude lower than those for their iron relatives. Structural modifications for the iron-based catalysts have in most cases also been applied to the cobalt complexes, and generally similar activity trends for ethylene oligomerization or polymerization are observed. However, the deviations away from the bis(imino)pyridine ligand framework sometimes afford higher activities with cobalt

for references, see page 11

complexes than their iron analogues. For example, cobalt complexes bearing bis(phosphinimide)pyridine (**B**, Scheme 5) are moderately active in ethylene polymerization.[30c] Cobalt complexes possessing a flexible ligand backbone without imino groups (**C**, Scheme 5), showed modest activity for ethylene oligomerization; the analogous iron system was not successfully prepared.[30d,32] Cobalt complexes bearing bis(imino)phenanthrolines also showed moderate activity for ethylene polymerization in the presence of MAO.[31b] Bianchini and co-workers reported the cobalt complexes of type **E**–**H**;[33] among them, complexes **F** (X = S) possessing a terminal sulfur donor that is not bound to the cobalt in the solid state, were most active for ethylene oligomerization. In fact, the ligand in **F** appears to bind in bidentate fashion in the catalysts, which likely explains why catalytic activity was not reported for the related iron systems.

Recently, there are several types of iron and cobalt complexes containing tridentate-N_3 ligands reported by our group in Beijing.[34] The same types of ligands as those used in nickel complexes (**H**–**L**, Scheme 3), including 2-benzimidazolyl-6-iminopyridines,[25a,35] 2-quinoxalinyl-6- iminopyridines,[37] 2-benzimidazolyl-1,10-phenanthrolines,[36] *N*-((Pyridin-2-yl)methylene)quinolin-8-amine,[38] are applied in the corresponding iron and cobalt complexes. These iron and cobalt complexes showed good catalytic activities for ethylene oligomerization on activation with MAO or MMAO. In this thesis, iron and cobalt complexes bearing 2-imino-1,10-phenathroline derivatives and their catalytic behavior for ethylene oligomerization were investigated and the detailed results will be discussed in Chapter II–IV.

for references, see page 11

References

1. Y. V. Kissen. Olefin Polymers-Polyethylene. In *Kirk-Othmer Encyclopedia of Chemical Technology,* 4th ed.; Kroschwitz, J. I., Howe-Grant, M., Eds.; Wiley-Interscience: New York, 1996; Vol. 17, p 702.
2. S. D. Ittel, L. K. Johnson, M. Brookhart, *Chem. Rev.* **2000**, *100*, 1169–1203.
3. D. Vogt, In Applied Homogeneous Catalysis with Organometallic Compounds; Cornils, B. Herrmann, W. A., Eds.; VCH: Weinheim, **2002**, Vol. 1, pp 240–253.
4. A. M. Al-Jarallah, J. A. Anabtawi, M. A. B. Siddiqui, A. M. Aitani, Al-Sa'doun, *Catal. Today* **1992**, *14*, 1–121.
5. J. Skupinska, *Chem. Rev.* **1991**, *91*, 613–648. (b) G. J. P. Britovsek, V. C. Gibson, D. F. Wass, *Angew. Chem. Int. Ed.* **1999**, *38*, 428–447.
6. (a) W. Keim, F. H. Kowaldt, R. Goddard, C. Kruger, *Angew. Chem.* **1978**, *90*, 493–494; *Angew. Chem., Int. Ed. Engl.* **1978**, *17*, 466–468. (b) W. Keim, A. Behr, B. Limbacker, C. Kruger, *Angew. Chem., Int. Ed. Engl.* **1983**, *22*, 503. (c) W. Keim, A. Behr, G. Kraus, *J. Organomet. Chem.* **1983**, *251*, 377–391. (d) P. Grenouillet, D. Neibecker, I. Tkatchenko, *J. Organomet. Chem.* **1983**, *243*, 213–222. (e) M. Peuckert, W. Keim, *Organometallics* **1983**, *2*, 594–597. (f) M. Peuckert, W. Keim, *J. Mol. Catal.* **1984**, *22*, 289–295. (g) W. Keim, *New J. Chem.* **1987**, *11*, 531–534. (h) U. Klabunde, S. D. Itten, *J. Mol. Catal.* **1987**, *41*, 123–134. (i) K. A. Ostoja Starzewski, J. Witte, *Angew. Chem.* **1987**, *99*, 76–77; *Angew. Chem., Int. Ed. Engl.* **1987**, *26*, 63–74. (j) W. Keim, *Angew. Chem.* **1990**, *102*, 251-260; *Angew. Chem., Int. Ed. Engl.* **1990**, *29*, 235–244. (k) K. Hirose, W. Keim, *J. Mol. Catal.* **1992**, *73*, 271–276. (l) W. Keim, *Macromol. Chem. Macromol. Symp.* **1993**, *66*, 225–230. (m) D. Matt, M. Huhn, J. Fischer, A. De Cian, W. Kläui, I. Tkatchenlo, M. C. Bonnet, *J. Chem. Soc., Dalton Trans.* **1993**, 1173–1178. (n) W. Keim, *New J. Chem.* **1994**, *18*, 93–96. (o) W. Keim, R. P. Schulz, *J. Mol. Catal.* **1994**, *92*, 21–33. (p) P. Braunstein, Y. Chauvin, S. Mecier, L. Saussine, A. De Cian, J. Fischer, *J. Chem. Soc., Chem. Commun.* **1994**, 2203–2204.
7. L. K. Johnson, C. M. Killian, M. Brookhart, *J. Am. Chem. Soc.* **1995**, *117*, 6414–6415.
8. S. Mecking, *Angew. Chem., Int. Ed. Engl.* **2001**, *40*, 534–540. (b) V. C. Gibson, S. K. Spitzmessor, *Chem. Rev.* **2003**, *103*, 283–315.
9. S. A. Svejda, M. Brookhart, *Organometallics* **1999**, *18*, 65–74. (b) C. M. Killian, L. K. Johnson, M. Brookhart, *Organometallics* **1997**, *16*, 2005–2007.
10. (a) T. V. Laine, M. Klinga, M. Leskelä, *Eur. J. Inorg. Chem.* **1999**, 959–964. (b) T. V. Laine, K. Lappalainen, J. Liimatta, E. Aitola, B. Löfgren, M. Leskelä, *Macromol. Rapid Commun.* **1999**, *20*, 487–491. (c) T. V. Laine, U. Piironen, K. Lappalainen, M. Klinga, E. Aitola, M. Leskelä, *J. Organomet. Chem.* **2000**, *606*, 112–114. (d) S. P. Meneghetti, P. J. Lutz, J. Kress, *Organometallics* **1999**, 18, 2734–2737. (e) A. Koppl, H. G. Alt, *J. Mol. Catal. A: Chem.* **2000**, *154*, 43–53. (e) M. Helldörfer, J. Backhaus, W. Milius, H. G. Alt, *J. Mol. Catal. A: Chem.* **2003**, *193*, 59–70. (f) M. Helldörfer, W. Milius, H. G. Alt, *J. Mol. Catal. A: Chem.* **2003**, *197*, 1–13.
11. C. M. Wang, S. Friedrich, T. R. Younkin, R. T. Li, R. H. Grubbs, D. A. Bansleben, M. W. Day, *Organometallics* **1998**, *17*, 3149–3151. (b) T. R. Younkin, E. F. Connor, J. I. Henderson, S. K. Friedrich, R. H. Grubbs, D. A. Bansleben, *Sicence* **2000**, *287*, 460–462.
12. F. M. Bauers, S. Mecking, *Angew. Chem., Int. Ed.* **2001**, *40*, 3020–3022. (b) F. M. Bauers, S. Mecking, *Macromolecules* **2001**, *34*, 1165–1171.

13. (a) C. Carlini, M. Marchionna, R. Patrini, A. M. R. Galletti, G. Sbrana, *Appl. Catal. A: Gen.* **2001**, *216*, 1–8. (b) C. Carlini, M. Marchionna, A. M. R. Galletti, G. Sbrana, *J. Mol. Catal. A: Chem.* **2001**, *169*, 79–88. (c) C. Carlini, M. Marchionna, A. M. R. Galletti, G. Sbrana, *Appl. Catal. A: Gen.* **2001**, *206*, 1–12. (d) C. Carlini, M. Isola, V. Liuzzo, A. M. R. Galletti, G. Sbrana, *Appl. Catal. A: Gen.* **2002**, *231*, 307–320.
14. Late Transition Metal Polymerization Catalysis; B. Rieger, L. Saunders Baugh, S. Kacker, S. Striegler, Eds.; Wiley-VCH: Weinheim, Germany, **2003**.
15. (a) P. Braunstein, M. D. Fryzuk, M. L. Dall, F. Naud, S. J. Rettig, F. Speiser, *J. Chem. Soc., Dalton Trans.* **2000**, 1067–1074. (b) P.-Y. Shi, Y.-H. Liu, S.-M. Peng, S.-T. Liu, *Organometallics* **2002**, *21*, 3203–3207.
16. (a) F. Speiser, P. Braunstein, L. Saussine, R. Welter, *Organometallics* **2004**, *23*, 2613–2624. (b) F. Speiser, P. Braunstein, L. Saussine, *Organometallics* **2004**, *23*, 2625–2632. (c) F. Speiser, P. Braunstein, L. Saussine, *Organometallics* **2004**, *23*, 2633–2640.
17. F. Speiser, P. Braunstein, L. Saussine, *Acc. Chem. Res.* **2005**, *38*, 784–793
18. F. Speiser, P. Braunstein, L. Saussine, *Inorg. Chem.* **2004**, *43*, 1649–1658.
19. S. A. Svejda, L. K. Johnson, M. Brookhart, *J. Am. Chem. Soc.* **1999**, *121*, 10634–10635.
20. (a) L. Deng, T. K. Woo, L. Cavallo, P. M. Margl, T. Ziegler, *J. Am. Chem. Soc.* **1997**, *119*, 6177–6186. (b) D. G. Musaev, R. D. J. Froese, M. Svensson, K. Morokuma, *J. Am. Chem. Soc.* **1997**, *119*, 367–374. (c) P. E. M. Siegbahn, S. Stromberg, K. Zetterberg, *Organometallics* **1996**, *15*, 5542–5550. (d) S. Strömberg, K. Zetterberg, P. E. M. Siegbahn, *J. Chem. Soc., Dalton Trans.* **1997**, 4147–4152.
21. (a) X. Tang, W.-H. Sun, T. Gao, J. Hou, J. Chen, W. Chen, *J. Organomet. Chem.* **2005**, *690*, 1570–1580. (b) W.-H. Sun, P. Hao, S. Zhang, Q. Shi, W. Zuo, X. Tang, *Organometallics* **2007**, *26*, 2439–2446. (c) Q.-Z. Yang, A. Kermagoret, M. Agostinho, O. Siri, P. Braunstein, *Organometallics* **2006**, *25*, 5518–5527.
22. F. Speiser, P. Braunstein, L. Saussine, *Dalton Trans.* **2004**, 1539–1545.
23. (a) J. Hou, W.-H. Sun, S. Zhang, H. Ma, Y. Deng, X. Lu, *Organometallics* **2006**, *25*, 236–244. (b) C. Zhang, W.-H. Sun, Z.-X. Wang, *Eur. J. Inorg. Chem.* **2006**, *23*, 4895–4902.
24. (a) D. M. Dawson, D. A. Walker, M. Thornton-Pett, M. Bochmann, *J. Chem. Soc., Dalton Trans.* **2000**, 459–466. (b) S. Al-Benna, M. J. Sarsfield, M. Thornton-Pett, D. Ormsby, P. J. Maddox, P. Bres, M. Bochmann, *J. Chem. Soc. Dalton Trans.* **2000**, 4247–4257. (c) F. A. Kunrath, R. F. de Souza, O. L. Casagrande Jr., N. R. Brooks, V. G. Young Jr., *Organometallics* **2003**, *22*, 4739–4743. (d) N. Ajellal, M. C. A. Kuhn, A. D. G.. Boff, M. Hörner, C. M. Thomas, J.-F. Carpentier, O. L. Casagrande Jr., *Organometallics* **2006**, *25*, 1213–1216.
25. (a) Y. Chen, P. Hao, W. Zuo, K. Gao, W.-H. Sun. *J. Organomet. Chem.* **2008**, *693*, 1829–1840. (b) S. Adewuyi, G. Li, S. Zhang, W. Wang, P. Hao, W.-H. Sun, N. Tang, J. Yi, *J. Organomet. Chem.* **2007**, *692*, 3532–3541. (c) W.-H. Sun, S. Zhang, S. Jie, W. Zhang, Y. Li, H. Ma, J. Chen, K. Wedeking, R. Fröhlich, *J. Organomet. Chem.* **2006**, *691*, 4196–4203. (d) M. Zhang, S. Zhang, P. Hao, S. Jie, W.-H. Sun, P. Li, X. Lu, *Eur. J. Inorg. Chem.* **2007**, 3816–3826. (e) W.-H. Sun, K. Wang, K. Wedeking, D. Zhang, S. Zhang, J. Cai, Y, Li. *Organometallics* **2007,** *26,* 4781–4790.
26. (a) B. L. Small, M. Brookhart, A. M. A. Bennett, *J. Am. Chem. Soc*. **1998**, *120*, 4049–4050. (b) B. L. Small, M. Brookhart, *J. Am. Chem. Soc*. **1998**, *120*, 7143–7144.
27. (a) G. J. P. Britovsek, V. C. Gibson, B. S. Kimberley, P. J. Maddox, S. J. McTavish, G. A. Solan, A. J. P. White, D. J. Williams, *Chem. Commun.* **1998**,

849–850. (b) G. J. P. Britovsek, M. Bruce, V. C. Gibson, B. S. Kimberley, P. J. Maddox, S. Mastroianni, S. J. McTavish, C. Redshaw, G. A. Solan, S. Stromberg, A. J. P. White, D. J. Williams, *J. Am. Chem. Soc.* **1999**, *121*, 8728–8740. (c) G. J. P. Britovsek, S. Mastroianni, G. A. Solan, S. P. D. Baugh, C. Redshaw, V. C. Gibson, A. J. P. White, D. J. Williams, M. R. J. Elsegood, *Chem. Eur. J.* **2000**, *6*, 2221–2231.

28. (a) C. Bianchini, G. Giambastiani, I. G. Rios, G. Mantovani, A. Meli, A. M. Segarra, *Coord. Chem. Rev.* **2006**, *250*, 1391–1418 and references therein. (b) V. C. Gibson, C. Redshaw, G. A. Solan. *Chem. Rev.* **2007**, *107*, 1745–1776 and references therein.
29. (a) R. Quijada, R. Rojas, G. Bazan, Z. J. A. Komon, R. S. Mauler, G. B. Galland, *Macromolecules* **2001**, *34*, 2411–2417. (b) G. B. Galland, R. Quijada, R. Rojas, G. Bazan, Z. J. A. Komon, *Macromolecules* **2002**, *35*, 339–345. (c) H. Wang, Z. Ma, Y. Ke, Y. Hu, *Polym. Int.* **2003**, *52*, 1546–1552.
30. (a) G. J. P. Britovsek, V. C. Gibson, O. D. Hoarau, S. K. Spitzmesser, A. J. P. White, D. J. Williams, *Inorg. Chem.* **2003**, *42*, 3454–3465. (b) G. J. P. Britovsek, V. C. Gibson, B. S. Kimberley, S. Mastroiannni, C. Redshaw, G. A. Solan, A. J. P. White, D. J. Williams, *J. Chem. Soc., Dalton Trans.* **2001**, 1639–1644. (c) S. Al-Benna, M. J. Sarsfield, M. Thornton-Pett, D. L. Ormsby, P. J. Maddox, P. Brès, M. Bochmann. *J. Chem. Soc., Dalton Trans.* **2000**, 4247–4257. (e) R. Cowdell, C. J. Davies, S. J. Hilton, J.-D. Maréchal, G. A. Solan, O. Thomas, J. Fawcett, *Dalton Trans.* **2004**, 3231–3240.
31. G. J. P. Britovsek, S. P. D. Baugh, O. Hoarau, V. C. Gibson, D. F. Wass, A. J. P. White, D. J. Williams, *Inorg. Chim. Acta* **2003**, *345*, 279–291. (b) L. Wang, W. -H. Sun, L. Han, H. Yang, Y. Hu, X. Jin, *J. Organomet. Chem.* **2002**, *658*, 62–70.
32. C. J. Davies, J. Fawcett, R. Shutt, G. A. Solan, *Dalton Trans.* **2005**, 2630–2640.
33. (a) C. Bianchini, D. Gatteschi, G. Giambastiani, I. G. Rios, A. Ienco, F. Laschi, C. Mealli, A. Meli, L. Sorace, A. Toti, F. Vizza. *Organometallics* **2007**, *26*, 726–739. (b) C. Bianchini, G. Giambastiani, G. Mantovani, A. Meli, D. Mimeau. *J. Organomet. Chem.* **2004**, *689*, 1356–1361. (c) C. Bianchini, G. Mantovani, A. Meli, F. Migliacci, F. Laschi. *Organometallics* **2003**, *22*, 2545–2547.
34. W.-H. Sun, S. Zhang, W. Zuo, *C. R. Chim.* **2008**, *10*, 307–316.
35. W.-H. Sun, P. Hao, S. Zhang, Q. Shi, W. Zuo, X. Tang. *Organometallics* **2007**, *26*, 2720–2734.
36. W.-H. Sun, P. Hao, G. Li, S. Zhang, W. Wang, J. Yi, M. Asma, N. Tang. *J. Organomet. Chem.* **2007**, *692*, 4506–4518.
37. M. Zhang, P. Hao, W. Zuo, S. Jie, W.-H. Sun. *J. Organomet. Chem.* **2008**, *693*, 483–491.
38. K. Wang, K. Wedeking, W. Zuo, D. Zhang, W.-H. Sun. *J. Organomet. Chem.* **2008**, *693*, 1073–1080.

Chapitre I

Complexes de nickel à pont bis-pyridinylimino et leur application en catalyse d'oligomerization et polymerization de l'éthylène

Abstract of Chapter I

A series of bridged bis(pyridinylimino) ligands were efficiently synthesized through the condensation reaction of 4,4'-methylene-bis(2,6-disubstituted aniline) with 2-pyridinecarboxaldehyde or 2-benzoylpyridine. They reacted with (DME)$NiBr_2$ to form dinuclear Ni(II) complexes. All resultant compounds were characterized by elemental analysis, IR spectra as well as the single-crystal X-ray diffraction to confirm their structures. Activated with methylaluminoxane (MAO), these nickel complexes showed considerably good activities for ethylene oligomerization and polymerization. Their catalytic activities and the properties of PEs obtained were depended on the arched environment of ligand and reaction conditions.

This chapter has been published. My contribution to this publication is the preparation of ligands, complexes and catalytic studies, and the manuscript, in collaboration with Dr. Tianzhu Zhang.

Bridged Bis-pyridinylimino Dinickel(II) Complexes: Syntheses, Characterization, Ethylene Oligomerization and Polymerization

J. Orangomet. Chem. **2005**, *690*, 1739–1749.

Suyun Jie,[a] Dongheng Zhang,[a] Tianzhu Zhang,[a] Wen-Hua Sun,[a,*] Jiutong Chen,[b] Qing Ren,[b] Dongbing Liu,[c] Gang Zheng[c] and Wei Chen[c,*]

[a] *Key Laboratory of Engineering Plastics, Institute of Chemistry, Chinese Academy of Sciences, Beijing 100080, China*

[b] *State Key Laboratory of Structural Chemistry, Fujian Institute of Research on the Structure of Matter, Chinese Academy of Sciences, Fuzhou 350002, China*

[c] *Polyolefin National Engineering and Research Center, Beijing Research Institute of Chemical Industry, China Petroleum & Chemical Corporation, Beijing, 100013, China*

Bridged Bis-pyridinylimino Dinickel(II) Complexes: Syntheses, Characterization, Ethylene Oligomerization and Polymerization

Introduction

In the past decade, homogeneous "non-metallocene" catalytic systems for the ethylene polymerization have drawn much attention, particularly late-transition metal derivatives [1]. The nickel complex was evidentially proved as good catalyst for ethylene oligomerization in SHOP process [2]. In 1995, the pioneering work by Brookhart's group on α-diimino nickel complexes for high-molecular-weight polyethylene broke out the silence of late-transition metal catalysts for polyolefins [3], and resulted in the remarkable increase of academic publications and patents about polyolefins obtained with Group VIII metal complexes as catalysts [1]. The various Schiff-base ligands such as N^N [3,4] and N^N^N [5] ligands have been extensively studied based on their easy preparation and the promising catalytic properties of their late-transition metal complexes. Involved in the exploring alternative nickel complexes as catalysts for ethylene activation, the bidentate and tridentate pyridinylimino derivatives are also generally considered in our group [6]. Pyridinylimino nickel complexes were observed as the centrosymmetric dimers with two bridging bromine atoms around each five-coordination nickel center [4] or the monomers with one acetonitrile molecule around five-coordination nickel center [7] in different solvents, all these nickel complexes showed good activities for ethylene polymerization. Investigating the scope of such nickel complexes and their catalytic activities, it would be interesting to synthesize the bridged bis(pyridinylimino) ligands and their nickel complexes. The 4,4'-methylene-bis(2,6-disubstituted anilines) were employed in the reaction with 2-pyridinecarboxaldehyde or 2-benzoylpyridine to form the bridged bis(pyridinylimino) ligands (**L1**–**L4**) and (**L5**–**L8**) [8], respectively. The bridged bis(pyridinylimino) ligands reacted with (DME)$NiBr_2$ to form their corresponding dinuclear nickel complexes (**C1**–**C8**). In the presence of methylaluminoxane (MAO), these nickel complexes showed considerably good activities for ethylene oligomerization and polymerization. Herein the synthesis and characterization of

for references, see page 32

ligands and nickel complexes were reported, and the nickel complexes for ethylene oligomerization and polymerization were carefully examined with various catalytic conditions.

Results and Discussion

Synthesis and characterization of the ligands and complexes

All the bridged bis(pyridinylimino) ligands were synthesized in the high yields by the condensation reaction. The ligands **L1**–**L4** were prepared by simply mixing 4,4'-methylene-bis(2,6-disubstituted aniline) and 2-pyridinecarboxaldehyde in ethanol with the catalytic amount of *p*-toluene sulfonic acid. On stirring for one day at room temperature, the products precipitated from the reaction mixture were isolated by filtration and purified by re-crystallization from their ethanol solutions (Scheme 1). All the four ligands were characterized by elemental analysis, IR and ^{1}H NMR spectra. In the synthesis of bulky **L5**–**L8**, it was necessary to remove the water formed in the reaction by using tetraethyl orthosilicate according to our previous work [8].

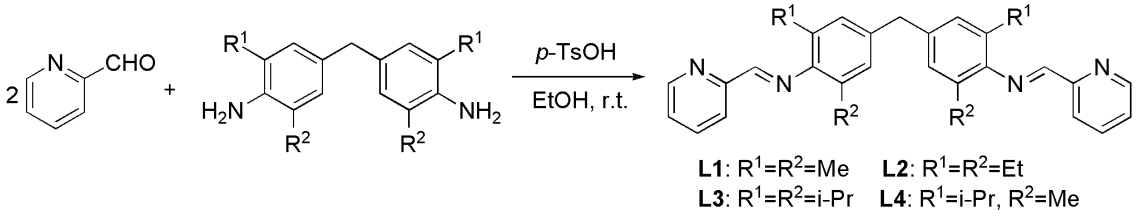

Scheme 1.
Synthesis of ligands **L1**–**L4**.

The bridged bis(pyridinylimino) ligands easily reacted with 2 equiv. of dibromo(1,2-dimethoxyethane)nickel(II) [(DME)$NiBr_2$] in CH_2Cl_2 to form the corresponding bridged bis(pyridinylimino) dinuclear nickel complexes (Scheme 2). The complexes **C1**–**C8** were characterized with elemental analysis and IR spectra. In the IR spectra of ligands **L1**–**L4** and **L5**–**L8**, strong and sharp peaks observed in the ranges of 1638–1643 cm^{-1} and 1627–1632 cm^{-1}, respectively, were ascribed to the stretching vibration of C=N, while the IR absorption bands of C=N appeared in the ranges of 1631–1632 cm^{-1} and 1590–1591 cm^{-1} for their corresponding nickel complexes **C1**–**C4** and **C5**–**C8**. The elemental analysis confirmed the components of ligands and nickel complexes. However, some elemental data of nickel complexes showed incorporation of solvent or water molecules due to the samples prepared by re-crystallization. The real structures of the ligands and nickel complexes were confirmed by the single-crystal X-ray diffraction analysis.

for references, see page 32

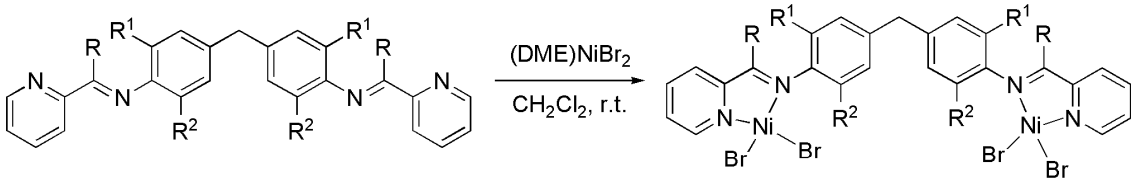

C1: R=H, R^1=R^2=Me **C2**: R=H, R^1=R^2=Et
C3: R=H, R^1=R^2=i-Pr **C4**: R=H, R^1=i-Pr, R^2=Me
C5: R=Ph, R^1=R^2=Me **C6**: R=Ph, R^1=R^2=Et
C7: R=Ph, R^1=R^2=i-Pr **C8**: R=Ph, R^1=i-Pr, R^2=Me

Scheme 2.
Synthesis of nickel complexes **C5**–**C8**.

Crystal structures

Single crystals suitable for the X-ray diffraction analysis were obtained by crystallization from the hexane solution of ligand **L4**, the acetonitrile solution of complex **C1** and slow diffusion of diethyl ether to the CH_3OH-DMF solution of complex **C7**, respectively.

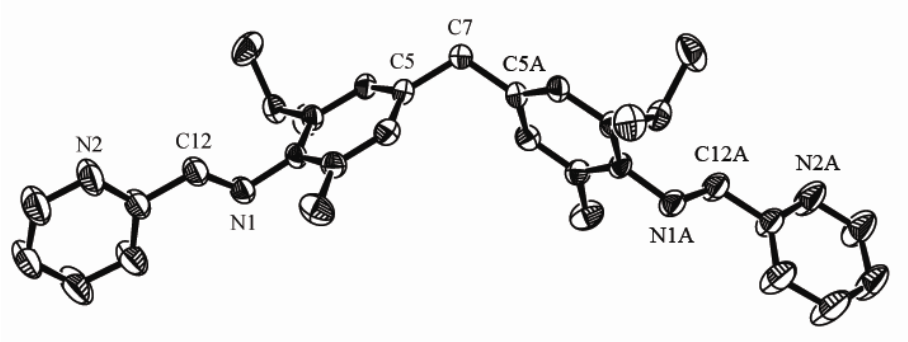

Fig. 1.
Crystal structure of **L4**. Displacement ellipsoids are drawn at the 30% probability level. Hydrogen atoms are omitted for clarity.

Table 1.
Selected bond lengths (Å) and angles (º) for **L4**

Bond lengths			
N(1)–C(12)	1.249(5)	N(2)–C(13)	1.325(5)
N(1)–C(2)	1.436(4)	N(2)–C(17)	1.338(6)
Bond angles			
C(12)–N(1)–C(2)	118.2(3)	C(13)–N(2)–C(17)	117.7(4)
C(3)–C(2)–N(1)	120.2(3)	C(1)–C(2)–N(1)	118.5(3)
N(1)–C(12)–C(13)	123.5(4)	N(2)–C(13)–C(12)	115.4(4)
N(2)–C(13)–C(14)	121.9(4)	N(2)–C(17)–C(16)	124.4(5)
C(5A)–C(7)–C(5)	114.3(4)		

The molecular structure of ligand **L4** is showed in Fig. 1 and the selected bond lengths and angles are listed in Table 1. The molecule is composed of two equivalent parts connected by atom C(7) with the bond angle C(5A)–C(7)–C(5) of 114.3(4)º. The distance between N(1) and C(12) (1.249(5) Å) is corresponding to the typical bond length of C=N [9]. The two phenyl ring planes, connected through C(7), are almost orthorhombic (the dihedral angle between the two rings is 87.9 º).

for references, see page 32

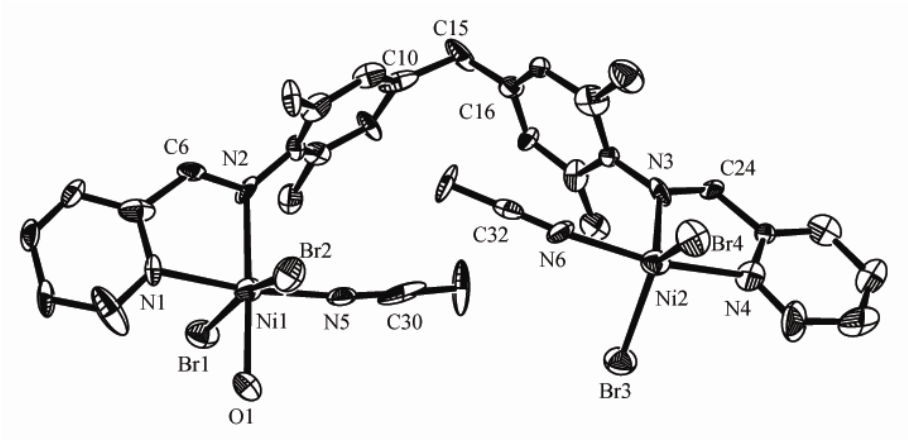

Fig. 2.
Molecular structure of **C1**. Displacement ellipsoids are drawn at the 30% probability level. Hydrogen atoms are omitted for clarity.

Table 2.
Selected bond lengths (Å) and angles (º) for **C1**

Bond lengths			
Br(1)–Ni(1)	2.592(4)	Ni(2)–N(3)	2.114(17)
Br(2)–Ni(1)	2.620(3)	N(1)–C(1)	1.31(3)
Br(3)–Ni(2)	2.410(3)	N(1)–C(5)	1.34(2)
Br(4)–Ni(2)	2.436(3)	N(2)–C(6)	1.29(2)
Ni(1)–N(5)	2.10(2)	N(2)–C(7)	1.42(2)
Ni(1)–O(1)	2.118(15)	N(3)–C(24)	1.21(2)
Ni(1)–N(1)	2.123(14)	N(3)–C(19)	1.41(2)
Ni(1)–N(2)	2.143(17)	N(4)–C(29)	1.33(3)
Ni(2)–N(6)	2.050(16)	N(4)–C(25)	1.36(2)
Ni(2)–N(4)	2.070(16)	N(6)–C(32)	1.107(19)
Bond angles			
N(5)–Ni(1)–O(1)	91.4(6)	N(2)–Ni(1)–Br(2)	95.6(4)
N(5)–Ni(1)–N(1)	172.3(7)	Br(1)–Ni(1)–Br(2)	163.18(14)
O(1)–Ni(1)–N(1)	94.6(6)	N(6)–Ni(2)–N(4)	166.8(7)
N(5)–Ni(1)–N(2)	92.7(7)	N(6)–Ni(2)–N(3)	89.5(6)
O(1)–Ni(1)–N(2)	174.0(6)	N(4)–Ni(2)–N(3)	77.8(7)
N(1)–Ni(1)–N(2)	81.1(6)	N(6)–Ni(2)–Br(3)	93.7(4)
N(5)–Ni(1)–Br(1)	95.2(5)	N(4)–Ni(2)–Br(3)	94.1(5)
O(1)–Ni(1)–Br(1)	83.7(4)	N(3)–Ni(2)–Br(3)	109.8(4)
N(1)–Ni(1)–Br(1)	90.3(4)	N(6)–Ni(2)–Br(4)	91.2(4)
N(2)–Ni(1)–Br(1)	100.3(4)	N(4)–Ni(2)–Br(4)	91.9(4)
N(5)–Ni(1)–Br(2)	89.4(5)	N(3)–Ni(2)–Br(4)	120.0(4)
O(1)–Ni(1)–Br(2)	80.0(4)	Br(3)–Ni(2)–Br(4)	129.95(14)
N(1)–Ni(1)–Br(2)	86.7(4)	C(16)–C(15)–C(10)	113.8(19)

The molecular structure of complex **C1** is shown in Fig. 2 and the selected bond lengths and angles are listed in Table 2. In complex **C1**, one ligand coordinates with two metal nickel(II) cations. The molecule is composed of two similar parts connected by C(15) and the C(10)–C(15)–C(16) bond angle is 113.8(19)º. The dihedral angle between the two aromatic rings connected by C(15) is 78.3º. In the molecule, one nickel (Ni2) is five-coordinated with one acetonitrile molecule on the axial coordination site and the other nickel (Ni1) is six-coordinated with one acetonitrile molecule and one H_2O molecule. Comparing the bond lengths of N–Ni bonds of two nickel atoms, Ni(1)–N(1)

for references, see page 32

(2.123(14) Å) to Ni(2)–N(4) (2.070(16) Å) and Ni(1)–N(5) (2.10(2) Å) to Ni(2)–N(6) (2.050(16) Å), they are relatively longer for nitrogen atoms bonding with Ni1 due to the coordinated water molecule. However, Ni(1)–N(2) (2.143(17) Å) to Ni(2)–N(3) (2.114(17) Å), their bond lengths are the approximately same for the nitrogen atoms of imino groups to two nickel atoms, and there are slight effects on N=C bonds, N(2)–C(6) (1.29(2) Å) to N(3)–C(24) (1.21(2) Å). In the structure, the geometry around Ni(2) is slightly distorted trigonal bipyramidal with the equatorial angles ranging from 109.8(4)º to 129.95(14)º and the trans-axial angle of the N(6)–Ni(2)–N(4) is 166.8(7)º, while the geometry around Ni(1) is slightly distorted octahedronal.

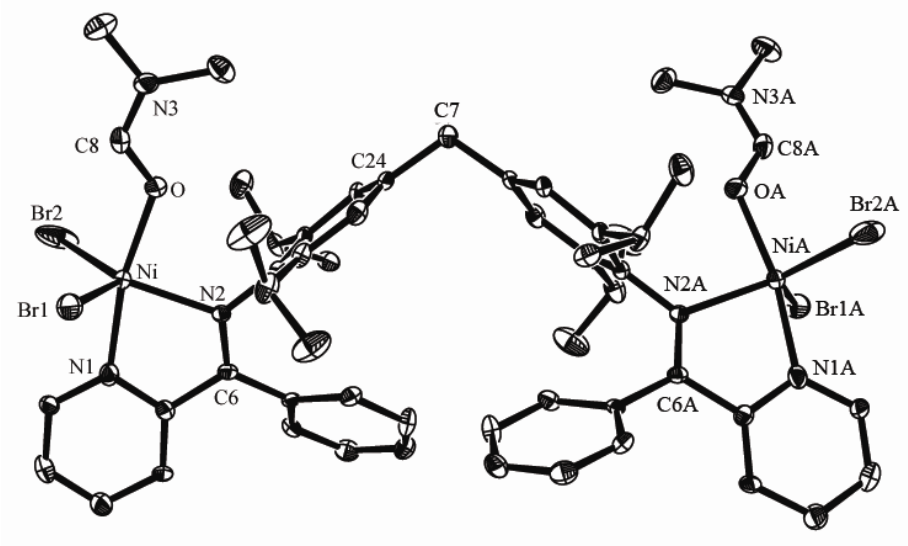

Fig. 3.
Molecular structure of **C7**. Displacement ellipsoids are drawn at the 30% probability level. Hydrogen atoms are omitted for clarity.

Table 3.
Selected bond lengths (Å) and angles (º) for **C7**

Bond lengths			
Ni–O	2.026(4)	O–C(8)	1.269(7)
Ni–N(1)	2.033(5)	N(1)–C(1)	1.352(7)
Ni–N(2)	2.076(4)	N(1)–C(5)	1.358(7)
Ni–Br(2)	2.4323(16)	N(2)–C(6)	1.310(7)
Ni–Br(1)	2.4538(17)	N(2)–C(21)	1.425(6)
Bond angles			
O–Ni–N(1)	168.59(17)	Br(2)–Ni–Br(1)	122.01(6)
O–Ni–N(2)	90.11(16)	C(1)–N(1)–Ni	125.4(4)
N(1)–Ni–N(2)	78.60(17)	C(5)–N(1)–Ni	116.7(3)
O–Ni–Br(2)	94.83(12)	C(6)–N(2)–C(21)	121.4(4)
N(1)–Ni–Br(2)	90.66(13)	C(6)–N(2)–Ni	114.9(3)
N(2)–Ni–Br(2)	126.52(11)	C(21)–N(2)–Ni	122.1(3)
O–Ni–Br(1)	92.90(12)	N(2)–C(6)–C(11)	125.7(4)
N(1)–Ni–Br(1)	92.66(13)	C(22)–C(21)–N(2)	121.0(4)
N(2)–Ni–Br(1)	110.81(11)	C(24A)–C(7)–C(24)	110.2(6)

The molecular structure of complex **C7** is shown in Fig. 3 and the selected bond lengths and angles are listed in Table 3. It can be seen from Fig. 3 that the complex **C7**

for references, see page 32

is composed of the two equivalent parts, in which two phenyl ring planes are connected by atom C(7) with a dihedral angle of 81.7º, and the bond angle C(24A)–C(7)–C(24) is 110.2(6)º. In this molecule, one ligand also coordinates with two nickel(II) cations. Each nickel(II) cation is five-coordinated with one DMF molecule. The X-ray structure shows that the geometry around nickel(II) is slightly distorted trigonal bipyramidal with one DMF molecule on the axial coordination site, in which Br1, Br2 and N2 compose an equatorial plane along with two atoms of N(1) and O occupying the two axial coordination sites, respectively. The nickel is slightly deviated from the triangular plane by –0.0809 Å.

It should be addressed about the previous works of using bridged bis(pyridinylimino) ligands that the nickel analogues reported by Hannon showed a pseudo-octahedral geometry due to three ligands coordinating with two nickel cations [10]. In addition, their silver analogues were also investigated [8,11]. The variation of their coordination was attributed to the bulk of ligands and it is necessary of the steric effects on enforcing the catalytic activity of the nickel complexes [3]. In our concern, the bridged substituted bis(pyridinylimino) ligands were needed, and their preparations were relatively difficult and lower yield of the 4,4'-methylene-bis(2,6-disubstituted aniline) than 4,4'-methylene-di-aniline. Therefore the reagents removing the resultant water are necessary in the reaction with 2-benzoylpyridine for the desired bulky bridged bis(pyridinylimino) ligands [8].

Ethylene oligomerization and polymerization

The catalyst precursor **C1**–**C8** could be activated for ethylene oligomerization and polymerization with methylaluminoxane (MAO). The results with one atmosphere of ethylene were summarized in Tables 4. The catalytic system of **C2** was typically investigated through varying reaction conditions, such as the molar ratio of cocatalyst (MAO) to nickel complex (Al/Ni), reaction temperature, reaction period and the pressure of ethylene, for the optimum.

(i) Effects of reaction temperature and Al/Ni molar ratio on catalyst activity

With the fixed Al/Ni molar ratio of 1000:1, the reaction temperature significantly affected on the catalytic activity, and the good polymerization activity was obtained at 0 °C (entry 2, Table 4). Along with elevating reaction temperature in the range of –10 °C to 40 °C, the polymerization activity significantly declined, while the amount of oligomers were increased. Up to 60 °C, only trace of polymer was obtained, in addition, the oligomerization activity was also lowered to 42.8 kg mol^{-1}(Ni) h^{-1} (entry 5, Table 4).

for references, see page 32

Elevating the reaction temperature speeds up combined catalytic reactions of oligomerization and polymerization, however, further increasing reaction temperature results in lower catalytic activities due to the lower solubility of ethylene and deactivation of some active centers [6a].

The variation of Al/Ni molar ratio in catalytic system of **C2** was explored at 0 °C. At the Al/Ni molar ratio of 100:1, only oligomer C_4 was formed with lower activity (entry 8, Table 4). When the Al/Ni molar ratio was further enhanced, the polymerization activity efficiently increased. At the Al/Ni molar ratio of 2000, the catalytic system displayed the higher polymerization activity of 712 kg mol^{-1}(Ni) h^{-1} (entry 13, Table 4).

Table 4.
The ethylene activation with complexes **C1**–**C8** at 1 atm [a]

Entry	Cat.	Al/Ni	T (°C)[b]	Olig-		Poly-		
				A_o[c]	A_p[c]	T_m[d]	M_w[e]	M_w/M_n[e]
1	**C2**	1000	–10	32.5	48.4	n.d.[f]	n.d.	n.d.
2	**C2**	1000	0	48.4	334	124.3, 110.7[i]	8 204	3.66
3	**C2**	1000	20	72.6	177	wax	n.d.	n.d.
4	**C2**	1000	40	122	25.4	wax-oil	n.d.	n.d.
5	**C2**	1000	60	42.8	trace	-	-	-
6[g]	**C2**	1000	0	16.6	324	123.8, 109.0[i]	n.d.	n.d.
7[h]	**C2**	1000	0	9.9	260	124.6, 109.1[i]	n.d.	n.d.
8	**C2**	100	0	41.3	-	-	-	-
9	**C2**	250	0	45.0	4.2	n.d.	n.d.	n.d.
10	**C2**	500	0	38.9	180	125.2, 116.2[i]	n.d.	n.d.
11	**C2**	750	0	13.3	290	124.1, 111.1[i]	n.d.	n.d.
12	**C2**	1500	0	22.1	372	122.6, 105.4[i]	n.d.	n.d.
13	**C2**	2000	0	39.1	712	124.6, 96.4[i]	n.d.	n.d.
14	**C1**	1000	0	13.6	256	124.5, 113.6[i]	7 864	5.28
15	**C3**	1000	0	9.4	638	122.0, 92.2[i]	3 648	3.42
16	**C4**	1000	0	40.2	280	124.4, 108.2[i]	7 381	5.64
17	**C3**	2000	0	108	792	wax	1 621	2.04
18	**C5**	1000	0	56.0	73.8	wax	n.d.	n.d.
19	**C6**	1000	0	49.9	2.60	wax	n.d.	n.d.
20	**C7**	1000	0	60.3	25.2	wax	n.d.	n.d.
21	**C8**	1000	0	72.0	12.8	wax	n.d.	n.d.

[a] Reaction conditions: cat.: 2.5 μmol; solvent: toluene (30 mL); reaction time: 0.5 h; ethylene pressure: 1 atm. [b] Reaction temperature. [c] Activity: in units of kg mol^{-1}(Ni) h^{-1}. [d] T_m values were determined by DSC with the second heat curves. [e] M_w and M_w/M_n values were determined by GPC. [f] Not determined. [g] Reaction time: 1 h. [h] Reaction time: 2 h. [i] Broad melting peak.

(ii) Lifetime of the active catalytic species

The lifetime of a catalyst is one significant factor in the industrial consideration. The effect of reaction time on catalytic activity was studied using **C2**/MAO system at the Al/Ni molar ratio of 1000:1 and 0 °C. The polymerization activity slightly decreased with the reaction time from 0.5 h to 2 h (compare entry 6–7 and 2, Table 4). The active species of **C2** were prolonged somehow during the catalytic reaction; however, it was often reported for nickel catalytic species to be deactivated as time going.

for references, see page 32

(iii) Effects of the ligand environment on the catalytic performance

To compare the catalytic results of the analogues as **C1**, **C3** and **C4** at the Al/Ni (1000:1) and 0 °C, **C3** containing the ligand with isopropyl substituents performed the highest polymerization activity (entry 16, Table 4). According to the better polymerization activity of **C2** (entry 13, Table 4) with the Al/Ni (2000:1) at 0 °C, as expected, the polymerization activity of **C3** was improved to 792 kg mol^{-1}(Ni) h^{-1} (entry 17, Table 4). Based on those data, the catalytic activity of the nickel complex is greatly affected by the arched environment of corresponding ligand, and the bulkier substituents, the higher catalytic activity [3].

In addition, to verify the role of the R substituent in the imino-C of the ligands on the catalytic performances, the complexes **C5**–**C8** bearing phenyl on carbon were also studied for ethylene oligomerization and polymerization. Under the same reaction conditions, the complexes **C5**–**C8** displayed the lower polymerization activities and the PEs obtained were wax-like (entry 18-21, Table 4). Though the bulkier group is recognized to increase the catalytic activity of late-transition metal complexes, the conjugated system with phenyl substituent decrease the net charge of the active metal center and reduced its activity as the final result [12].

(iv) Effects of ethylene pressure on the catalyst performance

Table 5.
The ethylene activation with complexes **C1**–**C8** at 10 atm [a]

Entry	Cat.	Al/Ni	Olig-	Poly-			
			A_o [b]	A_p [b]	T_m [c]	M_w [d]	M_w/M_n [d]
1	**C1**	894	85.2	2135	127.0, 121.6[e]	55 984	18.09
2	**C2**	927	328	874	125.5, 119.4[e]	15 405	9.49
3	**C3**	1000	55.1	2830	124.8, 116.7[e]	7 261	3.43
4	**C4**	927	153	1808	125.5, 118.3[e]	13 612	6.60
5	**C5**	1000	127	954	135.4, 128.3	271 625	45.79
6	**C6**	1000	56.7	1104	124.9, 105.6[e]	14 045	4.58
7	**C7**	1000	93.6	916	85.3[e]	4 531	2.20
8	**C8**	1000	57.2	2454	126.1, 104.8[e]	15 023	4.89

[a] Reaction conditions: cat: 10 μmol; solvent: toluene (1000 mL); the Al/Ni molar ratio: 1000; reaction temperature: 20 °C; reaction time: 1 h; ethylene pressure: 10 atm. [b] Activity: in units of kg mol^{-1}(Ni) h^{-1}. [c] T_m values were determined by DSC with the second heat curves. [d] M_w and M_w/M_n values were determined by GPC. [e] Broad melting peak.

The catalytic reaction was carried out at 10 atm of ethylene pressure and all nickel catalysts showed much better catalytic activity (Table 5). In the system of **C3**/MAO, the polymerization activity was obtained as high as 2830 kg mol^{-1}(Ni) h^{-1}, and the resultant polyethylene absolutely predominated (entry 3, Table 5). For complexes **C5**–**C8**/MAO, it was very clear that the ethylene pressure largely affected the catalytic performance

for references, see page 32

(entry 5–8, Table 5). At 10 atm of ethylene pressure, the PEs obtained became powder and the complex **C8** displayed higher polymerization activity (entry 8, Table 5). When the complex **C7** was used, however, lower polymerization activity was observed (entry 7, Table 5). Catalyst **C7** bearing the bulkier isopropyl substituents in the *orthro*-positions of imino N-aryl ring probably limited the insertion ability of ethylene and ethylene cannot easily contact with the cationic active centers in the catalytic system, so the polymerization activity decreased.

As a matter of fact, it is common for the late-transition metal catalytic system to carry out catalytic reaction of ethylene oligomerization and polymerization at the same time. With different views, major products of polyethylene or oligomers have been focused in most publications. In the dinuclear nickel complexes discussed herein, some catalytic systems gave good selectivity for ethylene polymerization with very low proportion of oligomers.

(v) Characterization of Polyethylene

The obtained PE samples showed intense bands at about 2920 cm^{-1} ($\nu_{as}CH_2$) and 2851 cm^{-1} (ν_sCH_2). Moreover, two single peaks were present around 1469 cm^{-1} and 721 cm^{-1}, respectively, assigned to scissoring and rocking vibrations in the solid state of sequential methylene groups. And a weak peak was found in 1374–1376 cm^{-1} due to the branched methyl symmetrical deformation vibration [13,14]. There were additional bands in characteristic presence of the double bond: a weak peak at 1642–1648 cm^{-1} attributed to stretching vibration absorption band of C=C and similar characteristic peaks of polyethylene obtained by its monomer nickel catalysts [4b].

The melting points (T_m) of resultant PEs were determined by differential scanning calorimetry analysis (DSC). The melting points were varied with the different catalysts and various catalytic conditions in Table 4 and 5. Examining the data of PEs by using complex **C2** at 1 atm of ethylene and 0 °C, the variation of the Al/Ni molar ratio gave slightly different melting points with two peaks. However, there was a great effect of reaction temperature. At either 1 atm or 10 atm of ethylene pressure, DSC curves gave two melting peaks. The results suggested that the interaction between two metals possibly created more than one kind of active species during the polymerization.

The molecular weights (M_w) and molecular weight distributions (M_w/M_n) of the obtained PEs were measured by GPC analysis. The relatively wide molecular weight distributions were different from those of PEs obtained using pyridinylimino nickel(II) complexes reported by Laine's group [4c] (see Fig. 4–6). In the catalytic system of

for references, see page 32

C3/MAO, when the Al/Ni molar ratio was changed from 1000:1 to 2000:1, both M_w and M_w/M_n became lower (compare entry 15 with 17, Table 4). Higher Al/Ni molar ratio increased the chain transfer reaction to MAO and resulted in lower polymer molecular weight. The narrow molecular distribution could be reasoned as a good ratio of cocatalyst to activate the nickel catalyst and produce the catalytic centers. The effect of ethylene pressure was very clear that the M_w significantly increased and M_w/M_n became broader when the pressure enhanced from 1 atm to 10 atm (compare Table 4 with 5). For complex **C5**, the highest molecular weight and broadest molecular weight distribution were achieved and as shown by the GPC traces in Fig. 6, the PE sample obtained displayed bimodal molecular weight distribution.

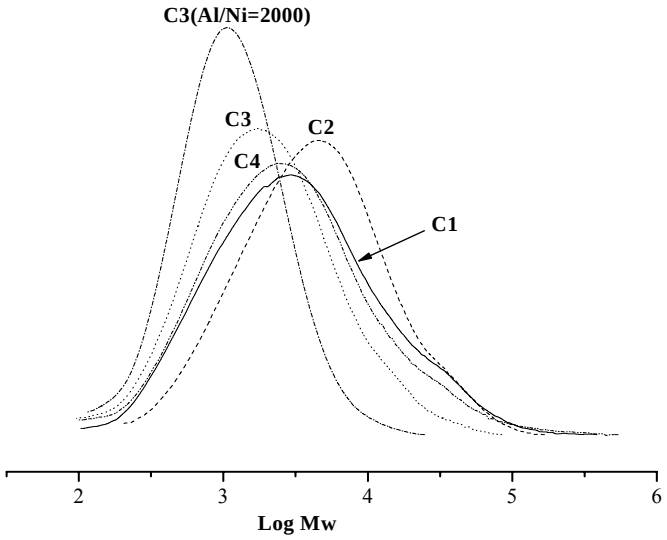

Fig. 4.
GPC traces of PE samples obtained by entries 2 and 14–17 in Table 4.

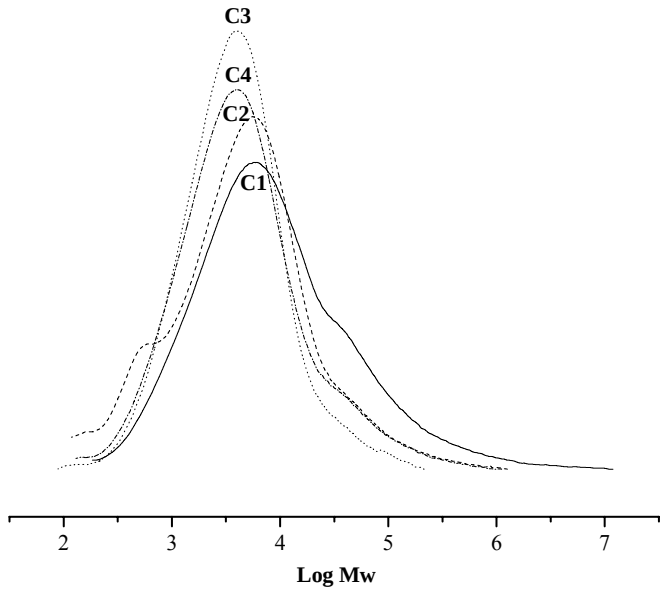

Fig. 5.
GPC traces of PE samples obtained by entries 1–4 in Table 5.

for references, see page 32

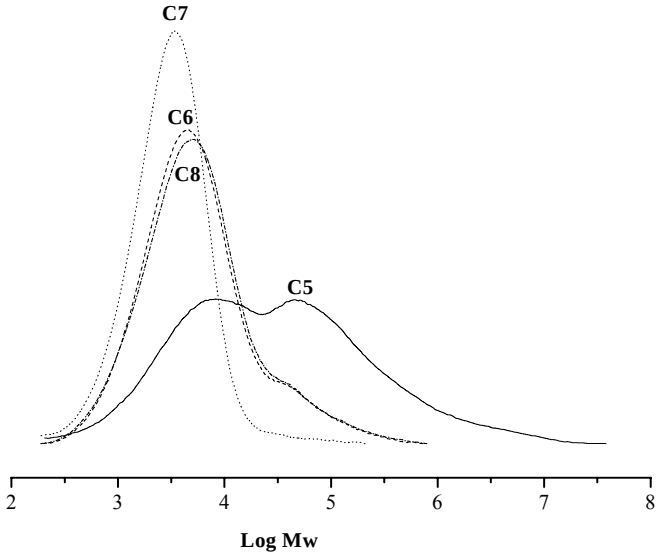

Fig. 6.
GPC traces of PE samples obtained by entries 5–8 in Table 5.

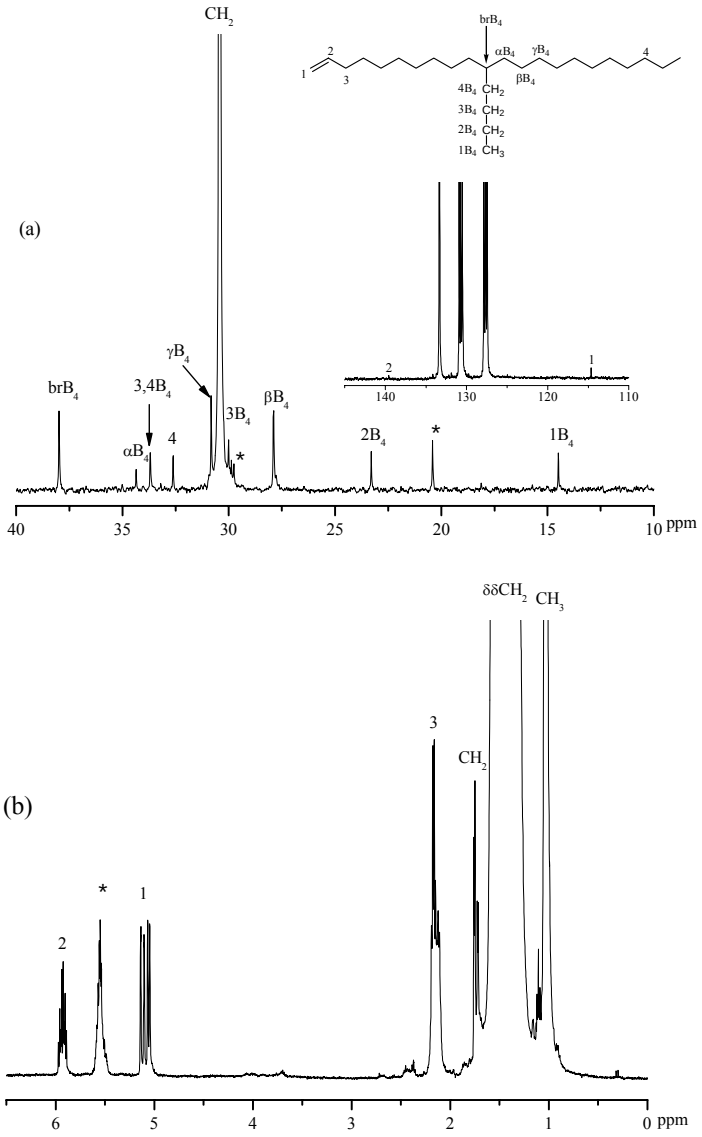

Fig. 7.
NMR spectra of polyethylene obtained by entry 3 in Table 5. (a) ^{13}C NMR; (b) ^{1}H NMR.

for references, see page 32

The ^{1}H, ^{13}C NMR spectra were recorded with the PE sample dissolved in *o*-dichlorobenzene-d_4 (see Fig. 7). The ^{13}C NMR spectra of the PE obtained by complex **C3** at 10 atm of ethylene pressure (entry 3, Table 5) indicated that the branched polyethylene with main butyl branch formed and the extent of branching was counted equal to 5 branches per 1000 carbon atoms according to the calculation method reported [15]. The single peaks at δ 114.64 and 139.58 ppm showed the property of vinyl-unsaturated chain end. The assignments were determined according to the literatures [15, 16] and the nomenclature of Usami and Takayama [17] for isolated branches was used.

Experimental

General

All manipulations involving air- and/or moisture-sensitive compounds were carried out under an atmosphere of nitrogen using standard Schlenk techniques. Solvents were refluxed over the appropriate drying reagents and distilled under nitrogen prior to use. IR spectra were recorded on a Perkin-Elmer System FT-IR 2000 spectrometer using KBr disc. ^{1}H NMR spectra were recorded on a Bruker DMX 300 MHz instrument at ambient temperature using TMS as the internal standard. Mass spectra were measured on a Bruker BIFLEX^{TM} III MALDI-TOF. Melting points were measured with a digital electrothermal apparatus without calibration. Elemental analyses were carried out using Flash EA1112 microanalyzer. GC analyses were performed with a Carlo Erba Strumentazione gas chromatograph equipped with a flame ionization detector and a 30 m (0.25 mm i.d., 0.25 μm film thickness) DM-1 silica capillary column. ^{1}H and ^{13}C NMR spectra of the PE sample were recorded on a Bruker DMX 400 MHz instrument at 135 °C in *o*-dichlorobenzene-d_4 using TMS as the internal standard. The molecular weight and the molecular weight distribution of the PEs were determined by a PL-GPC220 instrument at 150 °C with 1,2,4-trichlorobenzene as the eluent. Melting points of the PEs were obtained on a Perkin-Elmer DSC-7 instrument. The instrument was initially calibrated for the melting point of an indium standard at a heating rate of 10 °C/min. (DME)$NiBr_2$ was purchased from Alfa Aesar. Methylaluminoxane (MAO, 1.4 mol L^{-1} in toluene) was purchased from Albemarle Corp (USA). All other chemicals were obtained from commercial sources unless stated otherwise.

Preparation of the ligands (L1–L4)

The ligands (**L1**–**L4**) were prepared by condensing corresponding

for references, see page 32

4,4'-methylene-bis(2,6-bissubstituated-aniline) with 2-pyridinecarboxaldehyde in ethanol. Typically, 4,4'-Methylene-*N,N'*-(2-pyridinylmethylene)-bis(2,6-dimethylanil) (**L1**) was synthesized by mixing 4,4'-methylene-bis(2,6-dimethylaniline) (0.631 g, 2.5 mmol) and 2-pyridinecarboxaldehyde (0.614 g, 5.7 mmol) in 10 ml ethanol (95%) along with the catalytic amount of p-toluene sulfonic acid. The reaction mixture was stirred for one day at room temperature, and resulting yellow precipitate was isolated by filtration and re-crystallized from its ethanol solution to give **L1** in 63.3% yield. m.p. 174–176 °C. FT-IR (cm^{-1}): 3435, 2967, 2915, 1643, 1586, 1567, 1479, 1463, 1377, 1202, 1146, 874, 845, 778, 743. ^{1}H NMR (δ, ppm): 8.69 (d, 2H), 8.33 (s, 2H, C*H*=N), 8.27 (d, 2H), 7.82 (t, 2H), 7.39 (m, 2H), 6.93 (s, 4H), 3.84 (s, 2H, CH_2), 2.14 (t, 12H, PhCH_3). Anal. Calc. for $C_{29}H_{28}N_4$: C, 80.52; H, 6.52; N, 12.95. Found: C, 80.63; H, 6.64; N, 12.72 %.

4,4'-Methylene-*N,N'*-(2-pyridinylmethylene)-bis(2,6-diethyl-anil) (**L2**) was prepared as yellow crystals in 61.0% yield. m.p. 117–119 °C. FT-IR (cm^{-1}): 3054, 2966, 2932, 2872, 1640, 1584, 1569, 1468, 1439, 1199, 1145, 993, 880, 776. ^{1}H NMR (δ, ppm): 8.72 (t, 2H), 8.36 (s, 2H, C*H*=N), 8.28 (d, 2H), 7.85 (t, 2H), 7.41 (m, 2H), 6.97 (s, 4H), 3.95 (s, 2H, CH_2), 2.51 (m, 8H, CH_2Me), 1.13 (t, 12H, CH_3). Anal. Calc. for $C_{33}H_{36}N_4$: C, 81.11; H, 7.43; N, 11.47. Found: C, 80.99; H, 7.45; N, 11.23 %.

4,4'-Methylene-*N,N'*-(2-pyridinylmethylene)-bis(2,6-diisopropyl-anil) (**L3**) was prepared as yellow crystals in 76.0% yield. m.p. 163–164 °C. FT-IR (cm^{-1}): 3433, 2961, 2929, 2868, 1638, 1585, 1568, 1468, 1439, 1120, 1167, 992, 875, 780. ^{1}H NMR (δ, ppm): 8.73 (d, 2H), 8.32 (s, 2H, C*H*=N), 8.27 (d, 2H), 7.85 (t, 2H), 7.42 (m, 2H), 7.02 (s, 4H), 4.02 (s, 2H, CH_2), 2.96 (m, 2H, C*H*Me$_2$), 1.15 (d, 24H, i-Pr-*H*). Anal. Calc. for $C_{37}H_{44}N_4$: C, 81.57; H, 8.14; N, 10.28. Found: C, 81.28; H, 8.17; N, 10.15 %.

4,4'-Methylene-*N,N'*-(2-pyridinylmethylene)-bis(2-isopropy-6-methyl-anil) (**L4**) was prepared as yellow crystals in 58.7% yield. m.p. 152–154 °C. FT-IR (cm^{-1}): 3433, 2959, 2927, 2869, 1639, 1586, 1569, 1473, 1438, 1201, 1170, 1133, 887, 865, 774. ^{1}H NMR (δ, ppm): 8.72 (d, 2H), 8.34 (s, 2H, C*H*=N), 8.28 (d, 2H), 7.85 (t, 2H), 7.41 (m, 2H), 7.04 (s, 2H), 6.92 (s, 2H), 3.93 (s, 2H, CH_2), 3.03 (m, 2H, C*H*Me$_2$), 2.13 (t, 6H, PhCH_3), 1.17 (d, 12H, i-Pr-*H*). Anal. Calc. for $C_{33}H_{36}N_4$: C, 81.11; H, 7.43; N, 11.47. Found: C, 80.73; H, 7.55; N, 11.29 %.

Preparation of the nickel(II) complexes

The nickel complex (**C1**) was obtained in mixing ligand **L1** (0.35 g, 0.8 mmol) and (DME)$NiBr_2$ (0.50 g, 1.6 mmol) in 20 ml dichloromethane using the Schlenk technique,

for references, see page 32

and the reaction mixture was stirred for 24 hrs at room temperature. The resulting precipitate was filtered, washed with diethyl ether and dried in vacuum to form **C1** as a yellow powder in 93.5% yield. FT-IR (cm^{-1}): 3353, 2965, 2923, 1632, 1598, 1482, 1447, 1305, 1199, 1145, 1024, 774. Anal. Calc. for $C_{29}H_{28}Br_4N_4Ni_2 \cdot CH_2Cl_2$: C, 37.75; H, 3.17; N, 5.87. Found: C, 38.02; H, 3.67; N, 5.50%.

In a similar manner, the complex **C2** to **C8** were prepared from the ligand **L2** and (DME)$NiBr_2$. **C2** is a yellow powder in 98.1 % yield. FT-IR (cm^{-1}): 3371, 2965, 1630, 1597, 1459, 1305, 1197, 1142, 1023, 911, 774. Anal. Calc. for $C_{33}H_{36}Br_4N_4Ni_2$: C, 42.82; H, 3.92; N, 6.05. Found: C, 42.61; H, 4.37; N, 5.96 %.

C3 is a yellow powder in 88.5% yield. FT-IR (cm^{-1}): 3372, 2965, 2869, 1631, 1598, 1464, 1446, 1363, 1305, 1198, 1163, 1118, 1023, 910, 775. Anal. Calc. for $C_{37}H_{44}Br_4N_4Ni_2$: C, 45.26; H, 4.52; N, 5.71. Found: C, 45.82; H, 4.97; N 5.54 %.

C4 is a yellow powder in 90.7% yield. FT-IR (cm^{-1}): 3347, 2965, 2870, 1632, 1599, 1479, 1447, 1306, 1199, 1161, 1131, 1024, 774. Anal. Calc. for $C_{33}H_{36}Br_4N_4Ni_2 \cdot 2H_2O$: C, 41.21; H, 4.19; N, 5.83. Found: C, 41.54; H, 4.34; N, 5.55 %.

C5 is a brown powder in 69.0% yield. FT-IR (cm^{-1}): 3371, 2019, 1590, 1475, 1443, 1381, 1329, 1262, 1217, 1176, 1135, 1108, 1026, 985, 852, 800, 752, 704. MALDI-TOF MS Calcd for $C_{41}H_{37}{}^{79}Br_2N_4Ni_2$ [M-2Br]: 859.8, Found: 860.2. Anal. Calc. for $C_{41}H_{36}Br_4N_4Ni_2 \cdot 2Et_2O$: C, 50.26; H, 4.79; N, 4.79. Found: C, 50.26; H, 4.89; N, 5.32%.

C6 is a brown powder in 66.0% yield. FT-IR (cm^{-1}): 3367, 2970, 2936, 2879, 2319, 1989, 1590, 1445, 1378, 1328, 1262, 1176, 1131, 1061, 1026, 984, 940, 882, 853, 801, 751, 703. MALDI-TOF MS Calcd for $C_{45}H_{45}{}^{79}Br_2N_4Ni_2$ [M-2Br]: 915.9, Found: 916.1. Anal. Calc. for $C_{45}H_{44}Br_4N_4Ni_2 \cdot 1.5Et_2O$: C, 51.47; H, 4.96; N, 4.71. Found: C, 51.01; H, 5.51; N, 4.88 %.

C7 is a brown powder in 60.0% yield. FT-IR (cm^{-1}): 3377, 2969, 2871, 2318, 1591, 1465, 1444, 1384, 1363, 1328, 1261, 1158, 1111, 1071, 1028, 985, 958, 799, 753, 703. MALDI-TOF MS Calcd for $C_{49}H_{53}{}^{79}Br_2N_4Ni_2$ [M-2Br]: 972.0, Found: 972.4. Anal. Calc. for $C_{49}H_{52}Br_4N_4Ni_2 \cdot Et_2O$: C, 52.64; H, 5.13; N, 4.64. Found: C, 52.76; H, 5.36; N, 4.67 %.

C8 is a brown powder in 80.0% yield. FT-IR (cm^{-1}): 3370, 2965, 2928, 2869, 2355, 2589, 1591, 1470, 1443, 1384, 1328, 1262, 1160, 1123, 1082, 1060, 1026, 984, 857, 800, 753, 703. MALDI-TOF MS Calcd for $C_{45}H_{45}{}^{79}Br_2N_4Ni_2$ [M-2Br]: 915.9, Found: 916.2. Anal. Calc. for $C_{45}H_{44}Br_4N_4Ni_2 \cdot 1.5Et_2O$: C, 51.47; H, 4.96; N, 4.71. Found: C, 51.68; H, 5.38; N, 4.64 %.

for references, see page 32

X-ray crystallography of L2, C1 and C7

Data sets were collected with a RIGAKU SMART CCD diffractometer with graphite monochromatic Mo-K_α radiation (λ=0.71073Å). Cell parameters were obtained by the global refinement of the positions of all collected reflections. Intensities were corrected for Lorentz and polarization effects and empirical absorption. The structures were solved by direct methods, and refined by full-matrix least-square on F^2. Each hydrogen atom was placed in a calculated position, and refined using a riding model. All non-hydrogen atoms were refined anisotropically. Structure solution and refinement were performed using Shelxl-97 package [18]. The crystal data and refinement parameters were summarized in Table 6.

Table 6.
Crystal data and structure refinement for **L4, C1** and **C7**

	L4	**C1**·2CH_3CN·H_2O	**C7**·2DMF
Empirical formula	$C_{33}H_{36}N_4$	$C_{29}H_{28}Br_4N_4Ni_2$·2CH_3CN·H_2O	$C_{49}H_{52}Br_4N_4Ni_2$·2DMF
Formula weight	488.66	969.74	1280.20
Crystal color	Yellow	Brown	Red
Temperature(K)	293(2)	293(2)	123.15
Crystal system	Monoclinic	Monoclinic	Orthorhombic
Space group	C 2/c	P 2(1)	F dd2
a (Å)	14.4681(7)	8.1176(16)	34.60(3)
b (Å)	9.5641(4)	13.245(3)	35.76(3)
c (Å)	21.7672(6)	16.774(3)	9.049(7)
α (º)	90	90	90
β (º)	99.846(2)	95.36(3)	90
γ (º)	90	90	90
Volume (Å^3)	2967.7(2)	1795.7(6)	11196(15)
Z	4	2	8
D_{calc} (Mg m^{-3})	1.094	1.794	1.519
μ (mm^{-1})	0.065	5.535	3.572
F(000)	1048	960	5200
Crystal size(mm)	0.46×0.40×0.36	0.20×0.20×0.06	0.45×0.18×0.15
θ range (º)	1.90–25.01	1.22–27.40	2.28–28.28
Limiting indices	–17 ≤ h ≤ 14, –7 ≤ k ≤ 11, –25 ≤ l ≤ 23	0 ≤ h ≤ 10, 0 ≤ k ≤ 17, –21 ≤ l ≤21	–38 ≤ h ≤46, –47 ≤ k ≤47, –12 ≤ l ≤12
Reflections collected	4543	4217	22907
Unique reflections	2593	4217	6845
Completeness to *θ* (%)	98.7 (θ = 25.01)	98.8 (θ = 27.40)	99.8 (θ = 28.28)
Data/restraints/ parameters	2593/0/241	4217/1/415	6845/1/312
Goodness-of-fit on F^2	1.145	0.873	1.005
R1	0.0873	0.0731	0.0432
wR2	0.2081	0.1246	0.1250
Largest diff peak and hole (e Å^{-3})	0.181, –0.222	0.629, –0.514	0.984, –0.884

Ethylene oligomerization and polymerization

Ethylene oligomerization and polymerization at 1 atm of ethylene pressure was carried out as follows: The catalyst precursor (nickel complex) was dissolved with

for references, see page 32

toluene in a Schlenk tube stirred with a magnetic stirrer under ethylene atmosphere (1 atm), and the reaction temperature was controlled by water bath. The reaction was initiated by adding the desired amount of methylaluminoxane (MAO). After the desired period of time, a small amount of the reaction solution was collected with a syringe, terminated by the addition of 5% aqueous hydrogen chloride, and the analysis by gas chromatography (GC) was carried out for determining the distribution of oligomers obtained. The residual solution was quenched with HCl-acidified ethanol (5%), its precipitated polyethylene was collected by filtration, washed with ethanol, dried in vacuum at 60 ºC until constant weight, weighed and finally characterized.

Ethylene oligomerization and polymerization at 10 atm of ethylene pressure was carried out in a 2000-mL autoclave stainless steel reactor equipped with a mechanical stirrer and a temperature controller. The desired amount of MAO, 10 ml toluene solution of nickel complex and 1000 ml of toluene were added to the reactor in this order under ethylene atmosphere. When being to the reaction temperature, ethylene with the desired pressure (10 atm) was introduced to start the reaction. After 1 h, the reaction was stopped. And then a small amount of the reaction solution was collected, terminated by the addition of 5% aqueous hydrogen chloride and then analyzed by gas chromatography (GC) for determining the distribution of oligomers obtained. Then the residual solution was quenched with HCl-acidified ethanol (5%). The precipitated polymer was collected by filtration, washed with ethanol, dried in vacuum at 60 ºC until constant weight, weighed and finally characterized.

Acknowledgement

We are grateful to the National Natural Science Foundation of China for financial supports under Grant No.20473099 and 20272062, National 863 Foundation (2002AA333060). This work was partly carried out in Polymer Chemistry Laboratory, Chinese Academy of Sciences and China-Petro-Chemical Corporation.

for references, see page 32

References

[1] (a) S.D. Ittle, L.K. Johnson, M. Brookhart, Chem. Rev. 103 (2000), 1169;
(b) V.C. Gibson, S.K. Spitzmessor, Chem. Rev. 103 (2003), 283;
(c) S. Mecking, Angew. Chem., Int. Ed. Engl. 40 (2001), 534.
[2] W. Keim, F.H. Kowalt, R. Goddard, C. Kriiger, Angew. Chem., Int Ed. Engl. 17 (1978), 466.
[3] L.K. Johnson, C.M. Killian, M. Brookhart, J. Am. Chem. Soc. 117 (1995), 6414.
[4] (a) T.V. Laine, M. Klinga, M. Leskelä, Eur. J. Inorg. Chem. (1999), 959;
(b) T.V. Laine, K. Lappalainen, J. Liimatta, E. Aitola, B. Löfgren, M. Leskelä, Macromol. Rapid Commun. 20 (1999), 487;
(c) T.V. Laine, U. Piironen, K. Lappalainen, M. Klinga, E. Aitola, M. Leskelä, J. Organomet. Chem. 606 (2000), 112.
[5] (a) B.L. Small, M. Brookhart, A.M.A. Bennett, J. Am. Chem. Soc. 120 (1998), 4049;
(b) G.J.P. Britovsek, V.C. Gibson, B.S. Kimberley, D.J. Williams, Chem. Commun. (1998), 849.
[6] (a) W.-H. Sun, Z. Li, H. Hu, B. Wu, H. Yang, N. Zhu, X. Leng, H. Wang, New J. Chem., 26 (2002), 1474;
(b) L. Wang, W.-H. Sun, L. Han, H. Yang, Y. Hu, X. Jin, J. Organomet. Chem. 658 (2002), 62;
(c) X. Tang, Y. Cui, W.-H. Sun, Z. Miao, S. Yan, Polym. Int., 53 (2004), 2155;
(d) C. Shao, W.-H. Sun, Z. Li, Y. Hu, L. Han, Cat. Commun., 3 (2002), 405.
[7] G.J.P. Britovsek, S.P.D. Baugh, C. Redshaw, O. Hoarau, V.C. Gibson, D.F. Wass, A.J.P. White, D.J. Williams, Inorganica Chimica Acta, 345 (2003), 279.
[8] W.-H. Sun, T. Zhang, L. Wang, Y. Chen, R. Froehlich, J. Organomet. Chem., 689 (2004), 43.
[9] D.R. Lide; CRC Handbook of chemistry and Physics, 73rd, 6-9 (1992-1993).
[10] (a) L. J. Childs, N. W. Alcock, M. J. Hannon, Angew. Chem. Int. Ed., 40 (2001), 1079;
(b) M. J. Hannon, C.L. Painting, A. Jackson, J. Hamblin, W. Errinton. Chem. Commun., (1997), 1807.
[11] M. J. Hannon, C.L. Painting, N. W. Alcock, Chem. Commun., (1999), 2023;
[12] T. Zhang, D. Guo, S. Jie, W.-H Sun, T. Li, X,.Yang, J Polym Sci Part A: Polym Chem., 42 (2004), 4765.
[13] T. Usami, S. Takayama, Polym. J., 16 (10) (1984), 731.
[14] C. Baker, W.F. Maddams, Makromol. Chem., 177 (1976), 437.
[15] G.B. Galland, R. Quijada, R. Rojas, G.C. Bazan, Z.J.A. Komon, Maromolecules, 35 (2002), 339.
[16] G.B. Galland, R.F. De Souza, R. S. Mauler, F.F. Nunes, Macromolecules, 32 (1999), 1620.
[17] T. Usami, S. Takayama, Macromolecules, 17 (1984), 1756.
[18] G.M. Sheldrick, SHELXTL-97, Program for the Refinement of Crystal Structures, University of Gottingen: Germany, 1997.

Chapitre II

Complexes 2-imino-1,10- phénanthrolinyl du fer et leur application en catalyse d'oligomerization de l' éthylène

Abstract of Chapter II

A series of iron complexes ligated by 2-imino-1,10-phenanthrolinyl ligands, $LFeCl_2$ (L = 2-(ArN=CR)-1,10-phen), were synthesized and sufficiently characterized by elemental and spectroscopic analysis along with X-ray diffraction analysis. Activated with methylaluminoxane (MAO) or modified methylaluminoxane (MMAO), these iron(II) complexes show high catalytic activities up to 8.95×10^7 g mol^{-1}(Fe) h^{-1} for ethylene oligomerization. The distribution of oligomers produced follows Schulz-Flory rules with high selectivity for α-olefins. Both the steric and electronic effects of coordinative ligands affect the catalytic activity and the properties of the catalytic products. The parameters of the reaction conditions were also investigated to explore the catalytic potentials of these complexes.

This chapter has been published. I participated in the exploration of synthetic methods, prepared most of ligands and complexes, carried out all the catalytic experiments and wrote the manuscript. This work has been done in collaboration with Shu Zhang, Dr. Wen Zhang and Yingxia Song.

Iron Complexes Bearing 2-Imino-1,10-phenanthrolinyl Ligands as Highly Active Catalysts for Ethylene Oligomerization

Organometallics **2006**, *25*, 666–677.

Wen-Hua Sun*, Suyun Jie, Shu Zhang, Wen Zhang, Yingxia Song, Hongwei Ma

Key Laboratory of Engineering Plastics, Institute of Chemistry, Chinese Academy of Sciences, Beijing 100080, China

Jiutong Chen

State Key Laboratory of Structural Chemistry, Fujian Institute of Research on the Structure of Matter, Chinese Academy of Sciences, Fuzhou 350002, China

Katrin Wedeking and Roland Fröhlich

Organisch-Chemisches Institut der Universität Münster, Corrensstr. 40, 48149 Münster, Germany

Iron Complexes Bearing 2-Imino-1,10-phenanthrolinyl Ligands as Highly Active Catalysts for Ethylene Oligomerization

Introduction

α-Olefins are major industrial reactants that are extensively used in the preparation of detergents, lubricants, plasticizers, oil field chemicals as well as monomers for copolymerization. The α-olefin industry's increasing demand for higher fractions has been growing at around 5% per year, and the oligomerization of ethylene is currently one of the major industrial processes for the production of α-olefins. α-Olefin production falls into two categories: the full range process of ethylene oligomerization with a range of C_4/C_6 up to $C_{20}+$ generated, and the deliberate dimerization and trimerization of ethylene. The selective dimerization reaction was first described in 1954 by Ziegler,[1] and later the selectivity was improved by modification of the catalysts and optimization of the reaction conditions.[2] Phillips has developed chromium-based catalysts, which can selectively trimerize ethylene to 1-hexene with high selectivity.[3] On the base of chromium catalysts, the tetramerization of ethylene have been also developed with reasonable selectivity.[4] However, these processes could not provide higher order α-olefins, and the full range process of ethylene oligomerization provides various chemical substances and plays a more important role in large scale industry. The full range process of ethylene oligomerization was originally achieved with the Ziegler (Alfen) process, while currently the catalysts widely employed in industrial processes are alkylaluminum compounds, a combination of alkylaluminum compounds with early transition metal compounds, or nickel (II) complexes.[5] Homogeneous nickel-based catalysts with monoanionic [P,O] ligands (**A**, Chart 1) for ethylene oligomerization were developed as the well-known Schell Higher Olefin Process (SHOP) and have been extensively investigated.[6] In the past decade significant progress was achieved in the development of late-transition metal catalysts for the oligomerization of ethylene. Nickel and palladium complexes based on α-diimine ligands (**B**, Chart 1)[7] and iminophosphines (**C** and **D**, Chart 1)[8] were reported to be very active and selective catalysts for ethylene oligomerization. In 1998, extremely active iron- and cobalt-based catalysts bearing 2,6-bis(imino)pyridyl ligands for the linear polymerization of ethylene

for references, see page 63

were reported independently by Brookhart[9] and Gibson.[10] By tuning the steric and electronic properties of the ligands, the catalytic products of these metal complexes varied from polyethylene to oligomers (**E**, Chart 1),[11] in which both the catalytic activity and selectivity for α-olefins are highly interesting.

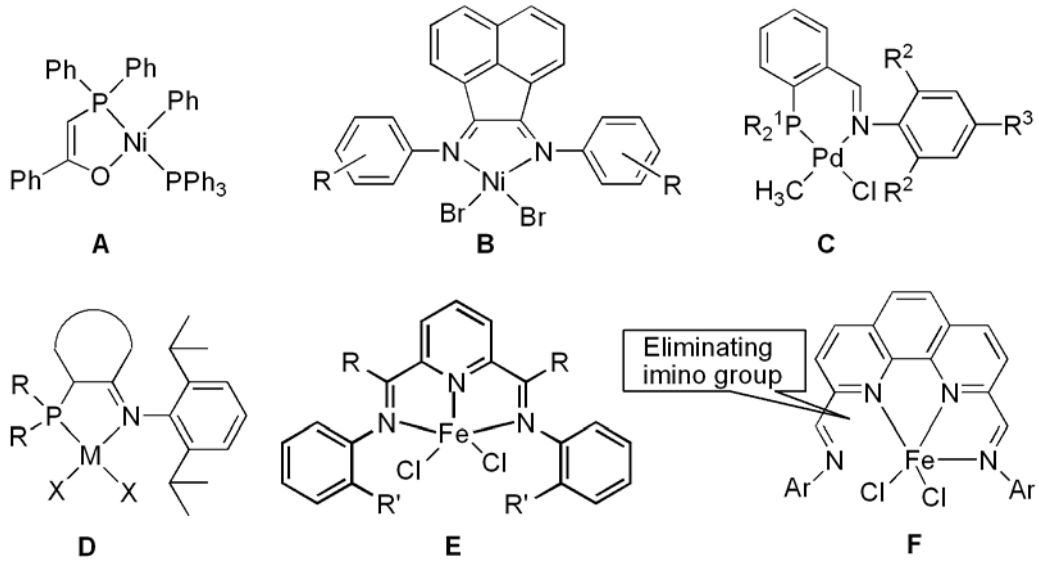

Chart 1.
Complex models of ethylene oligomerization catalysts.

Extending the iron complexes including other tridentate ligands, however, commonly leads to lower catalytic activities for ethylene oligomerization and polymerization.[12] In scanning suitable tridentate metal complexes, the late-transition metal complexes ligated by 2,9-bis(imino)-1,10-phenanthrolinyl ligands were investigated in our group.[13] The nickel and cobalt complexes showed considerable to good catalytic activities for ethylene oligomerization and polymerization, but the iron complexes (**F**, Chart 1) only showed negligible activities for ethylene polymeriztaion. This result was confirmed by Gibson group.[14] It could be argued that the nitrogen atom of the additional imino group can coordinate to the active catalytic center (iron) which is a necessary site for the coordination of ethylene for oligomerization and polymerization.[15] To verify this hypothesis, the additional imino group in **F** should be eliminated. The synthesis of 2-formyl-, 2-acetyl- and 2-benzoyl-1,10-phenanthrolines would be required for this work, but the multi-step syntheses have thus blocked further work. Fortunately, a convenient synthetic method for 2-acetyl-1,10-phenanthroline has been developed in our group, and accordingly the various 2-imino-1,10-phenanthrolinyl ligands and their corresponding iron(II) complexes have been synthesized. The catalytic investigation showed that these iron(II) complexes could oligomerize ethylene to linear α-olefins with high activity and selectivity. Herein the syntheses of 2-formyl-, 2-acetyl-

for references, see page 63

and 2-benzoyl-1,10-phenanthrolines are reported along with an improved synthetic method for 2-acetyl-1,10-phenanthroline. The 2-imino-1,10-phenanthrolinyl ligands and corresponding iron(II) complexes are investigated and discussed for ethylene oligomerization with various catalytic reaction parameters.

Results and Discussion

Preparation of 2-formyl-, 2-acetyl- and 2-benzoyl-1,10-phenanthroline

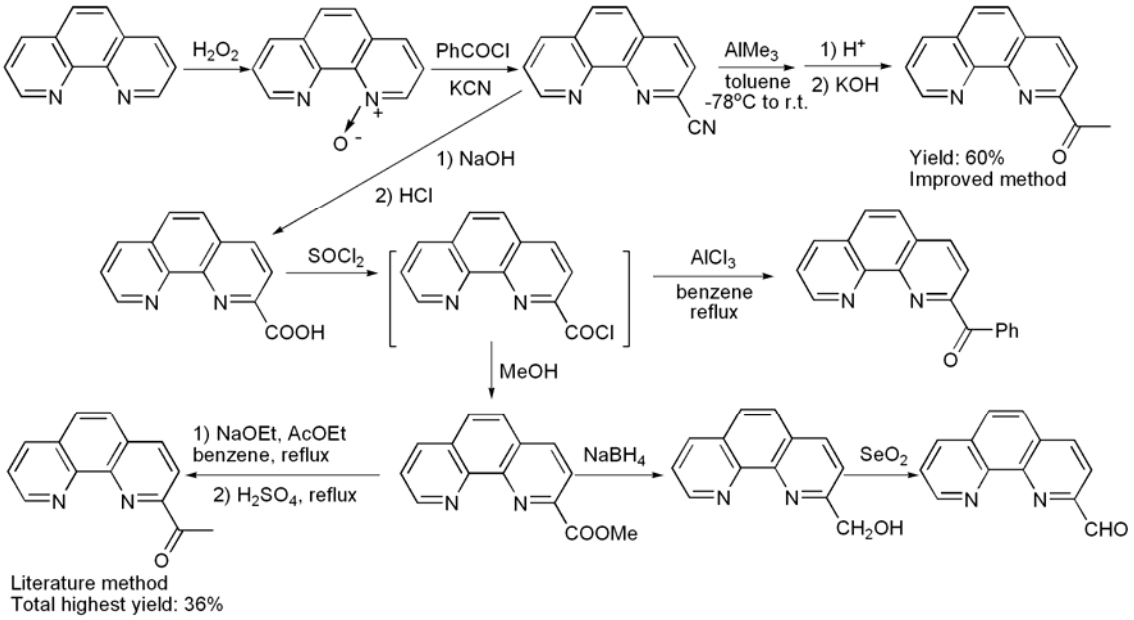

Scheme 1.
Synthesis of 2-formyl-, 2-acetyl- and 2-benzoyl-1,10-phenanthroline.

Neither the 2-formyl, 2-acetyl and 2-benzoyl 1,10-phenanthroline derivatives are commercially available, nor their synthetic intermediates except 1,10-phenanthroline. Therefore the literature procedures and improved synthetic methods have been explored to prepare the three reactants (Scheme 1). Firstly, 1,10-phenanthroline was oxidized with 30% hydrogen peroxide in glacial acetic acid to form 1,10-phenanthroline 1-oxide.[16,*] Following the procedure in the same report,[16] the oxide was converted to 2-cyano-1,10-phenanthroline through cyanation using KCN and benzoyl chloride. Further treatment gave 2-carbomethoxy-1,10-phenanthroline. Subsequently the ester was reduced to the carbinol with $NaBH_4$,[17] and the resulting carbinol was oxidized by SeO_2 to produce the aldehyde, 2-formyl-1,10-phenanthroline.[18] The attempts to convert

* Caution: The explosion easily happened during the concentration of the resulting acetic acid solution. The modified method included the least amount of acetic acid to dissolve 1,10-phenanrhroline and no rotary evaporation before being neutralized and extracted.

for references, see page 63

2-cyano-1,10-phenanthroline into the aldehyde by employing the reported one-step reaction employing Raney nickel and sodium hypophosphite were not successful.[19] In the preparation of 2-acetyl-1,10-phenanthroline, the literature procedure through a Claisen condensation reaction of 2-carbomethoxy-1,10-phenanthroline gave the highest total yield of 36% from 2-cyano-1,10-phenanthroline due to multi-step reactions and manipulations.[20] To shorten the synthetic route and improve the total yield, an alternative synthetic methodology was established through the direct reaction of 2-cyano-1,10-phenanthroline and trimethylaluminum (Scheme 1) for preparing 2-acetyl-1,10-phenanthroline in 60% yield in a somewhat scale-up reaction. But other methyl metal reagents such as methyllithium or methylmagnesium iodide did not work well. 2-Benzoyl-1,10-phenanthroline was first synthesized from 1,10-phenanthroline-2-carbonyl chloride followed by a Friedel-Crafts acylation reaction of benzene with $AlCl_3$ as catalyst.

Synthesis of 2-imino-1,10-phenanthrolinyl ligands and their iron complexes

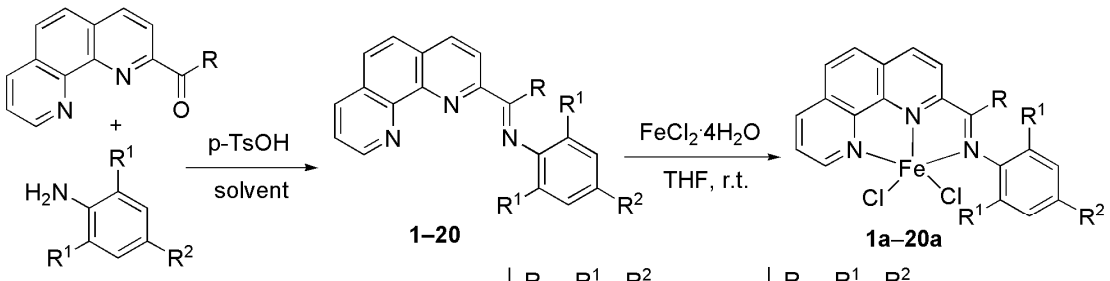

	R	R^1	R^2		R	R^1	R^2
1(**a**)	Me	Me	H	**11**(**a**)	Me	Br	Br
2(**a**)	Me	Et	H	**12**(**a**)	H	Me	H
3(**a**)	Me	*i*-Pr	H	**13**(**a**)	H	Et	H
4(**a**)	Me	Me	Me	**14**(**a**)	H	*i*-Pr	H
5(**a**)	Me	Me	Br	**15**(**a**)	H	F	H
6(**a**)	Me	F	H	**16**(**a**)	H	Cl	H
7(**a**)	Me	Cl	H	**17**(**a**)	H	Br	H
8(**a**)	Me	Br	H	**18**(**a**)	Ph	Me	H
9(**a**)	Me	Br	Me	**19**(**a**)	Ph	Et	H
10(**a**)	Me	Br	Cl	**20**(**a**)	Ph	*i*-Pr	H

Scheme 2.
Synthesis of the ligands **1**–**20** and the iron(II) complexes **1a**–**20a**.

The 2-imino-1,10-phenanthrolinyl ligands (**1**–**20**, 2-(ArN=CR)-1,10-phen) were prepared through the condensation reaction of aldehydes or ketones and the corresponding substituted anilines using *p*-toluene sulfonic acid as catalyst (Scheme 2). Because of the difference in the reactive nature between aldehydes and ketones, alkyl- and halogen-substituted anilines, the various solvents such as ethanol, toluene or tetraethyl silicate were employed in order to improve the product yields. The

for references, see page 63

2-imino-1,10-phenanthrolinyl ligands can be classified according to the nature of R on the imino-C as methyl-ketimine (R = Me, **1**–**11**), aldimine (R = H, **12**–**17**) and phenyl-ketimine (R = Ph, **18**–**20**), and all compounds were sufficiently characterized and confirmed by the analysis of IR, ^{1}H and ^{13}C NMR spectra as well as their elemental analysis.

The iron(II) complexes **1a**–**20a** were easily prepared by mixing the corresponding ligand and one equivalent of $FeCl_2 \cdot 4H_2O$ in THF at room temperature under argon (Scheme 2). The resulting complexes were precipitated from the reaction solution and separated as blue, purple or brown air-stable powders. All the complexes were characterized by FT-IR spectra and elemental analysis. In the IR spectra, the stretching vibration bands of C=N of these iron(II) complexes (1602–1614 cm^{-1}) apparently shifted to lower wave number and the peak intensity greatly reduced, as compared to the corresponding ligands (1618–1656 cm^{-1}), indicating the coordination interaction between the imino nitrogen atom and the metal cation. Some elemental data of complexes showed incorporation of solvent molecule because the samples were prepared through the re-crystallization. These iron(II) complexes are paramagnetic. As one representative species, complex **2a** was characterized in its methanol-d_4 solution by the Evans method[21] and afforded magnetic moment of 5.5 BM, consistent with four unpaired electrons of the high-spin iron(II). Their unambigious structures were confirmed by the single-crystal X-ray diffraction analysis.

Crystal structures

Single crystals of complexes **2a**, **4a**, **7a** and **8a** suitable for X-ray diffraction analysis were individually obtained by slow diffusion of diethyl ether into their methanol solutions under argon atmosphere, while crystals of **14a** suitable for X-ray diffraction analysis were grown through slowly layering of the chloroform solution of ligand **14** over the ethanol solution of $FeCl_2$ in a Schlenk tube under argon atmosphere. According to their structures, the coordination geometry around the iron center can be described as a distorted trigonal bipyramidal, in which the nitrogen (next to the imino-C) of the phenanthrolinyl group and two chlorides compose an equatorial plane. Their crystal structures are shown in Figure 1–5, individually, and the selected bond lengths and angles are collected in Table 1.

In the structure of **2a** (Figure 1), the iron atom slightly deviates by 0.0465 Å from the triangular plane of N2, Cl1 and Cl2 with equatorial angle ranges between 103.06(8)º and 146.74(8)º, deviating from 120º. This equatorial plane is nearly perpendicular to the

for references, see page 63

phenanthrolinyl plane with a dihedral angle of 91.2º. The dihedral angle between the phenyl ring and the phenanthrolinyl plane is 79.8º. The Fe–N(2)(phenanthrolinyl) bond (2.110(3) Å) is shorter by about 0.16 Å than the Fe-N(1)(phenanthrolinyl) (2.271(3) Å) and Fe-N(3)(imino) (2.275(3) Å) bonds, which is similar to the 2,6-bis(imino)pyridyl iron(II) complexes.[10] The two Fe–Cl bond lengths show a slight difference between the Fe–Cl(2) (2.3046(13) Å) and Fe–Cl(1) (2.2806(11) Å). The imino N(3)–C(13) bond length is 1.273(5) Å with the typical character of C=N double-bond.

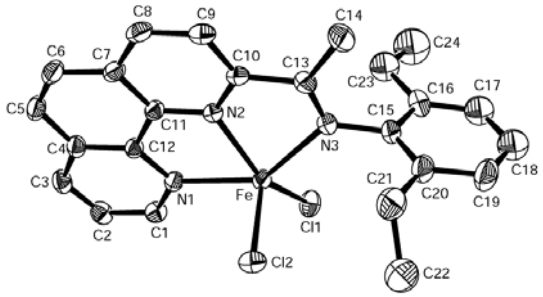

Figure 1.
ORTEP drawing of complex **2a** with thermal ellipsoids at 30% probability level.

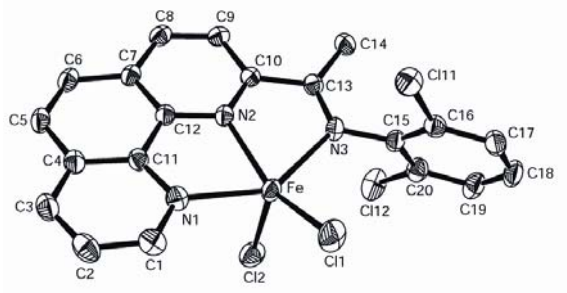

Figure 3.
ORTEP drawing of complex **7a** with thermal ellipsoids at 50% probability level.

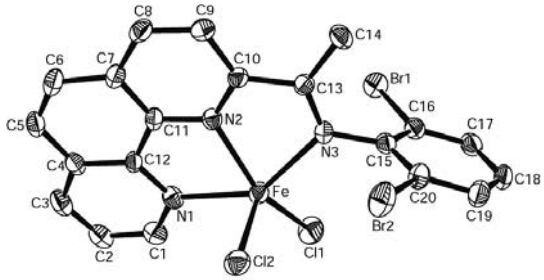

Figure 4.
ORTEP drawing of complex **8a** with thermal ellipsoids at 30% probability level.

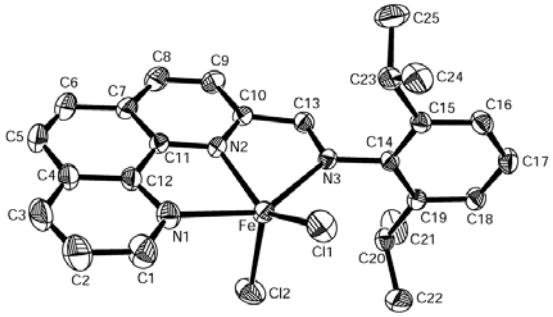

Figure 5.
ORTEP drawing of complex **14a** with thermal ellipsoids at 30% probability level.

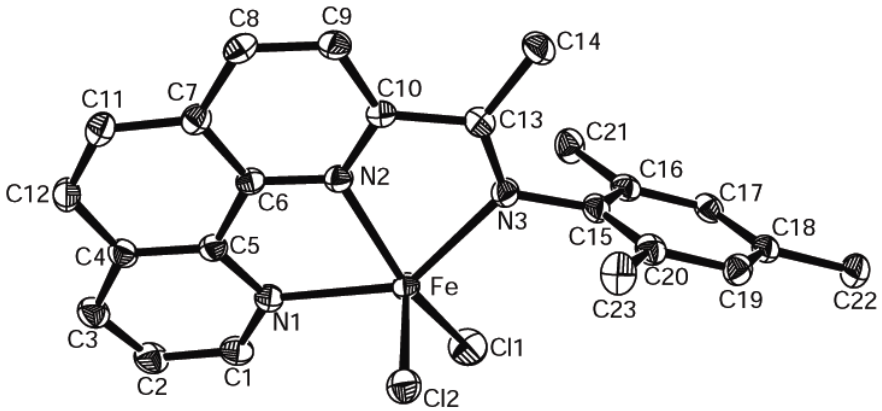

Figure 2.
ORTEP drawing of complex **4a** with thermal ellipsoids at 60% probability level. Hydrogen atoms have been omitted for clarity.

for references, see page 63

Table 1.
Selected bond lengths (Å) and angles (º) for complexes **2a**, **4a**, **7a**, **8a** and **14a**.

	2a	**4a**	**7a**	**8a**	**14a**
Bond lengths					
Fe–N(1)	2.271(3)	2.2643(16)	2.2387(17)	2.241(4)	2.259(3)
Fe–N(2)	2.110(3)	2.1262(15)	2.1223(17)	2.128(4)	2.097(2)
Fe–N(3)	2.275(3)	2.2296(16)	2.2750(17)	2.279(4)	2.276(2)
Fe–Cl(1)	2.2806(11)	2.2923(5)	2.2760(6)	2.2727(16)	2.2496(12)
Fe–Cl(2)	2.3046(13)	2.3321(5)	2.3292(7)	2.3228(17)	2.2921(12)
N(3)–C(13)	1.273(5)	1.286(2)	1.288(3)	1.283(6)	1.277(3)
N(3)–C(15)	1.438(4)	1.437(2)	1.419(3)	1.419(6)	1.449(3) (N3–C14)
Bond angles					
N(2)–Fe–N(1)	73.80(10)	73.36(6)	74.34(6)	74.19(16)	73.83(10)
N(2)– Fe–N(3)	71.86(10)	71.86(6)	71.30(6)	71.21(15)	72.58(9)
N(1)– Fe–N(3)	144.10(10)	143.38(6)	144.52(6)	144.14(16)	145.10(10)
N(1)–Fe–Cl(1)	97.95(7)	99.57(4)	101.91(5)	101.21(12)	101.26(8)
N(2)–Fe–Cl(1)	146.74(8)	150.53(5)	148.63(5)	148.98(12)	139.89(8)
N(3)–Fe–Cl(1)	104.97(8)	105.01(4)	102.72(5)	103.49(11)	98.26(7)
N(1)–Fe–Cl(2)	98.20(8)	98.35(4)	93.62(5)	93.87(12)	94.10(8)
N(2)–Fe–Cl(2)	103.06(8)	99.54(4)	100.50(5)	99.02(11)	103.50(8)
N(3)–Fe–Cl(2)	99.37(8)	98.32(4)	100.97(5)	100.47(11)	102.63(7)
Cl(1)–Fe–Cl(2)	110.04(4)	109.86(2)	110.85(3)	111.96(7)	116.60(5)

According to complex **4a** (Figure 2), the phenanthrolinyl nitrogen atom (N2) and two chlorides form the equatorial plane, and the iron atom slightly deviates by 0.0330 Å from this plane. The three equatorial angles N(2)–Fe–Cl(1), N(2)–Fe–Cl(2) and Cl(1)–Fe–Cl(2) are respectively 150.53(5), 99.54(4) and 109.86(2)º with the larger distortion of N(2)–Fe–Cl(1) and the axial Fe–N bonds subtend an angle of 143.38(6)º (N(1)–Fe–N(3)). The dihedral angles between the equatorial plane and the phenanthrolinyl plane, and the phenyl plane and the phenanthrolinyl plane are 85.5 and 77.3º, respectively. Their two axial Fe–N bond lengths, 2.2643(16) and 2.2296(16) Å, are longer than that of Fe–N(2) of the equatorial plane (2.1262(15) Å), which is similar to that observed in the bis(2,4,6-trimethylphenylimino)pyridyliron(II) complex,[11b] also with a trigonal bipyramical geometry at the iron center. The difference of the two Fe–Cl linkages, Fe–Cl(2) (2.3321(5) Å) and Fe–Cl(1) (2.2923(5) Å), is about 0.04 Å. The imino N(3)–C(13) bond length is 1.286(2) Å with the typical character of C=N double-bond, but slightly longer than that of **2a** (1.273(5) Å). The difference is probably due to the less bulky methyl at the *ortho*-positions of the phenyl ring in **4a**. This steric effect of the substituents also influences the Fe-N(imino) bonds. For instance, the Fe-N(imino) bond length of **4a** (2.2296(16) Å) is noticeably shorter than that of **2a** (2.275(3) Å) with the relatively bulkier ethyl groups at the *ortho*-positions of the phenyl ring.

Complex **7a** (Figure 3) with 2,6-dichlorophenyl and complex **8a** (Figure 4) with 2,6-dibromophenyl almost have the same structural characters, as shown in Figure 3 and

for references, see page 63

4 (their bond distances and angles listed in Table 1). One nitrogen atom (N2) of the phenanthrolinyl group and two chlorides form the equatorial plane, while the iron atom lies 0.0155 Å and 0.0246 Å out of the equatorial plane in **7a** and **8a**, respectively. The bond angles N(1)–Fe–N(3) are nearly identical for the two complexes, (144.52(6)º (**7a**) and 144.14(16)º (**8a**)), as well as the N(2)–Fe–Cl angles of **8a** (148.98(12) and 99.02(11)º) and those of **7a** (148.63(5) and 100.50(5)º) and the angles Cl(1)–Fe–Cl(2) of **7a** and **8a** (110.85(3) and 111.96(7)º, respectively). The equatorial planes of these two complexes are nearly orthogonal to the phenanthrolinyl plane with dihedral angles of 83.3º in **7a** and 84.7º in **8a**. The dihedral angels between the phenyl plane and the phenanthrolinyl plane are 103.9º in **7a** and 102.0º in **8a**, respectively, which are different from the corresponding alkyl-substituted analogues **2a** (79.8º) and **4a** (77.3º). The difference in bond distance is about 0.05 Å between the Fe–Cl(1) and Fe-Cl(2) bonds, such as 2.2760(6) and 2.3292(7) Å in **7a**, and 2.2727(16) and 2.3228(17) Å in **8a**, respectively. Interestingly, the Fe–Cl distances on the same sides of the complex frame are almost equal. The two imino C=N bonds have distinctive double-bond character, with C–N distances of 1.288(3) Å (**7a**) and 1.283(6) Å (**8a**). The electronic properties of the substituents at the *ortho*-positions of the phenyl ring also have some influence on the adjacent N(3)–C(15)(phenyl) bond length. The N(3)–C(15) bonds of **7a** (1.419(3) Å) and **8a** (1.419(6) Å) with 2,6-dihalogenphenyl are shorter by 0.02 Å than those of **2a** (1.438(4) Å) and **4a** (1.437(2) Å) with 2,6-dialkylphenyl.

Complex **14a** (Figure 5) has a similar structural character to complex **2a**. One phenanthrolinyl nitrogen atom and two chlorides form the equatorial plane with the iron atom slightly deviating by 0.012 Å from this plane. The three equatorial angles are respectively 139.89(8), 103.50(8) and 116.60(5)º with a smaller N(2)–Fe–Cl(1) angle and a larger Cl(1)–Fe–Cl(2) angle than those of the ketimine analogues, while the axial N(1)–Fe–N(3) angle is 145.10(10)º. Both the equatorial plane and the phenyl plane are almost perpendicular to the phenanthrolinyl plane with dihedral angles of 87.3 and 81.3º, respectively. The two axial Fe–N bond lengths, 2.259(3) and 2.276(2) Å, are longer than that of Fe–N(2) in the equatorial plane (2.097(2) Å). The two Fe-Cl distances show an obvious difference, 2.2496(12) and 2.2921(12) Å. Furthermore, they are shorter than those of the ketimine complexes, as shown in Table 1. The imino C(13)–N(3) bond has typical C=N double-bond character with a bond length of 1.277(3) Å and it also has a longer N(3)–C(14)(phenyl) (1.449(3) Å), which is slightly longer than that of the ketimine analogues.

for references, see page 63

Ethylene oligomerization

All the synthesized iron(II) complexes, when activated with methylaluminoxane (MAO), display high catalytic activities for ethylene oligomerization with high selectivity for α-olefins at 10 atm of ethylene pressure. The detailed results are summarized in Table 2. The distribution of oligomers obtained in all cases follows Schulz-Flory rules which is characteristic of the constant α; where α represents the probability of chain propagation (α = rate of propagation/((rate of propagation) + (rate of chain transfer)) = (moles of C_{n+2})/(moles of C_n)).[22] The α values are determined by the molar ratio of C_{12} and C_{14} fractions.

Table 2.
The results of ethylene oligomerization by complexes **1a**–**20a**/MAO[a]

entry	cat.	Al/Fe	T^b (°C)	oligomers			waxes
				$A_o{}^c$	α	% α-O[e]	$A_w{}^d$
1	**2a**	200	40	1.20	0.68	>99	1.01
2	**2a**	500	40	21.2	0.64	>96	1.56
3	**2a**	1000	40	49.1	0.62	>94	14.6
4	**2a**	1500	40	25.5	0.62	>97	9.13
5	**2a**	2000	40	7.50	0.64	>98	1.25
6	**2a**	1000	20	16.4	0.49	>96	10.1
7	**2a**	1000	30	21.4	0.55	>95	26.3
8	**2a**	1000	50	35.5	0.61	>93	5.87
9	**2a**	1000	60	14.4	0.44	>95	4.88
10	**1a**	1000	40	38.9	0.67	>96	102
11	**3a**	1000	40	9.42	0.50	>98	0.21
12	**4a**	1000	40	12.4	0.72	>96	138
13	**5a**	1000	40	48.2	0.67	>91	174
14	**6a**	1000	40	23.7	0.37	>79	trace
15	**7a**	1000	40	35.1	0.52	>79	trace
16	**8a**	1000	40	40.6	0.61	>80	65.5
17	**9a**	1000	40	38.9	0.73	>80	241
18	**10a**	1000	40	19.6	0.49	>90	14.6
19	**11a**	1000	40	22.2	0.64	>87	64.1
20	**12a**	1000	40	13.3	0.58	>94	48.6
21	**13a**	1000	40	1.60	0.54	>99	trace
22	**14a**	1000	40	9.00	0.48	>97	0.88
23	**15a**	1000	40	6.99	0.39	>97	trace
24	**16a**	1000	40	7.30	0.59	>97	4.51
25	**17a**	1000	40	1.08	0.62	>99	trace
26	**18a**	1000	40	12.7	0.57	>91	304
27	**19a**	1000	40	23.0	0.52	>95	3.25
28	**20a**	1000	40	1.31	0.50	>98	3.18

[a] General conditions: cat.: 2 μmol; reaction time: 1 h; solvent: toluene (100 mL); ethylene pressure: 10 atm. [b] Reaction temperature. [c] Activity for oligomers: 10^6 g mol^{-1}(Fe) h^{-1}. [d] Activity for low-molecular-weight waxes: 10^5 g mol^{-1}(Fe) h^{-1}. [e] % α-olefin content determined by GC and GC-MS.

(i) Effects of the molar ratio of Al/Fe and reaction temperature

The catalytic system of **2a**/MAO was typically investigated with varying reaction conditions, such as the molar ratio of Al/Fe and reaction temperature. When the Al/Fe molar ratio was enhanced from 200 to 2000, the catalytic activities of **2a** for both

for references, see page 63

oligomers and low-molecular-weight waxes initially increased, and then decreased, while the α value showed little change. With increasing reaction temperature, both the catalytic activity and α value initially increased, and then decreased; however, the activity had no great change. Complex **2a** exhibited an activity of 4.91×10^7 g mol^{-1}(Fe) h^{-1} at the Al/Fe molar ratio of 1000:1 and 40 °C under 10 atm of ethylene pressure.

(ii) Effect of the ligand environment

The variation of the R substituent on the imino-C of ligands, 2-(ArN=CR)-1,10-phen, resulted in changes of the catalytic performance. Aldimine (R = H) and phenyl-ketimine (R = Ph) complexes showed relatively lower catalytic activities than the corresponding methyl-ketimine (R = Me) complexes. Furthermore, the R substituent had different influences on the catalytic performances of methyl- or phenyl-ketimine and aldimine analogues. Consider the 2,6-dialkyl-substituted ketimine and aldimine complexes as examples. Both the methyl-ketimine complex **2a** and the phenyl-ketimine complex **19a** have 2,6-diethyl groups on the phenyl ring of imino nitrogen, and showed the highest activity among their analogues. However, the corresponding aldimine complex **13a** showed much lower activity under the same reaction conditions (entry 3, 27 and 21 in Table 2). Comparing the complexes ligated by the ketimine or aldimine containing the 2,6-diisopropylphenyl group on imino nitrogen, both **3a** and **14a** (entries 11 and 22 in Table 2) showed much better catalytic activity than **20a** (entry 28 in Table 2), which also showed lower activity than its analogues (entries 26 and 27 in Table 2), perhaps due to the bulky phenyl-ketimine. In general, all methyl-ketimine complexes bearing electron-donating alkyl groups showed high catalytic activity and good selectivity for α-olefins. On the contrary, relatively lower selectivity was observed with the complexes containing electron-withdrawing halogen groups, such as complexes **6a**–**9a**, despite their good productivity.

The substituents on the imino-N aryl ring had a great influence on the catalytic performances of both the ketimine and aldimine complexes. For the 2,6-dialkyl-substituted methyl-ketimine complexes **1a**–**3a**, somewhat reduced catalytic activity was observed for the sterically bulkier catalyst systems. This could be demonstrated by comparing 2,6-diisopropyl-substituted **3a** with 2,6-dimethyl-substituted **1a** or 2,6-diethyl-substituted **2a** (entry 11 vs 10 or 3 in Table 2). The greater bulkiness of the isopropyl groups at the *ortho*-positions of imino-N aryl ring of complex **3a** may prevent the access of ethylene to the active center in the catalytic system, therefore resulting in the decrease of catalytic activity. Furthermore, the bulkier the substituents, the smaller α value and a smaller amount of low-molecular-weight waxes

for references, see page 63

produced. Complexes **5a**–**11a**, which bear mono- or multi-halogen groups, exhibited comparable catalytic activity and relatively lower selectivity for α-olefins in the oligomerization of ethylene than complex **1a**–**4a** bearing only alkyl groups. In the catalytic systems of complexes **6a**–**8a** containing a 2,6-dihalogen-substituted ligands, the bulkier substituents at the *ortho*-positions of imino-N aryl ring resulted in higher catalytic activities as well as higher α value (bromo- > chloro- > fluoro-, entry 14–16 in Table 2). In addition, the substituent at the 4-position of the aryl ring had an obvious influence on the catalytic activity and α value. The 2,6-dibromo-substituted complex **9a** which also bears an electron-donating methyl group at the 4-position of the aryl ring, exhibited higher catalytic activity and a larger α value than the corresponding complex **10a** (4-chloro) and **11a** (4-bromo) which bear an electron-withdrawing halogen group at the 4-position of the aryl ring. However, complex **5a** bearing 4-bromo-2,6-dimethyl groups showed higher oligomerization activity than 2,4,6-trimethyl-substituted **4a**.

For the aldimine complexes **12a**–**17a**, 2,6-dimethyl-substituted complex **12a** displayed the higher catalytic activity of 1.33×10^7 g mol^{-1}(Fe) h^{-1} (entry 20 in Table 2), while a much lower catalytic activity was obtained for 2,6-diethyl-substituted complex **13a** (entry 21 in Table 2) under the same reaction condition. For the 2,6-dihalogen-substituted complexes **15a**–**17a**, complex **17a** with bromine atoms at the *ortho*-positions of the imino *N*-aryl ring gave the lower activity, while the 2,6-dichloro-substituted complex **16a** displayed a higher oligomerization activity with some waxes produced and 2,6-difluoro-substituted complex **15a** showed comparable oligomerization activity with a lower α value. This probably resulted from the interaction of their steric and electronic effects. For the phenyl-ketimine complexes, complex **20a** bearing bulkier isopropyl groups at the *ortho*-positions of the aryl ring had much lower oligomerization activity than the 2,6-dimethyl-substituted **18a** and the 2,6-diethyl-substituted **19a**, probably because of the cooperative interaction of bulkier isopropyl groups on the imino-N aryl ring and bulkier phenyl on the imino-C.

(iii) Effect of the different cocatalyst

When modified methylaluminoxane (MMAO) was employed as cocatalyst, methyl-ketimine complexes **1a**–**4a** and **6a**–**8a** also displayed high catalytic activity for ethylene oligomerization with high selectivity for α-olefins at 10 atm and the distribution of oligomers obtained in all cases followed Schulz-Flory rules. The detailed results are listed in Table 3.

In the presence of MMAO, ethylene was consumed very quickly over the first 5 minutes, but after this time, the consumption rate slowed down gradually. In the

for references, see page 63

presence of MAO, the consumption rate of ethylene slightly decreased during the reaction time. As an example, the lifetime of complex **1a**/MMAO system was studied by varying the reaction time from 5 to 60 minutes. The highest activity of 8.95×10^7 g mol^{-1}(Fe) h^{-1} was obtained at 5 min (entry 1 in Table 3). With prolonged reaction time, the oligomerization activity decreased and the yield of low-molecular-weight waxes increased progressively, while the α value and the activity for waxes had no remarkable change (entry 1–5 in Table 3). But under the same reaction condition, complex **1a** showed lower a catalytic activity (1.22×10^7 g mol^{-1}(Fe) h^{-1}) than that when using MAO as cocatalyst (3.89×10^7 g mol^{-1}(Fe) h^{-1}, entry 5 in Table 3 and entry 10 in Table 2). On treatment with MMAO, the other alkyl- and halogen-substituted methyl-ketimine complexes displayed the comparable ethylene oligomerization activities and high selectivities for α-olefins. However, the 2,6-diisopropyl-substituted complex **3a** and the 2,6-difluoro-substituted complex **6a** gave lower α values and no waxes were formed.

Table 3.
The ethylene oligomerization with complexes **1a**–**4a** and **6a**–**8a**/MMAO[a]

entry	cat.	*t* (min)	oligomers			waxes	
			A_o[b]	α	% α-O[d]	yield(g)	A_w[c]
1	**1a**	5	8.95	0.67	>98	0.67	40.2
2	**1a**	10	4.77	0.65	>98	0.73	22.1
3	**1a**	20	2.99	0.67	>98	1.88	28.2
4	**1a**	30	2.97	0.68	>97	2.63	26.3
5	**1a**	60	1.22	0.70	>97	3.99	20.0
6	**2a**	30	1.70	0.64	>97	0.06	0.61
7	**3a**	30	1.37	0.46	>98	trace	-
8	**4a**	30	2.07	0.55	>98	2.55	25.5
9	**6a**	30	1.72	0.42	>95	-	-
10	**7a**	30	1.80	0.65	>96	0.13	1.32
11	**8a**	30	1.87	0.62	>93	0.15	1.45

[a] General conditions: cat.: 2 μmol; reaction temperature: 40 °C; solvent: toluene (100 mL); ethylene pressure: 10 atm. [b] Activity for oligomers: 10^7 g mol^{-1}(Fe) h^{-1}. [c] % α-olefin content determined by GC and GC-MS. [d] Activity for low-molecular-weight waxes: 10^5 g mol^{-1}(Fe) h^{-1}.

(iv) Characterization for low-molecular-weight waxes

In many cases, some low-molecular-weight waxes as higher oligomers were obtained in addition to lower oligomers. Characterized by IR spectra recorded using KBr disc in the range of 4000–400 cm^{-1}, the waxes can be conformed to be mainly linear α-olefins from the characteristic vibration absorption bands of C=C and various C–H bonds. ^{1}H and ^{13}C NMR spectra of the waxes obtained by complex **1a**/MAO were recorded in *o*-dichlorobenzene-d_4 using TMS as the internal standard. NMR spectra of the waxes were shown in Figure 6 and the assignments were determined according to the literatures.[23, 24] The ^{13}C NMR spectra further demonstrated that linear α-olefins of the waxes absolutely predominated in the waxes and the single peaks at δ 139.14 and

for references, see page 63

114.17 ppm showed the property of vinyl-unsaturated chain end. The obtained average molecular weight from ^{1}H NMR indicated that the carbon number of the waxes was about 40.

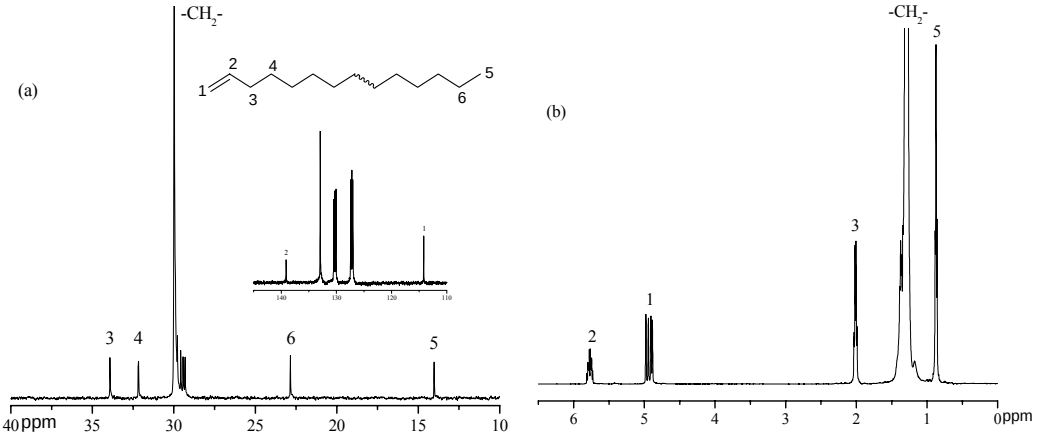

Figure 6.
NMR spectra of the waxes obtained by complex **1a**/MAO. (a) ^{13}C NMR; (b) ^{1}H NMR.

Conclusion

A series of tridentate iron(II) complexes bearing 2-imino-1,10-phenanthrolinyl ligands have been synthesized and fully characterized. Upon treatment with MAO or MMAO, these iron(II) complexes showed high catalytic activities of up to 8.95×10^{7} g mol^{-1}(Fe) h^{-1} for ethylene oligomerization with high selectivity for α-olefins. However, MAO was found to be more effective cocatalyst than MMAO. Both the R on the imino-C and the substituents on the N-aryl rings had an obvious influence on the catalytic activity, distribution of oligomers, and selectivity for α-olefins due to their different steric and electronic properties. The methyl ketimine complexes were proved to be relatively more active than either the corresponding aldimine or phenyl ketimine complexes under the same reaction conditions. Electron-donating groups placed on the N-aryl rings increased the selectivity for α-olefins. The placement of bulkier *o*-alkyl groups on the N-aryl rings led to the reduced activity because of steric interaction, however, bulkier halogen groups gave the reverse effect.

Experimental section

General considerations

All manipulations for air or moisture-sensitive compounds were carried out under an atmosphere of argon using standard Schlenk techniques. Melting points (Mp) were measured with a digital electrothermal apparatus without calibration. IR spectra were

for references, see page 63

recorded on a Perkin-Elmer FT-IR 2000 spectrometer by using KBr disc in the range of 4000–400 cm^{-1}. ^{1}H NMR and ^{13}C NMR spectra were recorded on a Bruker DMX-300 instrument with TMS as the internal standard. Splitting patterns are designated as follows: s, singlet; d, doublet; dd, double doublet; t, triplet; quad, quadruplet; sept, septet; m, multiplet. Elemental analysis was performed on a Flash EA1112 microanalyzer. GC analysis was performed with a Carlo Erba gas chromatograph equipped with a flame ionization detector and a 30 m (0.25 mm i.d., 0.25 μm film thickness) DM-1 silica capillary column.

Toluene and tetrahydrofuran were refluxed over sodium-benzophenone and distilled under argon prior to use. Trimethylaluminum was purchased from Acros Chemicals and diluted to 2 M with dried toluene. Methylaluminoxane (MAO, 1.46 M in toluene) and modified methylaluminoxane (MMAO, 1.93 M in heptane) were purchased from Akzo Corp (USA). All the anilines were purchased from Aldrich or Acros Chemicals. Iron(II) chloride tetrahydrate was synthesized from iron power reduced and aqueous hydrogen chloride and kept under inert atmosphere. All other chemicals were obtained commercially and used without further purification unless otherwise stated.

Preparation of the starting materials (aldehyde and ketones)

(i) Preparation of 2-formyl-1,10-phenanthroline

1,10-Phenanthroline 1-oxide: 30 mL of 30% Hydrogen peroxide was added dropwise to a solution of 50.0 g (0.25 mol) 1,10-phenanthroline monohydrate in 60 mL of glacial acetic acid. The reaction mixture was maintained at 70–75 ºC for 3 hrs, after which an addition 30 mL of 30% hydrogen peroxide was added dropwise and the heating continued for 3hrs. After cooling, the mixture was neutralized to pH≈10 with saturated aqueous potassium hydroxide, and then was extracted repeatedly with chloroform. The combined chloroform extracts were dried over anhydrous sodium sulfate and evaporated to give a yellow solid (39.0 g) in 79% yield. Mp: 178–180 ºC [lit.[16] 176–179 ºC].

2-Cyano-1,10-phenanthroline: To a solution consisting of 25.0 g (0.13 mol) 1,10-phenanthroline 1-oxide and 25.0 g potassium cyanide dissolved in 200 mL of water, 25 mL of benzoyl chloride was added dropwise under stirring magnetically. The total addition required 1 h and the reaction mixture was stirred for an additional 2 hrs. The resulting precipitate was collected by suction filtration, washed with water and dried as a brown solid in 87% yield. Mp: 230–232 ºC [lit.[16] 233–234 ºC].

for references, see page 63

2-Carboxy-1,10-phenanthroline: A solution of 10.0 g sodium hydroxide in 60 mL of water was added to a solution of 12.0 g (59.0 mmol) 2-cyano-1,10-phenanthroline in 120 mL of 95% ethanol and the reaction mixture was refluxed for 2 hrs. Some of ethanol was removed at reduced pressure and the residue was made slightly acidic with concentrated hydrochloric acid at ice-water bath. The precipitate was filtrated, washed with water and dried in vacuum and a yellow brown solid (10.4 g) was obtained in 79% yield. Mp: 212–214 ºC [lit.[16] 209–210 ºC].

2-Carbomethoxy-1,10-phenanthroline: 6.10 g (27.0 mmol) 2-Carboxy-1,10-phenanthroline was suspended in 250 mL of thionyl chloride and refluxed until the solid had dissolved to give a red solution (about 4 hrs) and then the residual $SOCl_2$ was removed at reduced pressure. To the residue 200 mL of anhydrous methanol was added and the mixture was stirred overnight at room temperature. The resulting red solution was eluted through basic alumina column and the methanol effluent was then concentrated to approximately 10 mL on the rotatory evaporator. The addition of 200 mL water caused the ester to precipitate from the solution. And the product was collected by filtration, washed with water and dried as a yellow solid (5.10 g) in 80% yield. Mp: 110–112 ºC [lit.[17] 112–114 ºC].

2-Carbinol-1,10-phenanthroline: To a red solution of 6.30 g (26.4 mmol) 2-carbomethoxy-1,10-phenanthroline dissolved in 60 mL of anhydrous methanol, 7.0 g sodium borohydride was slowly added over 30 min at 0–5 ºC. The reaction solution was stirred for 1 h at room temperature and then refluxed for 2 hrs. After the solution was allowed to cool down, 100 mL distilled water was added and methanol was removed on the rotatory evaporator. The resulting solution was then extracted four times with chloroform which were combined and dried over sodium sulfate. The chloroform was evaporated and the residue was eluted with ethanol on an alumina column. The second eluting part was collected and concentrated to give an orange solid (4.0 g) in 72% yield. Mp: 136–138 ºC [lit.[17] 139–143 ºC].

2-Formyl-1,10-phenanthroline: 1.40 g (12.5 mmol) Selenium dioxide was added to a solution of 5.25 g (25.0 mmol) 2-carbinol-1,10-phenanthroline in 200 mL of pyridine with constant stirring. The mixture was then heated for 4 hrs at 80–90 ºC and the color changed from orange to a dirty brown, characteristic of selenium metal precipitate. After cooling to room temperature, the selenium precipitate was removed by filtration. And pyridine of the filtrate was removed at reduced pressure and the residue was eluted with methanol on an alumina column. The eluent was concentrated to give a

for references, see page 63

yellow solid (4.70 g) in 90% yield. Mp: 152–154 ºC [lit.[18] 152–153 ºC]. FT-IR (KBr disc, cm^{-1}): 1705 ($\nu_{C=O}$).

(ii) Preparation of 2-acetyl-1,10-phenanthroline

To the suspension of 2-cyano-1,10-phenanthroline (2.10 g, 10.0 mmol) in 50 mL toluene, 2 equiv. of trimethylaluminum (10 mL, 20.0 mmol) toluene solution was added dropwise at –78 °C, and then the temperature was slowly elevated to room temperature. After stirred for 12 hrs at room temperature, small amount of water was added dropwise to the reaction mixture at ice-water bath and yellow precipitate appeared. Then the mixture was extracted with dilute aqueous hydrogen chloride. The combined water layer was made alkaline with solid potassium hydroxide and the resulting precipitate was filtered, dried and then purified through basic alumina column. The desired product was obtained as an ivory-white solid (1.37 g) in 60% yield. Mp: 152–154 °C. FT-IR (KBr disc, cm^{-1}): 1693 ($\nu_{C=O}$). ^{1}H NMR (300 MHz, $CDCl_3$): δ 9.26 (d, *J* = 3.9 Hz, 1H); 8.37 (s, 2H); 8.29 (d, *J* = 8.1 Hz, 1H); 7.87 (dd, *J* = 8.7 Hz, 2H); 7.69 (dd, *J* = 7.8 Hz, 1H); 3.09 (s, 3H, C*H*$_3$). Anal. Calc. for $C_{19}H_{10}N_2O$ (222.24): C, 75.66; H, 4.54; N, 12.60. Found: C, 75.50; H, 4.64; N, 12.41.

(iii) Preparation of 2-benzoyl-1,10-phenanthroline

1,10-phenanthroline-2-carboxylic acid (12.0 g, 53.0 mmol) was refluxed with thionyl chloride (250 mL) for 6 hrs and the residual $SOCl_2$ was removed at reduced pressure. The resulting yellowish solid was refluxed with anhydrous aluminium chloride (9.00 g, 66.0 mmol) in benzene (70 mL) for 4 hrs. The resulting red solution was cooled to room temperature, and it was stirred for 12 hrs and then refluxed for 6 hrs. After the solution was cooled to room temperature, it was poured into distilled water (125 mL) at 0 °C. The organic layer was extracted with chloroform (20 mL × 4). The combined organic phases were dried over anhydrous sodium sulfate and evaporated in vacuum to afford a white solid in 48% yield. Mp: 110–112 °C. FT-IR (KBr disc, cm^{-1}): 1655 ($\nu_{C=O}$). ^{1}H NMR (300 MHz, $CDCl_3$): δ 9.18 (dd, *J* = 2.1 Hz, 1H); 8.44 (s, 1H); 8.41 (s, 1H); 8.39 (d, *J* = 3.3 Hz, 1H); 8.27–8.23 (m, 2H); 7.86–7.83 (m, 2H), 7.66–7.58 (m, 2H); 7.54–7.49 (m, 2H). ^{13}C NMR (100 MHz, $CDCl_3$): δ 193.2, 154.8, 150.7, 146.3, 144.8, 136.9, 136.1, 135.9, 133.1, 131.8, 129.5, 129.0, 128.4, 128.2, 126.0, 123.1, 122.9. Anal. Calc. for $C_{19}H_{12}N_2O$ (284.31): C, 80.27; H, 4.25; N, 9.85. Found: C, 80.24; H, 4.24; N, 9.83.

for references, see page 63

Synthesis of the 2-imino-1,10-phenanthroline ligands 1–20

2-Acetyl-1,10-phenanthroline(2,6-dimethylanil) (1). A reaction mixture of 2-acetyl-1,10-phenanthroline (0.445 g, 2.00 mmol), 2,6-dimethylaniline (0.315 g, 2.60 mmol), *p*-toluenesulfonic acid (0.040 g) and absolute ethanol (20 mL) was refluxed under N_2 atmosphere for 2 days. The solvent was rotary evaporated and the resulting solid was eluted with petroleum ether/ethyl acetate (v:v = 2:1) on an alumina column. The second eluting part was collected and concentrated to give a yellow solid in 72% yield. Mp: 170–172 °C. FT-IR (KBr disc, cm^{-1}): 3435, 2970, 2933, 1645, 1590, 1553, 1490, 1469, 1446, 1366, 1324, 1207, 1138, 1117, 1091, 866, 777, 747. ^{1}H NMR (300 MHz, $CDCl_3$): δ 9.24 (t, *J* = 2.1 Hz, 1H); 8.80 (dd, *J* = 8.7 Hz, 1H); 8.34 (dd, *J* = 8.4 Hz, 1H); 8.27 (d, *J* = 7.8 Hz, 1H); 7.85 (s, 2H); 7.65 (m, 1H); 7.10 (d, J = 7.5 Hz, 2H); 6.96 (t, J = 7.5 Hz, 1H); 2.56 (s, 3H, C*H*$_3$); 2.08 (s, 6H, PhC*H*$_3$). ^{13}C NMR (75 MHz, $CDCl_3$): δ 168.0, 156.0, 150.6, 148.9, 146.2, 145.0, 136.4, 136.2, 129.4, 128.9, 127.8, 127.5, 126.4, 125.2, 123.0, 122.9, 120.8, 17.9, 16.9. Anal. Calc. for $C_{22}H_{19}N_3$ (325.41): C, 81.20; H, 5.89; N, 12.91. Found: C, 80.99; H, 5.94; N, 12.87.

2-Acetyl-1,10-phenanthroline(2,6-diethylanil) (2). In a similar manner as described for **1**, the ligand **2** was prepared as a yellow solid in 68% yield. Mp: 188–190 °C. FT-IR (KBr disc, cm^{-1}): 3424, 2966, 2930, 2870, 1639, 1587, 1553, 1491, 1453, 1363, 1322, 1257, 1197, 1138, 1116, 1079, 867, 824, 782, 747. ^{1}H NMR (300 MHz, $CDCl_3$): δ 9.25 (dd, *J* = 3.0 Hz, 1H); 8.80 (d, *J* = 8.3 Hz, 1H); 8.35 (d, *J* = 8.3 Hz, 1H); 8.27 (dd, *J* = 7.8 Hz, 1H); 7.86 (s, 2H); 7.66 (m, 1H); 7.15 (d, J = 7.6 Hz, 2H); 6.96 (t, J = 7.5 Hz, 1H); 2.58 (s, 3H, C*H*$_3$); 2.43 (m, 4H, C*H*$_2$CH$_3$), 1.16 (t, J = 7.5 Hz, 6H, CH$_2$C*H*$_3$). ^{13}C NMR (75 MHz, $CDCl_3$): δ 167.8, 156.2, 150.7, 148.0, 146.4, 145.2, 136.5, 131.1, 129.5, 129.0, 127.5, 126.5, 126.0, 123.4, 122.9, 120.8, 24.6, 17.3, 13.7. Anal. Calc. for $C_{24}H_{23}N_3$ (353.46): C, 81.55; H, 6.56; N, 11.89. Found: C, 80.88; H, 6.59; N, 11.78.

2-Acetyl-1,10-phenanthroline(2,6-diisopropylanil) (3). In a similar manner as described for **1**, the ligand **3** was prepared as a yellow solid in 72% yield. Mp: 196–198 °C. FT-IR (KBr disc, cm^{-1}): 3434, 2961, 2870, 1646, 1588, 1552, 1490, 1459, 1363, 1321, 1191, 1115, 861, 821, 772, 745. ^{1}H NMR (300 MHz, $CDCl_3$): δ 9.25 (d, *J* = 2.7 Hz, 1H); 8.82 (d, *J* = 8.7 Hz, 1H); 8.33 (m, 2H); 7.85 (s, 2H); 7.65 (m, 1H); 7.17 (m, 3H); 2.86 (sept, *J* = 6.6 Hz, 2H, C*H*(CH$_3$)$_2$), 2.60 (s, 3H, C*H*$_3$); 1.17 (d, 12H, CH(C*H*$_3$)$_2$). ^{13}C NMR (75 MHz, $CDCl_3$): δ 167.7, 156.1, 150.7, 146.7, 146.4, 145.2, 136.5, 136.3, 135.7, 129.5, 129.0, 127.5, 126.5, 123.7, 123.0, 122.9, 120.9, 28.3, 23.3,

for references, see page 63

22.9, 17.6. Anal. Calc. for $C_{26}H_{27}N_3$ (381.51): C, 81.85; H, 7.13; N, 11.01. Found: C, 81.82; H, 7.25; N, 10.71.

2-Acetyl-1,10-phenanthroline(2,4,6-trimethylanil) (4). In a similar manner as described for **1**, the ligand **4** was prepared as yellow solid in 80% yield. Mp: 146–148 °C. FT-IR (KBr disc, cm^{-1}): 2937, 1634, 1586, 1551, 1480, 1364, 1323, 1216, 1136, 1115, 824, 773, 744. ^{1}H NMR (400 MHz, $CDCl_3$): δ 9.25 (dd, *J* = 4.5 Hz, 1H); 8.80 (d, *J* = 8.4 Hz, 1H); 8.35 (d, *J* = 8.4 Hz, 1H); 8.30 (dd, *J* = 8.1 Hz, 1H); 7.88 (s, 2H); 7.68 (quad, *J* = 4.5 Hz, 1H); 6.93 (s, 2H); 2.56 (s, 3H, C*H*$_3$); 2.32 (s, 3H, PhC*H*$_3$); 2.05 (s, 6H, PhC*H*$_3$). ^{13}C NMR (75 MHz, $CDCl_3$): δ 168.3, 156.2, 150.5, 146.4, 146.2, 145.0, 136.4, 136.3, 132.2, 129.4, 128.9, 128.5, 127.4, 126.4, 125.1, 122.9, 120.9, 20.7, 17.9, 16.9. Anal. Calc. for $C_{23}H_{21}N_3$ (339.43): C, 81.38; H, 6.24; N, 12.38. Found: C, 81.42; H, 6.26; N, 12.14.

2-Acetyl-1,10-phenanthroline(4-bromo-2,6-dimethylanil) (5). A reaction mixture of 2-acetyl-1,10-phenanthroline (0.445 g, 2.00 mmol), 4-bromo-2,6-dimethylaniline (0.520 g, 2.60 mmol), *p*-toluenesulfonic acid (0.040 g) and anhydrous sodium sulfate in 30 mL toluene were refluxed under N_2 atmosphere for 30 hrs. After filtration, the solvent was removed through rotary evaporation and the resulting solid was eluted with petroleum ether/ethyl acetate (v:v = 4:1) on an alumina column. The second eluting part was collected and concentrated to give a yellow solid in 65% yield. Mp: 196–198 °C. FT-IR (KBr disc, cm^{-1}): 3036, 2969, 2913, 1641, 1584, 1550, 1462, 1397, 1366, 1323, 1284, 1201, 1113, 1077, 997, 880, 853, 780, 743, 710, 661. ^{1}H NMR (300 MHz, $CDCl_3$): δ 9.25 (dd., *J* = 4.2 Hz, 1H); 8.76 (d, *J* = 8.4 Hz, 1H); 8.37 (d, *J* = 8.4 Hz, 1H); 8.31 (dd, *J* = 7.8 Hz, 1H); 7.89 (s, 2H); 7.68 (dd, J = 7.8 Hz, 1H); 7.25 (d, J = 5.7 Hz, 2H); 2.55 (s, 3H, C*H*$_3$); 2.05 (s, 6H, PhC*H*$_3$). ^{13}C NMR (75 MHz, $CDCl_3$): δ 168.6, 155.5, 150.4, 147.7, 146.0, 1449, 136.3, 136.0, 130.2, 129.3, 128.7, 127.4, 127.3, 126.1, 122.7, 120.5, 115.3, 17.5, 16.8. Anal. Calc. for $C_{22}H_{18}BrN_3$ (404.30): C, 65.36; H, 4.49; N, 10.39. Found: C, 64.97; H, 4.49; N, 10.39.

2-Acetyl-1,10-phenanthroline(2,6-difluoroanil) (6). In a similar manner as described for **5**, the ligand **6** was prepared as a yellow solid in 54% yield. Mp: 180–182 °C. FT-IR (KBr disc, cm^{-1}): 3429, 3015, 1637, 1585, 1556, 1473, 1421, 1391, 1368, 1322, 1277, 1237, 1121, 1066, 1027, 999, 888, 852, 821, 766, 744, 697, 658. ^{1}H NMR (300 MHz, $CDCl_3$): δ 9.25 (dd, *J* = 4.2 Hz, 1H); 8.70 (d, *J* = 8.4 Hz, 1H); 8.36 (d, *J* = 8.7 Hz, 1H); 8.30 (dd, *J* = 8.7 Hz, 1H); 7.88 (s, 2H); 7.68 (dd, *J* = 7.8 Hz, 1H); 7.11-6.97 (m, 3H); 2.76 (s, 3H, C*H*$_3$). ^{13}C NMR (75 MHz, $CDCl_3$): δ 173.6, 155.7, 154.5, 151.3, 151.2, 150.7, 146.3, 145.1, 136.6, 136.3, 129.7, 129.0, 127.8, 126.4,

for references, see page 63

124.1, 123.0, 121.4, 111.8, 111.5, 18.2. Anal. Calc. for $C_{20}H_{13}F_2N_3$ (333.33): C, 72.06; H, 3.93; N, 12.61. Found: C, 71.89; H, 3.90; N, 12.87.

2-Acetyl-1,10-phenanthroline(2,6-dichloroanil) (7). 2-Acetyl-1,10-phenanthroline (0.445 g, 2.00 mmol), 2,6-dichloroaniline (0.388 mg, 2.40 mmol) and *p*-toluenesulfonic acid (0.040 g) were combined with tetraethyl silicate (5 mL) in a flask. The flask was equipped with a condenser along with a water knockout trap, and the mixture was heated at 140–150 °C under nitrogen for 36 hrs. Tetraethyl silicate was removed at reduced pressure and the resulting solid was eluted with petroleum ether/ethyl acetate (v:v = 4:1) on an alumina column. The second eluting part was collected and concentrated to give a yellow solid in 32% yield. Mp: 184–186 °C. FT-IR (KBr disc, cm^{-1}): 2966, 2926, 1641, 1629, 1585, 1554, 1489, 1448, 1432, 1390, 1367, 1324, 1285, 1260, 1223, 1119, 1079, 854, 782, 761, 738, 658. ^{1}H NMR (300 MHz, $CDCl_3$): δ 9.26 (d, *J* = 4.2 Hz, 1H); 8.78 (d, *J* = 8.4Hz, 1H); 8.38 (d, *J* = 8.4 Hz, 1H); 8.31 (d, *J* = 7.8 Hz, 1H); 7.89 (s, 2H); 7.69 (dd, J = 8.1 Hz, 1H); 7.39 (d, J = 8.1 Hz, 2H); 7.02 (t, J = 8.1 Hz, 1H); 2.68 (s, 3H, C*H*$_3$). ^{13}C NMR (75 MHz, $CDCl_3$): δ 172.3, 155.4, 150.7, 136.7, 136.4, 129.8, 129.0, 128.3, 127.9, 126.5, 124.4, 123.1, 121.5, 18.1. Anal. Calc. for $C_{20}H_{13}Cl_2N_3$ (366.24): C, 65.59; H, 3.58; N, 11.47. Found: C, 65.29; H, 3.70; N, 11.28.

2-Acetyl-1,10-phenanthroline(2,6-dibromoanil) (8). In a similar manner as described for **7**, the ligand **8** was prepared as a yellow solid in 22% yield. Mp: 170–172 °C. FT-IR (KBr disc, cm^{-1}): 3011, 2966, 1639, 1625, 1587, 1550, 1503, 1489, 1448, 1426, 1391, 1365, 1323, 1284, 1263, 1220, 1194, 1137, 1118, 1080, 889, 855, 818, 775, 759, 739, 725, 658. ^{1}H NMR (300 MHz, $CDCl_3$): δ 9.26 (d, *J* = 4.2 Hz, 1H); 8.81 (d, *J* = 8.4Hz, 1H); 8.39 (d, *J* = 8.4 Hz, 1H); 8.31 (d, *J* = 8.1 Hz, 1H); 7.89 (s, 2H); 7.69 (dd, J = 8.1 Hz, 1H); 7.60 (d, J = 8.1 Hz, 2H); 6.88 (t, J = 8.1 Hz, 1H); 2.67 (s, 3H, C*H*$_3$). ^{13}C NMR (75 MHz, $CDCl_3$): δ 172.0, 155.2, 150.7, 148.3, 146.3, 145.2, 136.7, 136.4, 132.0, 129.9, 129.0, 127.9, 126.5, 125.3, 123.1, 121.5, 113.5, 18.1. Anal. Calc. for $C_{20}H_{13}Br_2N_3$ (455.15): C, 52.78; H, 2.88; N, 9.23. Found: C, 52.78; H, 2.92; N, 9.16.

2-Acetyl-1,10-phenanthroline(2,6-dibromo-4-methylanil) (9). In a similar manner as described for **7**, the ligand **9** was prepared as a yellow solid in 37% yield. Mp: 213–215 °C. FT-IR (KBr disc, cm^{-1}): 2966, 2921, 1628, 1585, 1551, 1486, 1449, 1388, 1363, 1319, 1284, 1229, 1195, 1116, 1079, 853, 775, 740, 658. ^{1}H NMR (300 MHz, $CDCl_3$): δ 9.26 (dd, *J* = 4.2 Hz, 1H); 8.80 (d, *J* = 8.4Hz, 1H); 8.38 (d, *J* = 8.4 Hz, 1H); 8.31 (dd, *J* = 7.5 Hz, 1H); 7.89 (s, 2H); 7.68 (d, J = 8.1 Hz, 1H); 7.43 (s, 2H); 2.66 (s, 3H, C*H*$_3$); 2.18 (s, 3H, PhC*H*$_3$). ^{13}C NMR (75 MHz, $CDCl_3$): δ 172.2, 155.4, 150.7,

for references, see page 63

146.3, 145.7, 145.2, 136.7, 136.3, 135.4, 132.5, 129.8, 129.0, 127.8, 126.5, 123.0, 121.4, 113.1, 20.2, 18.0. Anal. Calc. for $C_{21}H_{15}Br_2N_3$ (469.17): C, 53.76; H, 3.22; N, 8.96. Found: C, 53.95; H, 3.49; N, 8.80.

2-Acetyl-1,10-phenanthroline(4-chloro-2,6-dibromoanil) (10). In a similar manner as described for **7**, the ligand **10** was prepared as a yellow solid in 22% yield. Mp: 214–216 °C. FT-IR (KBr disc, cm^{-1}): 3070, 3045, 2987, 1656, 1619, 1587, 1552, 1531, 1491, 1450, 1439, 1425, 1390, 1365, 1322, 1285, 1229, 1190, 1137, 1117, 1081, 858, 821, 773, 742, 699, 659. ^{1}H NMR (300 MHz, $CDCl_3$): δ 9.25 (d, *J* = 3.3 Hz, 1H); 8.77 (d, *J* = 8.4Hz, 1H); 8.38 (d, *J* = 8.4 Hz, 1H); 8.31 (d, *J* = 7.8 Hz, 1H); 7.89 (s, 2H); 7.69 (dd, J = 7.8 Hz, 1H); 7.62 (s, 2H); 2.66 (s, 3H, C*H*$_3$). ^{13}C NMR (75 MHz, $CDCl_3$): δ 172.7, 155.0, 150.7, 147.2, 146.3, 145.2, 136.7, 136.4, 131.6, 129.9, 129.2, 129.0, 128.0, 126.4, 123.1, 121.4, 113.6, 18.2. Anal. Calc. for $C_{20}H_{12}Br_2ClN_3$ (489.59): C, 49.06; H, 2.47; N, 8.58. Found: C, 49.17; H, 2.49; N, 8.43.

2-Acetyl-1,10-phenanthroline(2,4,6-tribromoanil) (11). In a similar manner as described for **7**, the ligand **11** was prepared as a yellow solid in 22% yield. Mp: 206–208 °C. FT-IR (KBr disc, cm^{-1}): 3066, 1644, 1586, 1551, 1529, 1489, 1450, 1421, 1393, 1363, 1323, 1286, 1225, 1192, 1136, 1114, 1079, 887, 854, 829, 775, 741, 681, 658. ^{1}H NMR (300 MHz, $CDCl_3$): δ 9.25 (d, *J* = 3.3 Hz, 1H); 8.77 (d, *J* = 8.4Hz, 1H); 8.38 (d, *J* = 8.4 Hz, 1H); 8.30 (d, *J* = 7.8 Hz, 1H); 7.88 (s, 2H); 7.75 (s, 2H); 7.68 (dd, *J* = 7.8 Hz, 1H); 2.66 (s, 3H, C*H*$_3$). ^{13}C NMR (100 MHz, $CDCl_3$): δ 172.5, 154.9, 150.7, 147.6, 146.3, 145.2, 136.7, 136.3, 134.3, 129.9, 129.0, 128.0, 126.4, 123.1, 121.3, 116.0, 113.9, 18.2. Anal. Calc. for $C_{20}H_{12}Br_3N_3$ (534.04): C, 44.98; H, 2.26; N, 7.87. Found: C, 45.16; H, 2.32; N, 7.94.

2-Formyl-1,10-phenanthroline(2,6-dimethylanil) (12). In a similar manner as described for **1**, the ligand **12** was prepared as a yellow solid in 78% yield. Mp: 164–166 °C. FT-IR (KBr disc, cm^{-1}): 3513, 3446, 2956, 2917, 1628, 1590, 1556, 1490, 1470, 1394, 1192, 1089, 855, 764, 743. ^{1}H NMR (300 MHz, $CDCl_3$): δ 9.23 (s, 1H); 8.89 (s, 1H, C*H*=N); 8.69 (d, *J* = 8.4 Hz, 1H); 8.32 (d, *J* = 8.4 Hz, 1H); 8.21 (d, J =7.8 Hz, 1H); 7.79 (s, 2H), 7.63 (s, 1H); 7.10 (d, J = 7.2 Hz, 2H); 7.00 (dd, J = 6.9 Hz, 1H); 2.21 (s, 6H, PhC*H*$_3$). ^{13}C NMR (100 MHz, $CDCl_3$): δ 164.3, 154.7, 150.8, 150.5, 146.2, 146.0, 137.0, 136.4, 129.9, 129.1, 128.3, 128.0, 126.7, 126.6, 124.2, 123.4, 120.4, 18.5. Anal. Calc. for $C_{21}H_{17}N_3 \cdot 0.5H_2O$ (320.39): C, 78.72; H, 5.66; N, 13.412. Found: C, 78.23; H, 5.70; N, 12.84.

2-Formyl-1,10-phenanthroline(2,6-diethylanil) (13). In a similar manner as described for **1**, the ligand **13** was prepared as a yellow solid in 70% yield. Mp: 94–96

for references, see page 63

°C. FT-IR (KBr disc, cm^{-1}): 3507, 3436, 2964, 2933, 2875, 1631, 1589, 1556, 1505, 1491, 1454, 1395, 1324, 1185, 1093, 867, 748. ^{1}H NMR (300 MHz, $CDCl_3$): δ 9.31 (dd, *J* = 4.2 Hz, 1H); 8.85 (s, 1H, C*H*=N); 8.72 (d, *J* = 8.4 Hz, 1H); 8.40 (d, *J* = 8.4 Hz, 1H); 8.36 (d, J =7.8 Hz, 1H); 7.90 (s, 2H), 7.72 (dd, *J* = 8.1 Hz, 1H); 7.12 (m, 2H); 6.98 (d, J = 7.5 Hz, 1H); 2.57 (q, *J* = 7.5 Hz, 4H, C*H*$_2$CH$_3$), 1.15 (t, *J* = 7.5 Hz, 6H, CH$_2$C*H*$_3$). ^{13}C NMR (100 MHz, $CDCl_3$): δ163.6, 154.8, 150.2, 149.4, 145.2, 137.1, 136.9, 132.5, 129.9, 129.0, 127.6, 126.8, 126.2, 126.1, 124.3, 123.3, 120.6, 24.7, 14.4. Anal. Calc. for $C_{23}H_{21}N_3$·0.5EtOH (362.47): C, 79.53; H, 6.67; N, 11.59. Found: C, 79.45; H, 6.45; N, 11.47.

2-Formyl-1,10-phenanthroline(2,6-diisopropylanil) (14). In a similar manner as described for **1**, the ligand **14** was prepared as a yellow solid in 88% yield. Mp: 192–194 °C. FT-IR (KBr disc, cm^{-1}): 3426, 3063, 2960, 2868, 1639, 1587, 1555, 1490, 1455, 1395, 1321, 1182, 1090, 859, 787, 751. ^{1}H NMR (300 MHz, $CDCl_3$): δ 9.25 (d, *J* = 1.5 Hz, 1H); 8.84 (s, 1H, C*H*=N); 8.73 (d, *J* = 8.4 Hz, 1H); 8.39 (d, *J* = 8.1 Hz, 1H); 8.29 (d, J =7.8 Hz, 1H); 7.87 (s, 2H), 7.67 (m, 1H); 7.17 (m, 3H); 3.06 (sept, J = 3.3 Hz, 2H, C*H*(CH$_3$)$_2$); 1.17 (d, J = 4.5 Hz, 12H, CH(C*H*$_3$)$_2$). ^{13}C NMR (100 MHz, $CDCl_3$): δ 163.4, 154.6, 150.7, 148.2, 146.1, 145.9, 136.8, 136.3, 129.8, 128.9, 127.8, 126.4, 124.3, 123.4, 123.1, 122.8, 120.4, 27.9, 23.2. Anal. Calc. for $C_{25}H_{25}N_3$ (367.49): C, 81.71; H, 6.86; N, 11.43. Found: C, 81.36; H, 6.82; N, 11.31.

2-Formyl-1,10-phenanthroline(2,6-difluoroanil) (15). In a similar manner as described for **5**, the ligand **15** was prepared as a yellow solid in 36% yield. Mp: 156–158 °C. FT-IR (KBr disc, cm^{-1}): 3072, 3037, 1634, 1584, 1555, 1469, 1397, 1316, 1274, 1239, 1012, 970, 793, 741. ^{1}H NMR (300 MHz, $CDCl_3$): δ 9.32 (s, 1H, C*H*=N); 9.26 (d, *J* = 3.6 Hz, 1H); 8.67 (d, *J* = 8.4Hz, 1H); 8.35 (d, *J* = 8.4 Hz, 1H); 8.28 (d, *J* = 7.5 Hz, 1H); 7.85 (s, 2H); 7.67 (dd, J = 8.1 Hz, 1H); 7.14 (m, 1H); 7.01 (m, 2H). ^{13}C NMR (100 MHz, $CDCl_3$): δ 167.7, 156.5, 152.2, 150.6, 146.0, 145.9, 137.3, 136.7, 131.1, 129.4, 128.0, 126.4, 123.6, 123.2, 120.5, 119.6, 116.5. Anal. Calc. for $C_{19}H_{11}F_2N_3$ (319.31): C, 71.47; H, 3.47; N, 13.16. Found: C, 70.64; H, 3.56; N, 12.76.

2-Formyl-1,10-phenanthroline(2,6-dichloroanil) (16). In a similar manner as described for **5**, the ligand **16** was prepared as a yellow solid in 58% yield. Mp: 116–118 °C. FT-IR (KBr disc, cm^{-1}): 3523, 3419, 1634, 1619, 1586, 1558, 1507, 1492, 1434, 1395, 1216, 1083, 856, 781, 743. ^{1}H NMR (300 MHz, $CDCl_3$): 9.25 (d, *J* = 3.9 Hz, 1H); 9.00 (s, 1H, C*H*=N); 8.70 (d, *J* = 8.1 Hz, 1H); 8.39 (d, *J* = 8.1 Hz, 1H); 8.29 (d, *J* = 8.1 Hz, 1H); 7.87 (s, 2H); 7.68 (dd, J = 7.8 Hz, 1H); 7.38 (d, *J* = 8.1 Hz, 2H);

for references, see page 63

7.04 (t, *J* = 8.1 Hz, 1H). ^{13}C NMR (100 MHz, $CDCl_3$): δ 194.0, 152.2, 150.9, 146.0, 140.0, 137.3, 136.3, 131.1, 129.3, 129.0, 128.3, 127.7, 126.1, 123.6, 119.6, 119.5, 118.0. Anal. Calc. for $C_{19}H_{11}Cl_2N_3$ (352.22): C, 64.79; H, 3.15; N, 11.93. Found: C, 65.14; H, 3.50; N, 11.79.

2-Formyl-1,10-phenanthroline(2,6-dibromoanil) (17). In a similar manner as described for **5**, the ligand **17** was prepared as a yellow solid in 51% yield. Mp: 198–200 °C. FT-IR (KBr disc, cm^{-1}): 3417, 3043, 1639, 1614, 1585, 1550, 1504, 1490, 1451, 1426, 1390, 1334, 1211, 854, 781, 737. ^{1}H NMR (300 MHz, $CDCl_3$): 9.25 (dd, *J* = 4.8 Hz, 1H); 8.93 (s, 1H, C*H*=N); 8.71 (d, *J* = 8.4 Hz, 1H); 8.38 (d, *J* = 8.1 Hz, 1H); 8.27 (dd, *J* = 8.4 Hz, 1H); 7.85 (s, 2H); 7.67 (dd, J = 8.1 Hz, 1H); 7.59 (d, *J* = 8.1 Hz, 2H); 6.89 (t, *J* = 8.1 Hz, 1H). ^{13}C NMR (100 MHz, $CDCl_3$): δ 170.4, 156.0, 153.1, 151.5, 148.4, 148.3, 139.3, 138.7, 134.5, 132.5, 131.3, 130.6, 128.7, 128.6, 125.7, 123.1, 116.6. Anal. Calc. for $C_{19}H_{11}Br_2N_3$ (441.12): C, 51.73; H, 2.51; N, 9.53. Found: C, 51.28; H, 2.45; N, 9.34.

2-Benzoyl-1,10-phenanthroline(2,6-dimethylanil) (18). In a similar manner as described for **7**, the ligand **18** was prepared as a yellow solid in 56% yield. Mp: 206–208 °C. FT-IR (KBr disc, cm^{-1}): 3420, 3057, 2917, 1618, 1589, 1550, 1487, 1446, 1387, 1323, 1208, 1161, 1091, 969, 851, 777, 693. ^{1}H NMR (300 MHz, $CDCl_3$): δ 9.21–6.67 (m, 15H); 2.26 (s, 6H, PhC*H*$_3$). ^{13}C NMR (100 MHz, $CDCl_3$): δ 165.8, 155.6, 150.5, 148.6, 146.2, 145.6, 137.7, 136.4, 135.8, 135.7, 130.8, 129.9, 129.3, 128.9, 128.2, 127.8, 127.4, 127.2, 126.3, 126.1, 125.4, 123.2, 123.0, 122.7, 121.6, 18.9, 18.5. Anal. Calc. for $C_{27}H_{21}N_3$ (387.48): C, 83.69; H, 5.46; N, 10.84. Found: C, 83.56; H, 5.47; N, 10.68.

2-Benzoyl-1,10-phenanthroline(2,6-diethylanil) (19). In a similar manner as described for **7**, the ligand **19** was prepared as a yellow solid in 76% yield. Mp: 178–180 °C. FT-IR (KBr disc, cm^{-1}): 3433, 3058, 2966, 2931, 1618, 1587, 1552, 1489, 1449, 1324, 1159, 964, 854, 695. ^{1}H NMR (300 MHz, $CDCl_3$): δ 9.17–6.80 (m, 15H); 2.85–2.71 (m, 2H, C*H*$_2$CH$_3$); 2.56–2.44 (m, 2H, C*H*$_2$CH$_3$); 1.17 (t, J = 7.5 Hz, 6H, CH$_2$C*H*$_3$). ^{13}C NMR (100 MHz, $CDCl_3$): δ 165.1, 155.5, 150.5, 147.7, 146.3, 145.6, 137.9, 136.5, 135.9, 135.7, 131.9, 130.8, 130.1, 129.5, 129.0, 128.3, 127.9, 127.5, 127.3, 126.3, 125.6, 125.1, 123.7, 123.1, 122.0, 24.9, 24.6, 13.5. Anal. Calc. for $C_{29}H_{25}N_3$ (415.53): C, 83.82; H, 6.06; N, 10.11. Found: C, 83.56; H, 6.10; N, 9.98.

2-Benzoyl-1,10-phenanthroline(2,6-diisopropylanil) (20). In a similar manner as described for **7**, the ligand **20** was prepared as a yellow solid in 82% yield. Mp:

for references, see page 63

224–226 °C. FT-IR (KBr disc, cm^{-1}): 3060, 2963, 1630, 1449, 1285, 1159, 974, 850, 766, 698. ^{1}H NMR (300 MHz, $CDCl_3$): δ 9.21-6.84 (m, 15H); 3.30 (sept, J = 6.6 Hz, 2H, C*H*$(CH_3)_2$); 1.19 (d, J = 6.3 Hz, 6H, CH(C*H*$_3)_2$); 0.98 (d, J = 6.3 Hz, 6H, CH(C*H*$_3)_2$). ^{13}C NMR (100 MHz, $CDCl_3$): 164.2, 155.3, 150.4, 146.1, 145.6, 137.9, 136.4, 135.9, 135.6, 130.6, 129.2, 128.9, 128.2, 127.7, 127.4, 127.2, 126.2, 123.4, 123.0, 122.4, 122.2, 28.4, 24.0, 21.7. Anal. Calc. for $C_{31}H_{29}N_3$ (443.58): C, 83.94; H, 6.59; N, 9.47. Found: C, 82.99; H, 6.59; N, 9.29.

Synthesis of the complexes 1a–20a

General procedure. The ligand and one equivalent of $FeCl_2 \cdot 4H_2O$ were added together in a Schlenk tube that was purged three times with argon and then charged with THF. The reaction mixture was stirred at room temperature for 9 hrs. The resulting precipitate was filtered, washed with diethyl ether and dried in vacuum. All the iron(II) complexes were prepared in high yield in this manner.

2-Acetyl-1,10-phenanthroline(2,6-dimethylanil)$FeCl_2$ (1a). Isolated as a dark blue powder in 96% yield. FT-IR (KBr disc, cm^{-1}): 3436, 3407, 2978, 2915, 1612, 1584, 1512, 1491, 1467, 1406, 1374, 1287, 1209, 1153, 1093, 864, 790, 772, 742, 657. Anal. Calc. for $C_{22}H_{19}Cl_2FeN_3$ (452.16): C, 58.44; H, 4.24; N, 9.29. Found: C, 58.51; H, 4.49; N, 9.07.

2-Acetyl-1,10-phenanthroline(2,6-diethylanil)$FeCl_2$ (2a). Isolated as a dark blue powder in 89% yield. FT-IR (KBr disc, cm^{-1}): 3436, 2965, 2933, 2876, 1609, 1583, 1513, 1493, 1447, 1406, 1374, 1287, 1194, 874, 836, 786, 741, 658. Anal. Calc. for $C_{24}H_{23}Cl_2FeN_3$ (480.21): C, 60.03; H, 4.83; N, 8.75. Found: C, 59.86; H, 4.88; N, 8.58.

2-Acetyl-1,10-phenanthroline(2,6-diisopropylanil)$FeCl_2$ (3a). Isolated as a dark blue powder in 89% yield. FT-IR (KBr disc, cm^{-1}): 3440, 2967, 2928, 2869, 1605, 1512, 1464, 1446, 1407, 1289, 1191, 1146, 850, 789, 759, 655. Anal. Calc. for $C_{26}H_{27}Cl_2FeN_3$ (508.26): C, 61.44; H, 5.35; N, 8.27. Found: C, 61.44; H, 5.58; N, 8.05.

2-Acetyl-1,10-phenanthroline(2,4,6-trimethylanil)$FeCl_2$ (4a). Isolated as a dark blue powder in 63% yield. FT-IR (KBr disc, cm^{-1}): 2915, 1606, 1580, 1513, 1480, 1406, 1286, 1221, 1161, 857, 785, 741, 657. Anal. Calc. for $C_{23}H_{21}Cl_2FeN_3$ (466.18): C, 59.26; H, 4.54; N, 9.01. Found: C, 58.24; H, 4.54; N, 8.56.

2-Acetyl-1,10-phenanthroline(4-bromo-2,6-dimethylanil)$FeCl_2$ (5a). Isolated as a purple powder in 80% yield. FT-IR (KBr disc, cm^{-1}): 3048, 2952, 2911, 1618, 1580, 1515, 1494, 1466, 1436, 1406, 1286, 1206, 854, 796, 738, 657. Anal. Calc. for

for references, see page 63

$C_{22}H_{18}BrCl_2FeN_3$ (531.05): C, 49.76; H, 3.42; N, 7.91. Found: C, 49.89; H, 3.53; N, 7.83.

2-Acetyl-1,10-phenanthroline(2,6-difloroanil)$FeCl_2$ (6a). Isolated as a dark blue powder in 97% yield. FT-IR (KBr disc, cm^{-1}): 3447, 3056, 2969, 2868, 1612, 1587, 1514, 1472, 1405, 1373, 1284, 1241, 1227, 1150, 1061, 1026, 1005, 861, 775, 743, 658. Anal. Calc. for $C_{20}H_{13}Cl_2F_2FeN_3$ (460.08): C, 52.21; H, 2.85; N, 9.13. Found: C, 52.32; H, 3.43; N, 8.83.

2-Acetyl-1,10-phenanthroline(2,6-dichloroanil)$FeCl_2$ (7a). Isolated as a purple powder in 88% yield. FT-IR (KBr disc, cm^{-1}): 3447, 3066, 2992, 2911, 1614, 1580, 1561, 1516, 1495, 1439, 1407, 1376, 1332, 1286, 1231, 1209, 1160, 1150, 1090, 859, 832, 788, 749, 684, 657. Anal. Calc. for $C_{20}H_{13}Cl_4FeN_3 \cdot Et_2O$ (567.11): C, 50.83; H, 4.09; N, 7.41. Found: C, 50.86; H, 3.75; N, 7.49.

2-Acetyl-1,10-phenanthroline(2,6-dibromoanil)$FeCl_2$ (8a). Isolated as a purple powder in 96% yield. FT-IR (KBr disc, cm^{-1}): 3462, 3059, 2969, 2909, 1614, 1578, 1551, 1515, 1493, 1432, 1406, 1376, 1331, 1286, 1266, 1231, 1204, 1150, 863, 833, 784, 732, 658. Anal. Calc. for $C_{20}H_{13}Br_2Cl_2FeN_3$ (581.90): C, 41.28; H, 2.25; N, 7.22. Found: C, 41.07; H, 2.46; N, 7.15.

2-Acetyl-1,10-phenanthroline(2,6-dibromo-4-methylanil)$FeCl_2$ (9a). Isolated as a purple powder in 77% yield. FT-IR (KBr disc, cm^{-1}): 3469, 3057, 2911, 1611, 1579, 1537, 1515, 1492, 1449, 1407, 1376, 1333, 1287, 1235, 1149, 860, 744, 658. Anal. Calc. for $C_{21}H_{15}Br_2Cl_2FeN_3$ (595.92): C, 42.33; H, 2.54; N, 7.05. Found: C, 41.76; H, 2.68; N, 6.77.

2-Acetyl-1,10-phenanthroline(4-chloro-2,6-dibromoanil)$FeCl_2$ (10a). Isolated as a purple powder in 95% yield. FT-IR (KBr disc, cm^{-1}): 3449, 3050, 2910, 1613, 1572, 1539, 1512, 1491, 1433, 1407, 1372, 1288, 1263, 1232, 1155, 1138, 875, 858, 842, 792, 747, 732, 699, 658. Anal. Calc. for $C_{20}H_{12}Br_2Cl_3FeN_3$ (616.34): C, 38.97; H, 1.96; N, 6.82. Found: C, 39.34; H, 2.30; N, 6.44.

2-Acetyl-1,10-phenanthroline(2,4,6-tribromoanil)$FeCl_2$ (11a). Isolated as a gray powder in 80% yield. FT-IR (KBr disc, cm^{-1}): 3450, 3050, 2910, 1613, 1581, 1562, 1538, 1512, 1491, 1430, 1408, 1369, 1288, 1155, 1138, 876, 856, 789, 746, 732, 692, 658. Anal. Calc. for $C_{20}H_{12}Br_3Cl_2FeN_3$ (660.79): C, 36.35; H, 1.83; N, 6.36. Found: C, 35.47; H, 2.11; N, 6.31.

2-Formyl-1,10-phenanthroline(2,6-dimethylanil)$FeCl_2$ (12a). Isolated as a dark blue powder in 94% yield. FT-IR (KBr disc, cm^{-1}): 3436, 3061, 2918, 1607, 1512, 1472,

for references, see page 63

1406, 1297, 1182, 1142, 1117, 1093, 963, 861, 780, 737. Anal. Calc. for $C_{21}H_{17}Cl_2FeN_3$ (438.13): C, 57.57; H, 3.91; N, 9.59. Found: C, 57.09; H, 4.20; N, 9.06.

2-Formyl-1,10-phenanthroline(2,6-diethylanil)$FeCl_2$ (13a). Isolated as a gray blue powder in 63% yield. FT-IR (KBr disc, cm^{-1}): 3436, 3059, 2965, 2934, 1605, 1584, 1514, 1452, 1405, 1177, 1141, 963, 860, 769, 737. $C_{23}H_{21}Cl_2FeN_3$ (466.18): C, 59.26; H, 4.54; N, 9.01. Found: C, 59.05; H, 4.50; N, 8.83.

2-Formyl-1,10-phenanthroline(2,6-diisopropylanil)$FeCl_2$ (14a). Isolated as a dark blue powder in 99% yield. FT-IR (KBr disc, cm^{-1}): 3395, 3.60, 2964, 2868, 1601, 1580, 1514, 1494, 1462, 1447, 1407, 1175, 1117, 849, 806, 766. Anal. Calc. for $C_{25}H_{25}Cl_2FeN_3$ (494.24): C, 60.75; H, 5.10; N, 8.50. Found: C, 60.36; H, 5.49; N, 8.00.

2-Formyl-1,10-phenanthroline(2,6-difluoroanil)$FeCl_2$ (15a). Isolated as a gray green powder in 90% yield. FT-IR (KBr disc, cm^{-1}): 3397, 3060, 3019, 1610, 1588, 1513, 1470, 1434, 1404, 1363, 1342, 1284, 1236, 1198, 1144, 1117, 1058, 1015, 963, 862, 786, 736. Anal. Calc. for $C_{19}H_{11}Cl_2F_2FeN_3$ (446.06): C, 51.16; H, 2.49; N, 9.42. Found: C, 51.17; H, 2.90; N, 9.07.

2-Formyl-1,10-phenanthroline(2,6-dichloroanil)$FeCl_2$ (16a). Isolated as a dark blue powder in 56% yield. FT-IR (KBr disc, cm^{-1}): 3370, 3063, 3005, 1607, 1580, 1563, 1513, 1441, 1405, 1360, 1342, 1297, 1200, 1117, 963, 863, 788, 737, 643. Anal. Calc. for $C_{19}H_{11}Cl_4FeN_3$ (478.97): C, 47.64; H, 2.31; N, 8.77. Found: C, 47.05; H, 2.66; N, 8.30.

2-Formyl-1,10-phenanthroline(2,6-dibromoanil)$FeCl_2$ (17a). Isolated as a dark gray powder in 86% yield. FT-IR (KBr disc, cm^{-1}): 3420, 3058, 1606, 1579, 1555, 1512, 1435, 1405, 1298, 1199, 1142, 1116, 961, 863, 780, 740, 643. Anal. Calc. for $C_{19}H_{11}Br_2Cl_2FeN_3$ (567.87): C, 40.19; H, 1.95; N, 7.40. Found: C, 40.25; H, 2.11; N, 7.35.

2-Benzoyl-1,10-phenanthroline(2,6-dimethylanil)$FeCl_2$ (18a). Isolated as a dark brown powder in 97% yield. FT-IR (KBr disc, cm^{-1}): 3409, 3060, 2908, 1602, 1511, 1492, 1442, 1402, 1297, 1216, 1000, 866, 790, 701. Anal. Calc. for $C_{27}H_{21}Cl_2FeN_3 \cdot 0.5H_2O$ (523.24): C, 61.98; H, 4.24; N, 8.03. Found: C, 61.95; H, 4.05; N, 8.03.

2-Benzoyl-1,10-phenanthroline(2,6-diethylanil)$FeCl_2$ (19a). Isolated as a dark brown powder in 87% yield. FT-IR (KBr disc, cm^{-1}): 3436, 3065, 2972, 1605, 1583, 1508, 1444, 1403, 1284, 1001, 881, 783, 703. Anal. Calc. for $C_{29}H_{25}Cl_2FeN_3$ (542.28): C, 64.23; H, 4.65; N, 7.75. Found: C, 64.04; H, 4.70; N, 7.66.

for references, see page 63

2-Benzoyl-1,10-phenanthroline(2,6-diisopropylanil)$FeCl_2$ (20a). Isolated as a dark brown powder in 64% yield. FT-IR (KBr disc, cm^{-1}): 2964, 2867, 1604, 1586, 1510, 1437, 1402, 1292, 1209, 1112, 999, 863, 783, 701. Anal. Calc. for $C_{31}H_{29}Cl_2FeN_3 \cdot EtOH$ (616.40): C, 64.30; H, 5.72; N, 6.82. Found: C, 64.27; H, 5.27; N, 7.04.

General Procedure for Ethylene Oligomerization

A 250-mL autoclave stainless steel reactor equipped with a mechanical stirrer and a temperature controller was heated in *vacuo* for at least 2 hrs over 80 °C, allowed to cool to the required reaction temperature under ethylene atmosphere, and then charged with toluene, the desired amount of cocatalyt, toluene solution of catalytic precursor, and the total volume was 100 mL. At the reaction temperature, the reactor was sealed and pressurized to 10 atm of ethylene pressure, and the ethylene pressure was kept with feeding of ethylene. After the reaction was carried out for the required time, the pressure was released and a small amount of the reaction solution was collected and terminated by the addition of 5% aqueous hydrogen chloride, which was then analyzed by gas chromatography (GC) for determining the composition and mass distribution of oligomers obtained. Then the residual reaction solution was quenched with 5% hydrochloric acid ethanol (5%). The precipitated low-molecular-weight waxes were collected by filtration, washed with ethanol, dried in vacuum until constant weight.

X-ray Crystallography Measurements

Single-crystal X-ray diffraction studies for **2a** and **8a** were carried out on a Rigaku RAXIS Rapid IP diffractometer with graphite monochromated Mo-Kα radiation (λ = 0.71073 Å). Intensity data for crystals of **4a** and **14a** were collected on a Bruker SMART 1000 CCD diffractometer with graphite monochromated Mo-K_α radiation (λ = 0.71073 Å). And data set for **7a** was collected with a Nonius Kappa CCD diffractometer, equipped with a rotating anode generator Nonius FR591. Cell parameters were obtained by global refinement of the positions of all collected reflections. Intensities were corrected for Lorentz and polarization effects and empirical absorption. The structures were solved by direct methods and refined by full-matrix least-squares on F^2. All non-hydrogen atoms were refined anisotropically. All hydrogen atoms were placed in calculated positions. Structure solution and refinement were performed by using the SHELXL-97 Package.[25] Crystallographic data and processing parameters for complexes **2a**, **4a**, **7a**, **8a** and **14a** are summarized in Table 4.

for references, see page 63

Table 4.
Crystal data and structure refinement for complexes **2a**, **4a**, **7a**, **8a** and **14a.**

Data	**2a**	**4a**	**7a**	**8a**	**14a**
formula	$C_{24}H_{23}Cl_2FeN_3$	$C_{23}H_{21}Cl_2FeN_3$	$C_{20}H_{13}Cl_4FeN_3$	$C_{20}H_{13}Br_2Cl_2FeN_3$	$C_{25}H_{25}Cl_2FeN_3$
Formula weight	480.20	466.18	492.98	581.90	494.23
Temperature (K)	293(2)	293(2)	198(2)	293(2)	293(2)
Crystal system	Triclinic	Monoclinic	Monoclinic	Monoclinic	Orthorhombic
Space group	P-1	P2(1)/c	P2(1)/c	P2(1)/c	Pbca
a (Å)	8.3051(17)	7.8710(5)	7.925(1)	8.0359(16)	14.974(5)
b (Å)	8.9970(18)	20.0610(11)	18.526(1)	18.611(4)	15.993(5)
c (Å)	16.173(3)	13.3304(8)	13.606(1)	13.788(3)	19.474(6)
α (º)	103.05(3)	90.00	90.00	90.00	90.00
β (º)	91.74(3)	104.979(2)	104.17(1)	103.90(3)	90.00
γ (º)	108.94(3)	90.00	90.00	90.00	90.00
Volume ($Å^3$)	1106.4(4)	2033.3(2)	1936.8(3)	2001.8(7)	4663(3)
Z	2	4	4	4	8
D_{calc} (Mg m^{-3})	1.441	1.523	1.691	1.931	1.408
μ (mm^{-1})	0.939	1.019	1.342	5.024	0.893
F(000)	496	960	992	1136	2048
Crystal size (mm)	0.56×0.19×0.10	0.53×0.20×0.12	0.15×0.15×0.10	0.288×0.232×0.211	0.18×0.17×0.15
θ range (º)	1.30-25.01	3.16-27.48	1.90-28.26	1.87-27.48	2.50-27.56
Limiting indices	$0 \le h \le 10$, $-11 \le k \le 10$, $-20 \le l \le 20$	$-10 \le h \le 10$, $-25 \le k \le 26$, $-17 \le l \le 17$	$-10 \le h \le 10$, $-22 \le k \le 24$, $-18 \le l \le 17$	$0 \le h \le 10$, $0 \le k \le 24$, $-17 \le l \le 17$	$-19 \le h \le 14$, $-20 \le k \le 20$, $-25 \le l \le 25$
Reflections collected	4459	4611	15954	4448	5373
Unique reflections	3709	4324	4747	2512	3375
Completeness to θ (%)	92.8(θ = 25.01º)	99.1(θ = 27.48º)	98.8(θ = 28.26º)	96.8(θ = 27.48º)	99.7(θ = 27.56º)
Absorption correction	empirical	empirical	empirical	empirical	empirical
Number of parameters	251	262	254	253	280
Goodness-of-fit on F^2	1.086	0.940	1.030	0.969	1.079
Final R indices [I>2σ(I)]	R1=0.0467, wR2=0.1266	R1=0.0353, *w*R2=0.0947	R1=0.0354, *w*R2=0.0744	R1=0.0561, *w*R2=0.1045	R1=0.0565, *w*R2=0.0925
R indices(all data)	R1=0.0531, wR2=0.1311	R1=0.0379, *w*R2=0.0969	R1=0.0541, *w*R2=0.0811	R1=0.1045, *w*R2=0.1202	R1=0.1102, *w*R2=0.1130
Largest diff. peak, hole ($eÅ^{-3}$)	0.602, -0.470	0.552, -0.537	0.309, -0.382	0.454, -0.582	0.358, -0.274

for references, see page 63

Acknowledgement. The project supported by NSFC Nos.20272062 and 20473099 along with National 863 Project (2002AA333060), and partly sponsored by CNPC Innovation Fund (04E7054). We thank Dr. Jinkui Niu and Mr. Steven Scheltz for English correction.

Supporting Information Available: X-ray crystallographic data (CIF) for complexes **2a**, **4a**, **7a**, **8a** and **14a**. This material is available free of charge via the Internet at http://pubs.acs.org. OM050891P

for references, see page 63

References

(1) Zieger, K.; Martin, H. US 2.943.125, **1954**.

(2) Al-Jarallah, A. M.; Anabtawi, J. A.; Siddiqui, M. A. B.; Aitani, A. M. *Catal. Today* **1992**, *14*, 1-121.

(3) (a) Reagen, W. K. *Am. Chem. Soc. Symp.*, *Division of Petroleum Chemistry* **1989**, *34*, 583, 3. (b) Phillips Petroleum (Reagen, W. K.; Conroy, B. K.), US 5.288.823, **1994**. (c) *Eur. Chem. News* **2000**, 2-8 October, 29.

(4) (a) Bollmann, A.; Blann, K.; Dixon, J. T.; Hess, F. M.; Killian, E.; Maumela, H.; McGuinness, D. S.; Morgan, D. H.; Neveling, A.; Otto, S.; Overett, M. J.; Slawin, A. M. Z.; Wasserscheid, P.; Kuhlmann, S. *J. Am. Chem. Soc.* **2004**, *126*, 14712-14713. (b) Overett, M. J.; Blann, K.; Bollmann, A.; Dixon, J. T.; Hess, F. M.; Killian, E.; Maumela, H.; Morgan, D. H.; Neveling, A.; Otto, S. *Chem. Commun.* **2005**, 622-624.

(5) Vogt, D. In Applied Homogeneous Catalysis with Organometallic Compounds; Cornils, B. Herrmann, W. A., Eds.; VCH: Weinheim, 2002, Vol. 1, pp 240-253.

(6) (a) Keim, W.; Kowaldt, F. H.; Goddard, R.; Kruger, C. *Angew. Chem.* **1978**, *90*, 493-494; *Angew. Chem., Int. Ed. Engl.* **1978**, *17*, 466-468. (b) Keim, W.; Behr, A.; Limbacker, B.; Kruger, C. *Angew. Chem., Int. Ed. Engl.* **1983**, *22*, 503. (c) Keim, W.; Behr, A.; Kraus, G. *J. Organomet. Chem.* **1983**, *251*, 377-391. (d) Grenouillet, P.; Neibecker, D.; Tkatchenko, I. *J. Organomet. Chem.* **1983**, *243*, 213-222. (e) Peuckert, M.; Keim, W. *Organometallics* **1983**, *2*, 594-597. (f) Peuckert, M.; Keim, W. *J. Mol. Catal.* **1984**, *22*, 289-295. (g) Keim, W. *New J. Chem.* **1987**, *11*, 531-534. (h) Klabunde, U.; Itten, S. D. *J. Mol. Catal.* **1987**, *41*, 123-134. (i) Ostoja Starzewski, K. A.; Witte, J. *Angew. Chem.* **1987**, *99*, 76-77; *Angew. Chem., Int. Ed. Engl.* **1987**, *26*, 63-74. (j) Keim, W. *Angew. Chem.* **1990**, *102*, 251-260; *Angew. Chem., Int. Ed. Engl.* **1990**, *29*, 235-244. (k) Hirose, K.; Keim, W. *J. Mol. Catal.* **1992**, *73*, 271-276. (l) Keim, W. *Macromol. Chem. Macromol. Symp.* **1993**, *66*, 225-230; (m) Matt, D.; Huhn, M.; Fischer, J.; De Cian, A.; Kläui, W.; Tkatchenlo, I.; Bonnet, M. C. *J. Chem. Soc. Dalton Trans.* **1993**, 1173-1178. (n) Keim, W.; Schulz, R. P. *J. Mol. Catal.* **1994**, *92*, 21-33. (o) Braunstein, P.; Chauvin, Y.; Mecier, S.; Saussine, L.; De Cian, A.; Fischer, J. *J. Chem. Soc. Chem. Commun.* **1994**, 2203-2204.

(7) (a) Svejda, S. A.; Brookhart, M. *Organometallics* **1999**, *18*, 65-74. (b) Killian, C. M.; Johnson, L. K.; Brookhart, M. *Organometallics* **1997**, *16*, 2005-2007.

(8) (a) van den Beuken, E. K.; Smeets, W. J. J.; Spek, A. L.; Feringa, B. L. *Chem. Commun.* **1998**, 223-224. (b) Guan, Z.; Marshall, W. J. *Organometallics* **2002**, *21*, 3580-3586.

(9) Small, B. L.; Brookhart, M.; Bennett, A. M. A. *J. Am. Chem. Soc*. **1998**, *120*, 4049-4050.

(10) Britovsek, G. J. P.; Gibson, V. C.; Kimberley, B. S.; Maddox, P. J.; McTavish, S. J.; Solan, G. A.; White, A. J. P.; Williams, D. J. *Chem. Commun.* **1998**, 849-850.

(11) (a) Small, B. L.; Brookhart, M. *J. Am. Chem. Soc*. **1998**, *120*, 7143-7144. (b) Britovsek, G. J. P.; Bruce, M.; Gibson, V. C.; Kimberley, B. S.; Maddox, P. J.; Mastroianni, S.; McTavish, S. J.; Redshaw, C.; Solan, G. A.; Stromberg, S.; White, A. J. P.; Williams, D. J. *J. Am. Chem. Soc.* **1999**, *121*, 8728-8740. (c) Britovsek, G. J. P.; Mastroianni, S.; Solan, G. A.; Baugh, S. P. D.; Redshaw, C.; Gibson, V. C.; White, A. J. P.; Williams, D. J.; Elsegood, M. R. J. *Chem. Eur. J.* **2000**, *6*, 2221-2231. (d) Chen, Y.; Chen, R.; Qian, C.; Dong, X.; Sun, J. *Organometallics* **2003**, *22*, 1231-1236. (e) Chen, Y.; Chen, R.; Qian, C.; Dong, X.; Sun, J. *Organometallics* **2003**, *22*, 4312-1321.

(12) (a) Qian, M.; Wang, M.; He, R. *J. Mol. Cat. A.* **2000**, *160*, 243-247. (b) Qian, M.; Wang, M.; Zhou, B.; He, R. *Appl. Cat. A.* **2001**, *209*, 11-15. (c) LePichon, L.;

Stephan, D. W.; Gao, X.; Wang, Q. *Organometallics* **2002,** *21,* 1362-1366. (d) Bianchini, C.; Mantovani, G.; Meli, A.; Migliacci, F.; Laschi, F. *Organometallics* **2003**, *22,* 2545-2547. (e) Zhou, M.-S.; Huang, S.-P.; Weng, L.-H.; Sun, W.-H.; Liu, D.-S. *J. Organomet. Chem.* **2003**, *665*, 237-245. (f) Britovsek, G. J. P.; Gibson, V. C.; Hoarau, O. D.; Spitzmesser, S. K.; White, A. J. P.; Williams, D. J. *Inorg. Chem.* **2003**, *42*, 3454-3465. (g) Cowdell, R.; Davies, C. J.; Hilton, S. J.; Maréchal, J-D; Solan, G. A.; Thomas, O.; Fawcett, J. *Dalton Trans.* **2004**, 3231-3240.

(13) Wang, L.; Sun, W. -H.; Han, L.; Yang, H.; Hu, Y.; Jin, X. *J. Organomet. Chem.* **2002**, *658*, 62-70.

(14) Britovsek, G. J. P.; Baugh, S. P. D.; Hoarau, O.; Gibson, V. C.; Wass, D. F.; White, A. J. P.; Williams, D. J. *Inorg. Chim. Acta* **2003**, *345*, 279-291.

(15) Ameerunisha, S.; Schneider, J.; Meyer, T.; Zacharias, P. S.; Bill, E.; Henkel, G. *Chem. Commun.* **2000**, 2155-2156.

(16) Corey, E. J.; Borror, A. L.; Foglia, T. *J. Org. Chem.* **1965**, *30*, 288-290.

(17) Sigman, D. S.; Wahl, G. M.; Greighton, D. J. *Biochemistry* **1972**, *11*, 2236-2242.

(18) Greighton, D. J.; Hajdu, J.; Sigman, D. S. *J. Am. Chem. Soc.* **1976**, 4619-4624.

(19) (a) Backeberg, O. G.; Ataskun, B. *J. Chem. Soc.* **1962**, 3961-3963. (b) Staskun, B.; Backeberg, O. G. *J. Chem. Soc.* **1964**, 5880-5881. (c) van Es, T.; Staskun, B. *J. Chem. Soc.* **1965**, 5775-5777.

(20) Case, F. H.; Schilt, A. A. *J. Heterocyclic Chem.* **1979**, *16*, 1135-1139.

(21) (a) Evans, D. F. *J. Chem. Soc.* **1959**, 2003-2005. (b) Löliger, J.; Scheffold, R. *J. Chem. Educ.* **1972**, *49*, 646-647. (c) Sur, S. K. *J. Magn. Reson.* **1989**, *82*, 169-173.

(22) (a) Schulz, G. V. Z. *Phys. Chem., Abt. B* **1935**, 30, 379-398. (b) Schulz, G. V. Z. *Phys. Chem., Abt. B* **1939**, 43, 25-46. (c) Flory, P. J. *J. Am. Chem. Soc.* **1940**, 62, 1561-1565. (d) Henrici-Olivé, G.; Olivé, S. *Adv. Polym. Sci.* **1974**, 15, 1-30.

(23) Galland, G. B.; De Souza, R. F.; Mauler, R. S.; Nunes, F. F. *Macromolecules* **1999**, *32*, 1620-1625.

(24) Galland, G. B.; Quijada, R.; Rojas, R.; Bazan, G. C.; Komon, Z. J. A. *Maromolecules* **2002**, *35*, 339-345.

(25) G.M. Sheldrick, SHELXTL-97, Program for the Refinement of Crystal Structures, University of Gottingen: Germany, 1997.

Chapitre III

Complexes 2-imino-1,10-phénanthrolinyl du cobalt et leur application en catalyse d'oligomerization de l'éthylène

Abstract of Chapter III

A series of cobalt(II) complexes containing 2-imino-1,10-phenanthrolines have been synthesized and characterized by elemental and spectroscopic analysis. The molecular structures of complexes **2**, **3**, **8** and **14** were confirmed by X-ray diffraction analysis. On treatment with methylaluminoxane (MAO) or modified methylaluminoxane (MMAO), these cobalt(II) complexes show moderate to high catalytic activities for ethylene oligomerization and butene predominates among the oligomers produced. The parameters of the reaction conditions and the effects of the ligands environment were investigated.

This chapter has been published. I synthesized most of complexes, carried out all the catalytic experiments and prepared the manuscript. This work has been done in collaboration with Shu Zhang and Dr. Wen Zhang.

Cobalt(II) Complexes Bearing 2-Imino-1,10-phenanthroline Ligands: Synthesis, Characterization and Ethylene Oligomerization

C. R. Chim. **2006**, *9*, 1500–1509.

Suyun Jie[†], Shu Zhang[†], Katrin Wedeking[†], Wen Zhang[†], Hongwei Ma[†], Xiaoming Lu[‡], Yuan Deng[‡] and Wen-Hua Sun[†,*]

[†] *Key Laboratory of Engineering Plastics and Beijing National Laboratory for Molecular Sciences, Institute of Chemistry, Chinese Academy of Sciences, Beijing 100080, China;*

[‡] *Department of Chemistry, Capital Normal University, Beijing 100037, China*

Cobalt(II) Complexes Bearing 2-Imino-1,10-phenanthroline Ligands: Synthesis, Characterization and Ethylene Oligomerization

Introduction

The oligomerization of ethylene represents one of major industrial processes [1]. Linear α-olefin oligomers with relatively short chain lengths are commonly used as comonomers for the preparation of linear low-density polyethylene (LLDPE). The selective dimerization reaction was first achieved in 1954 by *Ziegler* [2] and later the selectivity was improved by modification of the catalysts and optimization of the reaction conditions [3]. Until now, many efforts are still devoted to the development of highly active and selective ethylene oligomerization catalysts. The independent discovery by *Brookhart* [4] and *Gibson* [5] of highly active bis(imino)pyridyl iron- and cobalt-based catalysts for ethylene polymerization and oligomerization in 1998 has led to high interests in the catalytic chemistry of late-transition metal complexes bearing tridentate ligands [6]. Since that, many studies have been reported about the effects of ligand environment on activity, selectivity and the property of the products [7]. For the tridentate bis(imino)pyridyl ligands, it has generally been found that cobalt-based catalysts are at least an order of magnitude less active than their iron analogues. Furthermore, complexes bearing other tridentate ligands commonly lead to less catalytic activity for ethylene activation [8]. On the other hand, there were also cobalt complexes reported bearing bidentate ligands for ethylene oligomerization, such as dimine [9], 2-(2-pyridyl)quinoxaline [10], β-diketiminate [11], 2-(carbethoxy)-6-iminopyridine [12], 6-(organyl)-2-(imino)pyrine [13]. Again, those catalytic systems showed considerable to good catalytic activity for ethylene reactivity.

We previously reported that cobalt complexes ligated by 2,9-bis(imino)-1,10-phenanthrolines showed much higher activity than their iron analogues [14]. This unusual behavior was different from the bis(imino)pyridine systems. In order to eliminate the coordination effect of the additional imino group on the active center and improve the catalytic properties, 2-imino-1,10-phenanthroline ligands were synthesized and their iron(II) complexes were shown to be highly active catalysts with high

for references, see page 82

selectivity for ethylene oligomerization [15]. Extensive investigations on other late-transition metal complexes and their catalytic properties have also been carried out and nickel analogues showed high activity for ethylene oligomerization [16].

During the course of the preparation of this manuscript, the *Solan* group reported a series of 2-imino-1,10-phenanthroline cobalt(II) chloride complexes in which the steric bulk of the *ortho*-aryl substitution pattern has been kept constant and the electronic properties of the *para*-substituents were systematically varied for aldimine- and ketimine-based ligands [17]. Treatment of these complexes with excess methylaluminoxane (MAO) yields modestly active catalysts for the oligomerisation of ethylene (1 atm) which afford mainly linear α-olefins along with some degree of internal olefins. The nature of the *para*-position substitution pattern has little effect on the activity of the catalyst but does influence internal olefin ratio.

Herein we report our recent studies on a series of cobalt(II) complexes bearing 2-imino-1,10-phenanthroline ligands as active catalytic precursors for ethylene oligomerization. At variance with the work of the *Solan* group, the steric and electronic properties of the *ortho*-substituents have been changed systematically. Our work demonstrates the differences on catalytic performance between iron and cobalt complexes as well as the effects of the ligand backbone. Reaction parameters, such as different co-catalysts, Al/Co molar ratio, reaction temperature and ethylene pressure have also been studied and their effects on the catalytic activity will be discussed.

Results and Discussion

Synthesis and characterization

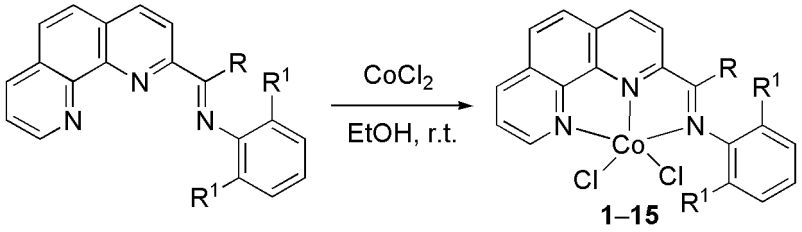

	1	2	3	4	5	6	7	8	9	10	11	12	13	14	15
R	H	H	H	H	H	H	Me	Me	Me	Me	Me	Me	Ph	Ph	Ph
R^1	Me	Et	i-Pr	F	Cl	Br	Me	Et	i-Pr	F	Cl	Br	Me	Et	i-Pr

Scheme 1.
Synthesis of cobalt complexes **1**–**15**.

All used 2-imino-1,10-phenanthroline ligands were synthesized according to our previous report [15]. The cobalt complexes **1**–**15** were easily prepared by mixing an

for references, see page 82

ethanol solution of the corresponding ligand and one equivalent of $CoCl_2$ at room temperature (Scheme 1). The resulting precipitate was separated from the reaction solution by filtration, washed with diethylether and dried in vacuum as air-stable powders. All the obtained cobalt complexes were characterized by FT-IR spectra and elemental analysis. In the IR spectra of these complexes, the stretching vibration bands of C=N was shifted to lower wave numbers and the peak intensity was greatly reduced when compared with the free ligands [15], thus demonstrating coordination of the imino nitrogen atom to the cobalt atom. The molecular structures of **2**, **3**, **8**, and **14** were determined by single-crystal X-ray diffraction analysis.

Single crystals of complexes **2**, **3**, **8** and **14** suitable for X-ray diffraction analysis were obtained by slow diffusion of diethylether into their methanol solutions. In these four cobalt complexes, the coordination geometry around the cobalt center can be regarded as a distorted trigonal bipyramidal in which the equatorial plane includes one nitrogen atom (next to the imino-C) of phenanthroline and two chlorine atoms. The asymmetric unit of complex **2**, however, contains the halves of two independent, nearly identical molecules (Figure 1) whereas one molecular structure can be found in the asymmetric unit of complex **3**, **8**, **14** (Figure 2–5, respectively). Their selected bond lengths and bond angles are listed in Tables 1 and 2.

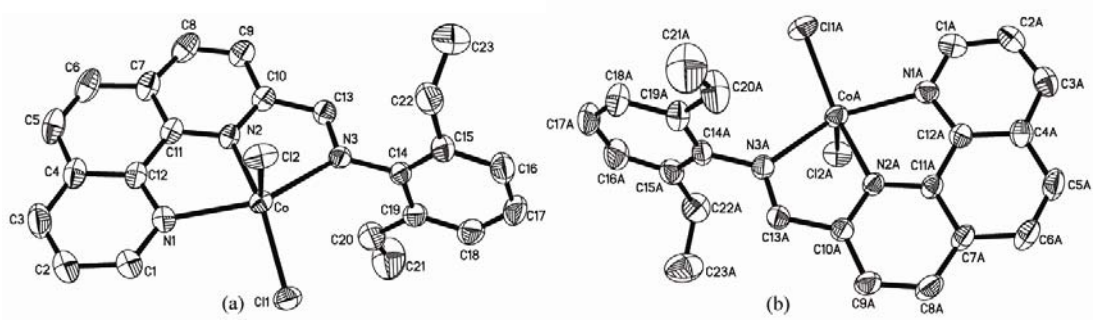

Figure 1.
Crystal structure of complex **2** showing the two independent molecules of the asymmetric unit. Displacement ellipsoids are drawn at 30%.

In the structure of complex **2**, the two independent molecules give slightly different bond lengths and bond angles (Table 1). In molecule (a), the cobalt center slightly deviates by 0.062 Å from the triangular plane formed by N2, Cl1 and Cl2, while this deviation is 0.035 Å in molecule (b). Furthermore, differences are observed for the dihedral angles between the equatorial plane and the phenanthroline plane, the phenyl ring attached to the imino-N and the phenanthroline plane (69.9º and 83.7º in (a), however, 94.9º and 74.4º in (b), respectively). In both molecules, the bond angles subtended by the axial Co–N bonds are 148.87(9)º (N(1)–Co–N(3)) and 145.26(8)º

for references, see page 82

(N(1A)–CoA–N(3A)), respectively. The Co–N distance in the equatorial plane and the imino C=N distance are nearly identical. In each molecule, the Co–N bond in the equatorial plane is shorter than that of the two axial Co–N bonds and the two Co–Cl bond distances show a slight difference, which is very similar to the situation in the iron(II) analogues [15].

Table 1.
Selected bond lengths (Å) and angles (º) for complex **2**.

Bond lengths			
Co–N(1)	2.199(2)	CoA–N(1A)	2.217(2)
Co–N(2)	2.035(2)	CoA–N(2A)	2.039(2)
Co–N(3)	2.293(2)	CoA–N(3A)	2.256(2)
Co–Cl(1)	2.251(1)	CoA–Cl(1A)	2.245(1)
Co–Cl(2)	2.270(1)	CoA–Cl(2A)	2.292(1)
N(3)–C(13)	1.277(3)	N(3A)–C(13A)	1.273(3)
Bond angles			
N(2)–Co–N(1)	76.58(9)	N(2A)–CoA–N(1A)	75.47(8)
N(2)–Co–N(3)	74.03(8)	N(2A)–CoA–N(3A)	73.80(8)
N(1)–Co–N(3)	148.87(9)	N(1A)–CoA–N(3A)	145.26(8)
N(1)–Co–Cl(1)	95.17(6)	N(1A)–CoA–Cl(1A)	95.67(6)
N(2)–Co–Cl(1)	143.28(6)	N(2A)–CoA–Cl(1A)	149.17(6)
N(3)–Co–Cl(1)	102.22(5)	N(3A)–CoA–Cl(1A)	102.44(6)
N(1)–Co–Cl(2)	94.96(7)	N(1A)–CoA–Cl(2A)	100.49(6)
N(2)–Co–Cl(2)	100.58(6)	N(2A)–CoA–Cl(2A)	96.19(6)
N(3)–Co–Cl(2)	100.24(5)	N(3A)–CoA–Cl(2A)	98.56(6)
Cl(1)–Co–Cl(2)	115.88(3)	Cl(1A)–CoA–Cl(2A)	114.55(3)

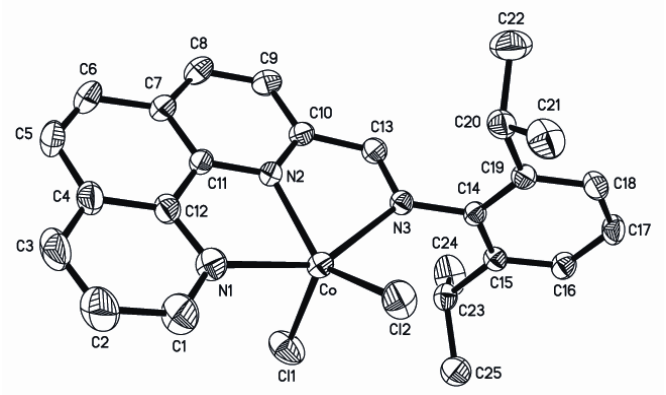

Figure 2.
Crystal structure of complex **3** with thermal ellipsoids at 30% probability level.

Unlike complex **2**, one complex molecule is found in the asymmetric unit of complex **3** (Figure 2). The cobalt atom is almost coplanar with the equatorial plane composed by N2, Cl1 and Cl2 with the deviation of 0.005 Å. The equatorial angles are 104.54(5)º, 137.24(5)º and 118.22(3)º, respectively and the axial Co–N bonds form a N(1)–Co–N(3) angle of 147.79(7)º. The dihedral angle between the equatorial plane and the phenanthroline plane is 73.0º, largely deviating from 90º. The phenyl ring on the imino-C is nearly perpendicular to the phenanthroline plane with a dihedral angle of 91.5º. The Co–N(2) bond (2.047(2) Å) on the equatorial plane is obviously shorter than the axial Co–N(1) (2.225(2) Å) and Co–N(3) (2.310(2) Å) bonds. The two Co-Cl bond

for references, see page 82

lengths show a slight difference: Co–Cl(1) = 2.2546(7) Å and Co–Cl(2) = 2.233(1) Å). The imino N(3)–C(13) bond length of 1.267(3) Å, which indicates a typical C=N double-bond character, is relatively shorter than that in other cobalt analogues, which is probably ascribed to the less bulky hydrogen atom on the imino-C and the bulkier isopropyl groups at the *ortho*-position of the phenyl ring on the imino-N.

Table 2.
Selected bond lengths (Å) and angles (º) for complexes **3**, **8** and **14**.

	3	**8**	**14**
Bond lengths			
Co–N(1)	2.225(2)	2.244(2)	2.223(1)
Co–N(2)	2.047(2)	2.055(2)	2.053(1)
Co–N(3)	2.310(2)	2.254(2)	2.316(1)
Co–Cl(1)	2.255(1)	2.264(1)	2.259(1)
Co–Cl(2)	2.233(1)	2.282(1)	2.255(1)
N(3)–C(13)	1.267(3)	1.284(3)	1.281(3)
Bond angles			
N(2)–Co–N(1)	75.91(7)	75.42(8)	76.27(7)
N(2)–Co–N(3)	73.47(6)	73.61(8)	72.88(7)
N(1)–Co–N(3)	147.79(7)	146.64(7)	148.62(7)
N(1)–Co–Cl(1)	94.77(5)	98.96(6)	96.37(6)
N(2)–Co–Cl(1)	104.54(5)	99.64(7)	112.88(6)
N(3)–Co–Cl(1)	102.29(5)	98.12(6)	100.69(6)
N(1)–Co–Cl(2)	99.06(6)	97.73(6)	96.55(6)
N(2)–Co–Cl(2)	137.24(5)	149.72(6)	132.63(6)
N(3)–Co–Cl(2)	96.63(5)	102.73(6)	100.02(5)
Cl(1)–Co–Cl(2)	118.22(3)	110.60(3)	114.44(3)

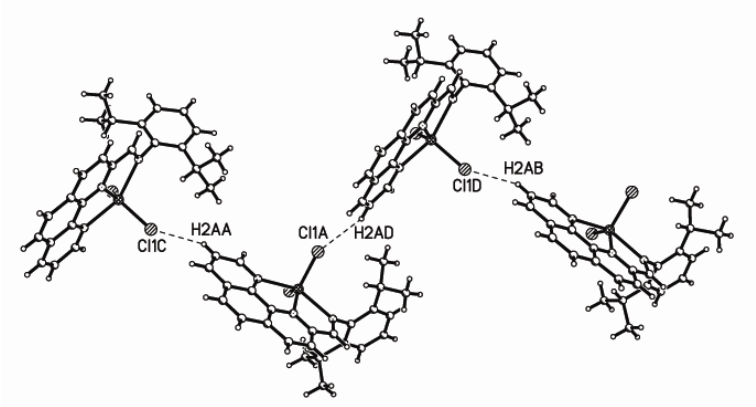

Figure 3.
The 1-D chain formed by intermolecular hydrogen bonding interactions (H2A···Cl1) in complex **3**.

In the solid state, complex **3** displays intermolecular hydrogen bonding interactions between one chlorine atom (Cl1) and one hydrogen atom (H(2A)) of the phenanthroline from another molecule. Hydrogen bonding between two neighboring molecules results in a 1-D infinite zigzag chain, as shown in Figure 3. The hydrogen bond angle of C2–H2A···Cl1 is 144.87º and the distances of H2A···Cl1 and C(2)···Cl1 are 2.757 and 3.558 Å, respectively.

In complex **8** (Figure 4), one nitrogen atom (N2) of the phenanthroline and two chlorine atoms form the equatorial plane, and the cobalt atom deviates slightly by 0.023

for references, see page 82

Å from this plane. The three equatorial angles N(2)–Co–Cl(1), N(2)–Co–Cl(2) and Cl(1)–Co–Cl(2) are respectively 99.64(7), 149.72(6) and 110.60(3)º whereas the axial Co–N bonds form an angle of 146.64(7)º. The equatorial plane is almost perpendicular to the phenanthroline plane with a dihedral angle of 91.8º and the phenyl ring on the imino-N and the phenanthroline plane form a dihedral angle of 77.0º. The two axial Co–N bond lengths, 2.244(2) and 2.254(2) Å, are longer by about 0.19 Å than that in the equatorial plane (Co–N(2) = 2.055(2) Å). The imino N(3)–C(13) bond length of 1.284(3) Å indicates a typical C=N double bond character, but is slightly longer than that in the corresponding aldimine complex **2**, which is probably due to the relatively bulky methyl on the imino-C.

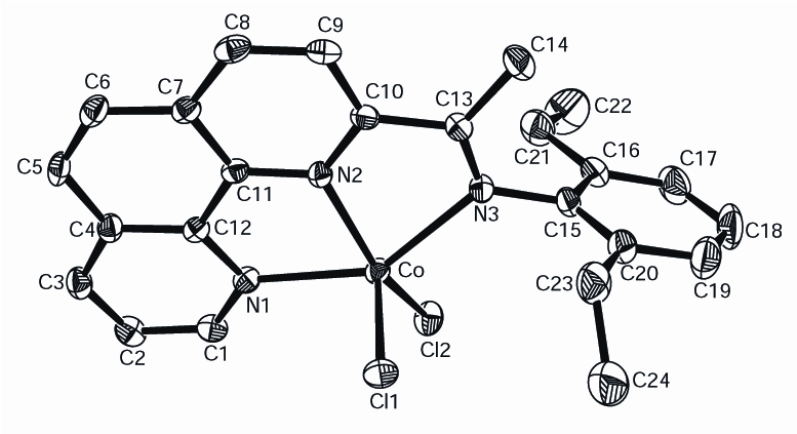

Figure 4.
Crystal structure of complex **8** with thermal ellipsoids at 30% probability level and all hydrogen atoms omitted for clarity.

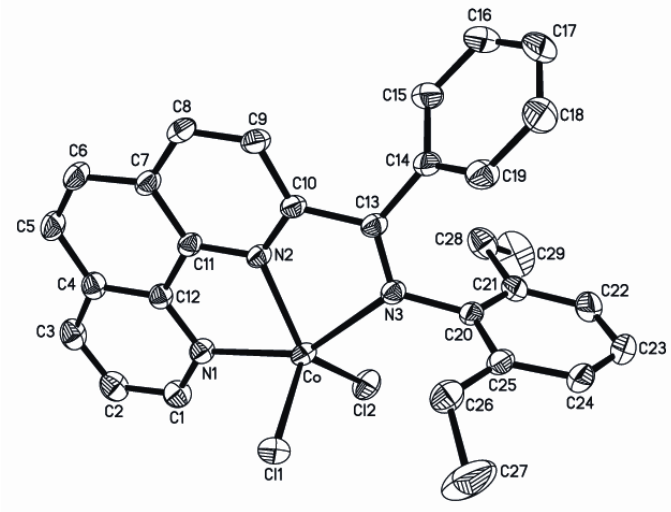

Figure 5.
Crystal structure of complex **14** with thermal ellipsoids at 30% probability level and all hydrogen atoms omitted for clarity.

In the structure of **14** (Figure 5), the cobalt atom slightly deviates by 0.0257 Å from the triangular plane of N2, Cl1 and Cl2 with equatorial angle ranging from 112.88(6)º and 132.63(6)º. This equatorial plane is nearly perpendicular to the

for references, see page 82

phenanthroline plane with a dihedral angle of 87.6º. The dihedral angles between the two phenyl rings, the phenyl ring on the imino-N and the phenanthroline plane are 82.9º and 93.6º, respectively. The Co–N(2) bond (2.053(2) Å) is much shorter than the axial bonds Co–N(1) (2.223(2) Å) and Co–N(3)(imino) (2.316(2) Å). The imino N(3)–C(13) bond length of 1.281(3) Å is similar to that in the corresponding methyl ketimine complex **8** but slightly longer than in the aldimine complex **2**.

Ethylene Oligomerization

Table 3.
The results of ethylene oligomerization by complexes **1**–**15** at 1 atm of ethylene.[a]

entry	complex	co-cat	Al/Co	T[b] (°C)	activity[c]	Oligomers distribution[d] (%)	
						C_4	C_6
1	**15**	Al(i-Bu)$_3$	500	20	0.652	100	-
2	**15**	MAO	250	20	0.822	95.4	4.6
3	**15**	MAO	500	20	1.19	95.3	4.7
4	**15**	MAO	1000	20	0.962	93.7	6.3
5	**15**	MMAO	100	20	1.17	95.5	4.5
6	**15**	MMAO	250	20	2.28	95.3	4.7
7	**15**	MMAO	500	20	3.53	94.5	5.5
8	**15**	MMAO	1000	20	7.00	94.2	5.8
9	**15**	MMAO	1500	20	4.15	95.2	4.8
10	**15**	MMAO	2000	20	4.05	92.9	5.1
11	**15**	MMAO	2500	20	3.98	93.7	6.3
12	**15**	MMAO	1000	0	3.14	95.9	4.1
13	**15**	MMAO	1000	40	4.03	97.2	2.8
14	**15**	MMAO	1000	60	1.21	100	-
15	**1**	MMAO	1000	20	1.58	100	-
16	**2**	MMAO	1000	20	1.93	99.5	0.5
17	**3**	MMAO	1000	20	2.65	100	-
18	**4**	MMAO	1000	20	1.46	100	-
19	**5**	MMAO	1000	20	2.95	100	-
20	**6**	MMAO	1000	20	3.23	99.4	0.6
21	**7**	MMAO	1000	20	1.93	100	-
22	**8**	MMAO	1000	20	2.34	97.5	2.5
23	**9**	MMAO	1000	20	2.57	99.3	0.7
24	**10**	MMAO	1000	20	1.66	100	-
25	**11**	MMAO	1000	20	2.16	99.2	0.8
26	**12**	MMAO	1000	20	4.18	97.0	3.0
27	**13**	MMAO	1000	20	3.08	97.3	2.7
28	**14**	MMAO	1000	20	3.60	98.0	2.0

[a] General conditions: complex: 5 μmol; solvent: toluene (30 ml); reaction time: 30 min. [b] Reaction temperature. [c] The unit of activity: 10^5 g mol^{-1} h^{-1}. [d] Determined by GC.

Various aluminum-based cocatalysts were used for exploring the catalytic activity of the cobalt complexes. When diethylaluminum chloride or ethylaluminum dichloride was used as a co-catalyst, only low catalytic activity (less than 10^4 g mol^{-1} h^{-1}) was observed. Considerable to good activities were obtained with methylaluminoxane (MAO), modified methylaluminoxane (MMAO) and triisobutylaluminum (Al(i-Bu)$_3$) as cocatalysts. Complex **15** was typically investigated under a range of reaction conditions, such as different co-catalysts, molar ratio of co-catalyst to cobalt and reaction

for references, see page 82

temperature at 1 atm of ethylene. The best catalytic activity (more than 10^5 g mol^{-1} h^{-1}) was observed upon activation with MMAO which was therefore used extensively. Butenes predominate among the oligomers produced. The results for ethylene oligomerization are summarized in Table 3.

(i) Effects of the molar ratio of Al/Co and reaction temperature

Upon activation with MAO, complex **15** showed the highest catalytic activity at the Al/Co molar ratio of 500. However, when MMAO was employed as a co-catalyst and the Al/Co molar ratio was changed from 100 to 2500, the catalytic activity of **15** firstly increased and then decreased and displayed the maximum at the Al/Co molar ratio of 1000. Between 1500 and 2500 almost no change in activity could be observed. The variation of the Al/Co molar ratio had no large influence on the distribution of oligomers.

With a fixed Al/Co molar ratio of 1000 using MMAO, the reaction temperature largely affected the catalytic activity. The highest activity was obtained at 20 °C (entry 8, Table 3). Higher reaction temperatures led to a large decrease in the catalytic activity (entry 14, Table 3), most likely due to the deactivation of some active centers and the lower solubility of ethylene in toluene.

(ii) Effect of the ligands environment

To compare the effect of the ligand environment on the catalytic activity, all cobalt complexes **1**–**15** were investigated under the same conditions (Al/Co molar ratio of 1000 and 20 °C). The 2,6-diisopropyl-substituted phenyl-ketimine complex **15** showed the highest catalytic activity (entry 8, Table 3).

Variation of the R substituent on the imino-C resulted in a change of the catalytic activity. For the complexes bearing the same alkyl groups at the *ortho*-positions of the imino-N aryl ring, the catalytic activities increased in turn according to aldimine (R = H), methyl-ketimine (R = Me) and phenyl-ketimine (R = Ph) complexes (Ph > Me > H). This trend was found to be different from the related iron systems.[15] Furthermore aldimine as well as ketimine complexes bearing bulky substituents on the *ortho*-position of the imino-N aryl ring displayed the highest catalytic activities (isopropyl > ethyl > methyl groups). For the cobalt complexes bearing 2,6-dihalogen-substituted ligands, the bulkiness and electronegativity of the halogen atoms had large influence on the catalytic activity. For both aldimine and methyl-ketimine complexes with the bulky and moderately electronegative bromine atoms at the *ortho*-position of the imino-N aryl ring, the catalytic activities were found to be highest (bromo- > chloro- > fluoro-, entry

for references, see page 82

18–20 and 24–26 in Table 3). Except for the 2,6-dichloro-substituted complexes, methyl-ketimine complexes showed higher catalytic activity than the corresponding aldimine complexes. Cobalt complexes bearing electron-withdrawing halogen groups displayed comparable catalytic activities and produced similar oligomeric products as the complexes bearing electron-donating alkyl groups. The substituents' effect was not so clearly observed in the recent paper by *Solan*,[17] possibly because of the fixed bulky *ortho*-isopropyl group and a weaker influence of the *para* substituents of the imino-N aryl ring.

(iii) Effect of ethylene pressure

Table 4.
The results of ethylene oligomerization by complexes **1**–**6** and **13**–**15** at 10 atm of ethylene.[a]

entry	complex	activity[b]	Oligomers distribution[c] (%)		
			C_4	C_6	$C_{\geq 8}$
1[d]	**15**	23.4	93.4	6.6	-
2	**15**	14.6	64.2	35.0	0.8
3	**1**	6.70	97.7	2.0	0.3
4	**2**	12.0	97.6	1.6	0.8
5	**3**	12.6	94.1	5.2	0.7
6	**4**	1.26	97.6	2.4	-
7	**5**	11.8	98.6	1.4	-
8	**6**	10.2	96.8	3.2	-
9	**13**	9.95	98.1	1.9	-
10	**14**	10.4	97.0	3.0	-

[a] General conditions: complex: 5 μmol; solvent: toluene (100 ml); co-cat: MAO; molar ratio of Al/Co: 500; reaction temperature: 40 °C; reaction time: 60 min. [b] The unit of activity: 10^5 g mol^{-1} h^{-1}. [c] Determined by GC. [d] co-cat: MMAO; molar ratio of Al/Co: 1000; reaction temperature: 20 °C; reaction time: 30 min.

Firstly the catalytic performances of complex **15** were investigated using MMAO or MAO as co-catalyst at 10 atm of ethylene. The catalytic activity increased more than three times under similar conditions when MMAO was used as co-catalyst, but a higher pressure seems to have almost no influence on the oligomeric products formed. However, when the catalyst precursor was activated with MAO, the consumption of ethylene was observed to last for a longer time, consistent with a longer lifetime of the active species. The catalytic activity increased about 10 times, up to 1.46×10^6 g mol^{-1} h^{-1} in 60 min, compared with the result at 1 atm after 30 min (entry 2 in Table 4 and entry 3 in Table 3). More importantly, the amount of C_6 products among the oligomers increased up to 35 wt%. Therefore complexes **1**–**6** and **13**–**14** were also investigated in the presence of MAO and the results are summarized in Table 4. Except for the 2,6-difluoro-substituted aldimine complex **4**, these complexes showed higher catalytic activities under 10 atm of ethylene, but they are about one order of magnitude less

for references, see page 82

active than their corresponding iron analogues under similar conditions [15]. Furthermore at 10 atm for the 2,6-dialkyl-substituted aldimine complexes **1**–**3** and phenyl-ketimine complexes **13**–**15**, the same activity pattern was observed at 1 atm of ethylene pressure. The complexes with bulky isopropyl groups showed higher activities than those with less bulky methyl groups. Except for complex **4** with less bulky and high electronegative fluorine atoms, complexes **5** and **6** containing halogen groups also displayed higher catalytic activity (more than 10^6 g mol^{-1} h^{-1}) at 10 atm of ethylene pressure.

Conclusion

A series of tridentate cobalt(II) complexes bearing 2-imino-1,-10-phenanthrolinyl ligands have been synthesized and fully characterized. Upon treatment with MAO or MMAO, these cobalt(II) complexes showed moderate to high catalytic activities of up to 2.34×10^6 g mol^{-1}(Co) h^{-1} for ethylene oligomerization at 10 atm ethylene. Butenes were found to be predominant among the oligomers produced. MMAO was found to be a more effective cocatalyst when the reactions were carried out at 1 atm ethylene. By comparison with the data obtained with MAO as cocatalyst, the lifetime of the catalysts was prolonged at elevated ethylene pressure along with an improved catalytic activity. For the complexes bearing the same alkyl groups at the *ortho*-positions of the imino-N aryl ring, the catalytic activities increased in the sequence: aldimine (R = H), methyl-ketimine (R = Me) and phenyl-ketimine (R = Ph). For both aldimine and methyl-ketimine complexes, bulky and moderately electronegative atoms at the *ortho*-positions of the imino-N aryl ring resulted in the sequence of catalytic activities: bromo- > chloro- > fluoro.

Experimental Section

General Considerations

All manipulations for air or moisture-sensitive compounds were carried out under an atmosphere of nitrogen using standard Schlenk techniques. IR spectra were recorded on a Perkin-Elmer FT-IR 2000 spectrometer using KBr disc in the range of 4000 – 400 cm^{-1}. Elemental analyses were performed on a Flash EA1112 microanalyzer. GC analyses were performed with a Carlo Erba gas chromatograph equipped with a flame ionization detector and a 30 m (0.25 mm i.d., 0.25 μm film thickness) DM-1 silica capillary column. The yield of oligomers was calculated by referencing with the mass of

for references, see page 82

the solvent on the basis of the prerequisite that the mass of each fraction is approximately proportional to its integrated areas in the GC traces.

Toluene was refluxed over sodium/benzophenone and distilled under nitrogen prior to use. Diethylaluminum chloride and ethylaluminum dichloride were purchased from Acros Chemicals. Triisobutylaluminum ($Al(i\text{-}Bu)_3$), methylaluminoxane (MAO, 1.46 M in toluene) and modified-methylaluminoxane (MMAO-3A, 7% aluminum in heptane solution) were purchased from Akzo Nobel Chemical Inc. All other chemicals were obtained commercially and used without further purification unless otherwise stated.

Synthesis of the Complexes 1–15

General Procedure. A solution of anhydrous $CoCl_2$ in absolute ethanol was added dropwise to a solution of the ligand in absolute ethanol. Then the reaction mixture was stirred at room temperature for 9 h. The resulting precipitate was filtered, washed with diethyl ether and dried in vacuum. All complexes were prepared in high yield in this manner.

2-Formyl-1,10-phenanthroline(2,6-dimethylanil)$CoCl_2$ (1). Isolated as a brownish yellow powder in 82 % yield. FT-IR (KBr disc, cm^{-1}): 3437, 3063, 2953, 1612, 1513, 1495, 1472, 1437, 1407, 1297, 1183, 1142, 1117, 1094, 963, 861, 780, 738, 645. Anal. Calc. for $C_{21}H_{17}Cl_2CoN_3 \cdot 0.5$ EtOH (464.26): C, 56.92; H, 4.34; N, 9.05. Found: C, 56.53; H, 4.05; N, 8.84.

2-Formyl-1,10-phenanthroline(2,6-diethylanil)$CoCl_2$ (2). Isolated as a brown powder in 52 % yield. FT-IR (KBr disc, cm^{-1}): 3444, 3060, 2967, 2934, 2875, 1610, 1585, 1514, 1495, 1451, 1407, 1297, 1176, 1143, 1117, 963, 865, 762, 739, 645. Anal. Calc. for $C_{23}H_{21}Cl_2CoN_3$ (469.27): C, 58.87; H, 4.51; N, 8.95. Found: C, 58.64; H, 4.47; N, 8.78.

2-Formyl-1,10-phenanthroline(2,6-diisopropylanil)$CoCl_2$ (3). Isolated as a brownish yellow powder in 93 % yield. FT-IR (KBr disc, cm^{-1}): 3437, 3059, 2965, 2929, 2869, 1609, 1515, 1495, 1463, 1409, 1297, 1176, 1144, 1117, 961, 851, 806, 765, 737, 645. Anal. Calc. for $C_{25}H_{25}Cl_2CoN_3$ (497.33): C, 60.38; H, 5.07; N, 8.45. Found: C, 60.12; H, 5.24; N, 8.34.

2-Formyl-1,10-phenanthroline(2,6-difluoroanil)$CoCl_2$ (4). Isolated as a brownish yellow powder in 49 % yield. FT-IR (KBr disc, cm^{-1}): 3418, 3059, 3021, 1613, 1587, 1514, 1470, 1435, 1407, 1284, 1236, 1198, 1143, 1117, 1016, 965, 863, 787, 737. Anal. Calc. for $C_{19}H_{11}Cl_2CoF_2N_3$ (449.15): C, 50.81; H, 2.47; N, 9.36. Found: C, 50.60; H, 2.48; N, 9.18.

for references, see page 82

2-Formyl-1,10-phenanthroline(2,6-dichloroanil)$CoCl_2$ (5). Isolated as a yellowish green powder in 65 % yield. FT-IR (KBr disc, cm^{-1}): 3398, 3062, 3012, 1613, 1581, 1564, 1512, 1494, 1440, 1407, 1359, 1341, 1296, 1234, 1199, 1117, 1143, 963, 865, 788, 739, 644. Anal. Calc. for $C_{19}H_{11}Cl_4CoN_3$ (482.06): C, 47.34; H, 2.30; N, 8.72. Found: C, 47.35; H, 2.60; N, 8.64.

2-Formyl-1,10-phenanthroline(2,6-dibromoanil)$CoCl_2$ (6) Isolated as a bluish green powder in 62 % yield. FT-IR (KBr disc, cm^{-1}): 3420, 3064, 1642, 1585, 1572, 1549, 1512, 1496, 1459, 1429, 1397, 1212, 1198, 1143, 867, 777, 742, 728, 641. Anal. Calc. for $C_{19}H_{11}Br_2Cl_2CoN_3$ (570.96): C, 39.97; H, 1.94; N, 7.36. Found: C, 40.12; H, 2.15; N, 7.51.

2-Acetyl-1,10-phenanthroline(2,6-dimethylanil)$CoCl_2$ (7). Isolated as a brownish yellow powder in 86 % yield. FT-IR (KBr disc, cm^{-1}): 3435, 3049, 2978, 1612, 1583, 1511, 1492, 1467, 1406, 1373, 1287, 1211, 1152, 1093, 864, 790, 772, 743. Anal. Calc. for $C_{22}H_{19}Cl_2CoN_3$ (455.25): C, 58.04; H, 4.21; N, 9.23. Found: C, 58.02; H, 4.31; N, 8.95.

2-Acetyl-1,10-phenanthroline(2,6-diethylanil)$CoCl_2$ (8). Isolated as a brownish yellow powder in 58 % yield. FT-IR (KBr disc, cm^{-1}): 3448, 2964, 2876, 1611, 1584, 1512, 1493, 1449, 1407, 1373, 1286, 1197, 1154, 873, 836, 785, 741, 657. Anal. Calc. for $C_{24}H_{23}Cl_2CoN_3$ (483.30): C, 59.64; H, 4.80; N, 8.69. Found: C, 59.69; H, 4.86; N, 8.62.

2-Acetyl-1,10-phenanthroline(2,6-diisopropylanil)$CoCl_2$ (9). Isolated as a brownish yellow powder in 76 % yield. FT-IR (KBr disc, cm^{-1}): 3435, 2967, 2869, 1609, 1511, 1464, 1410, 1373, 1287, 1196, 1146, 850, 789, 654. Anal. Calc. for $C_{26}H_{27}Cl_2CoN_3$ (511.35): C, 61.07; H, 5.32; N, 8.22. Found: C, 60.86; H, 5.49; N, 7.83.

2-Acetyl-1,10-phenanthroline(2,6-difluoroanil)$CoCl_2$ (10). Isolated as a brownish yellow powder in 85 % yield. FT-IR (KBr disc, cm^{-1}): 3420, 3056, 1614, 1587, 1515, 1472, 1407, 1373, 1282, 1227, 1151, 1027, 1005, 862, 775, 744. Anal. Calc. for $C_{20}H_{13}Cl_2CoF_2N_3$ (463.19): C, 51.86; H, 2.83; N, 9.07. Found: C, 51.55; H, 3.01; N, 8.78.

2-Acetyl-1,10-phenanthroline(2,6-dichloroanil)$CoCl_2$ (11). Isolated as a greenish yellow powder in 81 % yield. FT-IR (KBr disc, cm^{-1}): 3446, 3060, 2973, 2867, 1616, 1560, 1515, 1493, 1438, 1406, 1375, 1284, 1233, 1064, 862, 788, 744, 658. Anal. Calc. for $C_{20}H_{13}Cl_4CoN_3$ (496.08): C, 48.42; H, 2.64; N, 8.47. Found: C, 48.29; H, 2.78; N, 8.26.

for references, see page 82

2-Acetyl-1,10-phenanthroline(2,6-dibromoanil)$CoCl_2$ (12). Isolated as a greenish yellow powder in 86 % yield. FT-IR (KBr disc, cm^{-1}): 3446, 3055, 2968, 2866, 1616, 1579, 1549, 1515, 1492, 1432, 1406, 1374, 1285, 1230, 1149, 1063, 862, 832, 787, 743, 727, 658. Anal. Calc. for $C_{20}H_{13}Br_2Cl_2CoN_3$ (584.98): C, 41.06; H, 2.24; N, 7.18. Found: C, 40.77; H, 2.25; N, 7.10.

2-Benzoyl-1,10-phenanthroline(2,6-dimethylanil)$CoCl_2$ (13). Isolated as a brown powder in 71 % yield. FT-IR (KBr disc, cm^{-1}): 3442, 3060, 2908, 1603, 1565, 1510, 1492, 1440, 1403, 1295, 1217, 1094, 998, 866, 789, 701. Anal. Calc. for $C_{27}H_{21}Cl_2CoN_3$ (517.31): C, 62.69; H, 4.09; N, 8.12. Found: C, 62.43; H, 4.08; N, 8.06.

2-Benzoyl-1,10-phenanthroline(2,6-diethylanil)$CoCl_2$ (14). Isolated as a greenish yellow powder in 69 % yield. FT-IR (KBr disc, cm^{-1}): 3443, 3063, 2971, 2933, 1608, 1586, 1557, 1507, 1491, 1444, 1404, 1326, 1282, 1211, 1147, 1109, 999, 882, 836, 782, 703. Anal. Calc. for $C_{29}H_{25}Cl_2CoN_3$ (545.37): C, 63.87; H, 4.62; N, 7.70. Found: C, 63.71; H, 4.42; N, 7.51.

2-Benzoyl-1,10-phenanthroline(2,6-diisopropylanil)$CoCl_2$ (15). Isolated as a greenish yellow powder in 83 % yield. FT-IR (KBr disc, cm^{-1}): 3060, 2964, 2867, 1606, 1583, 1510, 1491, 1438, 1404, 1291, 1270, 1209, 997, 864, 782, 701. Anal. Calc. for $C_{31}H_{29}Cl_2CoN_3$ (573.42): C, 64.93; H, 5.10; N, 7.33. Found: C, 64.78; H, 5.29; N, 7.22.

General procedure for ethylene oligomerization

Ethylene oligomerization at 1 atm of ethylene pressure. A flame dried three-neck round flask was loaded with the complex and vacuated-filled three times with nitrogen. Then ethylene was charged together with freshly distilled toluene and stirring was maintained for 10 min. A certain amount of co-catalyst was injected via a syringe. The reaction mixture was stirred for 30 min and then terminated with 5 % aqueous hydrogen chloride. The content and distribution of oligomers were determined by GC.

Ethylene oligomerization at 10 atm of ethylene pressure. A 250-mL autoclave stainless steel reactor equipped with a mechanical stirrer and a temperature controller was heated in vacuum for at least 2 h over 80 °C, allowed to cool to the required reaction temperature under ethylene atmosphere, and then charged with toluene, the desired amount of co-catalyst and a toluene solution of the catalytic precursor. The total volume was 100 mL. Reaching the reaction temperature, the reactor was sealed and pressurized to 10 atm of ethylene pressure. The ethylene pressure was kept constant during the reaction time by feeding the reactor with ethylene. To determine the

for references, see page 82

composition and mass distribution of the oligomers obtained, using gas chromatography, a small amount of the reaction solution was collected after the reaction was carried out for the required time and quenched by addition of 5 % aqueous hydrogen chloride. Then the residual reaction solution was quenched with 5 % hydrochloric acid ethanol.

Table 5.
Crystal data and structure refinement for complexes **2**, **3**, **8** and **14**.

data	**2**	**3**	**8**	**14**
formula	$2C_{23}H_{21}Cl_2CoN_3$	$C_{25}H_{25}Cl_2CoN_3$	$C_{24}H_{23}Cl_2CoN_3$	$C_{29}H_{25}Cl_2CoN_3$
Formula weight	938.52	497.31	483.28	545.35
Temperature(K)	293(2)	293(2)	293(2)	293(2)
Wavelength(Å)	0.71073	0.71073	0.71073	0.71073
Crystal system	Monoclinic	Orthorhombic	Triclinic	Triclinic
Space group	P2(1)/n	Pbca	P-1	P-1
a (Å)	9.4674(3)	14.9445(7)	8.1365(16)	8.7410(17)
b (Å)	18.6424(6)	16.0133(8)	9.0670(18)	8.7867(18)
c (Å)	24.9135(8)	19.4261(10)	16.194(3)	17.165(3)
α (º)	90	90	104.31(3)	87.87(3)
β (º)	94.0570(10)	90	90.04(3)	78.88(3)
γ (º)	90	90	110.21(3)	75.65(3)
Volume ($Å^3$)	4386.1(2)	4648.9(4)	1081.4(4)	1253.2(4)
Z	4	4	2	2
D_{calc} (Mg m^{-3})	1.421	0.711	1.484	1.445
μ (mm^{-1})	1.040	0.493	1.057	0.921
F(000)	1928	1028	498	562
Crystal size(mm)	0.26×0.20×0.10	0.30×0.21×0.15	0.21×0.16×0.03	0.30×0.20×0.20
θ range (º)	1.97-28.31	2.10-28.31	2.48-27.48	1.21-27.38
Limiting indices	$-12 \le h \le 12$, $-24 \le k \le 23$, $-28 \le l \le 33$	$-19 \le h \le 19$, $-12 \le k \le 21$, $-16 \le l \le 25$	$0 \le h \le 10$, $-11 \le k \le 11$, $-21 \le l \le 20$	$0 \le h \le 11$, $-10 \le k \le 11$, $-21 \le l \le 22$
Reflections collected	37063	24328	4833	5583
Unique reflections	10877	5767	3278	4583
Completeness to θ (%)	99.5 (θ= 28.31º)	99.8 (θ= 28.31º)	97.4 (θ= 27.48º)	98.1 (θ= 27.38º)
Absorption correction	empirical	empirical	empirical	empirical
Number of parameters	523	280	274	316
Goodness-of-fit on F^2	1.128	1.124	0.913	1.072
Final R indices [I>2σ(I)]	R1 = 0.0420, wR2 = 0.1141	R1 = 0.0390, wR2 = 0.0972	R1 = 0.0410, wR2 = 0.0704	R1 = 0.0391, wR2 = 0.1058
R indices(all data)	R1 = 0.0927, wR2 = 0.1318	R1 = 0.0819, wR2 = 0.1039	R1 = 0.0785, wR2 = 0.0770	R1 = 0.0517, wR2 = 0.1120
Largest diff. peak, hole($eÅ^{-3}$)	0.735, -0.285	0.321, -0.320	0.342, -0.441	0.622, -0.418

for references, see page 82

X-ray Crystallography Measurements

Single-crystal X-ray diffraction studies for **2** and **3** were carried out on a Bruker P4 diffractometer with graphite monochromated Mo-K_α radiation (λ = 0.71073 Å) at 293(2) K. Intensity data for crystals of **8** and **14** were collected with a Rigaku RAXIS Rapid IP diffractometer with graphite monochromated Mo-K radiation (λ = 0.71073 Å) at 293(2) K. Cell parameters were obtained by global refinement of the positions of all collected reflections. Intensities were corrected for Lorentz and polarization effects and empirical absorption. The structures were solved by direct methods and refined by full-matrix least-squares on F^2. All non-hydrogen atoms were refined anisotropically. All hydrogen atoms were placed in calculated positions. Structure solution and refinement were performed by using the SHELXL-97 Package [18]. Crystallographic data and processing parameters for complexes **2**, **3**, **8** and **14** are summarized in Table 5. The data of complexes **2**, **3**, **8** and **14** have been deposited with the Cambridge Crystallographic Data Center under CCDC 621104, 621105, 621106 and 621107, respectively.

Acknowledgements. This project was supported by NSFC No 20473099. K. W. was supported by DAAD postdoctoral fellowship.

for references, see page 82

References

[1] D. Vogt, In Applied Homogeneous Catalysis with Organometallic Compounds; B. Cornils, W. A. Herrmann, Eds.; *VCH: Weinheim*, **2002**, Vol. 1, pp 240-253.

[2] K. Zieger, H. Martin, US 2.943.125, **1954**.

[3] A. M. Al-Jarallah, J. A. Anabtawi, M. A. B. Siddiqui, A. M. Aitani, *Catal. Today* **1992**, *14*, 1-121.

[4] B. L. Small, M. Brookhart, A. M. A. Bennett, *J. Am. Chem. Soc*. **1998**, *120*, 4049-4050.

[5] G. J. P. Britovsek, V. C. Gibson, B. S. Kimberley, P. J. Maddox, S. J. McTavish, G. A. Solan, A. J. P. White, D. J. Williams, *Chem. Commun.* **1998**, 849-850.

[6] (a) B. L. Small, M. Brookhart, *J. Am. Chem. Soc*. **1998**, *120*, 7143-7144. (b) G. J. P. Britovsek, M. Bruce, V. C. Gibson, B. S. Kimberley, P. J. Maddox, S. Mastrojanni, S. J. McTavish, C. Redshaw, G. A. Solan, S. Stromberg, A. J. P. White, D. J. Williams, *J. Am. Chem. Soc.* **1999**, *121*, 8728-8740. (c) G. J. P. Britovsek, S. Mastroianni, G. A. Solan, S. P. D. Baugh, C. Redshaw, V. C. Gibson, A. J. P. White, D. J. Williams, M. R. J. Elsegood, *Chem. Eur. J.* **2000**, *6*, 2221-2231. (d) Y. Chen, C. Qian, J. Sun, *Organometallics* **2003**, *22*, 1231-1236. (e) Y. Chen, R. Chen, C. Qian, X. Dong, J. Sun, *Organometallics* **2003**, *22*, 4312-4321.

[7] (a) V. C. Gibson, S. K. Spitzmesser, *Chem. Rev.* **2003**, *103*, 283-315 and references therein. (b) C. Bianchini, G. Giambastiani, I. G. Rios, G. Mantovani, A. Meli, A. M. Segarra *Coord. Chem. Rev.* **2006**, 250, 1391-1418 and references therein.

[8] (a) M. Qian, M. Wang, R. He, *J. Mol. Cat. A.* **2000**, *160*, 243-247. (b) L. LePichon, D. W. Stephan, X. Gao, Q. Wang, *Organometallics* **2002,** *21,* 1362-1366. (c) G. J. P. Britovsek, V. C. Gibson, O. D. Hoarau, S. K. Spitzmesser, A. J. P. White, D. J. Williams, *Inorg. Chem.* **2003**, *42*, 3454-3465. (d) R. Cowdell, C. J. Davies, S. J. Hilton, J.-D. Maréchal, G. A. Solan, O. Thomas, J. Fawcett, *Dalton Trans.* **2004**, 3231-3240.

[9] (a) T. V. Laine, M. Klinga, A. Maninen, E. Aitola, M. Leskela, *Acta Chem. Scand.* **1999**, 53, 968-973. (b) M. Qian, M. Wang, B. Zhou, R. He, *Appl. Catal. A: Gen.* **2001**, *209*, 11-15.

[10] C. Shao, W.-H. Sun, Z. Li, Y. Hu, L. Han, *Catal. Commun.* **2002**, *3*, 405-410.

[11] M.-S. Zhou, S.-P. Huang, L.-H. Weng, W.-H. Sun, D.-S. Liu, *J. Organomet. Chem.* **2003**, *665*, 237-245.

[12] W.-H. Sun, X. Tang, T. Gao, B. Wu, W. Zhang, H. Ma, *Organometallics* **2004**, *23*, 5037-5047.

[13] (a) C. Bianchini, G. Mantovani, A. Meli, F. Migliacci, F. Laschi, *Organometallics* **2003**, *22,* 2545-2547. (b) C. Bianchini, G. Giambastiani, G. Mantovani, A. Meli, D. Mimeau, *J. Organomet. Chem.* **2004**, *689*, 1356-1361.

[14] L. Wang, W.-H. Sun, L. Han, H. Yang, Y. Hu, X. Jin, *J. Organomet. Chem.* **2002**, *658*, 62-70.

[15] W.-H. Sun, S. Jie, S. Zhang, W. Zhang, Y. Song, H. Ma, J. Chen, K. Wedeking, R. Fröhlich, *Organometallics*, **2006**, *25*, 666-677.

[16] W.-H. Sun, S. Zhang, S. Jie, W. Zhang, Y. Li, H. Ma, J. Chen, K. Wedeking, R. Fröhlich, *J. Organomet. Chem.,* in press

[17] J. D. A. Pelletier, Y. D. M. Champouret, J. Cadarso, L. Clowes, M. Gañete, K. Singh, V. Thanarajasingham, G. A. Solan, *J. Organomet. Chem.,* in press

[18] G. M. Sheldrick, SHELXTL-97, Program for the Refinement of Crystal Structures, University of Goettingen: Germany, **1997**.

Chapitre IV

Complexes 2-arylimino-9-phényl-1,10-phénanthrolinyl du fer, cobalt et nickel, et leur application en catalyse d'oligomerization de l'éthylène

Abstract of Chapter IV

A series of 2-imino-9-phenyl-1,10-phenanthrolines (**1**–**6**) was prepared and investigated as new tridentate-N3 ligands in coordination with metal chlorides. Their iron(II) (**1a**–**6a**), cobalt(II) (**1b**–**6b**) and nickel(II) (**1c**–**6c**) complexes were synthesized and characterized by elemental and spectroscopic analysis along with single-crystal X-ray diffraction analysis. Upon treatment with MAO or MMAO, some iron complexes showed good activities for selective dimerization of ethylene; while their cobalt analogues showed higher activities than iron analogues and formation of C_6 and C_8 oligomers. The nickel analogues displayed high catalytic activities toward ethylene oligomerization in the presence of Et_2AlCl with the assistance of PPh_3 as an auxiliary ligand.

This chapter has been published. I did all the synthesis and catalytic studies and prepared the manuscript. Shu Zhang gave some help in the refinement of crystallographic data and the revision of manuscript.

2-Arylimino-9-phenyl-1,10-phenanthrolinyl-iron, -cobalt and -nickel Complexes: Synthesis, Characterization and Ethylene Oligomerization Behavior

Eur. J. Inorg. Chem. **2007**, 5584–5598.

Suyun Jie, Shu Zhang and Wen-Hua Sun*

Key Laboratory of Engineering Plastics and Beijing National Laboratory for Molecular Sciences, Institute of Chemistry, Chinese Academy of Sciences, Beijing 100080, China

2-Arylimino-9-phenyl-1,10-phenanthrolinyl-iron, -cobalt and -nickel Complexes: Synthesis, Characterization and Ethylene Oligomerization Behavior

Introduction

Ethylene oligomerization is an important catalytic process for the production of linear α-olefins as basic chemicals.[1] Catalysts currently used in industrial processes include alkylaluminum compounds, a combination of alkylaluminum compounds with early-transition metal compounds, nickel(II) complexes[1a] and monoanionic [P,O] nickel-based catalysts (SHOP).[2] In the past decade, the research of late-transition metal complexes as catalysts for ethylene oligomerization and polymerization has been found considerable attraction in both academic and industrial consideration due to expectation of highly active and selective catalysts.[3–5] This was stimulated by the pioneering work by Brookhart's group in 1995[6] who discovered α-diimino cationic nickel complexes as effective catalysts for ethylene oligomerization and polymerization. After the investigation of tetra-coordinated nickel complexes, recently more attention was paid to penta-coordinated complexes of nickel incorporating tridentate ligands such as N^N^O,[7] N^P^N,[8] P^N^N,[9] P^N^P[9a] and N^N^N[10–15] in addition to their iron and cobalt analogues. The discovery of highly active iron- and cobalt-based olefin polymerization catalysts initially started with designing bis(imino)pyridines as tridentate ligands by Brookhart and Gibson groups, individually.[16] Regarding to metal complexes bearing bis(imino)pyridines, the detailed investigations were carried out with modifying the substituents on the aryl ring linked to imino-group and checking their influences on catalytic behaviors and the resulting products of oligomerization or polymerization.[4] In addition, the extensive researches for alternative models of iron and cobalt complexes ligated with new types of tridentate-N_3 ligands did not result in highly active precursors toward ethylene oligomerization or polymerization.[17] Even so, tridentate-N_3 ligands are of great interests in preparing late-transition metal complexes as catalysts for ethylene oligomerization and polymerization, [10–15, 17–20] and selective syntheses of short ethylene oligomers, in particular α-olefins, are of industrial importance.

Variations of catalyst models through designing new organic compounds as tridentate ligands have been targeted in our group for highly active catalysts of iron and

for references, see page 112

cobalt,[11,15,19,20] as well as nickel.[11–14] Some of them performed promising catalytic activities toward ethylene oligomerization and polymerization, such as highly active iron catalysts bearing 2-imino-1,10-phenanthrolines[19] and 2-(2-benzimidazolyl)-2-(1-(arylimino)ethyl) pyridines[15b] along with bimetallic iron complexes bearing 2-methyl-2,4-bis(6-iminopyridin-2-yl)-1*H*-1,5- benzodiazepines[15a], meanwhile their cobalt analogues also showed good activities.[15a,15b,20] Similarly to the bis(imino)pyridine catalytic systems,[4] it has been found that the above iron-based catalysts were generally more active than their cobalt analogues. However, the exceptional cobalt complexes ligated by 2,9-bis(imino)-1,10-phenanthrolines indicated the better activity than the iron analogues.[11] Moreover, all their corresponding nickel complexes showed good catalytic activities for ethylene oligomerization[11,12,14a] and so did the recent nickel complexes bearing 2-(benzimidazol-2-yl)-1,10-phenanthrolines.[13]

Beyond the decisive influence of ligands, especially the steric and electronic effects of substituents on catalytic activities and products, the nature of different metals greatly affects catalytic behaviors. Various metals complexes containing 2-imino-1,10-phenanthrolines generally performed good to high catalytic activities for ethylene oligomerization and polymerization.[12,19,20] The bulky hindrance was recognized as a critical issue of diimino nickel complexes performing high catalytic activity for ethylene polymerization.[6] On the contrary, in comparison with the 2-imino-1,10-phenanthrolinyl metal complexes,[12,19,20] the additional imino group in metal complexes bearing 2,9-diimino-1,10-phenanthrolines[11] showed negative effects, in which the additional imino group was assumed to coordinate to the active species and resulted in the deactivated species. In order to check the steric hindrance, 2-imino-9-phenyl-1,10-phenanthroline derivatives were targeted for their metal complexes as precursors for ethylene oligomerization.

Herein we report the synthesis of 2-acetyl- and 2-benzoyl-9-phenyl-1,10-phenanthrolines and their subsequent transformation into 2-imino-9-phenyl-1,10-phenanthrolines for use as ligands. These compounds keep the same coordinative framework as 2-imino-1,10-phenanthrolines but with an additional phenyl group at the 9-position. Their late transition metal (Fe, Co, and Ni) complexes are synthesized and characterized and the catalytic properties of these complexes for ethylene oligomerization are evaluated under various reaction conditions. The effects of ligand environment and reaction conditions on the activity and the distribution of oligomers obtained are investigated systematically.

for references, see page 112

Results and Discussion

Preparation of Ketones I and II

2-Cyano-1,10-phenanthroline and 2-acetyl-1,10-phenanthroline were prepared according to the literature procedures.[19a,21] 2-Acetyl-9-phenyl-1,10-phenanthroline (ketone I) was synthesized by attaching a phenyl group at the phenanthroline ring using 2-acetyl-1,10-phenanthroline as the starting material (Scheme 1). The carbonyl group of 2-acetyl-1,10-phenanthroline was first protected with ethylene glycol and the 2-(2-methyl-1,3-dioxolan-2-yl)-1,10-phenanthroline formed in this condensation reaction was purified on an alumina column.[22] A solution of 1.7 equivalents of phenyllithium in diethyl ether was added dropwise to a suspension of 2-(2-methyl-1,3-dioxolan-2-yl)-1,10-phenanthroline in toluene under nitrogen at low temperature (0 °C) and the reaction mixture was maintained for an additional 3 h at 0 °C.[23] This procedure gave 2-(2-methyl-1,3-dioxolan-2-yl)-9-phenyl-1,10-phenanthroline by elimination of lithium hydride.[24] 2-(2-Methyl-1,3-dioxolan-2-yl) -9-phenyl-1,10-phenanthroline was purified as a yellow oil on a silica column and then refluxed in acetone in the presence of *p*-toluenesulfonic acid to cleave the 1,3-dioxolane moiety. The desired product (2-acetyl-9-phenyl-1,10-phenanthroline) precipitated from the solution and was obtained by filtration as a pale-yellow solid.

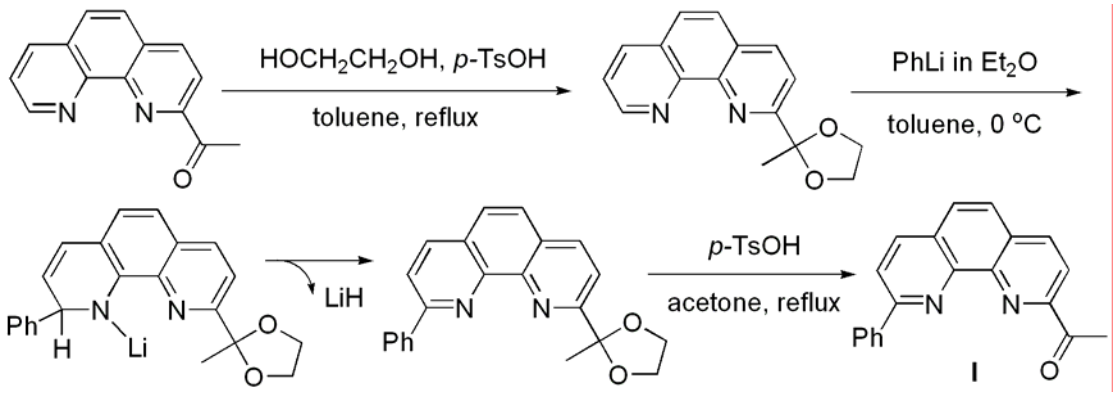

Scheme 1.
Synthesis of ketone **I**.

2-Benzoyl-9-phenyl-1,10-phenanthroline (ketone II) was prepared in a one-step reaction between 2-cyano-1,10-phenanthroline and three equivalents of phenyllithium (Scheme 2). Thus, a solution of phenyllithium in diethyl ether was added dropwise to a suspension of 2-cyano-1,10-phenanthroline in toluene at –78 °C, then the mixture was slowly warmed to room temperature and stirred overnight. The reaction proceeds by initial addition of phenyllithium to the nitrile group[25] followed by a Ziegler alkylation.[24] Subsequent hydrolysis gave the benzoyl-substituted product. The resultant

for references, see page 112

mixture was extracted with dichloromethane and the organic phase was purified on a silica column. The desired compound (2-benzoyl-9-phenyl-1,10-phenanthroline) was obtained as a slightly yellow solid in acceptable yield.

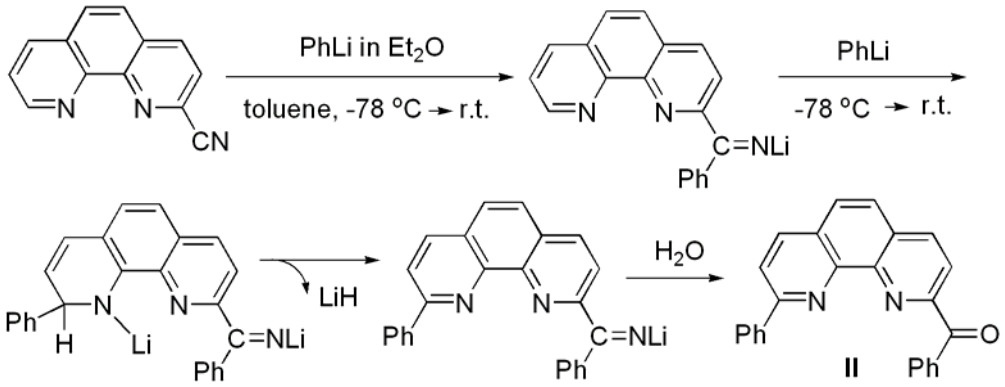

Scheme 2.
Synthesis of ketone **II**.

Synthesis and Characterization of Ligands and Complexes

The 2-imino-9-phenyl-1,10-phenanthrolinyl ligands (**1**–**6**) were prepared through the condensation reaction of the new ketones **I** or **II** and the corresponding substituted anilines with *p*-toluene sulfonic acid in toluene or tetraethyl silicate (Scheme 2). The ligands were obtained in high yield and were characterized by IR, ^{1}H and ^{13}C NMR spectra as well as their elemental analysis. The iron complexes **1a**–**6a** were readily prepared by mixing the corresponding ligand and one equivalent of $FeCl_2 \cdot 4H_2O$ in THF at room temperature under nitrogen (Scheme 2). The resulting complexes were precipitated from the reaction solution and separated as air-stable solid in green or brown color. Similarly, the cobalt complexes **1b**–**6b** and nickel complexes **1c**–**6c** were synthesized by the reaction of the corresponding ligand with one equivalent of $CoCl_2$ or $NiCl_2 \cdot 6H_2O$ in anhydrous ethanol at room temperature. The methyl-ketimine cobalt complexes **1b**–**3b** were obtained as green powders, whereas the phenyl-ketimine complexes **4b**–**6b** showed red brown color. The corresponding nickel complexes **1c**–**6c** were orange or yellow powders. All the complexes were well characterized by FT-IR spectra and elemental analysis. Comparing the IR spectra of the complexes and their corresponding ligands, the stretching vibration bands of C=N of these iron, cobalt and nickel complexes apparently shifted to lower wave number and the peak intensity greatly reduced, indicating the coordination interaction between the imino nitrogen atom and the central metal. Some samples for elemental analysis were prepared as crystals, therefore the analytical results showed the incorporation of solvent molecule. The

for references, see page 112

structures of ligand **2**, iron complex **2a**, cobalt complex **1b**, **4b**, **6b** and nickel complex **1c**, **5c** in solid state were confirmed by single-crystal X-ray diffraction analysis.

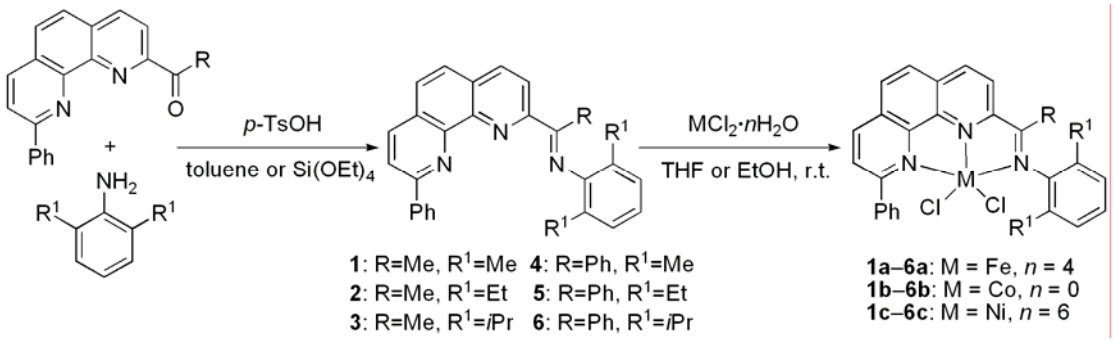

Scheme 3.
Synthesis of ligands **1**–**6** and complexes **1a**–**6a**, **1b**–**6b**, and **1c**–**6c**.

Crystal Structures

Single crystals of ligand **2** suitable for X-ray diffraction analysis were grown through recrystallization from its dichloromethane/hexane (1:5, v/v) solution. The molecular structure is shown in Figure 1 and the imino nitrogen atom is disposed *trans* with respect to the phenanthroline nitrogen atoms with the typical C=N double bond length of 1.270(2) Å. The phenyl ring on C1 is nearly coplanar to the phenanthrolinyl plane with the dihedral angle of 6.2°. However, the aryl ring on the imino-N is approximately perpendicular to the phenanthrolinyl plane and the phenyl plane on C1, and the corresponding dihedral angles are 92.1 and 89.6°, respectively.

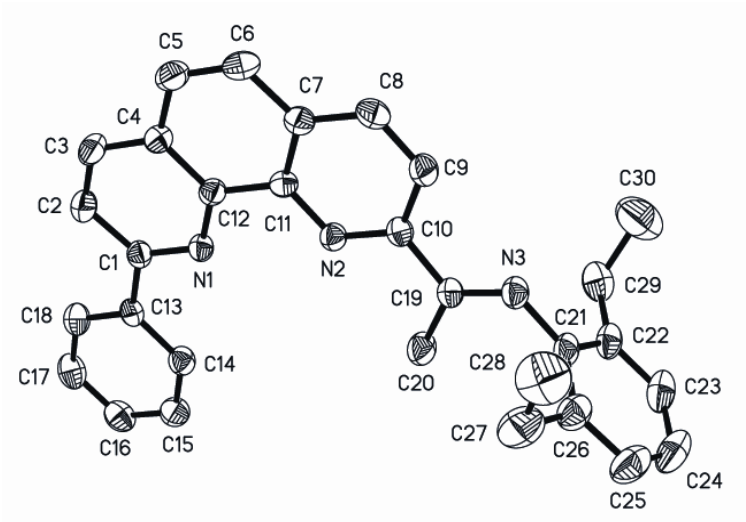

Figure 1.
Molecular structure of ligand **2** with all hydrogen atoms omitted for clarity. Selected bond lengths [Å] and bond angles [°]: N1–C1 1.330(2), N1–C12 1.355(3), N2–C11 1.356(3), N2–C10 1.327(2), N3–C19 1.270(2), N3–C21 1.422(3); C19–N3–C21 121.62(2), N3–C19–C10 117.6(2), N3–C19–C20 125.0(2).

for references, see page 112

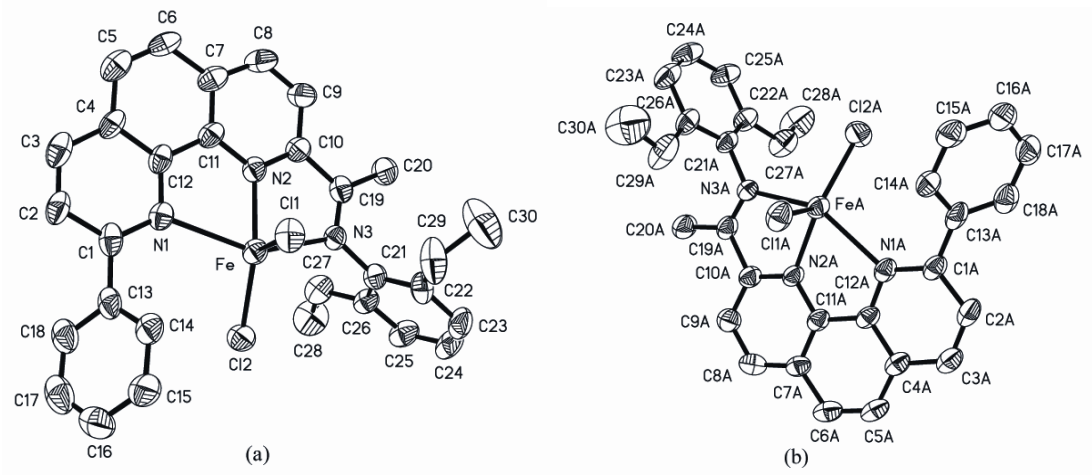

Figure 2.
Molecular structure of complex **2a** showing the two crystallographically independent molecules of the asymmetric unit, in which water molecules and all hydrogen atoms have been omitted for clarity.

Single crystals of complex **2a** suitable for X-ray diffraction analysis were obtained by slow evaporation diffusion of diethyl ether into its methanol solution under nitrogen. The asymmetric unit of complex **2a** contains the halves of two independent molecules, as shown in Figure 2. The coordination geometry around the iron center can be described as a distorted trigonal bipyramidal, in which N2 of phenanthrolinyl group and two chlorides compose an equatorial plane. The two independent molecules give slightly different bond lengths and bond angles, as shown in Table 1. In both molecules, the iron center is slightly deviated by 0.0469 Å from the equatorial plane, and the phenyl ring on C1 or C1A and the phenanthrolinyl plane make the same dihedral angle of 53.5º, which is largely different from that of the corresponding ligand **2** (6.2º). The phenanthrolinyl plane is nearly perpendicular to the equatorial plane (86.8º in (a) and 88.4º in (b)). The dihedral angles between the phenyl ring on C1 or C1A and the equatorial plane are also the same (139.1º) for the two molecules, while the angles between the aryl ring on the imino-N and the equatorial plane have large difference (56.8º in (a) and 78.9º in (b)). In each molecule, the Fe–N bond on the equatorial plane is obviously shorter than the two axial Fe–N bonds, and the axial Fe–N(phenanthroline) bond is about 0.1 Å longer than the Fe–N(imino) bond. The phenyl group on C1 resulted in a longer Fe–N1 bond length (av. 2.392(3) Å), in comparison with that of 2-acetyl-1,10-phenanthroline(2,6-diethylanil)$FeCl_2$ complex [2.271(3) Å].[19a] And the two Fe–Cl bond distances show the difference of about 0.1 Å. Although the two imino C=N bonds have some difference in distance [1.293(5) Å in (a) and 1.271(5) Å in (b)],

for references, see page 112

both of them keep the typical values of imino C=N double bond length. In molecule (b), the C=N bond distance is almost identical to the corresponding ligand **2** [1.270(2) Å].

Table 1.
Selected bond lengths [Å] and angles [º] for complex **2a**.

Fe–N1	2.391(3)	FeA–N1A	2.393(3)
Fe–N2	2.101(3)	FeA–N2A	2.104(3)
Fe–N3	2.298(3)	FeA–N3A	2.283(3)
Fe–Cl1	2.3405(1)	FeA–Cl1A	2.3456(1)
Fe–Cl2	2.2492(1)	FeA–Cl2A	2.2469(1)
N3–C19	1.293(5)	N3A–C19A	1.271(5)
N2–Fe–N1	73.77(1)	N2A–FeA–N1A	73.18(1)
N2–Fe–N3	73.18(1)	N2A–FeA–N3A	72.89(1)
N1–Fe–N3	145.86(1)	N1A–FeA–N3A	144.89(1)
N1–Fe–Cl1	93.70(8)	N1A–FeA–Cl1A	94.32(8)
N2–Fe–Cl1	98.23(9)	N2A–FeA–Cl1A	98.71(9)
N3–Fe–Cl1	99.19(8)	N3A–FeA–Cl1A	99.43(9)
N1–Fe–Cl2	104.73(9)	N1A–FeA–Cl2A	105.71(9)
N2–Fe–Cl2	141.53(9)	N2A–FeA–Cl2A	143.73(9)
N3–Fe–Cl2	95.87(9)	N3A–FeA–Cl2A	96.35(9)
Cl1–Fe–Cl2	120.09(5)	Cl1A–FeA–Cl2A	117.38(5)

Single crystals of cobalt complex **1b**, **4b** and **6b** were individually grown from slow diffusion of hexane into the solution by layering hexane on their corresponding dichloromethane solutions. Their molecular structures are shown in Figures 3–5, in which solvent molecules and all the hydrogen atoms have been omitted for clarity, and their selected bond lengths and bond angles are collected in Table 2. The coordination geometry around the cobalt center can be described as a distorted trigonal bipyramidal with N2 of phenanthrolinyl group and two chlorides composing an equatorial plane.

In the molecular structure of complex **1b**, the cobalt atom slightly deviates by –0.0517 Å from the equatorial plane composed by N2, Cl1 and Cl2 and the axial Co–N bonds form an angle of 149.22(1)º (N1–Co–N3). The phenyl ring on C1 and the phenanthrolinyl plane form the dihedral angle of 41.0º, and the phenanthrolinyl plane is almost perpendicular to the equatorial plane with the dihedral angle of 93.2º. The dihedral angles between the phenyl ring on C1 and the equatorial plane, the aryl ring on the imino-N and the equatorial plane are 134.0º and 133.7º, respectively. The two axial Co–N distances [2.313(4) and 2.279(4) Å] are much longer than that of the Co–N bond [2.035(4) Å] on the equatorial plane and the two Co–Cl linkages show the difference of 0.06 Å in distance. The imino N3–C19 bond length is 1.289(6) Å with the typical character of C=N double bond.

for references, see page 112

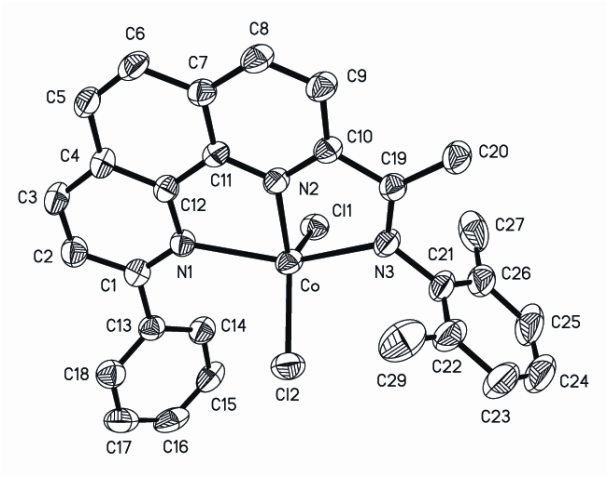

Figure 3.
Molecular structure of complex **1b** with water molecules and all the hydrogen atoms omitted for clarity.

For the phenyl-ketimine complex **4b**, the central cobalt also has a little deviation of 0.0196 Å from the equatorial plane of N2, Cl1 and Cl2. The bond lengths and bond angles around the cobalt center are very similar to those in 1b. However, the phenyl ring on C1 and the phenanthrolinyl plane make a dihedral angle (16.4º) different from that in **1b** (41.0º). The phenyl ring on C1, the phenanthrolinyl plane, the phenyl ring on the imino-C and the aryl ring on the imino-N are all approximately perpendicular to the equatorial plane with the dihedral angles of 80.1, 88.9, 91.5 and 86.0º, respectively.

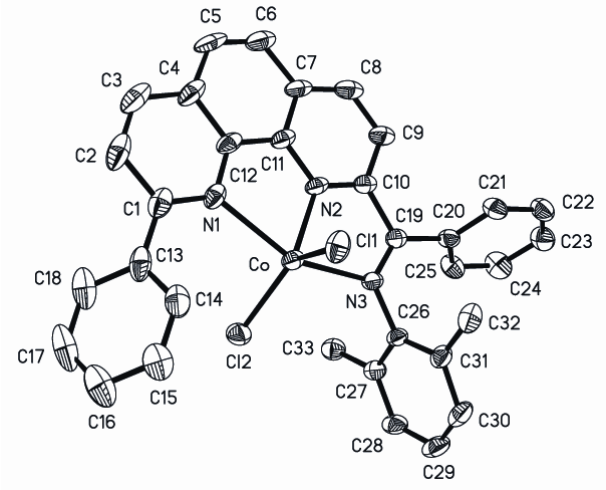

Figure 4.
Molecular structure of complex **4b** with one CH_2Cl_2 molecule and all the hydrogen atoms omitted for clarity.

For the phenyl-ketimine complex **6b** with the bulkier isopropyl groups at the *ortho*-positions of the imino-N aryl ring, there is a little larger deviation of 0.1829 Å from the equatorial plane of N2, Cl1 and Cl2 for the central cobalt than other complexes. Compared with the above complexes, it has the smaller bond angle of N2–Co–Cl1 [97.27(8)º] and larger bond angle of N2–Co–Cl2 [140.69(8)º]. The two axial Co–N bonds also make a slightly smaller angle of 143.99(9)º (N1–Co–N3). Differently from

for references, see page 112

other complexes, the phenyl ring on C1 is nearly coplanar to the phenanthrolinyl plane with the dihedral angle of 3.3º, which is greatly smaller than in other analogues and even smaller than in ligand **2** (6.2º). The dihedral angles between the phenyl ring on C1, the phenanthrolinyl plane, the phenyl ring on the imino-C, the aryl ring on the imino-N and the equatorial plane [82.8, 80.4, 88.9 and 89.2º, respectively] display the similar values to those in **4b**. In **6b**, the axial Co–N1(phenanthroline) bond is 0.19 Å shorter than the Co–N3(imino) bond, which is very different from other cobalt analogues (about 0.04 Å in **1b** and **4b**). The possible reason is that the bulkier isopropyl groups at the *ortho*-positions of the imino-N aryl ring take up more space and lead to the shortened Co–N1 bond [2.180(2) Å] and the lengthened Co–N3 bond [2.372(2) Å]. This kind of steric effect also contributes to the shorter imino N3–C19 bond length [1.255(4) Å].

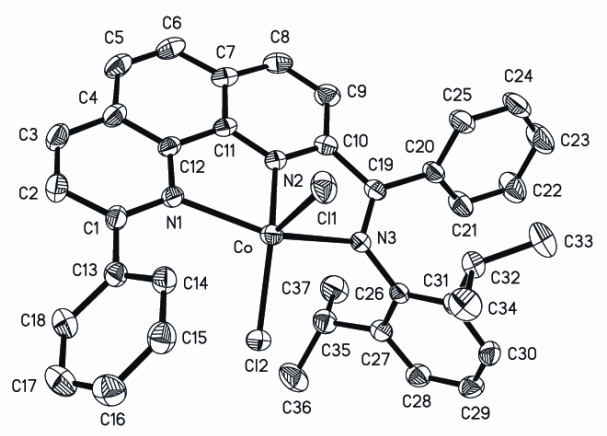

Figure 5.
Molecular structure of complex **6b** with one CH_2Cl_2 molecule and all the hydrogen atoms omitted for clarity.

Table 2.
Selected bond lengths [Å] and bond angles [º] of complexes **1b**, **4b**, **6b**, **1c** and **5c**.

	1b (M = Co)	**4b** (M = Co)	**6b** (M = Co)	**1c** (M = Ni)	**5c** (M = Ni)
M–N1	2.313(4)	2.299(3)	2.180(2)	2.300(7)	2.219(3)
M–N2	2.035(4)	2.034(3)	2.012(2)	1.962(6)	1.970(4)
M–N3	2.279(4)	2.257(3)	2.372(2)	2.238(6)	2.220(3)
M–Cl1	2.2923(2)	2.2745(1)	2.2192(1)	2.274(3)	2.2988(1)
M–Cl2	2.2357(2)	2.2404(1)	2.1917(9)	2.217(3)	2.2234(1)
N3–C19	1.289(6)	1.278(4)	1.255(4)	1.275(9)	1.276(5)
N1–M–N2	76.16(15)	76.64(12)	77.62(1)	78.4(3)	78.32(1)
N2–M–N3	74.00(15)	74.01(1)	70.50(9)	76.0(3)	75.40(1)
N1–M–N3	149.22(1)	149.77(1)	143.99(9)	154.1(2)	152.86(1)
N1–M–Cl1	97.95(11)	94.07(8)	103.79(7)	95.46(2)	91.79(1)
N1–M–Cl2	99.72(1)	96.22(8)	103.95(7)	92.28(2)	98.16(1)
N2–M–Cl1	104.94(1)	100.88(8)	97.27(8)	101.4(2)	99.41(1)
N2–M–Cl2	133.77(1)	131.09(8)	140.69(8)	120.9(2)	129.52(1)
N3–M–Cl1	96.80(1)	98.37(8)	96.55(7)	93.11(2)	99.04(1)
N3–M–Cl2	95.48(1)	97.55(8)	90.89(7)	97.66(2)	93.33(1)
Cl1–M–Cl2	121.12(6)	128.01(5)	119.62(4)	137.71(1)	131.07(6)

for references, see page 112

Single crystals of nickel complex **1c** and **5c** were individually obtained through layering hexane onto their corresponding dichloromethane solutions. X-ray diffraction analysis reveals that they display the distorted trigonal bipyramidal geometry, in which the central nickel atom is coordinated to three nitrogen atoms from the ligand and two halides. Similar to their iron and cobalt analogues, one nitrogen atom (N2) of phenanthrolinyl group and two chlorides compose the equatorial plane; correspondingly, the imino-N atom (N3) and another nitrogen atom (N1) of phenanthrolinyl group occupy the two axial coordination sites. Their molecular structures are shown in Figures 6 and 7 and the selected bond lengths and angles are collected in Table 2.

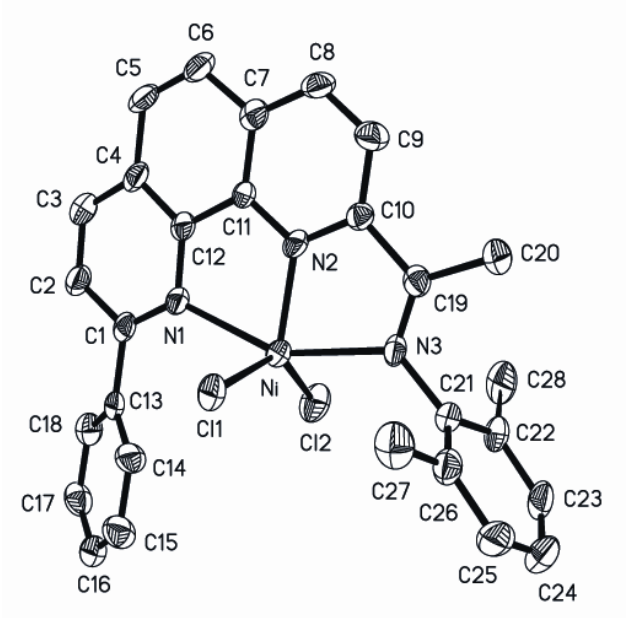

Figure 6.
Molecular structure of complex **1c** with one CH_2Cl_2 molecule and all the hydrogen atoms omitted for clarity.

The central nickel atom in **1c** deviates by 0.0128 Å from the equatorial plane of N2, Cl1 and Cl2 and the two axial Ni–Cl bonds make an axial angle N1–Ni–N3 of 154.1(2)°. Both the equatorial plane and the phenyl plane on the imino-N atom are almost perpendicular to the phenanthrolinyl plane with dihedral angles of 84.8° and 87.8°, respectively. The pendant phenyl plane on C1 makes a dihedral angle of 33.6° with the phenanthrolinyl plane and 51.2° with the equatorial plane. Similarly to 2-acetyl-1,10-phenanthroline(2,6-dimethylanil)$NiCl_2$, the Ni–N bond on the equatorial plane is obviously shorter than the axial Ni–N bonds; however, the presence of a phenyl group on C1 led to an elongate Ni–N1 bond [2.300(7) Å vs 2.157(3) Å],[12] while the two Ni–Cl bond distances just show a little difference. Despite the typical character of C=N double bond, the imino N3–C19 bond [1.275(9) Å] is slightly shorter than that of 2-acetyl-1,10-phenanthroline(2,6-dimethylanil)$NiCl_2$ [1.284(4) Å].[12] At the same time,

for references, see page 112

largely increased Cl1–Ni–Cl2 [137.71(1)°] and decreased N2–Ni–Cl1 [120.9(2)°] bond angles were observed after the addition of phenyl group at the 9-position of phenanthroline (110.62(4)° and 153.12(8)° in 2-acetyl-1,10-phenanthroline(2,6-dimethylanil)$NiCl_2$).[12]

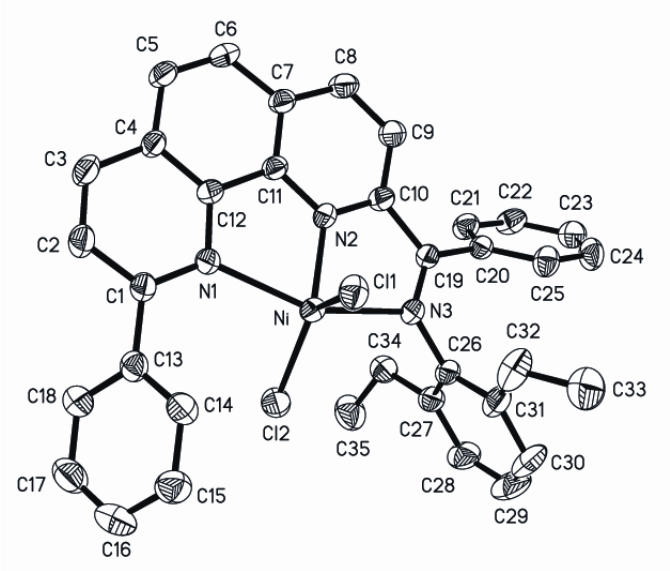

Figure 7.
Molecular structure of complex **5c** with two CH_2Cl_2 molecules and all the hydrogen atoms omitted for clarity.

Except for the similarity to **1c**, **c**omplex **5c** has its own structural characteristics due to the introduction of phenyl group on the imino-C atom replacing methyl group. The central nickel atom has a deviation of 0.0102 Å from the equatorial plane of N2, Cl1 and Cl2. The introduced phenyl group on the imino-C atom forms a dihedral angle of 5.7° with the phenanthrolinyl plane and is almost perpendicular to the equatorial plane with a dihedral angle of 82.2°. The equatorial plane is still almost perpendicular to the phenanthrolinyl plane with a dihedral angle of 87.5°, whereas the dihedral angle of phenyl plane on the imino-N atom and phenanthrolinyl plane greatly decreases to 7.2°. The pendant phenyl plane on C1 makes a decreased dihedral angle of 8.0° with the phenanthrolinyl plane and an increased dihedral angle of 79.9° with the equatorial plane. All bond lengths and angles in **5c** display the features similar to those in **1c**.

Ethylene Oligomerization

(i) Ethylene oligomerization with iron complexes 1a–6a

The iron(II) complexes **1a**–**6a** were first investigated as ethylene oligomerization catalysts at 1 atm of ethylene pressure (Table 3), although the results were not satisfactory as almost no absorption of ethylene was observed wigh diethylaluminum chloride as co-catalyst. Activation with methylaluminoxane (MAO) gave a low catalytic

for references, see page 112

activity for methyl-substituted complexes **1a** and **4a**, although ethyl-substituted complexes **2a** and **5a** were found to be less active and isopropyl-substituted complexes **3a** and **6a** completely inactive. Modified-methylaluminoxane (MMAO) was found to be a more effective co-catalyst than MAO with a similar effect of ligand environment on the catalytic activity. Thus, for complexes bearing the same substituents on the imino-N aryl ring, phenyl-ketimine (R = Ph) complexes **4a**–**6a** showed relatively higher catalytic activities than the corresponding methyl-ketimine (R = Me) complexes **1a**–**3a**. Complex **4a** exhibited the highest activity of 2.64×10^5 g mol^{-1}(Fe) h^{-1} with 1-butene as main product. Under the same reaction conditions, the variation of R^1 on the imino-N aryl ring was found to have a strong influence on the catalytic activity. Thus, increasing the bulkiness of R^1 in both methyl and phenyl ketimine complexes caused the catalytic activity to decrease dramatically (methyl- > ethyl- > isopropyl-), and in all cases essentially only dimerization was achieved, with a high selectivity for 1-butene.

Table 3.
Ethylene oligomerization with complexes **1a**–**6a**.[a]

Entry	Cat.	Co-cat.	P[b] [atm]	T[c] [°C]	Activity[d]	Oligomer distribution[e] [%]		Selectivity for 1-C4[e] [%]
						C4/∑C	C6/∑C	
1	**1a**	MAO	1	20	0.259	100	-	96.1
2	**2a**	MAO	1	20	0.059	100	-	100
3	**3a**	MAO	1	20	-	-	-	-
4	**4a**	MAO	1	20	0.295	100	-	100
5	**5a**	MAO	1	20	0.052	100	-	100
6	**6a**	MAO	1	20	-	-	-	-
7	**1a**	MMAO	1	20	4.78	100	-	100
8	**2a**	MMAO	1	20	1.63	100	-	100
9	**3a**	MMAO	1	20	0.199	100	-	100
10	**4a**	MMAO	1	20	26.4	100	-	100
11	**5a**	MMAO	1	20	5.13	100	-	100
12	**6a**	MMAO	1	20	0.275	100	-	100
13	**1a**	MAO	10	40	40.8	99.2	0.8	99.8
14	**2a**	MAO	10	40	29.1	98.7	1.3	99.8
15	**3a**	MAO	10	40	0.621	100	-	100
16	**4a**	MAO	10	40	194	99.2	0.8	99.9
17	**5a**	MAO	10	40	51.6	98.6	1.4	100
18	**6a**	MAO	10	40	0.409	100	-	100
19	**1a**	MMAO	10	40	269	99.4	0.6	100
20	**2a**	MMAO	10	40	47.9	100	-	100
21	**3a**	MMAO	10	40	1.90	100	-	100
22	**4a**	MMAO	10	40	211	99.1	0.9	100
23	**5a**	MMAO	10	40	54.3	98.7	1.3	100
24	**6a**	MMAO	10	40	0.465	100	-	100

[a] General conditions: cat.: 5 µmol, Al/Fe: 500, solvent (toluene): 30 mL for 1 atm and 100 mL for 10 atm, reaction time: 30 min. [b] Ethylene pressure. [c] Reaction temperature. [d] 10^4 g mol^{-1}(Fe) h^{-1}. [e] Weight percentage determined by GC.

The iron (II) complexes **1a**–**6a** were studied for ethylene oligomerization at 10 atm of ethylene pressure in the presence of MAO or MMAO; much higher catalytic

for references, see page 112

activities were observed than those at 1 atm (Table 3). With MAO as a co-catalyst, the highest activity of 1.94×10^6 g·mol^{-1}(Fe)·h^{-1} was obtained with complex **4a**. In general, however, under similar conditions, these complexes were found to be much less active than the corresponding 2-imino-1,10-phenanthroline iron complexes,[19] probably due to the presence of a phenyl group at the 9-position of 1,10-phenanthroline ligands, which hinders the insertion of ethylene. MMAO was found to be more effective than MAO at 10 atm of ethylene pressure, and the methyl-substituted **1a** [2.69×10^6 g mol^{-1}(Fe) h^{-1}] and **4a** [2.11×10^6 g mol^{-1}(Fe) h^{-1}] displayed the highest activity. The isopropyl-substituted **3a** and **6a** always showed lower catalytic activity, probably because the bulkier isopropyl groups at the *ortho* positions of the aryl ring at imine nitrogen affect the active species by preventing the coordination of an ethylene molecule at the metal center. A trend similar to that at 1 atm as regards the effect of ligand environment on the catalytic activities and catalytic products was obtained for both MAO and MMAO catalytic systems.

(ii) Ethylene oligomerization with cobalt complexes 1b–6b

Table 4.
Ethylene oligomerization with complexes **1b**–**6b**.[a]

Entry	Cat.	P[b] [atm]	Al/Co	T[c] [°C]	Activity[d]	Oligomer distribution[e] [%]			Selectivity for 1-C_4[e] [%]
						$C_4/\sum C$	$C_6/\sum C$	$C_{\geq 8}/\sum C$	
1[f]	**5b**	1	500	20	5.93	77.1	16.2	6.7	96.1
2	**5b**	1	100	20	0.76	90.7	5.9	3.4	98.0
3	**5b**	1	200	20	2.33	86.3	10.6	3.1	97.0
4	**5b**	1	500	20	6.42	78.5	15.2	6.3	96.7
5	**5b**	1	1000	20	5.70	77.8	15.1	7.1	97.4
6	**5b**	1	1500	20	5.42	76.0	16.7	7.3	96.1
7	**5b**	1	2000	20	4.31	82.2	14.8	3.0	98.2
8	**5b**	1	500	0	3.64	91.0	7.6	1.4	98.4
9	**5b**	1	500	40	5.05	81.1	16.0	2.9	95.9
10	**5b**	1	500	60	1.41	72.4	19.2	8.4	97.2
11	**5b**	1	500	80	0.874	72.5	16.6	10.9	96.3
12	**1b**	1	500	20	6.85	94.3	5.7	-	97.0
13	**2b**	1	500	20	6.71	91.9	5.4	2.7	97.9
14	**3b**	1	500	20	5.23	80.0	16.5	3.5	95.4
15	**4b**	1	500	20	5.58	84.4	14.8	0.8	96.4
16	**6b**	1	500	20	2.85	55.2	28.1	16.7	94.3
17	**1b**	10	500	30	43.2	92.1	7.6	0.3	99.8
18	**2b**	10	500	30	40.6	95.7	4.0	0.3	99.7
19	**3b**	10	500	30	65.2	75.7	23.0	1.3	99.7
20	**4b**	10	500	30	49.0	84.5	13.4	2.1	99.8
21	**5b**	10	500	30	73.3	80.5	16.8	2.7	99.7
22	**6b**	10	500	30	28.0	46.7	34.0	19.3	100

[a] General conditions: cat.: 5 µmol, co-cat.: MAO, solvent (toluene): 30 mL for 1 atm and 100 mL for 10 atm, reaction time: 30 min. [b] Ethylene pressure. [c] Reaction temperature. [d] 10^5 g mol^{-1}(Co) h^{-1}. [e] Weight percentage determined by GC. [f] Co-cat.: MMAO.

for references, see page 112

Complex **5b** was studied as a model for ethylene oligomerization under varying conditions at 1 atm of ethylene pressure (Table 4). No catalytic activity was observed with diethylaluminum chloride (Al/Co = 100 or 200) as co-catalyst at 20 °C, whereas in the presence of MAO or MMAO (Al/Co = 500) the catalytic activity increased remarkably and the products mainly consisted of butene and hexene with a high selectivity for 1-butene (> 96%). The catalytic system **5b**/MAO showed relatively higher activity than **5b**/MMAO, although both gave a similar distribution of oligomers and a similar selectivity for 1-butene (entry 1 and 4, Table 4). MAO was therefore chosen as a co-catalyst during the subsequent investigation at 1 atm and 10 atm of ethylene pressure. When the molar ratio of Al/Co was 100, The **5b**/MAO system showed a lowest activity with a butene content in the oligomeric products of more than 90% (entry 2, Table 4). Increasing the Al/Co molar ratio in the range of 200–2000 led to an increase in the activity to 6.42×10^5 g mol^{-1}(Co) h^{-1} at a Al/Co molar ratio of 500 and then a gradual decrease. The distribution of oligomers and the selectivity for 1-butene hardly changed.

The reaction temperature was found to have a remarkable influence on the catalytic activity and the distribution of oligomers. The highest activity was achieved at 20 °C and a slightly lower activity was obtained, although with a higher amount of butene produced (91.0%), at lower temperature (0 °C; entry 8, Table 4). An elevated reaction temperature also resulted in a decrease of the catalytic activity and butene content; for instance, **5b**/MAO showed an activity of 8.74×10^4 g mol^{-1}(Co) h^{-1} with a 72.5% butene content at 80 °C (entry 11, Table 4). No significant difference was observed between methyl- and ethyl-substituted complexes for both methyl and phenyl ketimine complexes. However, the isopropyl-substituted complexes **3b** and **6b** displayed lower catalytic activities and gave a smaller amount of butene and higher amount of hexene than the corresponding methyl- or ethyl-substituted complexes. In contrast to bis(imino)pyridine systems[4], 2-benzimidazolyl-6-iminopyridine systems[15b], 2-quinoxalinyl-6-iminopyridine systems[15c] and 2-imino-1,10-phenanthroline systems[19,20], these cobalt complexes displayed much higher catalytic activities than their corresponding iron analogues under similar reaction conditions.

When the ethylene pressure was increased from 1 atm to 10 atm, the catalytic activity of each complex increased greatly, with a very high selectivity for 1-butene. Complex **5b** was found to have the highest activity [7.33×10^6 g mol^{-1}(Co) h^{-1}; entry 21, Table 4]. For methyl ketimine complexes, methyl-substituted **1b** and ethyl-substituted **2b** showed comparable catalytic activities and a similar distribution of oligomers,

for references, see page 112

whereas isopropyl-substituted **3b** showed a higher activity and gave a larger amount of hexene than **1b** and **2b**. A slightly higher amount of hexene was obtained for the corresponding phenyl ketimine complexes than with the methyl ketimine complexes. Complex **6b**, which contains bulkier isopropyl groups on the aryl ring of the imino nitrogen, was found to be slightly less active and produce a wider distribution of oligomers (C_4 to C_{22}, along with small amount of polyethylene waxes) than **4b** or **5b** (entry 22, Table 4).

(iii) Ethylene oligomerization with nickel complexes 1c–6c

Table 5.
Ethylene oligomerization with complexes**1c**–**6c**.[a]

Entry	Cat	Equiv. of PPh_3[b]	P[c] [atm]	T[d] [°C]	t[e] [min]	Activity[f]	Oligomer distribution[g] [%]		Selectivity for 1-C_4[g] [%]
							$C_4/\sum C$	$C_6/\sum C$	
1[h]	**5c**	-	1	20	30	-	-	-	-
2[h]	**5c**	10	1	20	30	-	-	-	-
3[i]	**5c**	-	1	20	30	0.048	100	-	92.8
4[i]	**5c**	10	1	20	30	0.128	100	-	41.6
5	**5c**	-	1	20	30	0.143	100	-	78.5
6	**5c**	2	1	20	30	0.963	97.8	2.2	27.1
7	**5c**	5	1	20	30	2.29	98.1	1.9	24.0
8	**5c**	10	1	20	30	3.31	98.1	1.9	15.9
9	**5c**	10	1	20	60	3.71	96.5	3.5	3.5
10	**5c**	20	1	20	30	6.82	97.7	2.3	8.5
11	**5c**	30	1	20	30	2.75	98.8	1.2	27.2
12	**5c**	10	1	0	30	1.14	99.2	0.8	34.6
13	**5c**	10	1	0	60	1.91	98.4	1.6	16.3
14	**5c**	10	1	40	30	2.36	97.2	2.8	22.7
15	**5c**	10	1	60	30	1.58	95.4	4.6	20.2
16	**1c**	10	1	20	30	3.74	98.0	2.0	17.5
17	**1c**	10	1	20	60	3.49	96.7	3.3	4.3
18	**2c**	10	1	20	30	3.29	97.3	2.7	15.9
19	**2c**	10	1	20	60	4.67	97.0	3.0	5.8
20	**3c**	10	1	20	30	3.33	97.5	2.5	14.0
21	**3c**	10	1	20	60	3.68	96.1	3.9	3.2
22	**4c**	10	1	20	30	3.47	97.8	2.2	15.2
23	**4c**	10	1	20	60	4.71	95.7	4.3	2.8
24	**6c**	10	1	20	30	5.88	97.5	2.5	10.6
25	**6c**	10	1	20	60	3.89	96.4	3.6	6.6
26	**5c**	-	10	30	30	2.26	98.9	1.1	97.1
27	**5c**	10	10	30	30	5.87	100	-	93.0
28	**5c**	20	10	30	30	51.7	97.5	2.5	36.5
29	**1c**	20	10	30	30	36.8	98.1	1.9	36.2
30	**2c**	20	10	30	30	61.5	98.7	1.3	50.2
31	**3c**	20	10	30	30	39.6	98.9	1.1	63.4
32	**4c**	20	10	30	30	39.1	98.1	1.9	38.9
33	**6c**	20	10	30	30	57.7	98.4	1.6	34.9

[a] General conditions: cat.: 5 µmol, co-cat.: Et_2AlCl, Al/Ni: 300, solvent (toluene): 30 mL for 1 atm and 100 mL for 10 atm. [b] PPh_3 as an auxiliary ligand. [c] Ethylene pressure. [d] Reaction temperature. [e] Reaction time. [f] 10^5 g mol^{-1}(Ni) h^{-1}. [g] Weight percentage determined by GC. [h] Co-cat.: MAO, Al/Ni: 500. [i] Co-cat.: MMAO, Al/Ni: 500.

for references, see page 112

Complex **5c** was investigated for ethylene oligomerization in the presence of different co-catalysts at 1 atm of ethylene pressure. Unlike the nickel complexes ligated by other 1,10-phenanthroline derivatives,[11–13] almost no catalytic activity was observed with **5c** in the presence of MAO. When MMAO was used as a co-catalyst, however, slightly better activity was obtained and only butene was generated, with a high selectivity for 1-butene (entry 3, Table 5). However, Et_2AlCl was found to be more effective as a co-catalyst for nickel complexes, although the selectivity for 1-butene was slightly lower. For example, at an Al/Ni molar ratio of 300, **5c**/Et_2AlCl showed an activity of 1.43×10^4 g mol^{-1}(Ni) h^{-1}, with a selectivity of 78.5% for 1-butene, at 1 atm of ethylene pressure (entry 5, Table 5).

The addition of PPh_3 as an auxiliary ligand to the nickel-based catalytic systems has been demonstrated to improve catalytic activity and prolong catalyst lifetime,[7a,12,26] although the mechanism is still not clear. However, in the presence of MAO, the addition of 10 equiv. of PPh_3 had no effect and the system still had no activity. For the catalytic system **5c**/MMAO, the addition of 10 equiv. of PPh_3 resulted in an increase in catalytic activity but a drastic decrease in the selectivity for 1-butene (entry 4, Table 5). The effect of varying the amount of PPh_3 added on the catalytic activity and the selectivity for 1-butene was investigated with the catalytic system **5c**/Et_2AlCl at 1 atm of ethylene pressure. Addition of 2 equiv. of PPh_3 improved the catalytic activity to 9.63×10^4 g mol^{-1}(Ni) h^{-1}, with a small amount of hexene generated, whereas the selectivity for 1-butene decreased from 78.5% to 27.1% (entry 6, Table 5). Increasing the amount of PPh_3 (≤ 20) led to a further enhancement of catalytic activity and a further decrease of selectivity for 1-butene. The addition In the presence of 20 equivalvents of PPh_3 gave the highest activity [6.82×10^5 g mol^{-1}(Ni) h^{-1}] and the lowest selectivity (8.5%; entry 10, Table 5). Further increasing the amount of PPh_3 to 30 equivalents reduced the catalytic activity and increased the selectivity for 1-butene.

The effect of reaction temperature on the catalytic properties was also studied in the presence of 10 equiv. of PPh_3. When keeping the other conditions constant, the optimum catalytic activity was obtained at 20 °C ; both increasing and decreasing the reaction temperature led to a lower catalytic activity and higher selectivity for 1-butene. In general, an induction time of 10–20 min is observed after the addition of PPh_3, and a lower temperature led to a longer induction time and catalyst lifetime. For instance, the catalytic activity of **5c** at 0 or 20 °C after 60 min was found to be higher than that after 30 min, although a lower selectivity for 1-butene was obtained with a slightly larger amount of hexene produced after 60 min, which indicates that the isomerization reaction

for references, see page 112

of 1-butene to 2-butene takes place at the same time as oligomerization reaction. Generally, phenyl ketimine complexes display slightly higher activity than methyl ketimine complexes bearing the same substituents on the aryl ring of the imino nitrogen. The catalytic properties of methyl ketimine complexes after 30 min were found to be not greatly affected by the substituents on the aryl ring of the imino nitrogen, and complexes **1c**–**3c** showed comparable catalytic activity and similar selectivity for 1-butene. However, when the reaction time was prolonged to 60 min, a higher catalytic activity and slightly higher selectivity for 1-butene were achieved with ethyl-substituted **2c** than with methyl-substituted **1c** and isopropyl-substituted **3c**. For phenyl ketimine complexes, isopropyl-substituted **6c** showed the highest activity of 5.88×10^5 g mol^{-1}(Ni) h^{-1} after 30 min and methyl-substituted **4c** showed the highest activity of 4.71×10^5 g mol^{-1}(Ni) h^{-1} after 60 min (entry 23 and 24, Table 5).

The catalytic activity and selectivity for 1-butene of **5c** increased to 2.26×10^5 g mol^{-1}(Ni) h^{-1} and 97.1%, respectively (entry 26, Table 5) at 10 atm of ethylene pressure without PPh_3, whereas at 10 atm the catalytic activity and selectivity for 1-butene did not change greatly when 10 equiv. of PPh_3 was introduced into the catalytic system (entry 27, Table 5), which means that both the PPh_3/Ni molar ratio and the concentration of PPh_3 in the reaction solution affect on the catalytic properties. When the amount of PPh_3 was increased to 20 equivalents, the catalytic activity of **5c** increased to 5.17×10^6 g mol^{-1}(Ni) h^{-1}, with a lower selectivity for 1-butene (36.5%; entry 28, Table 5). Five other nickel complexes were therefore also investigated in the presence of 20 equiv. of PPh_3 at 10 atm of ethylene pressure. A higher catalytic activity and selectivity for 1-butene was obtained for each complex than at 1 atm, and the highest activity of 6.15×10^6 g mol^{-1}(Ni) h^{-1} was achieved with **2c**, with a selectivity of 50.2% for 1-butene. In general, the selectivity for 1-butene increases with increasing ethylene pressure, probably due to a competition between chain transfer and chain isomerization, and a higher ethylene concentration thus favors the formation of 1-butene due to rapid chain transfer rather than chain isomerization.[27]

Conclusion

A series of iron, cobalt and nickel complexes bearing 2-imino-9-phenyl-1,10-phenanthroline ligands have been synthesized, characterized, and evaluated as catalyst precursors in ethylene oligomerization. Some iron complexes gave good catalytic activities, with high selectivity for ethylene oligomerization [**1a**/MMAO: 2.69×10^6 g mol^{-1}(Fe) h^{-1}], upon treatment with MAO or MMAO.

for references, see page 112

Unexpectedly, in contrast to previous results with other tridentate N_3 catalytic systems, the cobalt complexes generally show much higher activities and broader oligomer distributions than the corresponding iron analogues. The ligand environment and the reaction parameters play an important role in influencing both the catalytic activity and the oligomer distributions for iron and cobalt complexes. The highest activity of up to 7.33×10^6 g mol^{-1}(Co) h^{-1} for ethylene oligomerization has been obtained with the catalytic system **5b**/MAO at 10 atm of ethylene pressure. Et_2AlCl is a more effective co-catalyst for nickel complexes, and the addition of PPh_3 significantly improves the catalytic activity and prolongs the catalyst lifetime. The addition of 20 equiv. of PPh_3 leads to higher catalytic activities at 10 atm of ethylene pressure.

Experimental Section

General Considerations: All manipulations for air or moisture-sensitive compounds were carried out under an atmosphere of nitrogen using standard Schlenk techniques. Melting points (m.p.) were measured with a digital electrothermal apparatus without calibration. IR spectra were recorded on a Perkin-Elmer FT-IR 2000 spectrometer by using KBr disc in the range of 4000–400 cm^{-1}. ^1H NMR and ^{13}C NMR spectra were recorded on a Bruker DMX-300 or DMX-400 instrument with TMS as the internal standard. Splitting patterns are designated as follows: s, singlet; d, doublet; dd, double doublet; t, triplet; quad, quadruplet; sept, septet; m, multiplet. Elemental analyses were performed on a Flash EA1112 microanalyzer. GC analyses were performed with a Varian CP-3800 gas chromatograph equipped with a flame ionization detector and a 30 m (0.2 mm i.d., 0.25 μm film thickness) CP-Sil 5 CB capillary column. The yield of oligomers was calculated by referencing to the mass of solvent on the basis of the prerequisite that the mass of each fraction was approximately proportional to its integrated area in the GC trace.

Toluene, diethyl ether and tetrahydrofuran were refluxed over sodium-benzophenone and distilled under nitrogen prior to use. Diethylaluminum chloride was purchased from Acros Chemicals. Methylaluminoxane (MAO, 1.46 M in toluene) and modified-methylaluminoxane (MMAO-3A, 7% aluminum in heptane solution) were purchased from Akzo Corp (USA). All other chemicals were obtained commercially and used without further purification unless otherwise stated.

Synthesis of 2-acetyl-9-phenyl-1,10-phenanthroline (I)

2-(2-Methyl-1,3-dioxolan-2-yl)-1,10-phenanthroline: The mixture of 2-acetyl-1,10-phenanthroline (2.230 g, 10.0 mmol), glycol (3.254 g, 52.4 mmol) and

for references, see page 112

p-toluenesulfonic acid (206 mg) was refluxed in toluene (100 mL) for 18 h until no further formation of water was observed in a Dean-Stark trap. And then the solvent was removed under reduced pressure and the residue was eluted with petroleum ether/ethyl acetate (1:2, v/v) on an alumina column. The second eluting fraction was collected and concentrated to give a slightly yellow solid in 50.0% yield (1.333 g). m.p. 119–121 °C. FT-IR (KBr disc): 3054, 2993, 2980, 2938, 2900, 1619, 1589, 1552, 1505, 1490, 1476, 1445, 1391, 1376, 1256, 1232, 1204, 1147, 1129, 1106, 1029, 1009, 953, 855, 789, 752, 675 cm^{-1}. ^{1}H NMR (400 MHz, $CDCl_3$): δ = 9.24 (d, J = 4.4 Hz, 1 H, phen), 8.25 (d, J = 8.4 Hz, 1 H, phen), 8.22 (d, J = 8.4 Hz, 1 H, phen), 7.93 (d, J = 8.4 Hz, 1 H, phen), 7.77 (s, 2 H, phen), 7.61 (dd, J = 4.4 Hz, 1 H, phen), 4.18 (t, J = 6.4 Hz, 2 H, CH_2), 4.01 (t, J = 6.4 Hz, 2 H, CH_2), 1.98 (s, 3 H, CH_3) ppm. ^{13}C NMR (100 MHz, $CDCl_3$): δ = 161.5, 150.5, 146.4, 145.8, 136.8, 136.0, 129.0, 128.1, 126.7, 126.3, 122.9, 119.5, 109.2, 65.2, 25.6 ppm. $C_{16}H_{14}N_2O_2$ (266.29): calcd. C 72.16, H 5.30, N 10.52; found C 72.18, H 5.23, N 11.00.

2-Acetyl-9-phenyl-1,10-phenanthroline (I): Phenyllithium solution was prepared through the slow addition of a bromobenzene (0.9 mL, 8.50 mmol) solution in diethyl ether (20 mL) to two equivalents of lithium (118 mg, 17.0 mmol) in diethyl ether (30 mL) at room temperature under nitrogen. Phenyllithium solution was thereafter added dropwise to a suspension of 2-(2-methyl-1,3-dioxolan-2-yl)-1,10-phenanthroline (1.333 g, 5.00 mmol) in toluene (40 mL) at 0 °C and the initial yellow suspension turned dark brown. After the addition, the resultant solution was stirred under nitrogen at 0 °C for an additional 3 h. Thereafter the reaction was quenched by slow addition of water (100 mL) and stirred. The yellow organic layer was separated and the aqueous layer was extracted several times with CH_2Cl_2, and then the organic phase was merged and dried over anhydrous sodium sulfate. After the evaporation of solvent, the residue was purified on a silica column and the pure product was obtained as a yellow oil. Thereafter the oil was dissolved in 50 mL acetone with p-toluenesulfonic acid (170 mg) as a catalyst and refluxed for 15 h. The desired product was precipitated from the solution and collected by filtration as a pale yellow solid in 47.5% yield (710 mg). m.p. 184–186 °C. FT-IR (KBr disc): 3103, 3026, 2916, 1694, 1633, 1620, 1597, 1565, 1537, 1495, 1367, 1285, 1219, 1190, 1120, 1034, 1011, 888, 817, 766, 741, 678, 566 cm^{-1}. ^{1}H NMR (300 MHz, $CDCl_3$): δ = 8.44 (d, J = 7.2 Hz, 2 H, Ph), 8.34 (d, J = 3.0 Hz, 2 H, phen), 8.30 (d, J = 8.4 Hz, 1 H, phen), 8.17 (d, J = 8.4 Hz, 1 H, phen), 7.88 (d, J = 8.7 Hz, 1 H, phen), 7.78 (d, J = 8.7 Hz, 1 H, phen), 7.59 (t, J = 7.2 Hz, 2 H, Ph), 7.50 (t, J = 7.2 Hz, 1 H, Ph), 3.14 (s, 3 H, $COCH_3$) ppm. ^{13}C NMR (75 MHz, $CDCl_3$): δ = 200.3,

for references, see page 112

156.6, 152.3, 145.4, 144.8, 138.5, 136.5, 130.4, 129.3, 128.4, 128.1, 127.3, 127.0, 125.3, 119.7, 119.6, 25.2 ppm. $C_{20}H_{14}N_2O$ (298.34): calcd. C 80.52, H 4.73, N 9.39; found C 80.00, H 4.77, N 9.36.

Synthesis of 2-benzoyl-9-phenyl-1,10-phenanthroline (II)

Phenyllithium solution was prepared through the slow addition of a bromobenzene (3.2 mL, 30.5 mmol) solution in diethyl ether (20 mL) to two equivalents of lithium (439 mg, 63.2 mmol) in diethyl ether (30 mL) at room temperature under nitrogen. Phenyllithium solution was thereafter added dropwise to a suspension of 2-cyano-1,10-phenanthroline (2.053 g, 10.0 mmol) in toluene (50 mL) at –78 °C and then the temperature was slowly warmed to room temperature. After stirred for 12 h at room temperature, the reaction was quenched by slow addition of water (100 mL) and stirred. The red organic layer was separated and the aqueous layer was extracted several times with CH2Cl2, and then the organic phase was merged and dried over anhydrous sodium sulfate. After the evaporation of the solvent, the residue was purified through a silica column and the pure product was obtained as a yellow solid in 21.3% yield (1.245 g). m.p. 162–164 °C. FT-IR (KBr disc): 3060, 3034, 1645, 1616, 1595, 1575, 1545, 1505, 1486, 1446, 1420, 1364, 1319, 1288, 1183, 1152, 1093, 1023, 944, 878, 865, 768, 716, 692 cm^{-1}. ^1H NMR (300 MHz, $CDCl_3$): δ = 8.93 (d, J = 7.2 Hz, 2 H, Ph), 8.55–8.39 (m, 4 H), 8.30 (d, J = 8.4 Hz, 1H, phen), 8.16 (d, J = 8.4 Hz, 1 H, phen), 7.89 (d, J = 8.7 Hz, 1 H, phen), 7.81 (d, J = 8.7 Hz, 1 H, phen), 7.72–7.62 (m, 3 H, Ph), 7.56–7.49 (m, 3 H, Ph) ppm. ^{13}C NMR (100 MHz, $CDCl_3$): δ = 191.4, 156.5, 153.4, 145.9, 144.6, 138.8, 136.7, 136.6, 132.7, 132.5, 129.8, 129.6, 128.6, 128.3, 127.8, 127.5, 127.3, 125.4, 122.6, 119.6 ppm. $C_{25}H_{16}N_2O$ (360.41): calcd. C 83.31, H 4.47, N 7.77; found C 82.94, H 4.45, N 7.73.

Synthesis of Ligands 1–6

Ligand 1: A reaction mixture of 2-acetyl-9-phenyl-1,10-phenanthroline (225 mg, 0.75 mmol), 2,6-dimethylaniline (184 mg, 1.50 mmol), p-toluenesulfonic acid (80 mg) in toluene (20 mL) was refluxed for 24 h under N2 atmosphere. The solvent was evaporated under reduced pressure and the residue was eluted with petroleum ether/ethyl acetate (20:1, v/v) on an alumina column. The second eluting part was collected and concentrated to give a yellow solid in 34.6% yield (105 mg). m.p. 190–192 °C. FT-IR (KBr disc): 3041, 3018, 2914, 1635, 1605, 1590, 1546, 1506, 1485, 1467, 1362, 1293, 1204, 1118, 1091, 855, 761, 739, 687 cm^{-1}. ^1H NMR (300 MHz, $CDCl_3$): δ = 8.80 (d, J = 8.4 Hz, 1 H, phen), 8.45 (d, J = 7.5 Hz, 2 H, Ph), 8.34 (d, J =

for references, see page 112

8.7 Hz, 2 H, phen), 8.18 (d, J = 8.4 Hz, 1 H, phen), 7.85 (d, J = 3.9 Hz, 2 H, phen), 7.56 (t, J = 7.5 Hz, 2 H, Ph), 7.47 (t, J = 7.5 Hz, 1 H, Ph), 7.11 (d, J = 7.5 Hz, 2H, Ar), 6.97 (t, J = 7.5 Hz, 1 H, Ar), 2.62 (s, 3 H, $COCH_3$), 2.09 (s, 6 H, 2 Me) ppm. ^{13}C NMR (75 MHz, $CDCl_3$): δ = 168.0, 156.9, 155.8, 149.0, 146.0, 145.1, 139.2, 137.1, 136.5, 129.8, 129.6, 128.9, 127.9, 127.8, 127.5, 127.3, 126.1, 125.3, 123.1, 120.6, 119.9, 18.0, 16.7 ppm. $C_{28}H_{23}N_3$ (401.50): calcd. C 83.76, H 5.77, N 10.47; found C 83.69, H 5.76, N 10.40.

Ligand 2: In a similar manner as described for ligand **1**, ligand **2** was prepared from 2-acetyl-9-phenyl-1,10-phenanthroline (446 mg, 1.50 mmol) and 2,6-diethylaniline (491 mg, 3.20 mmol) as a yellow solid in 44.2% yield (284 mg). m.p. 181–183 °C. FT-IR (KBr disc): 3060, 3037, 2960, 2929, 2868, 1639, 1608, 1589, 1546, 1507, 1486, 1452, 1418, 1369, 1296, 1258, 1194, 1119, 1099, 862, 828, 762, 740, 686 cm^{-1}. ^1H NMR (300 MHz, $CDCl_3$): δ = 8.80 (d, J = 8.4 Hz, 1 H, phen), 8.45 (d, J = 7.5 Hz, 2 H, Ph), 8.33 (d, J = 8.4 Hz, 2 H, phen), 8.17 (d, J = 8.4 Hz, 1 H, phen), 7.80 (d, J = 3.9 Hz, 2 H, phen), 7.56 (t, J = 7.5 Hz, 2 H, Ph), 7.47 (t, J = 7.5 Hz, 1 H, Ph), 7.16 (d, J = 7.2 Hz, 2 H, Ar), 7.07 (t, J = 7.2 Hz, 1 H, Ar), 2.64 (s, 3 H, $COCH_3$), 2.42 (q, J = 7.2 Hz, 4 H, 2 Et), 1.16 (t, J = 7.2 Hz, 6 H, 2 Et) ppm. ^{13}C NMR (75 MHz, $CDCl_3$): δ = 167.7, 156.9, 155.9, 148.0, 146.0, 145.1, 139.2, 137.1, 136.5, 131.1, 129.8, 129.6, 128.9, 127.8, 127.5, 127.3, 126.1, 126.0, 123.4, 120.5, 119.8, 24.7, 17.0, 13.8 ppm. $C_{30}H_{27}N_3$ (429.56): calcd. C 83.88, H 6.34, N 9.78; found C 83.66, H 6.40, N 9.60.

Ligand 3: n a similar manner as described for ligand **1**, ligand **3** was prepared from 2-acetyl-9-phenyl-1,10-phenanthroline (298 mg, 1.00 mmol) and 2,6-diisopropylaniline (448 mg, 2.50 mmol) as a yellow solid in 53.1% yield (243 mg). m.p. 256–258 °C. FT-IR (KBr disc): 3061, 2962, 2924, 2865, 1635, 1607, 1589, 1579, 1546, 1507, 1486, 1462, 1436, 1420, 1381, 1366, 1294, 1247, 1189, 1117, 1097, 860, 780, 761, 741, 685 cm^{-1}. ^1H NMR (400 MHz, $CDCl_3$): δ = 8.82 (d, J = 8.4 Hz, 1 H, phen), 8.45 (d, J = 7.6 Hz, 2 H, Ph), 8.33 (dd, J = 8.4 Hz, 2 H, phen), 8.17 (d, J = 8.4 Hz, 1 H, phen), 7.88 (d, J = 4.0 Hz, 2 H, phen), 7.56 (t, J = 7.6 Hz, 2 H, Ph), 7.47 (t, J = 7.6 Hz, 1 H, Ph), 7.21 (d, J = 7.6 Hz, 2 H, Ar), 7.13 (t, J = 7.6 Hz, 1 H, Ar), 2.86 (sept, J = 6.8 Hz, 2 H, 2 *i*Pr), 2.66 (s, 3 H, $COCH_3$), 1.18 (dd, J = 6.8 Hz, 12 H, 2 *i*Pr) ppm. ^{13}C NMR (75 MHz, $CDCl_3$): δ = 167.7, 156.9, 155.8, 146.7, 146.0, 145.2, 139.2, 137.1, 136.5, 135.8, 129.9, 129.7, 129.0, 127.8, 127.5, 127.3, 126.1, 123.7, 123.1, 120.6, 119.9, 28.3, 23.3, 23.0, 17.3 ppm. $C_{32}H_{31}N_3$ (457.61): calcd. C 83.99, H 6.83, N 9.18; found C 84.00, H 6.84, N 8.98.

for references, see page 112

Ligand 4: 2-Benzoyl-9-phenyl-1,10-phenanthroline (760 mg, 2.10 mmol), 2,6-dimethylaniline (585 mg, 4.80 mmol) and p-toluenesulfonic acid (100 mg) were combined with tetraethyl silicate (5 mL) in a flask. The flask was equipped with a condenser along with a Dean-Stark trap, and the mixture was heated at ~130 °C for 36 h under N_2 atmosphere. Tetraethyl silicate was removed under the reduced pressure and the residue was eluted with petroleum ether/ethyl acetate (6:1, v/v) on an alumina column. The second eluting part was collected and concentrated to give a yellow solid in 38.4% yield (376 mg). m.p. 142–144 °C. FT-IR (KBr disc): 3055, 2943, 1616, 1589, 1577, 1544, 1505, 1484, 1441, 1368, 1319, 1290, 1207, 1088, 1024, 969, 858, 773, 765, 740, 716, 694 cm^{-1}. ^1H NMR (400 MHz, $CDCl_3$): δ = 8.87 (d, J = 8.4 Hz, 1 H, phen), 8.37 (d, J = 8.4 Hz, 1 H, phen), 8.26–8.24 (m, 3 H), 8.11 (d, J = 8.4 Hz, 1 H, phen), 7.82 (s, 2 H, phen), 7.57 (d, J = 8.0 Hz, 2 H, Ph), 7.46 (m, 4 H, Ph), 7.38 (t, J = 7.2 Hz, 2 H, Ph), 6.96 (d, J = 7.2 Hz, 2 H, Ar), 6.86 (t, J = 7.2 Hz, 1 H, Ar), 2.12 (s, 6 H, 2 Me) ppm. ^{13}C NMR (100 MHz, $CDCl_3$): δ = 166.1, 155.9, 155.7, 148.2, 145.7, 144.7, 138.5, 136.3, 136.0, 135.4, 129.6, 129.2, 129.1, 128.9, 128.3, 127.9, 127.3, 127.0, 126.8, 126.7, 125.5, 125.2, 122.7, 121.7, 118.9, 18.2 ppm. $C_{33}H_{25}N_3$ (463.57): calcd. C 85.50, H 5.44, N 9.06; found C 85.14, H 5.47, N 8.94.

Ligand 5: In a similar manner as described for ligand **4**, ligand **5** was prepared from 2-benzoyl-9-phenyl-1,10-phenanthroline (570 mg, 1.58 mmol) and 2,6-diethylaniline (498 mg, 3.27 mmol) as a yellow solid in 72.8% yield (556 mg). m.p. 187–189 °C. FT-IR (KBr disc): 3060, 3034, 2962, 2918, 1618, 1586, 1542, 1504, 1485, 1440, 1363, 1294, 1200, 1090, 965, 869, 763, 697 cm^{-1}. ^1H NMR (400 MHz, $CDCl_3$): δ = 8.85 (d, J = 8.0 Hz, 1 H, phen), 8.37–8.22 (m, 4 H), 8.09 (d, J = 8.0 Hz, 1 H, phen), 7.80 (s, 2 H, phen), 7.58 (s, 2 H, Ph), 7.45–7.36 (m, 6 H, Ph), 7.01–6.97 (m, 3 H, Ar), 2.61 (q, J = 7.2 Hz, 2 H, Et), 2.34 (q, J = 7.2 Hz, 2 H, Et), 1.16 (t, J = 7.2 Hz, 6 H, 2 Et) ppm. ^{13}C NMR (100 MHz, $CDCl_3$): δ = 165.7, 156.2, 156.1, 147.6, 146.1, 145.1, 138.9, 136.7, 136.4, 135.4, 131.1, 130.3, 129.6, 129.2, 128.7, 128.5, 127.7, 127.5, 127.3, 127.2, 125.8, 125.5, 123.4, 122.1, 119.2, 24.5, 13.5 ppm. $C_{35}H_{29}N_3$ (491.62): calcd. C 85.51, H 5.95, N 8.55; found C 85.03, H 5.94, N 8.48.

Ligand 6: In a similar manner as described for ligand **4**, ligand **6** was prepared from 2-benzoyl-9-phenyl-1,10-phenanthroline (394 mg, 1.09 mmol) and 2,6-diisopropylaniline (433 mg, 2.44 mmol) as a yellow solid in 74.0% yield (420 mg). m.p. 170–171 °C. FT-IR (KBr disc): 3063, 2958, 2860, 1611, 1588, 1544, 1506, 1487, 1463, 1430, 1358, 1291, 1194, 1091, 966, 858, 777, 757, 701 cm^{-1}. ^1H NMR (300 MHz, $CDCl_3$): δ = 8.84 (d, J = 8.4 Hz, 1 H, phen), 8.38–8.24 (m, 4 H), 8.11 (d, J = 8.4 Hz, 1 H,

for references, see page 112

phen), 7.82 (s, 2 H, phen), 7.62 (m, 2 H, Ph), 7.49–7.39 (m, 6 H, Ph), 7.04(m, 3 H, Ar), 3.00 (sept, 2 H, 2 *i*Pr), 1.19 (d, 6 H, iPr), 0.97 (d, 6 H, *i*Pr) ppm. ^{13}C NMR (100 MHz, $CDCl_3$): δ = 164.9, 155.9, 145.7, 144.6, 138.5, 136.3, 136.0, 135.2, 134.5, 130.3, 129.1, 128.7, 128.4, 128.2, 128.1, 127.2, 127.1, 126.9, 126.7, 125.4, 123.2, 122.4, 121.8, 111.8, 28.1, 23.7, 21.6 ppm. $C_{37}H_{33}N_3$ (519.68): calcd. C 85.51, H 6.40, N 8.09; found C 84.91, H 6.36, N 7.84.

Synthesis of Iron(II) Complexes 1a–6a

General procedure: The ligand (0.20 mmol) and one equivalent of $FeCl_2·4H_2O$ (0.20 mmol) were added together in a Schlenk tube that was purged three times with nitrogen and then charged with THF. The reaction mixture was stirred at room temperature for 9 h. The resulting precipitate was filtered, washed with diethyl ether and dried in vacuum. All the iron(II) complexes were prepared in high yield in this manner.

Complex 1a: Isolated as a green powder in 98.4% yield (104 mg). FT-IR (KBr disc): 3059, 2953, 2918, 2867, 1615, 1590, 1555, 1504, 1491, 1468, 1451, 1435, 1374, 1299, 1205, 865, 792, 772, 745, 702 cm^{-1}. $C_{28}H_{23}Cl_2FeN_3·1/2CH_2Cl_2$ (570.72): calcd. C 59.98, H 4.24, N 7.36; found C 59.61, H 4.34, N 7.28.

Complex 2a: Isolated as a green powder in 95.9% yield (107 mg). FT-IR (KBr disc): 3063, 2966, 2929, 2872, 1617, 1584, 1558, 1504, 1490, 1442, 1374, 1289, 1243, 1205, 1193, 1152, 1141, 1060, 859, 786, 759, 744, 701 cm^{-1}. $C_{30}H_{27}Cl_2FeN_3$ (556.31): calcd. C 64.77, H 4.89, N 7.55; found C 64.26, H 4.59, N 7.50.

Complex 3a: Isolated as a green powder in 66.2% yield (78 mg). FT-IR (KBr disc): 3062, 2969, 2926, 2865, 1611, 1590, 1557, 1501, 1490, 1463, 1440, 1374, 1330, 1286, 1247, 1185, 1152, 1138, 870, 786, 748, 701 cm^{-1}. $C_{32}H_{31}Cl_2FeN_3$ (584.36): calcd. C 65.77, H 5.35, N 7.19; found C 65.15, H 5.32, N 6.95.

Complex 4a: Isolated as a gray-green powder in 86.9% yield (103 mg). FT-IR (KBr disc): 3056, 2922, 1620, 1588, 1549, 1489, 1445, 1368, 1300, 1212, 1155, 1001, 863, 774, 744, 703 cm^{-1}. $C_{33}H_{25}Cl_2FeN_3·H_2O$ (608.34): calcd. C 65.15, H 4.47, N 6.91; found C 65.12, H 4.11, N 6.85.

Complex 5a: Isolated as a brown powder in 79.8% yield (99 mg). FT-IR (KBr disc): 3061, 2966, 2874, 1594, 1553, 1490, 1444, 1368, 1291, 1261, 1107, 1059, 1000, 868, 781, 702 cm^{-1}. $C_{35}H_{29}Cl_2FeN_3$ (618.38): calcd. C 67.98, H 4.73, N 6.80; found C 67.94, H 4.78, N 6.57.

Complex 6a: Isolated as a green powder in 86.6% yield (112 mg). FT-IR (KBr disc): 3031, 2959, 2866, 1620, 1587, 1550, 1488, 1459, 1436, 1364, 1319, 1274, 1206,

for references, see page 112

995, 872, 850, 704 cm^{-1}. $C_{37}H_{33}Cl_2FeN_3$ (646.43): calcd. C 68.75, H 5.15, N 6.50; found C 68.42, H 5.23, N 6.59.

Synthesis of Cobalt(II) Complexes 1b–6b and Nickel(II) Complexes 1c–6c

General procedure: The ligand (0.20 mmol) and one equivalent of $CoCl_2$ or $NiCl_2·6H_2O$ (0.20 mmol) were added together in a Schlenk tube and then charged with anhydrous ethanol. The reaction mixture was stirred at room temperature for 9 h. The resulting precipitate was filtered, washed with diethyl ether and dried in vacuum. All the complexes were prepared in high yield in this manner.

Complex 1b: Isolated as a green powder in 65.6% yield (70 mg). FT-IR (KBr disc): 3063, 2945, 2914, 1619, 1585, 1557, 1504, 1490, 1451, 1437, 1374, 1290, 1256, 1206, 1142, 989, 919, 865, 791, 772, 745, 700, 653, 609 cm^{-1}. $C_{28}H_{23}Cl_2CoN_3·H_2O$ (549.36): calcd. C 61.22, H 4.59, N 7.65; found C 61.46, H 4.34, N 7.24.

Complex 2b: Isolated as a green powder in 80.3% yield (91 mg). FT-IR (KBr disc): 3061, 2969, 2924, 2865, 1613, 1582, 1557, 1501, 1489, 1463, 1441, 1375, 1330, 1288, 1185, 1153, 869, 786, 749, 700 cm^{-1}. $C_{30}H_{27}Cl_2CoN_3$ (559.39): calcd. C 64.41, H 4.86, N 7.51; found C 64.25, H 4.92, N 7.27.

Complex 3b: Isolated as a green powder in 85.6% yield (103 mg). FT-IR (KBr disc): 3450, 3062, 2964, 2932, 2875, 1618, 1585, 1558, 1504, 1490, 1441, 1375, 1290, 1193, 859, 787, 760, 745, 701 cm^{-1}. $C_{32}H_{31}Cl_2CoN_3$ (587.45): calcd. C 65.43, H 5.32, N 7.15; found C 64.48, H 5.55, N 6.61.

Complex 4b: Isolated as a red brown powder in 80.2% yield (95 mg). FT-IR (KBr disc): 3057, 2919, 1612, 1597, 1555, 1490, 1445, 1371, 1317, 1289, 1213, 999, 863, 774, 748, 721, 703 cm^{-1}. $C_{33}H_{25}Cl_2CoN_3·CH_2Cl_2$ (678.34): calcd. C 60.20, H 4.01, N 6.19; found C 60.25, H 4.02, N 6.28.

Complex 5b: Isolated as a red brown powder in 77.6% yield (84 mg). FT-IR (KBr disc): 3063, 2963, 2934, 2875, 1613, 1596, 1552, 1498, 1490, 1442, 1371, 1319, 1288, 1108, 995, 872, 782, 751, 720, 701 cm^{-1}. $C_{35}H_{29}Cl_2CoN_3·CH_2Cl_2$ (706.40): calcd. C 61.21, H 4.42, N 5.95; found C 60.68, H 4.28, N 5.63.

Complex 6b: Isolated as a red brown powder in 78.4% yield (103 mg). FT-IR (KBr disc): 3058, 3032, 2959, 2924, 2865, 1619, 1599, 1552, 1489, 1437, 1370, 1319, 1274, 1207, 1100, 995, 873, 850, 759, 718, 652 cm^{-1}. $C_{37}H_{33}Cl_2CoN_3·CH_2Cl_2$ (734.45): calcd. C 62.14, H 4.80, N 5.72; found C 62.17, H 4.82, N 5.54.

Complex 1c: Isolated as an orange powder in 89.3% yield (95 mg). FT-IR (KBr disc): 3445, 3056, 1611, 1587, 1556, 1503, 1489, 1453, 1376, 1294, 1204, 1148, 862,

for references, see page 112

793, 773, 745, 702 cm^{-1}. $C_{28}H_{23}Cl_2N_3Ni \cdot 1/2CH_2Cl_2$ (573.57): calcd. C 59.68, H 4.22, N 7.33; found C 59.89, H 4.44, N 7.20.

Complex 2c: Isolated as an orange powder in 89.7% yield (100 mg). FT-IR (KBr disc): 3442, 3062, 2958, 2871, 1616, 1584, 1559, 1502, 1489, 1442, 1377, 1302, 1292, 1192, 1060, 859, 787, 762, 744, 701 cm^{-1}. $C_{30}H_{27}Cl_2N_3Ni \cdot 1/2CH_2Cl_2$ (601.62): calcd. C 60.89, H 4.69, N 6.98; found C 60.46, H 4.96, N 6.67.

Complex 3c: Isolated as an orange powder in 76.5% yield (90 mg). FT-IR (KBr disc): 3426, 3060, 2967, 2865, 1609, 1586, 1558, 1489, 1443, 1378, 1330, 1293, 1185, 1151, 869, 787, 761, 749, 702 cm^{-1}. $C_{32}H_{31}Cl_2N_3Ni \cdot CH_2Cl_2$ (672.14): calcd. C 58.97, H 4.95, N 6.25; found C 58.44, H 5.02, N 6.20.

Complex 4c: Isolated as a yellow powder in 96.0% yield (114 mg). FT-IR (KBr disc): 3388, 1618, 1592, 1554, 1486, 1445, 1378, 1290, 1212, 1057, 1038, 1004, 868, 778, 754, 723, 703 cm^{-1}. $C_{33}H_{25}Cl_2N_3Ni \cdot H_2O$ (611.19): calcd. C 64.85, H 4.45, N 6.88; found C 65.09, H 4.16, N 6.82.

Complex 5c: Isolated as a orange powder in 90.6% yield (113 mg). FT-IR (KBr disc): 3061, 2963, 1597, 1558, 1489, 1443, 1377, 1291, 1209, 1148, 1108, 1065, 1040, 1004, 867, 784, 706 cm^{-1}. $C_{35}H_{29}Cl_2N_3Ni \cdot 1/2CH_2Cl_2$ (663.69): calcd. C 64.24, H 4.56, N 6.33; found C 64.50, H 4.75, N 6.60.

Complex 6c: Isolated as an orange powder in 75.1% yield (98 mg). FT-IR (KBr disc): 3440, 3057, 2962, 2866, 1621, 1595, 1554, 1490, 1439, 1377, 1322, 1293, 1207, 1151, 1101, 1024, 872, 784, 763, 707 cm^{-1}. $C_{37}H_{33}Cl_2N_3Ni \cdot 1/2CH_2Cl_2$ (691.75): calcd. C 65.11, H 4.95, N 6.07; found C 65.01, H 5.04, N 5.85.

General Procedure for Ethylene Oligomerization

Ethylene oligomerization at 1 atm of ethylene pressure: A flame dried three-neck flask was loaded with the catalyst precursor and vacuumized-filled three times by nitrogen. Then ethylene was charged together with freshly distilled toluene and stirred for 10 min under 1 atm of ethylene pressure. The reaction temperature was controlled by the water bath and the given amount of co-catalyst was injected via a syringe. The reaction mixture was stirred for the required time and then terminated with 5% aqueous hydrogen chloride. The contents and distribution of oligomers were determined by GC.

Ethylene oligomerization at 10 atm of ethylene pressure: A 250-mL autoclave stainless steel reactor equipped with a mechanical stirrer and a temperature controller was heated in *vacuo* for at least 2 h over 80 °C, allowed to cool to the required reaction

for references, see page 112

temperature under ethylene atmosphere and then charged with toluene, the desired amount of co-catalyst, toluene solution of catalyst precursor and the total volume was 100 mL. At the reaction temperature, the reactor was sealed and pressurized to 10 atm of ethylene pressure and the ethylene pressure was kept with feeding of ethylene. After the reaction was carried out for the required period, the pressure was released. A small amount of the reaction solution was collected and terminated by the addition of 5% aqueous hydrogen chloride. The organic layer was analyzed by gas chromatography (GC) for determining the composition and mass distribution of oligomers obtained. At last, the residual reaction solution was quenched with 5% hydrochloric acid ethanol.

X-ray Crystallography

Single-crystal X-ray diffraction studies for **2a**, **1b**, **1c** and **5c** were carried out on a Bruker P4 diffractometer with graphite monochromated Mo-K_α radiation (λ = 0.71073 Å) at 293(2) K. Intensity data for crystals of **2**, **4b** and **6b** were collected on a Bruker SMART 1000 CCD diffractometer with graphite monochromated Mo-K_α radiation (λ = 0.71073 Å). Cell parameters were obtained by global refinement of the positions of all collected reflections. Intensities were corrected for Lorentz and polarization effects and empirical absorption. The structures were solved by direct methods and refined by full-matrix least-squares on F^2. All non-hydrogen atoms were refined anisotropically. All hydrogen atoms were placed in calculated positions. Structure solution and refinement were performed by using the SHELXL-97 Package.[28] Crystallographic data and processing parameters for **2**, **2a**, **1b**, **4b**, **6b**, **1c** and **5c** are summarized in Table 6.

CCDC-650185 to -650191 contain the supplementary crystallographic data for this paper, which could be obtained free of charge from the Cambridge Crystallographic Data Centre via www.ccdc.cam.ac.uk/data_request/cif.

Acknowledgments: The project was supported by the National Natural Science Foundation of China (grant no. 20473099 and 20674089). We thank Mr. Saliu Alao Amolegbe (the CAS–TWAS Postgraduate Fellow from Nigeria) for the English corrections.

for references, see page 112

Table 6.
Crystal data and structure refinement for **2**, **2a**, **1b**, **4b**, **6b**, **1c** and **5c**.

	2	**2a**	**1b**	**4b**	**6b**	**1c**	**5c**
Formula	$C_{30}H_{27}N_3$	$C_{30}H_{27}C_{l2}FeN_3O_{0..5}$	$C_{28}H_{23}Cl_2CoN_3O$	$C_{33}H_{25}Cl_2CoN_3{\cdot}CH_2Cl_2$	$C_{37}H_{33}Cl_2CoN_3{\cdot}CH_2Cl_2$	$C_{28}H_{23}Cl_2N_3Ni{\cdot}CH_2Cl_2$	$C_{35}H_{29}Cl_2N_3Ni{\cdot}2CH_2Cl_2$
Formula weight	429.55	564.30	547.32	678.32	734.42	616.03	791.07
Crystal system	Triclinic	Triclinic	Monoclinic	Triclinic	Triclinic	Monoclinic	Triclinic
Space group	*P*–1	*P*–1	*C*2/c	*P*–1	*P*–1	*P*2(1)/c	*P*–1
a [Å]	7.869(2)	13.3880(6)	25.9027(8)	8.6610(14)	9.2300(18)	18.870(4)	9.2599(4)
b [Å]	11.840(3)	14.0560(6)	16.9116(6)	9.5741(15)	10.254(2)	9.7077(19)	9.6246(4)
c [Å]	13.547(4)	14.9754(6)	16.5805(5)	19.014(3)	17.912(4)	15.550(3)	20.9828(9)
α [º]	105.675(5)	83.065(3)	90	81.376(2)	96.51(3)	90	97.054(2)
β [º]	94.203(5)	86.114(3)	128.031(2)	88.499(3)	90.33(3)	96.26(3)	95.194(2)
γ [º]	99.069(5)	78.191(3)	90	86.065(3)	92.04(3)	90	98.629(2)
V [Å^3]	1191.1(6)	2735.6(2)	5721.0(3)	1555.0(4)	1683.2(6)	2831.6(10)	1823.54(13)
Z	2	4	8	2	2	4	2
$D_{calcd.}$ [g/cm^3]	1.198	1.370	1.271	1.449	1.449	1.445	1.441
μ [mm^{-1}]	0.071	0.772	0.810	0.925	0.860	1.086	1.003
F(000)	456	1168	2248	694	758	1264	812
Crystal size [mm]	0.24×0.15×0.12	0.20×0.14× 0.12	0.26×0.20× 0.15	0.25×0.12×0.08	0.30×0.18×0.12	0.26×0.19×0.11	0.31×0.22×0.20
θ range [º]	1.82–26.49	1.37–28.36	2.46–28.32	1.08–26.45	1.14–26.47	2.17–25.01	0.98–28.35
Limiting indices	–9≤h≤5, –14≤k≤14, –16≤l≤15	–17≤h≤17, –18≤k≤18, –19≤l≤19	–34≤h≤34, –22≤k≤22, –21≤l≤22	–10≤h≤7, –10≤k≤11, –23≤l≤19	–11≤h≤11, –12≤k≤10, –17≤l≤22	–19≤h≤22, –11≤k≤1, –18≤l≤18	–12≤h≤12, –10≤k≤12, –27≤l≤27
Completeness to *θ* (%)	97.7(θ=26.49º)	98.8(θ=28.36º)	99.1(θ=28.32º)	97.7(θ=26.45º)	97.4(θ=26.47º)	100.0(θ=25.01º)	98.7(θ=28.35º)
No. of parameters	302	667	334	379	415	334	424
Goodness-of-fit on F^2	0.981	0.734	0.931	1.018	1.038	1.00	0.87
*R*1 [I>2σ(I)]	0.0538	0.0494	0.0672	0.0522	0.0452	0.0917	0.0614
*wR*2	0.1183	0.1191	0.1895	0.1208	0.1048	0.1527	0.1661
Largest diff. peak/hole [eÅ^{-3}]	0.121/–0.171	0.381/–0.374	0.915/–0.349	0.491/–0.499	0.697/–0.629	0.360/–0.407	0.540/–0.531

for references, see page 112

References

[1] a) D. Vogt, *Applied Homogeneous Catalysis with Organometallic Compounds*; Cornils, B. Herrmann, W. A., Eds.; VCH, Weinheim, **2002**, Vol. 1, p. 240–253; b) A. M. Al-Jarallah, J. A. Anabtawi, M. A. B. Siddiqui, A. M. Aitani, A. W. Al-Sa'doun, *Catal. Today* **1992**, *14*, 1–121.

[2] a) W. Keim, F. H. Kowaldt, R. Goddard, C. Krüger, *Angew. Chem., Int. Ed. Engl.* **1978**, *17*, 466–467; b) W. Keim, *Angew. Chem., Int. Ed. Engl.* **1990**, *29*, 235–244; c) P. Braunstein, Y. Chauvin, S. Mercier, L. Saussine, A. D. Cian, J. Fisher, *J. Chem. Soc., Chem. Commun.* **1994**, 2203–2204; d) J. Heinicke, M. He, A. Dal, H.-F. Klein, O. Hetche, W. Keim, U. Flörke, H.-J. Haupt, *Eur. J. Inorg. Chem.* **2000**, 431–440.

[3] a) G. J. P. Britovsek, V. C. Gibson, D. F. Wass, *Angew. Chem. Int. Ed.* **1999**, *38*, 428–447; b) S. D. Ittel, L. K. Johnson, M. Brookhart, *Chem. Rev.* **2000**, *100*, 1169–1203; c) V. C. Gibson, S. K. Spitzmessor, *Chem. Rev.* **2003**, *103*, 283–316; d) W. Zhang, W. Zhang, W.-H. Sun, *Prog. Chem.* **2005**, *17*, 310–319; e) S. Jie, S. Zhang, W.-H. Sun, *Petrochem. Tech. (Shiyou Huagong)* **2006**, *35*, 295–300.

[4] a) C. Bianchini, G. Giambastiani, I. G. Rios, G. Mantovani, A. Meli, A. M. Segarra, *Coord. Chem. Rev.* **2006**, *250*, 1391–1418 and the references therein; b) V. C. Gibson, C. Redshaw, G. A. Solan, *Chem. Rev.* **2007**, *107*, 1745–1776 and the references therein.

[5] a) F. Speiser, P. Braunstein, L. Saussine, *Acc. Chem. Res.* **2005**, *38*, 784–793; b) W.-H. Sun, D. Zhang, S. Zhang, S. Jie, J. Hou, *Kinet. Catal.* **2006**, *47*, 278–283.

[6] a) L. K. Johnson, C. M. Killian, M. Brookhart, *J. Am. Chem. Soc.* **1995**, *117,* 6414–6415; b) D. P. Gates, S. A. Svejda, E. Oñate, C. M. Killian, L. K. Johnson, P. S. White, M. Brookhart, *Macromolecules* **2000,** *33,* 2320–2334.

[7] a) X. Tang, W.-H. Sun, T. Gao, J. Hou, J. Chen, W. Chen, *J. Organomet. Chem.* **2005**, *690*, 1570–1580; b) Q.-Z. Yang, A. Kermagoret, M. Agostinho, O. Siri, P. Braunstein, *Organometallics* **2006**, *25*, 5518–5527.

[8] F. Speiser, P. Braunstein, L. Saussine, *Dalton Trans.* **2004**, 1539–1545.

[9] a) J. Hou, W.-H. Sun, S. Zhang, H. Ma, Y. Deng, X. Lu, *Organometallics* **2006**, *25*, 236–244; b) C. Zhang, W.-H. Sun, Z.-X. Wang, *Eur. J. Inorg. Chem.* **2006**, *23*, 4895–4902.

[10] a) D. M. Dawson, D. A. Walker, M. Thornton-Pett, M. Bochmann, *J. Chem. Soc. Dalton Trans.* **2000**, 459–466; b) S. Al-Benna, M. J. Sarsfield, M. Thornton-Pett, D. Ormsby, P. J. Maddox, P. Bres, M. Bochmann, *J. Chem. Soc. Dalton Trans.* **2000**, 4247–4257; c) F. A. Kunrath, R. F. de Souza, O. L. Casagrande Jr., N. R. Brooks, V. G.. Young Jr., *Organometallics* **2003**, *22*, 4739–4743; d) N. Ajellal, M. C. A. Kuhn, A. D. G.. Boff, M. Hörner, C. M. Thomas, J.-F. Carpentier, O. L. Casagrande Jr., *Organometallics* **2006**, *25*, 1213–1216.

[11] L. Wang, W.-H. Sun, L. Han, H. Yang, Y. Hu, X. Jin, *J. Organomet. Chem.* **2002**, *658*, 62–70.

[12] W.-H. Sun, S. Zhang, S. Jie, W. Zhang, Y. Li, H. Ma, J. Chen, K. Wedeking, R. Fröhlich, *J. Organomet. Chem.* **2006**, *691*, 4196–4203.

[13] M. Zhang, S. Zhang, P. Hao, S. Jie, W.-H. Sun, P. Li, X. Lu, *Eur. J. Inorg. Chem.*, **2007**, 3816.

[14] a) P. Hao, S. Zhang, W.-H. Sun, Q. Shi, S. Adewuyi, X. Lu, P. Li, *Organometallics* **2007**, *26*, 2439–2446; b) S. Adewuyi, G. Li, S. Zhang, W. Wang, P. Hao, W.-H. Sun, N. Tang, J. Yi, *J. Organomet. Chem.* **2007**, *692*, 3532–3541.

[15] a) S. Zhang, I. Vystorop, Z. Tang, W.-H. Sun, *Organometallics* **2007**, *26*, 2456–2460; b) W.-H. Sun, P. Hao, S. Zhang, Q. Shi, W. Zuo, X. Tang, *Organometallics* **2007**, *26*, 2720–2734; c) W.-H. Sun, P. Hao, G. Li, S. Zhang, W.

Wang, J. Yi, M. Asma, N. Tang, *J. Organomet. Chem.*, DOI: 10.1016/j.jorganchem.2007.04.027.

[16] a) B. L. Small, M. Brookhart, A. M. A. Bennett, *J. Am. Chem. Soc.* **1998**, *120*, 4049–4050; b) B. L. Small, M. Brookhart, *J. Am. Chem. Soc*. **1998**, *120*, 7143–7144; c) G. J. P. Britovsek, V. C. Gibson, B. S. Kimberley, P. J. Maddox, S. J. McTavish, G. A. Solan, A. J. P. White, D. J. Williams, *Chem. Commun.* **1998**, 849–850; d) G. J. P. Britovsek, M. Bruce, V. C. Gibson, B. S. Kimberley, P. J. Maddox, S. Mastroianni, S. J. McTavish, C. Redshaw, G. A. Solan, S. Stromberg, A. J. P. White, D. J. Williams, *J. Am. Chem. Soc.* **1999**, *121*, 8728–8740.

[17] a) G. J. P. Britovsek, V. C. Gibson, O. D. Hoarau, S. K. Spitzmesser, A. J. P. White, D. J. Williams, *Inorg. Chem.* **2003**, *42*, 3454–3465; b) V. C. Gibson, S. K. Spitzmesser, A. J. P. White, D. J. Williams, *Dalton Trans.* **2003**, 2718–2727; c) R. Cowdell, C. J. Davies, S. J. Hilton, J.-D. Maréchal, G. A. Solan, O. Thomas, J. Fawcett, *Dalton Trans.* **2004**, 3231–3240.

[18] a) G. J. P. Britovsek, S. P. D. Baugh, O. Hoarau, V. C. Gibson, D. F. Wass, A. J. P. White, D. J. Williams, *Inorg. Chim. Acta* **2003**, *345*, 279–291; b) Y. Nakayama, Y. Baba, H. Yasuda, K. Kawakita, N. Ueyama, *Macromolecules* **2003**, *36*, 7953–7958; c) C. J. Davies, S. J. Hilton, G. A. Solan, W. Stannard, J. Fawcett, *Polyhedron* **2005**, *24*, 2017–2026; d) J. D. A. Pelletier, Y. D. M. Champouret, J. Cadarso, L. Clowes, M. Ganete, K. Singh, V. Thanarajasingham, G. A. Solan, *J. Organomet. Chem.* **2006**, *691*, 4114–4123.

[19] a) W.-H. Sun, S. Jie, S. Zhang, W. Zhang, Y. Song, H. Ma, J. Chen, K. Wedeking, R. Fröhlich, *Organometallics* **2006**, *25*, 666–677; b) S. Jie, S. Zhang, W.-H. Sun, X. Kuang, T. Liu, J. Guo, *J. Mol. Catal. A: Chem.* **2007**, *269*, 85–96.

[20] S. Jie, S. Zhang, K. Wedeking, W. Zhang, H. Ma, X. Lu, Y. Deng, W.-H. Sun, *C. R. Chim.* **2006**, *9*, 1500–1509.

[21] E. J. Corey, A. L. Borror, T. Foglia, *J. Org. Chem.* **1965**, *30*, 288–290.

[22] A. J. Showler, P. A. Darley, *Chem. Rev.* **1967**, *67*, 427–440.

[23] C. Dietrich-Buchecker, B. Colasson, D. Jouvenot, J.-P. Sauvage, *Chem. Eur. J.* **2005**, *11*, 4374–4386.

[24] K. Ziegler, H. G. Gellert, *Justus Liebigs Ann. Chem.* **1950**, *567*, 179–185.

[25] J. Einhorn, J. L. Luche, *Tetrahedron Lett.* **1986**, *26*, 501–504.

[26] a) C. Carlini, M. Isola, V. Liuzzo, A. M. R. Galletti, G. Sbrana, *Appl. Catal. A: Gen.* **2002**, *231*, 307–320; b) J. C. Jenkins, M. Brookhart, *Organometallics* **2003**, *22*, 250–256; c) W.-H. Sun, W. Zhang, T. Gao, X. Tang, L. Chen, Y. Li, X. Jin, *J. Organomet. Chem.* **2004**, *689*, 917–929.

[27] a) C. M. Killian, L. K. Johnson, M. Brookhart, *Organometallics* **1997**, *16*, 2005–2007; b) S. A. Svejda, M. Brookhart, *Organometallics* **1999**, *18*, 65–74.

[28] G. M. Sheldrick, *SHELXL-97*, *Program for the Refinement of Crystal Structures*, University of Göttingen, Göttingen, Germany, **1997**.

Chapitre V

Complexes phosphino- and phosphinito-oxazoline du cobalt, application en catalyse d'oligomerization de l'éthylène

Abstract of Chapter V

Cobalt(II) complexes of the type $[CoCl_2(P,N)]$, where P,N represents a heterobidentate phosphino- or phosphinito-oxazoline-type ligand, have been synthesised and characterised by infrared spectroscopy and elemental analysis. Their molecular structures were established by single-crystal X-ray diffraction in the solid state. Whereas the phosphino-oxazoline complex $[CoCl_2\{Ph_2PCH_2ox^{Me2}\}]$ ($Ph_2PCH_2ox^{Me2}$ = 2-[(diphenylphosphanyl)-methyl]-4,4-dimethyl-4,5-dihydrooxazole) (**8**) and the phosphinito-oxazoline complexes $[CoCl_2\{Ph_2POCH_2ox^{Me2}\}]$ ($Ph_2POCH_2ox^{Me2}$ = 1-[4,4-dimethyl-2{1-oxy(diphenylphosphino)-1-methyl}]-4,5- dihydro oxazole) (**9**) and $[CoCl_2\{Ph_2POCMe_2ox^{Me2}\}]$ ($Ph_2POCMe_2ox^{Me2}$ = 1-[4,4-dimethyl-2-[1-oxy(diphenylphosphino)-1-methylethyl]]-4,5-dihydrooxazole) (**10**) are mononuclear, the phosphino-oxazoline complexes $[CoCl_2\{i\text{-}Pr_2PCH_2ox\}]_2$ (i-Pr_2PCH_2ox = 2-[(diisopropyl-phosphanyl)-methyl]-4,5-dihydro-oxazole) (**6**) and $[CoCl_2\{\mu\text{-}Ph_2PCH_2ox\}]_2$ (Ph_2PCH_2ox = 2-[(diphenyl-phosphanyl)-methyl]-4,5-dihydro-oxazole) (**7**) are dinuclear compounds and contain two bridging phosphino-oxazoline ligands which form a 10-membered ring. In the course of this work, the zwitterionic complex $[CoCl_3\{Ph_2PCH_2C(O)OCH_2CMe_2NH_3]$ (**11**) was obtained and characterised by X-ray diffraction in which the oxazoline ring has been opened. Air-oxidation of the phosphine function of the mononuclear P,N chelate complex **8** yielded the blue N,O-bridged, centrosymmetric dinuclear complex $[CoCl_2\{\mu\text{-}OPPh_2CH_2C{=}NCMe_2CH_2O\}]_2$ (**12**) which contains a 12-membered ring. All these complexes are paramagnetic and their magnetic moments in solution were measured by the Evans method. Complexes **6**–**10** were evaluated in the catalytic oligomerisation of ethylene with $AlEtCl_2$ or methylaluminoxane (MAO) as cocatalysts and provided moderate activities. In the presence of $AlEtCl_2$ (6–14 equiv), the selectivities for ethylene dimers were higher than 92% and complex **8** showed the highest turnover frequency with 14 equiv of $AlEtCl_2$. When MAO was used as cocatalyst, the catalytic activities were similar to those with $AlEtCl_2$ but significant amounts of C_6–C_{12} oligomers were produced.

This chapter has been published. My contribution to this publication is the preparation of all the complexes, the catalytic studies, and the manuscript, in collaboration with Dr. Magno Agostinho and Dr. Anthony Kermagoret.

Mono- and Dinuclear Cobalt Complexes with Chelating or Bridging Bidentate P,N Phosphino- and Phosphinito-oxazoline Ligands: Synthesis, Structures and Catalytic Ethylene Oligomerisation

Dalton Trans. **2007**, 4472–4482.

Suyun Jie,[a,b] Magno Agostinho,[a] Anthony Kermagoret,[a] Catherine S. J. Cazin[a] and Pierre Braunstein*[a]

[a] *Laboratoire de Chimie de Coordination, Institut de Chimie (UMR 7177 CNRS), Université Louis Pasteur, 4 rue Blaise Pascal, F-67070 Strasbourg Cédex, France*

b *Key Laboratory of Engineering Plastics and Beijing National Laboratory for Molecular Sciences, Institute of Chemistry, Chinese Academy of Sciences, Beijing 100080, China*

Mono- and Dinuclear Cobalt Complexes with Chelating or Bridging Bidentate P,N Phosphino- and Phosphinito-oxazoline Ligands: Synthesis, Structures and Catalytic Ethylene Oligomerisation

Introduction

Heteroatom-containing ligands are of increasing interest in coordination and organometallic chemistry owing to the properties they confer to their metal complexes and also to their ability to act as hemilabile ligands.[1] Nitrogen- and phosphorus-based donor ligands are among the most used in molecular chemistry[2] and when nitrogen as a hard donor and phosphorus as a soft donor are associated within a functional ligand, they can act cooperatively to stabilize metal ions in optimum oxidation states and generate systems of considerable chemical and structural diversity and with important applications in homogeneous catalysis.[3,4] This combination can also provide the possibility to fine-tune steric and electronic requirements by appropriate chemical modifications and even relatively minor variations may lead to complete changes in the coordination properties and bonding mode of the ligand, as will be illustrated in the present work.

Chelating P,N ligands containing N-heterocycles, such as pyridyl- and oxazolyl-, are receiving considerable attention.[1c-e,1g,3,4d] In particular, their nickel complexes are active catalysts precursors in the catalytic oligomerisation of ethylene,[4d,5] which is of major industrial interest.[6] Much fewer P,N-cobalt complexes have been reported as catalyst precursors for ethylene oligomerisation, even when P,N-containing tridentate ligands are considered.[7] We have recently found that phosphino-oxazoline and phosphinito-oxazoline nickel complexes **I**[8a] and **II**,[8b] respectively, are very active for the dimerisation of ethylene in the presence of small amounts of a cocatalyst (2 or 6 equiv of $AlEtCl_2$). The following phosphino-oxazolines **1**–**3** and phosphinito-oxazolines **4**–**5** ligands have now been selected because of the easy modulation of their stereoelectronic properties with the aim to investigate their cobalt complexes and compare them with the corresponding nickel complexes. Ligand tuning can be done by variation of the substituents on P (**1** R = *i*-Pr and **2** R = Ph), by introducing substituents on the heterocycle (**2** R^1 = H and **3** R^1 = Me) or on the P-heterocycle bridge (**4** R^2 = H and **5** R^2

for references, see page 134

= Me). This can also be done by introduction of an oxygen atom (going from a phosphine to a phosphinite) which changes the ring size of the chelate and the electronic density of the metal centre (**3** and **4**). Phosphinite ligands are readily available from reactions between alcohols and chlorophosphines and find interesting applications in homogeneous catalysis.[9]

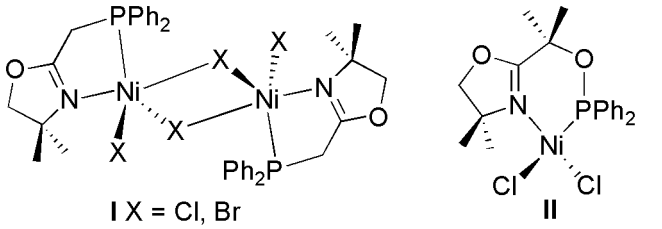

I X = Cl, Br

II

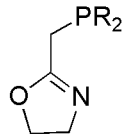

1 R = *i*-Pr
2 R = Ph

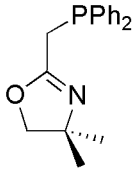

3

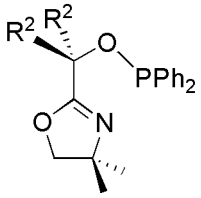

4 R^2 = H
5 R^2 = Me

Results and Discussion

Synthesis and characterization of the complexes

The phosphino-oxazoline ligands **1-3** were prepared from the corresponding oxazolines according to the literature methods (eq 1).[10]

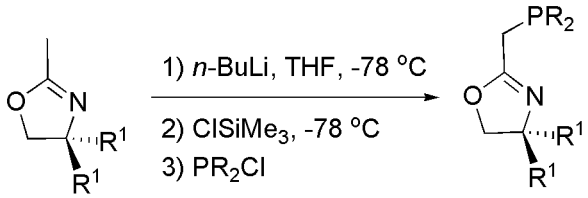

1) *n*-BuLi, THF, -78 °C
2) $ClSiMe_3$, -78 °C
3) PR_2Cl

1 R = *i*-Pr, R^1 = H
2 R = Ph, R^1 = H
3 R = Ph, R^1 = Me

(1)

Lithiation of the oxazolines in THF was carried out with 1.0 equiv of *n*-BuLi at -78 °C in order to avoid metallation on the oxazoline heterocycle,[11] followed by the addition of $SiClMe_3$ at low temperature to form the *N*-silyl derivatives. Finally, 1.0 equiv of chlorophosphine (PR_2Cl) was added and the solution was allowed to warm to room temperature overnight. After treatment and purification, the phosphino-oxazolines were isolated in high purity and good yield.

for references, see page 134

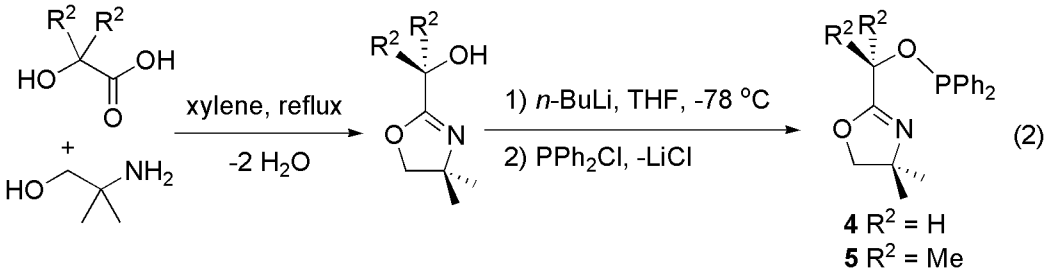

The phosphinito-oxazoline ligands **4** and **5** were prepared from the oxazoline alcohols, which were readily synthesised by refluxing glycolic acid or 2-hydroxy-2-methylpropionic acid with 2-amino-2-methyl-1-propanol in xylene until no further formation of water was observed in a Dean-Stark trap (eq 2).[12] The diphenylphosphino group was introduced by reaction of the deprotonated alcohol with PPh_2Cl (eq 2).[13]

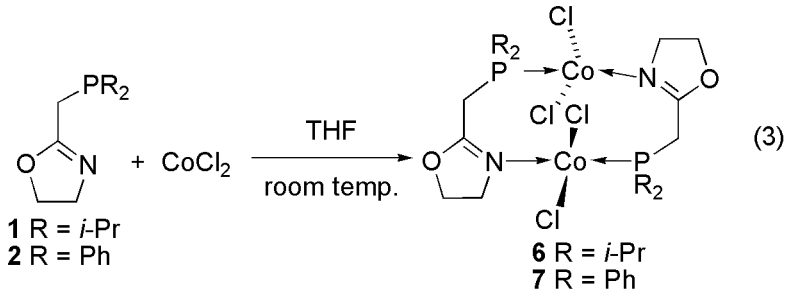

The cobalt complexes were readily obtained by reaction of the corresponding ligands with anhydrous cobalt dichloride in THF at room temperature. When ligands **1** and **2** were used, the complexes **6** and **7** precipitated from the solution and were isolated by filtration and washed with diethyl ether to give air-stable bright-blue powders (eq 3).

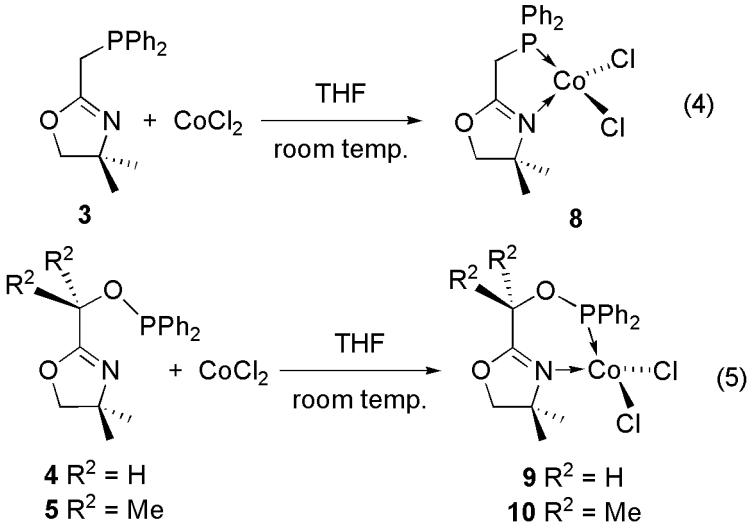

Since ligands **1**–**5** always behaved as chelates in their Ni(II) or Pd(II) complexes,[8,10,13,16] it was unexpected that **6** and **7** would be dinuclear complexes with bridging phosphino-oxazoline ligands, as was established by X-ray diffraction (see

for references, see page 134

below). In contrast, when ligands **3-5** were used, purple or blue chelated complexes were obtained (**8**–**10**) which are well soluble in THF (eq 4,5).

The infrared ν(C=N) stretching vibration bands shifted from 1660–1668 cm^{-1} (free ligands)[8b,10a,13] to 1612–1643 cm^{-1} (coordinated ligands) and the peak intensity became weaker, confirming coordination of the ligands to cobalt. All the complexes were paramagnetic and their magnetic moment was measured in CD_2Cl_2 solution by the Evans method.[14] Magnetic moments in the range 3.75–3.94 μB were found for complexes **8**–**10**, typical for the presence of three unpaired electrons on a cobalt(II) high spin system (S = 3/2) and values of 5.30 and 5.42 μ_B per complex for **6** and **7**, respectively.[15] The structures of **6** and **7** in the solid state were determined by single X-ray diffraction analysis (Figures 1 and 2). Selected bond lengths and angles are collected in Table 1.

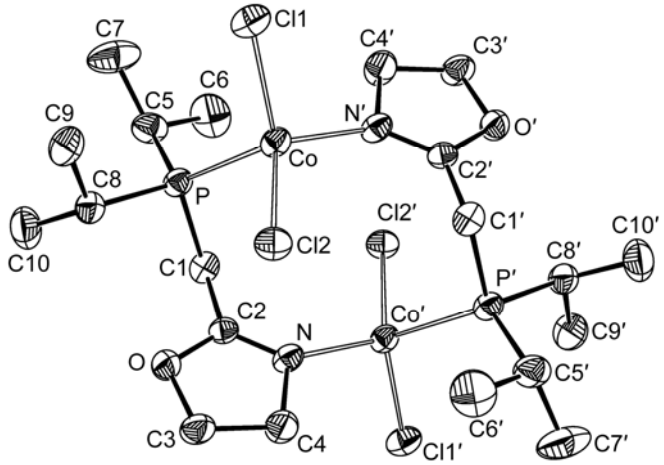

Figure 1.
ORTEP view of the molecular structure of complex **6** with thermal ellipsoids drawn at the 50% probability level. Symmetry operations generating equivalent atoms(‘): *–x*, *–y*, *–z*.

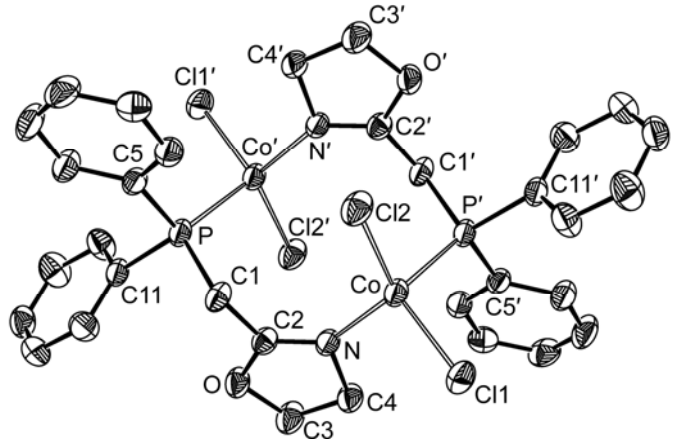

Figure 2.
ORTEP view of the molecular structure of complex **7** with thermal ellipsoids drawn at the 50% probability level. Symmetry operations generating equivalent atoms(‘): *–x*, *–y*, *–z*.

for references, see page 134

Table 1.
Selected bond lengths (Å) and bond angles (°) in complexes **6**–**8**.

	6	**7**	**8**
Co–N	2.015(2)	1.996(2)	2.003(2)
Co–Cl2	2.2466(8)	2.2281(8)	2.2177(9)
Co–Cl1	2.2385(9)	2.2306(8)	2.2245(8)
Co–P	2.4147(9)	2.4176(8)	2.3981(8)
N–C2	1.278(4)	1.281(3)	1.280(3)
C1–C2	1.479(4)	1.487(4)	1.493(4)
P–C1	1.863(3)	1.851(3)	1.856(3)
N–Co–Cl1	101.88(8)	102.44(7)	112.15(7)
N–Co–Cl2	113.70(7)	116.44(6)	119.13(7)
Cl1–Co–Cl2	116.44(3)	118.25(3)	113.88(4)
N–Co–P	115.30(8)	109.27(7)	84.65(7)
Cl1–Co–P	111.17(3)	107.41(3)	112.57(3)
Cl2–Co–P	99.03(3)	102.69(3)	111.04(3)
C2–N–Co	135.0(2)	134.23(2)	120.36(2)
N–C2–C1	127.0(3)	125.7(2)	126.4(2)
C2–C1–P	114.4(2)	114.81(2)	109.9(2)
C1–P–Co	111.49(1)	115.07(9)	97.61(9)

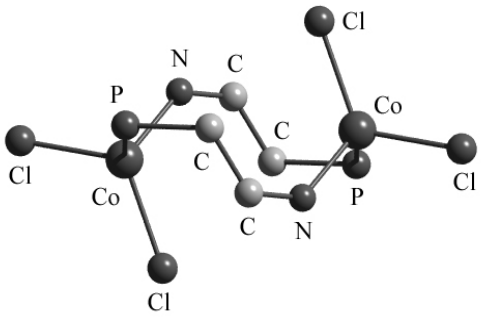

Figure 3.
Conformation of the ten-membered dimetallocyclic skeleton of the dinuclear phosphino-oxazoline cobalt complex **7**.

Whereas chelation of ligands **1** and **2** to $CoCl_2$ was anticipated by analogy with their behaviour in Pd(II) complexes,[10a,10c,16] complexes **6** and **7** possess in fact a centrosymmetric dinuclear structure with a distorted tetrahedral coordination geometry around the metal centres. The cobalt atoms are coordinated by the nitrogen atom from one ligand and the phosphorus from another ligand, which results in a ten-membered ring structure (Figures 1 and 2). The ten-membered dimetallocycles display a double boat-like conformation (Figures 1–3). The Cl1–Co–Cl2 angle is 116.44(3)° in **6** and 118.25(3)° in **7** (Table 1). Only the structure of **7** will be discussed in some detail because of its similarity with that of **6**. The P–Co–N angle (109.27(7)°) in **7** is nearly what is expected for a regular tetrahedral coordination, which results from the coordinated P and N atoms originating from two separate ligands (this P–Co–N angle will be much smaller, 84.65(7)°, in the chelate complex **8**, see below). The Co–N bond length (1.996(2) Å) is about 0.42 Å shorter than that of Co–P bond (2.4176(8) Å), while the two Co–Cl distances are very similar. The C2–N bond in the oxazoline heterocycle has a typical double-bond character with a length of 1.281(3) Å. Structuraly

for references, see page 134

characterised precedents for the exceptional bridging rather than chelating bonding mode of a phosphino-oxazoline ligand are [{(OC)$_4$Fe(μ-PCH$_2$ox-*P,N*)}$_2$CoCl$_2$] (**III**)[17] and [(OC)$_3$Fe(μ-PCH$_2$ox-*P,N*)$_2$Cu]BF$_4$ (**IV**).[18]

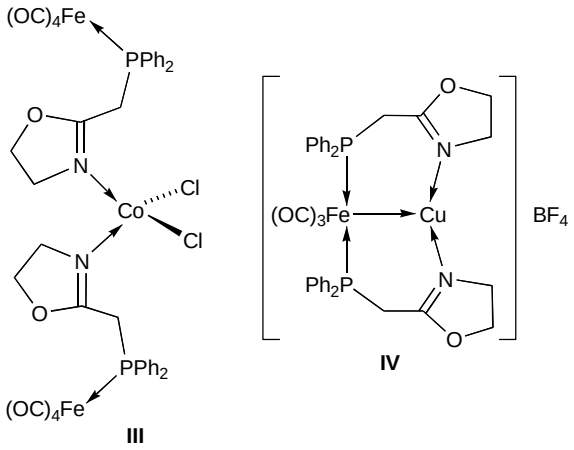

The phosphino-oxazoline ligand **3** with two *gem*-methyl groups on the oxazoline heterocycle formed the chelated mononuclear complex **8** (eq 4) and the coordination geometry around the cobalt centre was established by X-ray diffraction to be distorted tetrahedral (Figure 4).

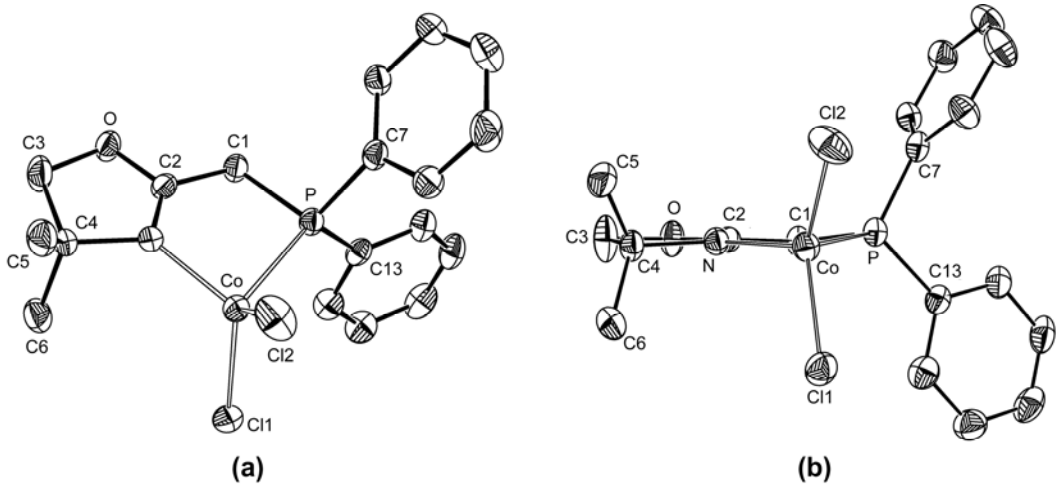

Figure 4.
ORTEP views of the molecular structure of complex **8** with thermal ellipsoids drawn at the 50% probability level.

This structure shows similar characteristics to that of the five-membered P,N-chelate cobalt(II) complex bearing 2-pyridylbis(diphenylphosphino)methane ligand.[19] Most bond lengths in **8** are similar to those observed for the dinuclear cobalt complexes **6** and **7** and the corresponding dinuclear nickel complex **I**.[8a] The N–Co–P bond angle (84.65(7)°) in **8** is larger than that in the dinuclear nickel complex **I** (80.83(7)°) but much smaller than in **6** or **7** (Table 1). The C1, C2, N, P and Co atoms in the chelate ring are nearly coplanar and the maximum deviation out of the mean plane defined by these atoms is 0.082 Å for C1 and the two chlorine atoms are located on

for references, see page 134

either side of this plane. In addition, this plane and the oxazoline ring are almost coplanar with a dihedral angle of only 2.0(1)° (Figure 4b). The two methyl groups on C4 may provide new steric hindrance compared to the situation in **6** and **7**. The geometry around the phosphorus atom is also distorted tetrahedral with a C1–P–Co bond angle of 97.61(9)°, which is much smaller than those in **6** and **7**.

Complex **8** was less stable in solution than **6** or **7**. In a Schlenk tube containing a solution of this complex in CH_2Cl_2 we observed the formation of few blue crystals upon slow layer diffusion with *n*-pentane. These were identified by X-ray diffraction which established that this product resulted from the cleavage of the C=N double bond of the oxazoline heterocycle. This must have been caused by the presence of adventitious water and the small quantity of product did not allow us to perform all the usual analyses. In this ring-opened complex **11**, the nitrogen atom is not coordinated but quaternised to form an ammonium salt (Figure 5).

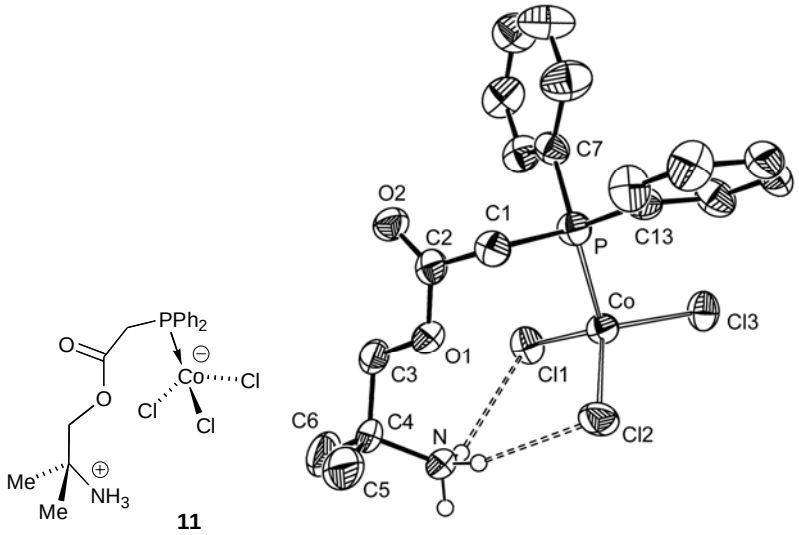

Figure 5.
ORTEP view of the molecular structure of ring-opened complex **11** (obtained from **8**) with thermal ellipsoids drawn at the 30% probability level. Selected bond lengths (Å) and angles (°): Co–Cl1 = 2.2590(2), Co–Cl2 = 2.2406(1), Co–Cl3 = 2.2496(1), Co–P = 2.3885(2), O2–C2 = 1.210(6), N–C4 = 1.535(6); Cl2–Co–Cl1 = 110.24(6), Cl2–Co–Cl3 = 115.90(6), Cl3–Co–Cl1 = 106.71(6), Cl1–Co–P = 113.61(6), Cl2–Co–P = 100.83(6), Cl3–Co–P = 109.72(6).

This transformation results in a zwitterionic complex in which the cobalt atom exhibits a slightly distorted tetrahedral geometry with the ester phosphine acting as a monodentate ligand through the phosphorus atom. The nitrogen atom lies far away from the cobalt centre with the Co···N separation of 4.039 Å. With an average length of 2.2497 Å, the Co–Cl bonds are a little longer than in **8** whereas the Co–P bond length is almost unchanged. The C2–O2 bond points away from the cobalt centre and its length is typical for a carbonyl group (1.210(6) Å).

for references, see page 134

Accidental air-oxidation of the phosphine function of the mononuclear P,N complex **8** in CH_2Cl_2 yielded after slow diffusion of *n*-pentane the blue N,O-bridged dinuclear complex $[CoCl_2\{\mu\text{-}OPPh_2CH_2C{=}NCMe_2CH_2O\}]_2$ (**12**) (Figure 6).

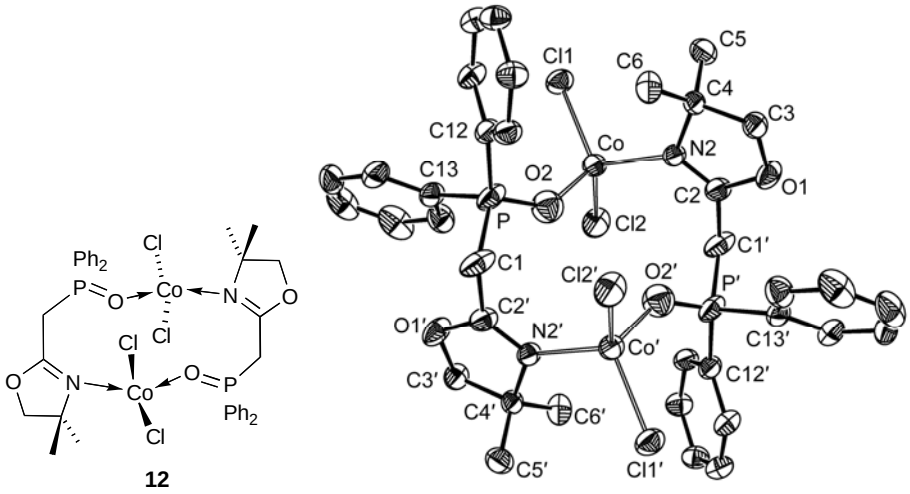

Figure 6.
ORTEP view of the molecular structure of oxidized complex **12** (obtained from **8**) with thermal ellipsoids drawn at the 50% probability level. Selected bond lengths (Å) and angles (°): Co–O2 = 1.910(4), Co–N2 = 2.033(3), Co–Cl1 = 2.2421(1), Co–Cl2 = 2.2599(1), P–O2 = 1.427(4), N2–C2 = 1.284(5); O2–Co–N2 = 106.24(2), O2–Co–Cl1 = 115.09(1), N2–Co–Cl1 = 110.48(1), O2–Co–Cl2 = 103.31(1), N2–Co–Cl2 = 112.68(10), Cl1–Co–Cl2 = 108.93(5).

In the centrosymmetric structure of **12**, the cobalt atoms also adopt a distorted tetrahedral coordination geometry, with coordination of a nitrogen atom from one ligand and an oxygen atom from another ligand to form a twelve-membered mesocycle. The corresponding bond lengths and angles are very similar to those in **8**. This dinuclear structure is obviously preferred to the alternative six-membered ring chelation in a mononuclear complex.

The X-ray structures of the phosphinito-oxazoline complexes **9** and **10** (eq 5) are shown in Figures 7 and 8 and selected bond lengths and angles are given in Table 2.

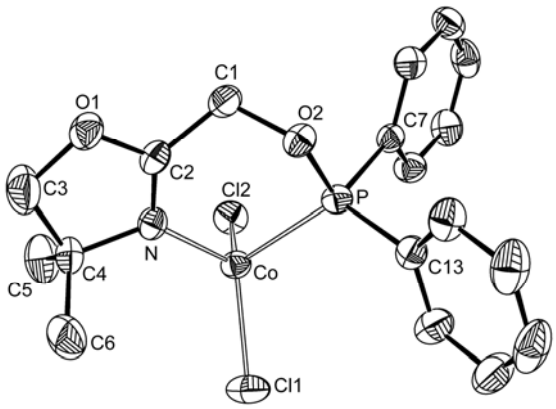

Figure 7.
ORTEP view of the molecular structure of complex **9** with thermal ellipsoids drawn at the 50% probability level.

for references, see page 134

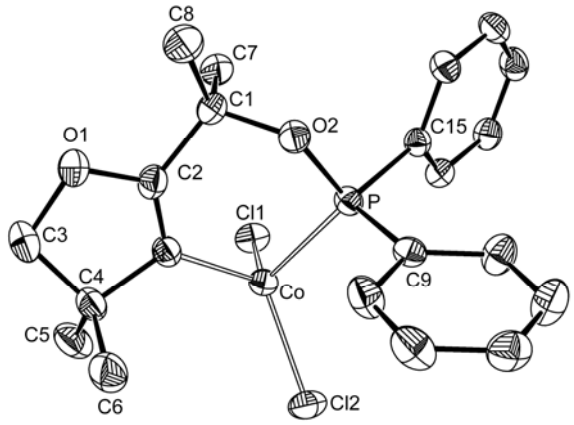

Figure 8.
ORTEP view of the molecular structure of complex **10** with thermal ellipsoids drawn at the 50% probability level.

Table 2.
Selected bond lengths (Å) and bond angles (°) in complexes **9** and **10**.

	9	**10**
Co–N	2.0073(2)	2.006(2)
Co–Cl1	2.2242(7)	2.2340(8)
Co–Cl2	2.2139(7)	2.2227(7)
Co–P	2.3648(7)	2.3281(7)
N–C2	1.272(3)	1.275(3)
C1–C2	1.500(3)	1.531(4)
C1–O2	1.441(3)	1.452(3)
P–O2	1.6300(2)	1.6288(2)
N–Co–Cl1	115.06(6)	110.31(7)
N–Co–Cl2	112.83(6)	117.09(7)
Cl1–Co–Cl2	113.28(3)	117.38(3)
N–Co–P	93.24(6)	91.21(6)
Cl1–Co–P	113.57(3)	110.92(3)
Cl2–Co–P	107.01(3)	106.62(3)
C2–N–Co	125.32(2)	127.28(2)
N–C2–C1	127.53(2)	128.6(2)
O2–C1–C2	112.24(2)	109.6(2)
C1–O2–P	118.43(1)	124.62(2)
O2–P–Co	107.65(6)	109.26(7)

In both complexes the cobalt centre has a distorted tetrahedral coordination geometry. Because these complexes have very similar geometries and structural parameters, only **10** will be described in some detail in order to compare it with the corresponding nickel complex **II**.[8b] The six-membered chelate ring shows a boat-like conformation, similar to that of the nickel complex **II**. However, the bond distances and angles are similar in the Co(II) and Ni(II) complexes. The bond angles around the cobalt centre are in the range of 91.21(6)° (N–Co–P) to 117.38(3)° (Cl1–Co–Cl2). The two Co–Cl bond distances are similar and the Co–P bond is much longer than Co–N, which resembles the situation in the phosphinooxazoline complexes **6**–**8**.

for references, see page 134

Catalytic Oligomerisation of Ethylene

The phosphino- (**6**–**8**) and phosphinito-oxazoline (**9** and **10**) cobalt(II) dichloride complexes have been evaluated as precatalysts for oligomerisation of ethylene in the presence of $AlEtCl_2$ or MAO as cocatalysts. The influence of the steric and electronic properties of the ligands and of the Al/Co molar ratio on the catalytic properties was examined (Tables 3 and 4). Even though they showed moderate catalytic activities for ethylene oligomerisation, it is interesting to compare them with their corresponding nickel complexes and other cobalt-based precatalysts in order to gain a better insight into the influence of different metal centres and ligands on the catalytic behaviour.

Use of $AlEtCl_2$ as cocatalyst

Table 3.
Ethylene dimerisation with precatalysts **6**–**10** using $AlEtCl_2$ as cocatalyst.[a]

	$AlEtCl_2$ (equiv.)	Selectivity (%)			Productivity/ $g_{C2H4}\ g_{Co}^{-1}\ h^{-1}$	TOF/ $mol_{C2H4}\ mol_{Co}^{-1}\ h^{-1}$	α-Olefin (C_4) (%)
		C_4	C_6	C_8			
6	6	95	4	<1	700	1500	52
6	10	93	7	<1	2100	4400	46
6	14	92	8	<1	2800	5800	43
7	6	98	2	0	1000	2100	46
7	10	94	5	1	1200	2400	41
7	14	94	5	1	1600	3300	37
8	2	97	3	0	<100	<200	57
8	6	96	4	<1	1800	3800	31
8	10	95	5	<1	2500	5300	23
8	14	93	7	<1	3700	7700	19
9	6	99	1	0	250	540	71
9	10	95	5	<1	1200	2400	54
9	14	93	6	<1	1700	3600	48
10	6	99	1	0	180	370	75
10	10	97	2	<1	380	800	73
10	14	95	4	1	560	1200	70

[a] Conditions: T = 25 °C, 10 bar of C_2H_4, 35 min, $4x10^{-2}$ mmol of Co, solvent = 15 mL of toluene. No C_{10} oligomers were detected.

When 2 equiv of cocatalyst ($AlEtCl_2$) were added, very low activities were observed. However, in the presence of 6, 10 or 14 equiv of $AlEtCl_2$, complexes **6**–**10** displayed moderate activities for the selective dimerisation of ethylene (C_4 fraction > 92%) (Table 3, Figures 9 and 10). Different quantities of cocatalyst led to the same trend of catalytic activities and selectivities for 1-butene for each complex. When the amount of $AlEtCl_2$ was increased from 6 to 14 equiv, the turnover frequencies (TOF) also increased, whereas the selectivities for 1-butene decreased slightly.

Under similar conditions, the dinuclear phosphino-oxazoline complex **6** showed a slightly higher TOF and selectivity for 1-butene than **7**. For exemple, in the presence of 14 equiv of $AlEtCl_2$, **6** gave a TOF of 5800 $mol_{C2H4}\ mol_{Co}^{-1}\ h^{-1}$ and a selectivity of 43%

for references, see page 134

for 1-butene. For comparison, **7** led to a TOF of 3300 mol_{C2H4} mol_{Co}^{-1} h^{-1} and a selectivity of 37% for 1-butene. The difference of catalytic properties between **6** and **7** can only be ascribed to the different stereoelectronic properties of the phosphorus substituents.

In the presence of 6, 10 or 14 equivalents of $AlEtCl_2$, the mononuclear phosphino-oxazoline complex **8** were more active than the dinuclear complexes **6** and **7** but slightly less selective for 1-butene. The introduction of the *gem*-methyl groups in the oxazoline heterocycle resulted for **8** in higher turnover frequencies than for **7**. In contrast to the corresponding dinuclear nickel complex **I**, complex **8** in the presence of 14 equiv of $AlEtCl_2$ was about five times less active but more selective for 1-butene (**8**, 19%; **I**, 3%).[8a] Complex **8** needs to be treated with only 6 equiv of $AlEtCl_2$ in order to lead to a TOF of 3800 mol_{C2H4} mol_{Co}^{-1} h^{-1} whereas under such conditions complex **I** is completely inactive.

When compared with the phosphine complex **8**, the phosphinite complex **9** showed lower catalytic activities and higher selectivities for 1-butene, which illustrates the effect of a different environment around the phosphorus atom and a different ring size of the metal chelate. The substituents on the carbon atom α to the oxazoline ring remarkably influenced the catalytic activities of the phosphinite cobalt complexes. When 10 or 14 equiv of $AlEtCl_2$ were used, complex **10** with two methyl groups on the carbon atom α to the oxazoline ring was twice less active than **9** whereas **10** displayed higher selectivities for 1-butene. In contrast, the corresponding nickel complex **II** provided high TOF of 49500 mol_{C2H4} mol_{Ni}^{-1} h^{-1} for ethylene dimerisation and trimerization in the presence of 6 equiv of $AlEtCl_2$ despite of lower selectivity for 1-butene (8%).[8b]

When a blank experiment was run with $CoCl_2$ in the presence of equiv of $AlEtCl_2$, no catalytic activity was found, which confirms the major role played by the ligands and indicates that they actually remain coordinated on the cobalt centre during catalysis.

Use of MAO as cocatalyst

Complexes **6**–**10** afforded TOF values between 600 and 6800 mol_{C2H4} mol_{Co}^{-1} h^{-1} (Table 4, Figures 11 and 12). Note that complex **I** decomposed in the presence of MAO.[8a] With 100–400 equiv of MAO, the catalytic activities and selectivities for 1-butene were comparable to those obtained with $AlEtCl_2$ as cocatalyst. Similarly, the phosphine complexes **6**–**8** showed higher activities than phosphinite complexes **9** and

for references, see page 134

10. The turnover frequencies were in the range of 600–4000 mol_{C2H4} mol_{Co}^{-1} h^{-1} with 100 equiv of MAO and 2700–6300 mol_{C2H4} mol_{Co}^{-1} h^{-1} with 400 equiv of MAO. The best results were obtained with **7** in the presence of 200 equiv of MAO, which afforded a TOF as high as 6800 mol_{C2H4} mol_{Co}^{-1} h^{-1}.

Table 4.
Ethylene oligomerisation with precatalysts **6**–**10** using MAO as cocatalyst.[a]

	MAO	Selectivity (%)					Productivity/	TOF/	α-Olefin
	(equiv.)	C_4	C_6	C_8	C_{10}	C_{12+}	g_{C2H4} g_{Co}^{-1} h^{-1}	mol_{C2H4} mol_{Co}^{-1} h^{-1}	(C_4) (%)
6	100	54	21	16	8	1	1700	3600	46
6	200	37	27	22	14	<1	3100	6600	46
6	400	48	19	18	12	3	3000	6300	44
7	100	36	25	18	14	7	1100	2300	25
7	200	22	29	26	19	3	3200	6800	34
7	400	26	29	26	17	2	2900	6200	43
8	100	32	28	23	13	4	1900	4000	31
8	200	29	32	27	11	1	3100	6500	38
8	400	21	26	27	23	3	2300	4900	43
9	100	29	24	21	15	11	800	1600	47
9	200	23	31	27	17	2	2400	5100	46
9	400	23	26	23	21	7	1900	4100	47
10	100	33	19	21	10	17	300	600	55
10	200	26	27	26	15	6	1000	2100	50
10	400	22	27	26	19	6	1300	2700	50

[a] Conditions: T = 25 °C, 10 bar of C_2H_4, 35 min, 10^{-2} mmol of Co, solvent = 20 mL of toluene.

When activated by MAO, these cobalt(II) precatalysts produced C_4–C_{12} olefins. When 100 equiv of MAO was used, the C_4 fractions were larger than C_6 for each complex. In contrast to the diisopropylphosphine complex **6**, complexes **7**–**10** gave more C_6 than C_4 products when the amount of MAO was increased to 200 and 400 equivalents. The fractions of the different C_6 oligomers are shown in Table 5. Depending on the nature of reinsertion of 1-butene or 2-butene (1,2- or 2,1-insertion) and further β-H elimination, various C_6 products can be formed.[15d,20] 1-Hexene was formed by a chain growth mechanism and its Co-catalyzed isomerization resulted in the formation of 2-hexene and 3-hexene.[20b]

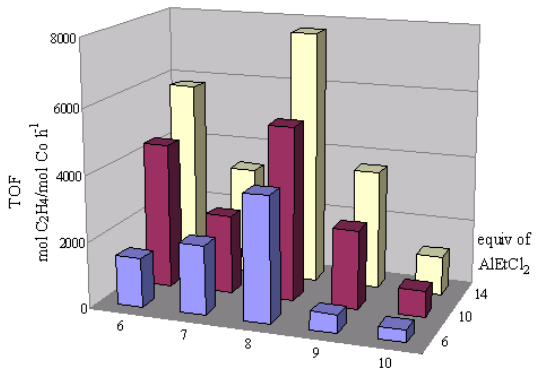

Figure 9.
Catalytic activities of precatalysts **6**–**10** in the oligomerisation of ethylene using $AlEtCl_2$ as cocatalyst.

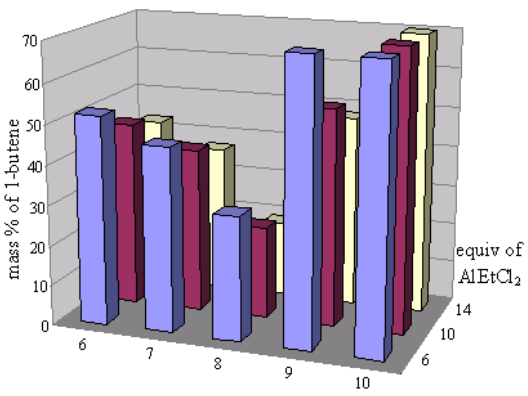

Figure 10.
Selectivity of precatalysts **6**–**10** for 1-butene, within the C_4 fraction, using $AlEtCl_2$ as cocatalyst.

for references, see page 134

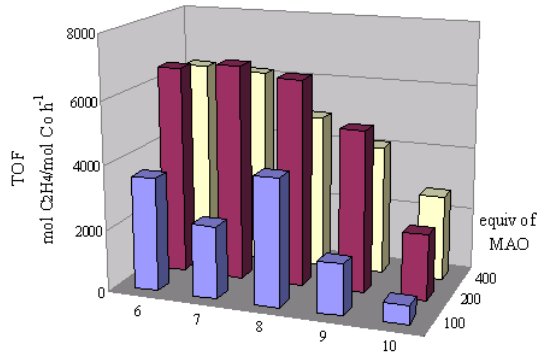

Figure 11.
Catalytic activities of precatalysts **6**–**10** in the oligomerisation of ethylene using MAO as cocatalyst.

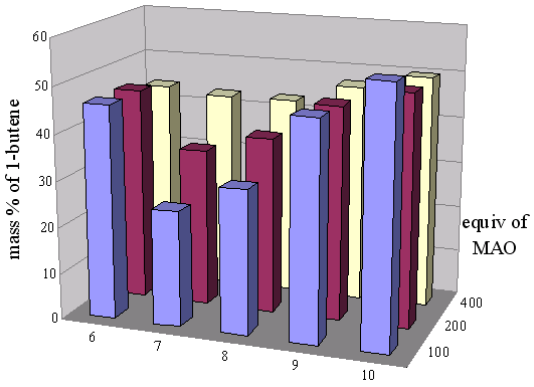

Figure 12.
Selectivity of precatalysts **6**–**10** for 1-butene within the C_4 fraction using MAO as cocatalyst.

Table 5.
Catalytic data for complexes **6**–**10** and distribution of the C_6 alkenes in the oligomerisation of ethylene with MAO as cocatalyst.[a]

	MAO (equiv.)	Selectivity (mass%)			
		1-hexene	Linear C_6[b]	C_6 from 1-butene[c]	C_6 from 2-butene[d]
6	100	29	63	1	7
6	200	26	62	2	10
6	400	24	63	2	11
7	100	13	81	0	6
7	200	22	66	1	11
7	400	26	62	1	11
8	100	22	70	1	7
8	200	23	65	2	10
8	400	23	62	3	12
9	100	33	58	0	9
9	200	27	60	2	11
9	400	27	58	2	13
10	100	33	62	0	5
10	200	34	59	0	8
10	400	28	59	2	10

[a] Conditions: T = 25 °C, 10 bar of C_2H_4, 35 min, 10^{-2} mmol of Co, solvent = 20 mL of toluene. [b]Sum of 3-*cis*-hexene, 3-*trans*-hexene, 2-*cis*-hexene, and 2-*trans*-hexene. [c] Corresponds to 2-ethyl-1-butene. [d] Sum of 3-methyl-1-pentene, 3-methyl-2-*cis*-pentene, and 3-methyl-2-*trans*- pentene.

Bianchini and co-workers[21] have reported that upon activation by MAO, tetrahedral cobalt(II) dichloride precursors with 6-substituted-2-(imino)pyridyl ligands catalyzed the selective conversion of ethylene to α-olefins with turnover frequencies as high as 1.5×10^6 mol C_2H_4/((mol Co)·h) but the most productive systems have been described by Gibson and co-workers[15d] with Co(II) catalysts containing CF_3 substituents on the ring of the bis(imino)pyridine ligand. In contrast, pentacoordinated imino-phenanthroline Co(II) complexes were only moderately active for the oligomerisation of ethylene.[22] Dinuclear tetrahedral imino-pyridyl Co(II) complexes and

for references, see page 134

pentacoordinated imino-pyridyl, phenolate-bridged Co(II) complexes displayed low activities in the presence of MAO.[23] Cobalt(II) complexes bearing P-containing ligands, such as bis(2-diphenylphosphinoethyl)methylamine[7b] and pyrazolyliminophosphorane[7c] ligands, were also found to be moderately active for this reaction in the presence of ethylaluminoxane (EAO) or MAO.

Conclusion

The cobalt(II) complexes **6**–**10** have been synthesised and characterised by single-crystal X-ray diffraction. Unexpectedly, complexes **6** and **7** with the bulkier ligands have a centrosymmetric dinuclear structure, in contrast to the mononuclear complexes **8**–**10** which are of the more usual five-membered and six-membered chelate type. The coordination geometry around cobalt can be described as a distorted tetrahedral for each complex. The magnetic moments of these paramagnetic complexes were measured in their D_2-dichloromethane solutions by Evans method.

Complexes **6**–**10** showed moderate catalytic activities as precatalysts for the oligomerisation of ethylene in the presence of MAO or $AlEtCl_2$. With the latter, all of the complexes displayed selectivities higher than 92% for ethylene dimerisation and the highest TOF were obtained with complex **8** under the same conditions. Although these cobalt(II) complexes were less active than the corresponding nickel complexes **I** and **II**,[8] much higher selectivities for 1-butene were observed. When MAO was used as catalyst, complexes **6**–**10** provided similar catalytic activities and selectivites for 1-butene. In contrast to $AlEtCl_2$, which afforded almost exclusively C_4 products, the use of MAO as cocatalyst gave a C_4–C_{12} distribution of oligomers.

Experimental Section

General Considerations. All solvents were dried and distilled using common techniques unless otherwise stated. All manipulations were carried out under an inert-gas atmosphere using standard Schlenk techniques. The compounds 2-[(diisopropyl-phosphanyl)-methyl]-4,5-dihydro-oxazole (**1**),[10b,c] 2-[(diphenylphosphanyl)-methyl]-4,5-dihydrooxazole (**2**),[10a] 2-[(diphenylphosphanyl)-methyl]-4,4-dimethyl-4,5-dihydrooxazole (**3**),[10a] 1-[4,4-dimethyl-2{1-oxy(diphenylphosphino)-1-methyl}]-4,5-dihydrooxazole (**4**)[13] and 1-[4,4-dimethyl-2-{1-oxy(diphenylphosphino)-1-methylethyl}]-4,5-dihydrooxazole (**5**)[8b-d,] were prepared according to the literature procedures. Other chemicals were commercially available and used without further purification unless otherwise stated. IR spectra in the range 4000–400 cm^{-1} were recorded on a Bruker IFS28FT instrument. For

for references, see page 134

all complexes whose magnetic moments were determined by the Evans method,[14] a CH_3NO_2-CD_2Cl_2 solution (20:80 v/v) was used as the reference and a solution of the paramagnetic complex 0.055-0.10 M in CD_2Cl_2 was prepared (a diamagnetic correction was introduced for the solvent). Gas chromatographic analyses were performed on an Thermoquest GC8000 Top Series gas chromatograph using an HP Pona column (50 m, 0.2 mm diameter, 0.5 μm film thickness).

Preparation of 2-[(diisopropylphosphanyl)-methyl]-4,5-dihydrooxazole) cobalt dichloride (6). To a solution of 2-[(diisopropyl-phosphanyl)-methyl]-4,5-dihydro-oxazole (**1**) (0.263 g, 1.31 mmol) in THF (15 mL) $CoCl_2$ (0.153 g, 1.18 mmol) was added. The reaction mixture was stirred for 15 h at room temperature. The resulting product precipitated from the solution and was isolated by filtration, washed with diethyl ether (2x15 mL) and dried in vacuum to give a bright-blue powder (0.198 g, 90% yield). FT-IR (KBr disc): 1640 cm^{-1} (ν(C=N)). Magnetic moment in solution (Evans method): 5.30 μ_B. Anal. Calcd for $C_{20}H_{40}Cl_4Co_2N_2O_2P_2$: C, 36.28; H, 6.09; N, 4.23. Found: C, 35.78; H, 6.15; N, 4.18.

Preparation of 2-[(diphenylphosphanyl)-methyl]-4,5-dihydrooxazole) cobalt dichloride (7). The ligand 2-[(diphenylphosphanyl)-methyl]-4,5-dihydrooxazole (**2**) (0.573 g, 2.12 mmol) and 0.8 equiv of anhydrous $CoCl_2$ (0.221 g, 1.70 mmol) were mixed in a Schlenk tube and then degassed THF (15 mL) was added. The reaction mixture was stirred for 18 h at room temperature. The resultant blue precipitate was collected by filtration, washed with diethyl ether (2x15 mL), dried in vacuum to give a bright-blue powder (0.442 g, 65% yield). FT-IR (KBr disc): 1643 cm^{-1} (ν(C=N)). Magnetic moment in solution (Evans method): 5.42 μ_B. Anal. Calcd for $C_{32}H_{32}Cl_4Co_2N_2O_2P_2$: C, 48.15; H, 4.04; N, 3.51. Found: C, 47.83; H, 4.31; N, 3.18.

Preparation of 2-[(diphenylphosphanyl)-methyl]-4,4-dimethyl-4,5-dihydro oxazole cobalt dichloride (8). To a solution of the ligand 2-[(diphenylphosphanyl)-methyl]-4,4-dimethyl-4,5-dihydrooxazole (**3**) (0.350 g, 1.18 mmol) in THF (20 mL), $CoCl_2$ (0.138 g, 1.06 mmol) was added. The reaction mixture was stirred for 15 h at room temperature to yield a blue-purple solution. The solvent was removed *in vacuo* and the residue was washed with diethyl ether (2x15 mL) and pentane (15 mL) and dried *in vacuum* to lead to a purple powder (0.420 g, 92% yield). FT-IR (KBr disc): 1615 cm^{-1} (ν(C=N)). Magnetic moment in solution (Evans method): 3.94 μ_B. Anal. Calcd for $C_{18}H_{20}Cl_2CoNOP$: C, 50.61; H, 4.72; N, 3.28. Found: C, 50.23; H, 4.79; N, 3.17.

for references, see page 134

Preparation of 1-[4,4-dimethyl-2{1-oxy(diphenylphosphino)-1-methyl}]-4,5-dihydrooxazole cobalt dichloride (9). To a solution of 1-[4,4-dimethyl-2{1-oxy(diphenylphosphino)-1-methyl}]-4,5-dihydrooxazole (**4**) (0.441 g, 1.41 mmol) in THF (15 mL), cobalt dichloride (0.171 g, 1.32 mmol) was added and the colourless solution immediately became dark blue. The reaction mixture was stirred for 15 h at room temperature, the solvent removed under reduced pressure and the residue washed with diethyl ether (2x15 mL). The product was collected by filtration and dried in vacuum. (blue-purple powder, 0.535 g, 92% yield). IR (KBr disc): 1639 cm^{-1} (ν(C=N)). Magnetic moment in solution (Evans method): 3.92 μ_B. Anal. Calcd for $C_{18}H_{20}Cl_2CoNO_2P$: C, 48.78; H, 4.55; N, 3.16. Found: C, 48.35; H, 4.61; N, 3.00.

Preparation of 1-[4,4-dimethyl-2-[1-oxy(diphenylphosphino)-1-methylethyl]]-4,5-dihydrooxazole cobalt dichloride (10). To a solution of 1-[4,4-dimethyl-2-{1-oxy(diphenylphosphino)-1-methylethyl}]-4,5-dihydrooxazole (**5**) (0.410 g, 1.20 mmol) in THF (20 mL), cobalt dichloride (0.094 g, 0.724 mmol) was added and the colourless solution rapidly became dark blue. The reaction mixture was stirred for 15 h at room temperature, the the solvent removed *in vacuo* and the residue washed with diethyl ether (2x20 mL) and pentane (20 mL). The product was dried *in vacuo* and obtained as a dark-blue powder (0.300 g, 88% yield). IR (KBr disc): 1612 cm^{-1} (ν(C=N)). Magnetic moment in solution (Evans method): 3.75 μ_B. Anal. Calcd for $C_{20}H_{24}Cl_2CoNO_2P$: C, 50.98; H, 5.13; N, 2.97. Found: C, 50.51; H, 5.08; N, 2.82.

Oligomerisation of Ethylene. All catalytic reactions were carried out in a magnetically stirred (900 rpm) 100 mL stainless steel autoclave. The interior of the autoclave was protected from corrosion with a glass container. All catalytic tests were started at 25 °C, and no cooling of the reactor was done during the reaction. In the catalytic experiments with $AlEtCl_2$, $4.0x10^{-2}$ mmol of cobalt complex was used. Depending on the amount of cocatalyst added (3, 5, or 7 mL of cocatalyst solution in toluene for 6, 10 or 14 equiv of $AlEtCl_2$, respectively, 12, 10 or 8 mL toluene were added to dissolve the precatalyst so that the total volume of all solutions was 15 mL. When MAO (1, 2, or 4 mL of cocatalyst solution in toluene for 100, 200 or 400 equiv of MAO, respectively) was used as cocatalyst, 10^{-2} mmol of cobalt complex was dissolved in 19, 18 or 16 mL of toluene, respectively, so that the total volume of all solutions was 20 mL. After injection of the catalyst solution under a constant low flow of ethylene, the reactor was brought to working pressure and continuously fed with ethylene, using a reserve bottle placed on a balance to allow continuous monitoring of the ethylene uptake. The modest temperature increase observed (from ca. 25 to 30 °C) resulted solely from the exothermicity of the

for references, see page 134

reaction. The oligomerisation products and remaining ethylene were only collected from the reactor at the end of the catalytic experiment. The gaseous and liquid products were analysed separately and combined results are given in the Tables. At the end of each test, the reactor was cooled to 10 °C before the gaseous phase was transferred into a 10 L polyethylene tank filled with water. An aliquot of this gaseous phase was transferred into a Schlenk flask, previously evacuated, for GC analysis. The products in the reactor were hydrolyzed in situ by addition of ethanol (10 mL), transferred into a Schlenk flask and separated from the metal complexes by trap-to-trap distillation (25 °C, 0.6 mbar). All volatiles were evaporated (25 °C, 0.6 mbar static pressure) and recovered in a second flask previously immersed in liquid nitrogen in order to avoid any loss of product. For gas chromatographic analyses, 1-heptene was used as internal reference.

X-ray Structure Determinations. Single crystals of complexes **6**–**10** suitable for X-ray diffraction analysis were obtained by slow layer-diffusion of *n*-pentane into their corresponding dichloromethane solutions under nitrogen atmosphere. Blue crystals of **11** were obtained from the same Schlenk tube as **8** (purple) by slow layer-diffusion of *n*-pentane into a CH_2Cl_2 solution of **8**. Blue crystals of **12** were obtained independently by slow layer-diffusion of *n*-pentane into a CH_2Cl_2 solution of **8**. Diffraction data were collected on a Kappa CCD diffractometer using graphite-monochromated Mo-Kα radiation (λ = 0.71073 Å). The relevant data are summarized in Table 6 and 7. Data were collected using Φ scans and the structures were solved by direct methods using the SHELX-97 software.[24,25] The refinements were conducted by full-matrix least squares on F^2. No absorption correction was used. All non-hydrogen atoms were refined anisotropically with H atoms mathematically introduced as fixed contributors (SHELXL procedure).

Acknowledgements

We thank the French Embassy in Beijing for a doctoral grant to S. J. to perform research in Strasbourg in the context of the Franco-Chinese Laboratory for Catalysis, and to the CNRS, the Ministère de la Recherche (Paris) and the Institut Français du Pétrole (IFP) for support. We are grateful to Professor Wen-Hua Sun, Institute of Chemistry, Chinese Academy of Sciences, Beijing 100080, China for his kind cooperation, to Dr. A. DeCian and Prof. R. Welter (ULP Strasbourg) for the crystal structure determinations and to M. Mermillon-Fournier for experimental assistance.

for references, see page 134

Table 6.
Crystallographic data for complexes **6–12**

	6	**7**	**8**	**9**	**10**	**11**	**12**
formula	$C_{20}H_{40}Cl_4Co_2N_2O_2P_2$	$C_{32}H_{32}Cl_4Co_2N_2O_2P_2$	$C_{18}H_{20}Cl_2CoNOP$	$C_{18}H_{20}Cl_2CoNO_2P$	$C_{20}H_{24}Cl_2CoNO_2P$	$C_{18}H_{20}Cl_3CoNO_2P$	$C_{36}H_{40}Cl_4Co_2N_2O_4P_2$
Formula weight	662.14	798.20	427.15	443.15	471.20	478.60	886.30
Crystal system	monoclinic	monoclinic	monoclinic	monoclinic	monoclinic	monoclinic	monoclinic
Space group	$P2_1/c$	$P2_1/c$	$P2_1/c$	$P2_1/c$	$P2_1/c$	$P2_1/c$	$P2_1/c$
a (Å)	12.4010(4)	13.1310(4)	7.0690(2)	11.3700(3)	8.9970(2)	14.2380(6)	8.6150(10)
b (Å)	9.8100(4)	10.0750(3)	28.7830(6)	18.1880(5)	14.5140(4)	12.8960(6)	18.264(3)
c (Å)	14.2570(5)	13.4300(5)	10.8560(2)	9.7290(4)	16.7880(4)	13.1040(9)	12.580(2)
α (º)	90.00	90.00	90.00	90.00	90.00	90.00	90.00
β (º)	122.6151(16)	100.3060(11)	120.5011(9)	95.4760(11)	93.2150(15)	111.8260(16)	104.325(5)
γ (º)	90.00	90.00	90.00	90.00	90.00	90.00	90.00
V (Å^3)	1460.92(9)	1748.05(10)	1903.18(8)	2002.75(11)	2188.77(9)	2233.6(2)	1917.8(5)
Z	2	2	4	4	4	4	2
Crystal size(mm)	0.18×0.14×0.14	0.10×0.10×0.10	0.16×0.14×0.10	0.16×0.16×0.14	0.14×0.14×0.12	0.16×0.10×0.10	0.10×0.10×0.10
D_{calcd} (g cm^{-3})	1.505	1.516	1.491	1.470	1.430	1.423	1.535
μ (mm^{-1})	1.631	1.378	1.271	1.214	1.116	1.210	1.268
θ range (º)	1.95-29.05	2.54-29.94	1.41-29.11	1.80-29.10	1.86-29.11	1.54-27.48	2.01-30.02
F(000)	684	812	876	908	972	976	908
R	0.0456	0.0478	0.0446	0.0401	0.0450	0.0775	0.0731
Rw	0.0974	0.1126	0.0957	0.0872	0.1063	0.1277	0.1594
GOF on F^2	1.049	1.052	1.007	1.010	1.029	1.004	1.016
Largest diff. peak, hole (e Å^{-3})	0.999, -0.777	1.623, -0.777	0.587, -0.707	0.619, -0.631	0.656, -0.840	0.534, -0.378	1.930, -1.477

for references, see page 134

References

1. (a) A. Bader and E. Lindner, *Coord. Chem. Rev.*, 1991, **108**, 27. (b) C. S. Slone, D. A. Weinberger and C. A. Mirkin, *Prog. Inorg. Chem.*, 1999, **48**, 233. (c) G. Helmchen and A. Pfaltz, *Acc. Chem. Res.*, 2000, **33**, 336. (d) P. Braunstein and F. Naud, *Angew. Chem., Int. Ed.*, 2001, **40**, 680. (e) H. A. McManus and P. J. Guiry, *Chem. Rev.*, 2004, **104**, 4151. (f) G. Margraf, R. Pattacini, A. Messaoudi and P. Braunstein, *Chem. Commun.*, 2006, 3098. (g) P. Braunstein, *Chem. Rev.*, 2006, **106**, 134.
2. (a) J. P. Collman, L. S. Hegedus, J. R. Norton and R. G. Finke, eds., *Principles and Applications of Organotransition Metal Chemistry*, University Science Book, CA, 1987. (b) A. Yamamoto, ed., *Organotransition Metal Chemistry*, Wiley, New York, 1986.
3. (a) J.-C. Hierso, R. Amardeil, E. Bentabet, R. Broussier, B. Gautheron, P. Meunier and P. Kalck, *Coord. Chem. Rev.*, 2003, **236**, 143. (b) P. Espinet and K. Soulantica, *Coord. Chem. Rev.*, 1999, **193-195**, 499. (c) G. R. Newkome, *Chem. Rev.*, 1993, **93**, 2067.
4. (a) A. N. Ajjou and H. Alper, *J. Am. Chem. Soc.*, 1998, **120**, 1466. (b) C. Bianchini, A. Meli, M. Peruzzini, F. Vizza and F. Zanobini, *Coord. Chem. Rev.*, 1992, **120**, 193. (c) M. Qadir, T. Mochel and K. K. Hii, *Tetrahedron*, 2000, **56**, 7975. (d) F. Speiser, P. Braunstein and L. Saussine, *Acc. Chem. Res.*, 2005, **38**, 784.
5. (a) M. E. Bluhm, C. Folli, O. Walter and M. Doering, *J. Mol. Catal. A: Chem.*, 2005, **229**, 177. (b) A. Mukherjee, U. Subramanyam, V. G. Puranik, T. P. Mohandas and A. Sarkar, *Eur. J. Inorg. Chem.*, 2005, 1254. (c) D. Sirbu, G. Consiglio and S. Gischig, *J. Organomet. Chem.*, 2006, **691**, 1143. (d) F. Speiser, P. Braunstein and L. Saussine, *Organometallics*, 2004, **23**, 2633. (e) F. Speiser, P. Braunstein and L. Saussine, *Organometallics*, 2004, **23**, 2625. (f) W.-H. Sun, Z. Li, H. Hu, B. Wu, H. Yang, N. Zhu, X. Leng and H. Wang, *New J. Chem.*, 2002, **26**, 1474. (g) X. Tang, D. Zhang, S. Jie, W.-H. Sun and J. Chen, *J. Organomet. Chem.*, 2005, **690**, 3918.
6. (a) D. Vogt, ed., *Applied Homogeneous Catalysis with Organometallic Compounds*, VCH, Weinheim, 2002. (b) V. C. Gibson and S. K. Spitzmesser, *Chem. Rev.*, 2003, **103**, 283 (c) S. D. Ittel, L. K. Johnson and M. Brookhart, *Chem. Rev*. 2000, **100**, 1169
7. (a) S. Al-Benna, M. J. Sarsfield, M. Thornton-Pett, D. L. Ormsby, P. J. Maddox, P. Brès and M. Bochmann, *J. Chem. Soc., Dalton Trans.*, 2000, 4247. (b) M. Wang, X. Yu, Z. Shi, M. Qian, K. Jin, J. Chen and R. He, *J. Organomet. Chem.*, 2002, **645**, 127. (c) C. Zhang, W.-H. Sun and Z.-X. Wang, *Eur. J. Inorg. Chem.*, 2006, 4895.
8. (a) F. Speiser, P. Braunstein, L. Saussine and R. Welter, *Organometallics*, 2004, **23**, 2613 (b) F. Speiser, P. Braunstein, L. Saussine and R. Welter, *Inorg. Chem.*, 2004, **43**, 1649. (c) F. Speiser, P. Braunstein and L. Saussine, *Fr. Pat.*, 2 837 725 A1, 2003. (d) P. Braunstein, J. Zhang and R. Welter, *Dalton Trans*. 2003, 507.
9. (a) J.-M. Basset, C. Copéret, D. Soulivong, M. Taoufik, J. Thivolle-Cazat, *Angew. Chem. Int. Ed.*, 2006, **45**, 6082. (b) R. B. Bedford, C. S. J. Cazin, D. Holder, *Coord. Chem. Rev.*, 2004, 2283. (c) F. Agbossou, J.-F. Carpentier, F. Hapiot, I. Suisse and A. Mortreux, *Coord. Chem. Rev.*, 1998, **178-180**, 1615. (d) S. J. Roseblade and A. Pfaltz, *C.R. Chimie* 2007, **10**, 178.

10 (a) P. Braunstein, M. D. Fryzuk, M. Le Dall, F. Naud, S. J. Rettig and F. Speiser, *Dalton Trans.*, 2000, 1067. (b) A. Kermagoret and P. Braunstein, *Unpublished results*. (c) M. Agostinho, P. Braunstein, *C. R. Chimie*, 2007, *in press.*

11. T. G. Gant and A. I. Meyers, *Tetrahedron*, 1994, **50**, 2297.

12. L. N. Pridgen and G. Miller, *J. Heterocycl. Chem.*, 1983, **20**, 1223.

13. M. Agostinho, P. Braunstein and R. Welter, *Dalton Trans.*, 2007, 759.

14. (a) D. F. Evans, *J. Chem. Soc.*, 1959, 2003. (b) J. Loeliger and R. Scheffold, *J. Chem. Educ.*, 1972, **49**, 646. (c) S. K. Sur, *J. Magn. Reson.*, 1989, **82**, 169.

15. (a) F. A. Cotton and G. Wilkinson, *Advanced Inorganic Chemistry*, J. Wiley, New York, 5th Edition, 1988, p. 729. (b) A. Panda, M. Stender, R. J. Wright, M. M. Olmstead, P. Klavins and P. P. Power, *Inorg. Chem*. 2002, **41**, 3909. (c) L. P. Spencer, R. Altwer, P. Wei, L. Gelmini, J. Gauld and D. W. Stephan, *Organometallics*, 2003, **22**, 3841. (d) K. P. Tellmann, V. C. Gibson, A. J. P. White and D. J. Williams, *Organometallics*, 2005, **24**, 280.

16. M. Agostinho, P. Braunstein, *Chem. Commun.*, 2007, 58.

17. P. Braunstein, G. Clerc, X. Morise, R. Welter and G. Mantovani, *Dalton Trans.*, 2003, 1601.

18. P. Braunstein, G. Clerc and X. Morise, *New J. Chem.*, 2003, **27**, 68.

19. J. T. Mague and J. L. Krinsky, *Inorg. Chem.*, 2001, **40**, 1962.

20. (a) V. C. Gibson, K. P. Tellmann, M. J. Humphries and D. F. Wass, *Chem. Commun.*, 2002, 2316. (b) B. L. Small, *Organometallics*, 2003, **22**, 3178. (c) B. L. Small and R. Schmidt, *Chem. Eur. J.* 2004, **10**, 1014. (d) J. Heinicke, M. Köhler, N. Peulecke, M. K. Kindermann, W. Keim and M. Köckerling, *Organometallics*, 2005, **24**, 344. (e) Q.-Z. Yang, A. Kermagoret, M. Agostinho, O. Siri and P. Braunstein, *Organometallics*, 2006, **25**, 5518.

21. (a) C. Bianchini, D. Gatteschi, G. Giambastiani, I. G. Rios, A. Ienco, F. Laschi, C. Mealli, A. Meli, L. Sorace, A. Toti and F. Vizza, *Organometallics*, 2007, **26**, 726. (b) C. Bianchini, G. Giambastiani, G. Mantovani, A. Meli and D. Mimeau, *J. Organomet. Chem.*, 2004, **689**, 1356. (c) C. Bianchini, G. Mantovani, A. Meli, F. Migliacci and F. Laschi, *Organometallics*, 2003, **22**, 2545.

22. (a) J. D. A. Pelletier, Y. D. M. Champouret, J. Cadarso, L. Clowes, M. Ganete, K. Singh, V. Thanarajasingham and G. A. Solan, *J. Organomet. Chem*. 2006, **691**, 4114. (b) S. Jie, S. Zhang, K. Wedeking, W. Zhang, H. Ma, X. Lu, Y. Deng and W.-H. Sun, *C.R. Chim*., 2006, **9**, 1500.

23. Y. D. M. Champouret, J. Fawcet, W. J. Nodes, K. Singh and G. A. Solan, *Inorg. Chem*. 2006, **45**, 9890.

24. *Kappa CCD Operation Manual*; Nonius BV, Delft, The Netherlands, 1997.

25. G. M. Sheldrick, *SHELX97, Program for the refinement of crystal structures*; University of Göttingen; Göttingen, Germany, 1997.

Conclusion Générale

General Conclusion

Driven by its fundamental importance and commercial applications, the research of late-transition metal complexes as catalysts for ethylene oligomerization and polymerization has been found considerable attraction in both academic and industrial consideration due to expectation of highly active and selective catalysts. This thesis focuses on designing and synthesis of late-transition metal complexes used as catalysts for catalytic oligomerization and polymerization of ethylene. Three types of ligands, including N^N, N^N^N and P^N ligands, were used in the preparation of late-transition metal complexes. Upon activation with Al-based cocatalyst, their catalytic properties were detailedly investigated and discussed.

Chapter I

A series of bridged bis(pyridinylimino) ligands were efficiently synthesized through the condensation reaction of 4,4'-methylene-bis(2,6-disubstituted aniline) with 2-pyridinecarboxaldehyde or 2-benzoylpyridine. The ligands **L1**–**L4** were prepared by mixing 4,4'-methylene-bis(2,6-disubstituted aniline) and 2-pyridinecarboxaldehyde in ethanol with the catalytic amount of *p*-toluene sulfonic acid (Scheme 1). The bulky ligands **L5**–**L8** were synthesized by the reaction of 2-benzoylpyridine and bis-aniline and it was necessary to remove the water formed in the reaction by using tetraethyl silicate.

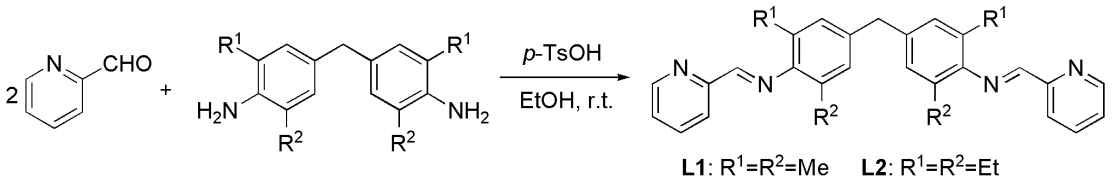

L1: R^1=R^2=Me **L2**: R^1=R^2=Et
L3: R^1=R^2=i-Pr **L4**: R^1=i-Pr, R^2=Me

Scheme 1.
Synthesis of ligands **L1**–**L4**.

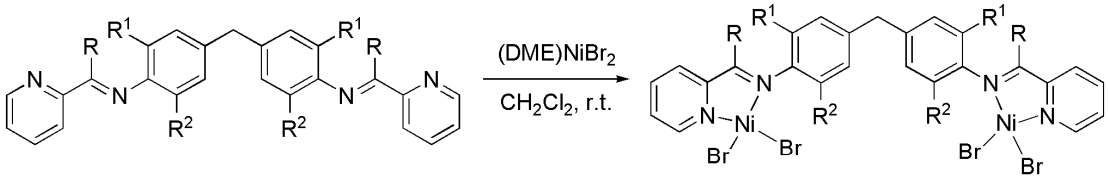

C1: R=H, R^1=R^2=Me **C2**: R=H, R^1=R^2=Et
C3: R=H, R^1=R^2=i-Pr **C4**: R=H, R^1=i-Pr, R^2=Me
C5: R=Ph, R^1=R^2=Me **C6**: R=Ph, R^1=R^2=Et
C7: R=Ph, R^1=R^2=i-Pr **C8**: R=Ph, R^1=i-Pr, R^2=Me

Scheme 2.
Synthesis of nickel complexes **C5**–**C8**.

The bridged bis(pyridinylimino) ligands **L1**–**L8** readily reacted with 2 equiv. of (DME)$NiBr_2$ in CH_2Cl_2 to form the corresponding bridged bis(pyridinylimino) dinuclear nickel complexes **C1**–**C8** (Scheme 2).

Activated with MAO, these nickel complexes showed considerably good activities for ethylene oligomerization and polymerization. The highest polymerization activity of 2830 kg mol^{-1}(Ni) h^{-1} was obtained with **C3**/MAO catalytic system at 10 atm of ethylene pressure. The resultant PEs were characterized by FT-IR, their melting points (T_m) were measured by DSC, and their molecular weights (M_w) and molecular weight distributions (M_w/M_n) were determined by GPC. The ^{13}C NMR spectra of PE obtained by **C3**/MAO indicated that the vinyl-unsaturated branched polyethylene with main butyl branches formed and the branching extent was counted equal to 5 branches per 1000 carbon atoms according to the calculation method reported.

Chapter II

In this chapter, 2-formyl-, 2-acetyl-, and 2-benzoyl-1,10-phenanthrolines, were prepared using 1,10-phenanthroline as starting material (Scheme 3). To shorten the synthetic route and improve the total yield, an improved synthetic method to prepare 2-acetyl-1,10-phenanthroline from 2-cyano-1,10-phenanthroline was established by using trimethylaluminum in the yield of 60%. 2-Benzoyl-1,10-phenanthroline was first synthesized from 1,10-phenanthroline-2-carbonyl chloride followed by a Friedel-Crafts acylation reaction of benzene with $AlCl_3$ as catalyst.

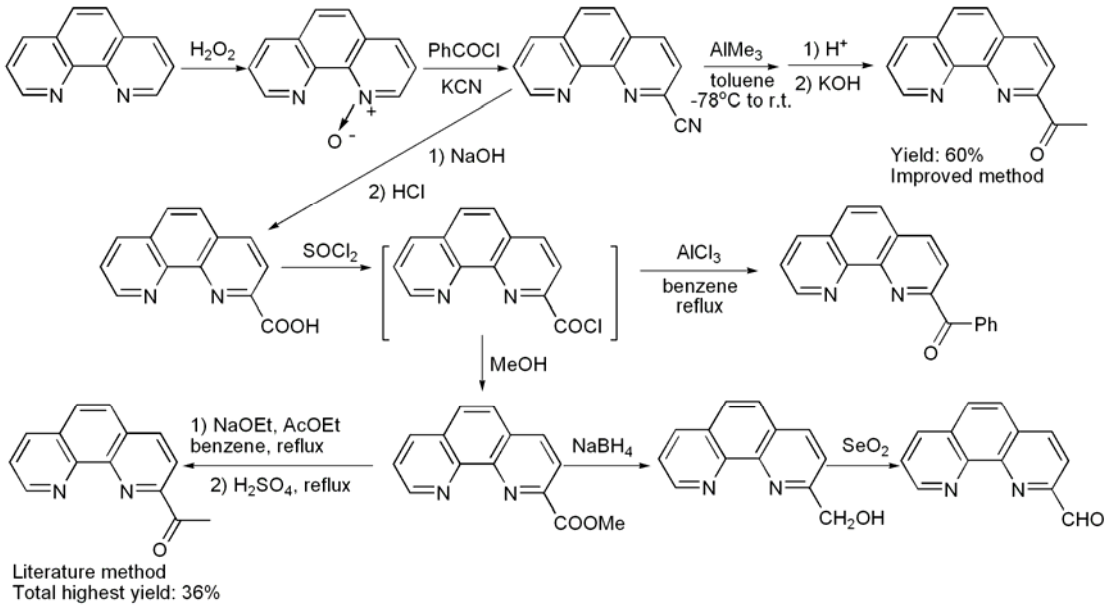

Scheme 3.
Synthesis of 2-formyl-, 2-acetyl- and 2-benzoyl-1,10-phenanthroline.

The 2-imino-1,10-phenanthrolinyl ligands (**1**–**20**, 2-(ArN=CR)-1,10-phen) were prepared through the condensation reaction of aldehyde or ketones and the corresponding substituted anilines using *p*-toluene sulfonic acid as catalyst (Scheme 4). Because of the difference in the reactive nature between aldehyde and ketones, alkyl- and halogen-substituted anilines, the various solvents such as ethanol, toluene or tetraethyl silicate were employed in order to improve the product yields. The iron(II) complexes **1a**–**20a** were easily prepared by mixing the corresponding ligand and one equivalent of $FeCl_2 \cdot 4H_2O$ in THF at room temperature under argon (Scheme 4) and the final products were obtained as blue, purple or brown air-stable powders.

Upon treatment with MAO or MMAO, these iron(II) complexes showed high catalytic activities of up to 8.95×10^7 g mol^{-1}(Fe) h^{-1} for ethylene oligomerization with high selectivity for α-olefins. However, MAO was found to be more effective than MMAO. The distribution of oligomers produced follows Schluz-Flory rules with high selectivity for α-olefins. Both steric and electronic effects of ligands affect the catalytic activity and the properties of catalytic products. In many cases, some low-molecular-weight waxes as higher oligomers were obtained in addition to lower oligomers. The ^{13}C NMR spectra further demonstrated that linear α-olefins absolutely predominated in the waxes. This is a new family of highly active iron catalysts for ethylene oligomerization since the bis(imino)pyridine iron systems.

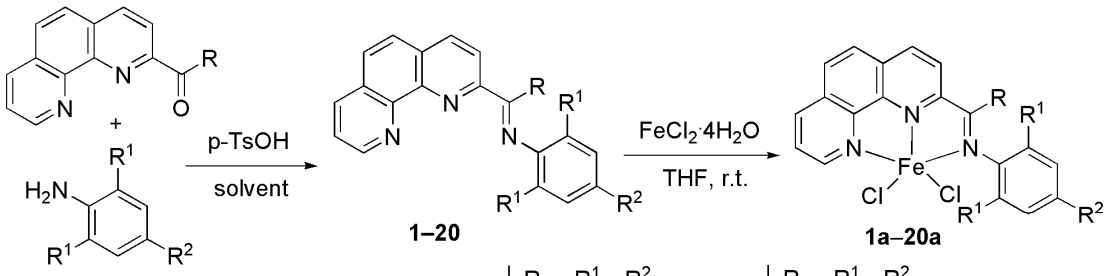

	R	R^1	R^2		R	R^1	R^2
1(**a**)	Me	Me	H	**11**(**a**)	Me	Br	Br
2(**a**)	Me	Et	H	**12**(**a**)	H	Me	H
3(**a**)	Me	*i*-Pr	H	**13**(**a**)	H	Et	H
4(**a**)	Me	Me	Me	**14**(**a**)	H	*i*-Pr	H
5(**a**)	Me	Me	Br	**15**(**a**)	H	F	H
6(**a**)	Me	F	H	**16**(**a**)	H	Cl	H
7(**a**)	Me	Cl	H	**17**(**a**)	H	Br	H
8(**a**)	Me	Br	H	**18**(**a**)	Ph	Me	H
9(**a**)	Me	Br	Me	**19**(**a**)	Ph	Et	H
10(**a**)	Me	Br	Cl	**20**(**a**)	Ph	*i*-Pr	H

Scheme 4.

Synthesis of the ligands **1**–**20** and the iron(II) complexes **1a**–**20a**.

Chapter III

The cobalt complexes **1**–**15** were readily prepared by mixing an ethanol solution of the corresponding ligand and $CoCl_2$ at room temperature (Scheme 5). The resulting precipitate was separated by filtration, washed with Et_2O and dried under vacuum as air-stable powders.

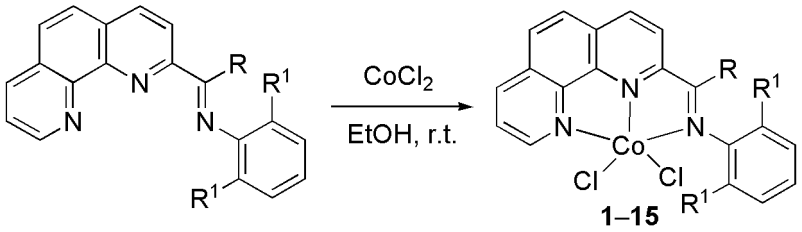

	1	2	3	4	5	6	7	8	9	10	11	12	13	14	15
R	H	H	H	H	H	H	Me	Me	Me	Me	Me	Me	Ph	Ph	Ph
R^1	Me	Et	i-Pr	F	Cl	Br	Me	Et	i-Pr	F	Cl	Br	Me	Et	i-Pr

Scheme 5.
Synthesis of cobalt complexes **1**–**15**

Upon treatment with MAO or MMAO, these cobalt(II) complexes showed moderate to high catalytic activities of up to 2.34×10^6 g mol^{-1}(Co) h^{-1} for ethylene oligomerization at 10 atm of ethylene pressure. Butenes were found to be predominant among the oligomers produced. MMAO was found to be a more effective cocatalyst at 1 atm of ethylene pressure. By comparison with the data obtained with MAO as cocatalyst, the lifetime of the catalysts was prolonged at 10 atm of ethylene pressure along with an improved catalytic activity. For the complexes bearing the same alkyl groups at the *ortho*-positions of the aryl ring, the catalytic activities increased in the sequence: aldimine (R=H), methyl-ketimine (R=Me) and phenyl-ketimine (R=Ph). For both aldimine and methyl-ketimine complexes, bulky and moderately electronegative atoms at the *ortho*-positions of the imino-N aryl ring resulted in the sequence of catalytic activities: bromo- > chloro- > fluoro.

Chapter IV

2-Acetyl-9-phenyl-1,10-phenanthroline (**I**) was synthesized through attaching a phenyl group at phenanthroline ring using 2-acetyl-1,10-phenanthroline as the starting material (Scheme 6).

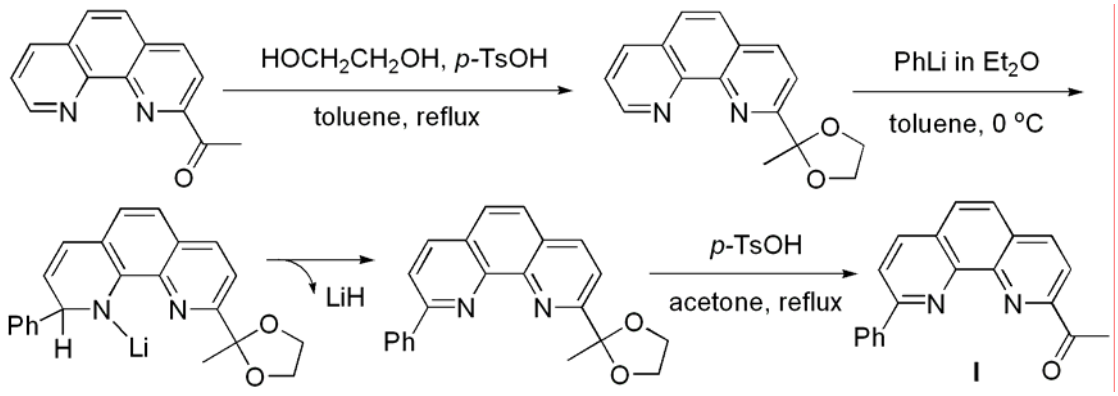

Scheme 6.
Synthesis of ketone **I**.

2-Benzoyl-9-phenyl-1,10-phenanthroline (**II**) was prepared through the one-step reaction of 2-cyano-1,10-phenanthroline and three equivalents of phenyllithium (scheme 7).

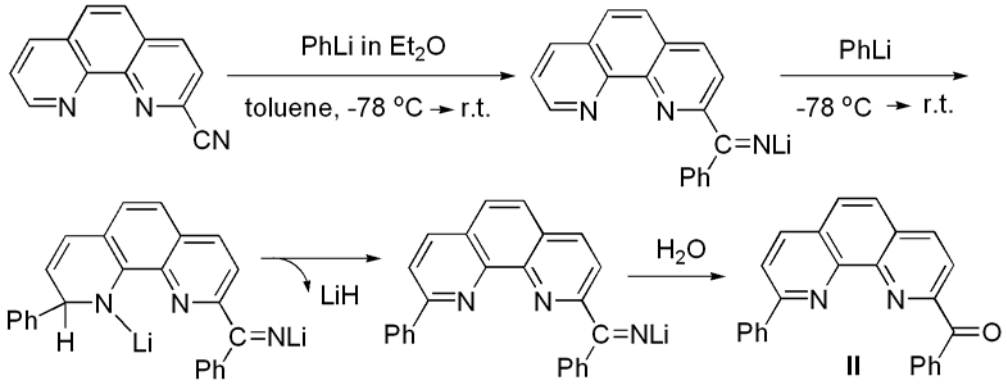

Scheme 7.
Synthesis of ketone **II**.

The 2-imino-9-phenyl-1,10-phenanthrolinyl ligands (**1**–**6**) were prepared through the condensation reaction of ketones **I** or **II** and the corresponding substituted anilines with *p*-toluene sulfonic acid in toluene or tetraethyl silicate (Scheme 8). The iron complexes **1a**–**6a** were readily prepared by mixing the corresponding ligand and $FeCl_2 \cdot 4H_2O$ in THF at room temperature under nitrogen, which were obtained as air-stable solid in green or brown color (Scheme 8). Similarly, the cobalt complexes **1b**–**6b** and nickel complexes **1c**–**6c** were synthesized by the reaction of the corresponding ligand with $CoCl_2$ or $NiCl_2 \cdot 6H_2O$ in anhydrous ethanol at room temperature. The methyl-ketimine cobalt complexes **1b**–**3b** were obtained as green powders, whereas the phenyl-ketimine complexes **4b**–**6b** showed red brown color. The corresponding nickel complexes **1c**–**6c** were orange or yellow powders.

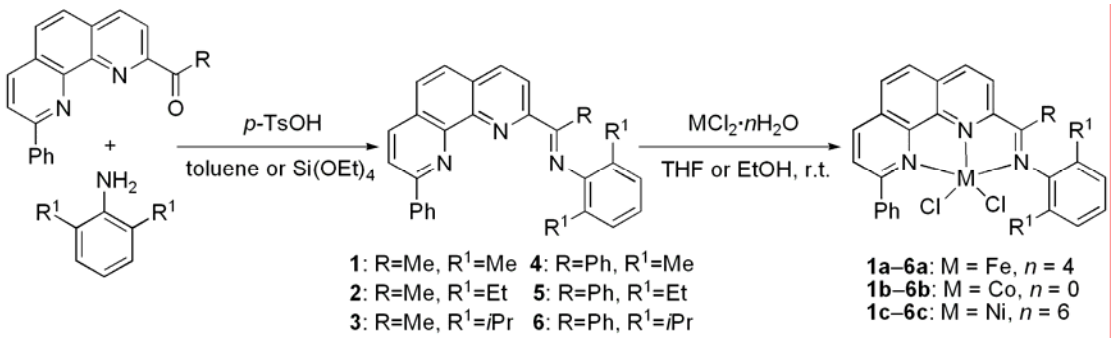

Scheme 8.
Synthesis of ligands **1**–**6** and complexes **1a**–**6a**, **1b**–**6b**, and **1c**–**6c**.

In the presence of MAO or MMAO, some iron complexes gave good catalytic activities with high selectivity for ethylene oligomerization (**1a**/MMAO: 2.69×10^6 g mol^{-1}(Fe) h^{-1}). Unexpectedly, the cobalt complexes generally showed much higher activities and broader distribution of oligomers than the corresponding iron analogues, which was greatly different from most of tridentate-N_3 catalytic systems. The ligand environment and the reaction parameters played an important role in influencing both the catalytic activity and the distribution of oligomers for iron and cobalt complexes. The highest activity up to 7.33×10^6 g mol^{-1}(Co) h^{-1} for ethylene oligomerization was obtained by **5b**/MAO at 10 atm of ethylene pressure. Et_2AlCl was a more effective co-catalyst for nickel complexes and the addition of PPh_3 could largely improve the catalytic activity and prolong the catalyst lifetime. The addition of 20 equiv. of PPh_3 led to higher catalytic activities at 10 atm of ethylene pressure.

Chapter V

The cobalt complexes were readily obtained by reaction of the corresponding ligands with anhydrous cobalt dichloride in THF at room temperature under nitrogen. When ligands **1** and **2** were used, the complexes **6** and **7** precipitated from the solution and were isolated by filtration and washed with diethyl ether to give air-stable bright-blue powders. It was unexpected that **6** and **7** would be dinuclear complexes with bridging phosphino-oxazoline ligands, as was established by X-ray diffraction. In contrast, when ligands **3**–**5** were used, purple or blue chelated complexes **8**–**10** were obtained.

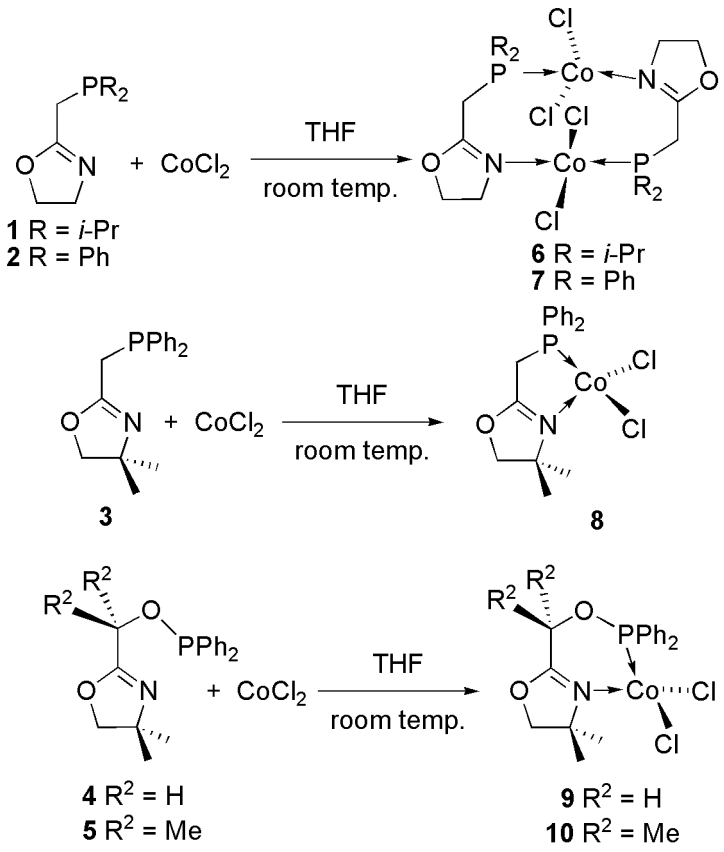

Complexes **6**–**10** showed moderate catalytic activities as precatalysts for the oligomerisation of ethylene in the presence of MAO or $AlEtCl_2$. With the latter (6–14 equiv), all of the complexes displayed selectivities higher than 92% for ethylene dimerisation and the highest TOF were obtained with complex **8** under the same conditions. Although these cobalt(II) complexes were less active than the corresponding nickel complexes, much higher selectivities for 1-butene were observed. When MAO was used as catalyst, complexes **6**–**10** provided similar catalytic activities and selectivites for 1-butene. In contrast to $AlEtCl_2$, which afforded almost exclusively C_4 products, the use of MAO as cocatalyst gave a C_4–C_{12} distribution of oligomers.